The University Of Sheffield.

An Investigation of Autoantibodies against the Calcium-Sensing Receptor in Patients with Autoimmune Polyendocrine Syndrome Type 1

Mahmoud Mohammad A Habibullah

A thesis submitted in partial fulfilment of the requirements for the degree of
Doctor of Philosophy

The University of Sheffield
Faculty of Medicine, Dentistry and Health
Department of Oncology and Metabolism

March, 2016

Summary

Context: Autoimmune polyendocrine syndrome type 1 (APS1) is characterised by multiple autoimmune endocrinopathies and results from mutations in the *AIRE* (autoimmune regulator) gene. Approximately 80% of patients present with hypoparathyroidism which is suggested to result from autoimmune responses against the parathyroid glands. The calcium-sensing receptor (CaSR), which plays a pivotal role in maintaining calcium homeostasis by sensing blood calcium levels and regulating release of parathyroid hormone, has been identified as a parathyroid autoantibody target in APS1.

Aims: The main aims of this study were to characterise APS1 patient anti-CaSR autoantibodies in relation to their prevalence, disease associations, epitopes, specificity, IgG subclass and effects upon CaSR function, and to develop an ELISA to detect CaSR autoantibodies in patient sera.

Methodology: Immunoprecipitation; radioligand binding assays; phage-display; ELISA; bioassays; protein expression.

Results: Autoantibodies against the CaSR were detected in 16 out of 44 (36%) APS1 patients and in none of 38 healthy control subjects (P = < 0.0001). No statistically significant associations were found between the presence of CaSR autoantibodies and the disease manifestations of APS1 including hypoparathyroidism. The detection of CaSR autoantibodies had a specificity of 83%, and a sensitivity of 39% for the diagnosis of hypoparathyroidism. There were no significant associations between the presence of CaSR antibodies and either sex, age or disease presentation age. However, a significant association between a shorter APS1 duration (< 10 years) and positivity for CaSR autoantibodies was noted (P = 0.019).

CaSR autoantibody epitopes were identified between amino acids 41–69, 114–126, 171–195 and 260-340 in the extracellular domain of the receptor. Autoantibodies against CaSR epitopes 41–69, 171-195 and 260-340 were exclusively of the IgG1 subclass. Autoantibody responses against CaSR epitope 114-126 were predominantly of the IgG1 with a minority of the IgG3 subclass. CaSR autoantibodies were analysed for their ability to increase Ca^{2+}-dependent inositol phosphate accumulation in HEK293 cells expressing the CaSR. The results indicated that 4/16 (25%) APS1 patients had anti-CaSR-activating autoantibodies, suggesting that although the majority of APS1 patients do not have CaSR-stimulating autoantibodies, there may be a small minority of patients in whom the hypoparathyroid state is the result of functional suppression of the parathyroid glands.

As part of this study, an ELISA was developed using the extracellular domain of the CaSR expressed in *Escherichia coli* as the antibody-capture antigen. Although this assay was able to detect the presence of autoantibodies in APS1 patient sera, the experimental method still requires further optimisations in order to attain a validated and robust ELISA, as this was not achievable during the present study.

Conclusion: The study provides a detailed analysis of the characteristics of CaSR autoantibodies in APS1 patients, although further investigations are required to determine the exact role played by the autoimmune response against the CaSR in the pathogenesis of APS1.

Declaration

I declare that this thesis has been written by me and has not been accepted in any earlier application for a higher degree. The work reported in this thesis has been carried out by me, except where specifically acknowledged in the text. All sources of information have been specifically acknowledged by means of references.

Mahmoud Habibullah

March, 2016

Dedication

I dedicate my thesis work to my family and many friends; to my loving parents, I have a special feeling of gratitude for their encouragement and prayers, to my beloved wife Arwa, for all the help and the love she gives me throughout this long journey, to my lovely daughters Seba and Ruba, to my sisters and brother, and to my friends and community.

Acknowledgments

It is a pleasure for me to acknowledge the many colleagues, friends, researchers, and other people who have played a great role through their support and help during my PhD journey. I do appreciate the help I received from everyone at various stages of my research. First, I owe a debt of gratitude to my supervisor Dr Helen Kemp for giving me an opportunity to do this project and help me understand research in the way she has. Her patient guidance at different stages of the project, continued support and encouragement, the positive energy she passes to me through her attitude, invaluable advice during writing, constant encouragement to present my work at meetings and conferences, and great help when things got tough, has made my PhD experience one of the unforgettable experiences of my life. Thank-you from bottom of my heart, your energy, smile, and patience has been inspirational.

I also like to extend my thanks to Professor Tony Weetman for his continued support, and to clinical collaborators Professor Annamari Ranki and Dr Nicolas Kluger (both from the Department of Dermatology, Allergology, and Venereology, the Institute of Clinical Medicine, University of Helsinki and Helsinki University Central Hospital, Helsinki, Finland), and Professor Kai Krohn (Clinical Research Institute, HUCH Ltd, HUS Helsinki, Finland). I would like to thank Professor Ravinder Goswami (Department of Endocrinology and Metabolism, All India Institute of Medical Sciences, New Delhi, India) for providing plasmid pPROEX-HTb-CaSREx, and Professor Olle Kampe (Department of Medical Sciences, Uppsala University Hospital, Uppsala, Sweden) for providing plasmid pCMV6-XL5-NALP5. Also, I would like to extend my thanks and appreciation to my colleagues, the academic and technical staff in our department, Miss Julie Porter, Miss Harpreet Sandhu, Dr Ian Wilkinson, Mrs Sue Justice, Dr Phil Watson, and all my friends who made my laboratory work more enjoyable. Also, I would like to acknowledge the patients participants.

Finally, I would like to say a massive thanks to my sponsors for their belief. Praise to King Abdullah who started the scholarship program. Thanks to Jazan University, the Saudi Arabian government, and the Royal Embassy of Saudi Arabia in London, UK.

All praise and thanks to Allah at the beginning and the end.

Table of Contents

Summary ..... **II**

Declaration ..... **III**

Dedication ..... **IV**

Acknowledgments ..... **V**

Table of Contents ..... **VI**

List of Figures ..... **X**

List of Tables ..... **XIII**

List of Abbreviations ..... **XIV**

List of Permissions ..... **XV**

List of Publications ..... **XVI**

1 Review of the Literature **2**

1.1 Autoimmune polyendocrine syndromes 2

1.2 Autoimmune polyendocrine syndrome type 1: aetiology and pathogenesis 3

1.2.1 The *AIRE* gene and AIRE protein 3

1.2.2 AIRE function in promoting central and peripheral tolerance 4

1.2.3 *AIRE* gene mutations in APS1 7

1.2.4 Models of pathogenesis in APS1 11

1.2.5 Organ-specific autoantibodies in APS1 15

1.2.6 Anti-cytokine autoantibodies in APS1 18

1.3 Autoimmune polyendocrine syndrome type 1: diagnosis, epidemiology and clinical features 20

1.3.1 Diagnosis 20

1.3.2 Epidemiology 20

1.3.3 Clinical manifestations 20

1.3.3.1 Chronic mucocutaneous candidiasis 21

1.3.3.2 Hypoparathyroidism 25

1.3.3.3 Addison's disease 25

1.3.3.4 Hypothyroidism 26

1.3.3.5 Type 1 diabetes mellitus 26

1.3.3.6 Gonadal insufficiency 27

1.3.3.7 Hypopituitarism 27

1.3.3.8 Chronic atrophic gastritis 28

1.3.3.9 Intestinal dysfunction 28

1.3.3.10 Hepatitis 29

1.3.3.11 Alopecia areata 29

1.3.3.12 Vitiligo 30

1.3.3.13 Ocular abnormalities 30

1.3.3.14 Nail dystrophy 31

1.3.3.15 Dental enamel dysplasia 31

1.3.3.16 Lung disease 31

1.3.3.17 Kidney impairment 32

1.3.3.18 Asplenia 32

1.4 Hypoparathyroidism in APS1 33

1.4.1 Animal models of autoimmunity against the parathyroid 33

1.4.2 T cells in hypoparathyroidism 33

1.4.3 Anti-parathyroid autoantibodies 35
1.4.4 Autoantibodies against NACHT leucine-rich-repeat protein 5 35
1.4.5 Autoantibodies against the calcium-sensing receptor 36
1.4.6 The calcium-sensing receptor 41
1.4.6.1 Structure of the calcium-sensing receptor 41
1.4.6.2 Functioning of the CaSR in the parathyroid in response to Ca^{2+} 46

1.5 Project Aims 49

2 General Materials and Methods 51
2.1 Reagents 51
2.2 Plasticware 51
2.3 Bacterial growth medium 51
2.4 Bacterial strains 52
2.5 Plasmids 52
2.6 Small-scale plasmid preparations 55
2.7 Large-scale plasmid preparations 55
2.8 Agarose gel electrophoresis 56
2.9 Restriction enzyme digests 57
2.10 Polymerase chain reaction amplification 59
2.11 Extraction and purification of DNA fragments from agarose gels 61
2.12 DNA ligations 61
2.13 Bacterial transformation 61
2.14 TOPO® cloning reactions 62
2.15 DNA sequencing 63
2.16 DNA and protein analyses 63
2.17 Sodium dodecyl sulphate-polyacrylamide gel electrophoresis 65
2.18 Antibodies 66
2.19 Western blotting 66

3 Prevalence and Clinical Associations of Calcium-Sensing Receptor and NALP5 Autoantibodies in Finnish Patients with Autoimmune Polyendocrine Syndrome Type 1 71

3.1 Introduction 71

3.2 Aims 73

3.3 Materials and Methods 74
3.3.1 Patients and controls 74
3.3.2 *AIRE* gene genotyping 74
3.3.3 Cytokine enzyme-linked immunosorbent assays 74
3.3.4 Detection of CaSR antibodies 76
3.3.4.1 Culture and maintenance of HEK293 cells 76
3.3.4.2 Transfection of HEK293 cells 76
3.3.4.3 Preparation of cell extracts and protein determination 80
3.3.4.4 Detection of CaSR expression 80
3.3.4.5 CaSR immunopreciptation assays 81
3.3.5 Detection of NALP5 antibodies 84
3.3.5.1 *In vitro* translation of NALP5 cDNA 84
3.3.5.2 NALP5 radioligand binding assays 87
3.3.6 Statistical analyses 88

3.4 Results 90
3.4.1 Clinical characteristics of APS1 patients 90
3.4.2 *AIRE* genotypes of the APS1 patients 94
3.4.3 Detection of cytokine antibodies in APS1 patients and controls 96
3.4.4 Detection of CaSR antibodies in APS1 patients and controls 101
3.4.4.1 Expression of CaSR-FLAG in HEK293 cells 101

3.4.4.2 Results of CaSR immunoprecipitation assays 101
3.4.5 Detection of NALP5 antibodies in APS1 patients and controls 106
3.4.5.1 *In vitro* translation of NALP5 106
3.4.5.2 Results of NALP5 radioligand binding assays 106
3.4.6 Associations of CaSR and NALP5 antibodies with the clinical and demographic characteristics and *AIRE* genotypes of APS1 patients 111
3.5 Discussion 116
4 Mapping of autoantibody binding sites on the calcium-sensing receptor 122
4.1 Introduction 122
4.1.1 Antibody-antigen interactions 122
4.1.2 B cell epitope mapping techniques 122
4.1.3 Phage-display technology 123
4.1.4 Identification of antibody binding sites on the CaSR 127
4.2 Aim 134
4.3 Materials and Methods 135
4.3.1 Patient and control sera 135
4.3.2 CaSR peptide phage-display library 135
4.3.3 Enrichment of the CaSR peptide phage-display library (panning experiments) 136
4.3.4 Analysis of the panned phage-display library 137
4.3.5 CaSR peptide ELISAs 137
4.3.6 Statistical analyses 139
4.3.7 DNA and protein sequences analyses 139
4.3.8 Antigenicity predictions 139
4.3.9 *In silico* modelling of CaSR epitopes 139
4.4 Results 141
4.4.1 Analysis of the unpanned CaSR peptide phage-display library 141
4.4.2 Panning of the CaSR peptide phage-display library with APS1 patient and anti-CaSR antibody 141
4.4.3 Identification of CaSR peptides enriched by panning 144
4.4.4 CaSR peptide ELISAs with APS1 patient and control sera 147
4.4.5 Summary of CaSR epitope identification 152
4.4.6 Features of the identified CaSR epitopes 156
4.5 Discussion 161
5 Characterisation of the properties of CaSR autoantibodies in APS1 patients 167
5.1 Introduction 167
5.1.1 Antibody functional affinity (avidity) 167
5.1.2 IgG subclasses 168
5.1.3 Antibody functional effects 169
5.2 Aims 171
5.3 Materials and Methods 172
5.3.1 Patient and control sera 172
5.3.2 Antibody titrations 172
5.3.3 Absorption experiments 176
5.3.4 Functional affinity experiments 177
5.3.5 IgG subclass ELISAs 180
5.3.6 IgG preparation 180
5.3.7 Ca^{2+}-stimulation of the CaSR expressed in human embryonic kidney cells 181
5.3.8 Inositol-1-phosphate ELISAs 182
5.3.9 Effect of IgG on Ca^{2+}-stimulation of the CaSR 183

5.4 Results 186
5.4.1 Determination of APS1 patient CaSR antibody titres 186
5.4.2 Determination of APS1 patient CaSR antibody specificity 192
5.4.3 Determination of APS1 patient CaSR antibody functional affinity 197
5.4.4 Determination of APS1 patient CaSR antibody IgG subclass 203
5.4.5 Effect of APS1 patient IgG on the response of the CaSR to Ca^{2+}-stimulation 207
5.5 Results Summary 213
5.6 Discussion 216
6 Development of an ELISA for the Detection of CaSR Autoantibodies 220
6.1 Introduction 220
6.2 Aims 223
6.3 Strategy for expressing the CaSR extracellular domain 224
6.4 Experiments and Results 229
6.4.1 Preparation of pPROEX-HTb-CaSREx 229
6.4.2 Cloning of the CaSR extracellular domain for expression in *E. coli* 229
6.4.2.1 PCR amplification of the CaSR extracellular domain 229
6.4.2.2 TOPO® cloning of the CaSR-ECD cDNA PCR product 230
6.4.2.3 Sequencing of cloned CaSR-ECD cDNA fragment 236
6.4.2.4 Preparation of the CaSR-ECD cDNA fragment for cloning into pET14b 236
6.4.2.5 Preparation of vector pET14b 236
6.4.2.6 Cloning of CaSR-ECD cDNA fragment into pET14b 237
6.4.2.7 Sequencing of the CaSR-ECD cDNA fragment cloned in pET14b 240
6.4.3 Expression of the CaSR-ECD in *E. coli* BL21 strains 240
6.4.3.1 Transformation of *E. coli* BL21 strains with pET14b-CaSR-ECD, pET14b, and pPROEX-HTb-CaSREX 240
6.4.3.2 Small-scale expression of the CaSR-ECD in *E. coli* BL21 strains 242
6.4.3.3 Western blotting of uninduced and induced *E. coli* BL21/pET14b-CaSR-ECD cell extracts 243
6.4.4 Purification of the His-tagged CaSR-ECD 248
6.4.4.1 Large-scale expression of the His-tagged CaSR-ECD 248
6.4.4.2 Solubility of the His-tagged CaSR-ECD 248
6.4.4.3 Purification and solubilisation of inclusion bodies containing the His-tagged CaSR-ECD 251
6.4.4.4 Purification of His-tagged CaSR-ECD by Ni^{2+}-chelation chromatography .. 253
6.4.4.5 Purification of His-tagged CaSR-ECD using gel-filtration chromatography 254
6.4.5 Use of the purified CaSR-ECD in an ELISA format 259
6.4.5.1 Assay procedure 259
6.4.5.2 Assay of APS1 patient sera in the CaSR-ECD ELISA 260
6.4.5.3 Analysis of the results of the CaSR-ECD ELISA 260
6.5 Discussion 263
7 General Discussion 266
References 271

List of Figures

Figure 1.1: Schematic representation of the human AIRE protein. 5
Figure 1.2: AIRE interaction with transcriptional partners 6
Figure 1.3: AIRE function in promoting central and peripheral tolerance 8
Figure 1.4: Current and alternative model of AIRE deficiency 13
Figure 1.5: Immunohistochemistry staining of the hair follicles from an APS1 patient. 14
Figure 1.6: Schematic picture of the possible role for AIRE in interferon-γ receptor signaling. 17
Figure 1.7: Clinical manifestations of APS1. 24
Figure 1.8: Infiltration of the parathyroid with lymphocytes. 34
Figure 1.9: Schematic representation of the calcium-sensing receptor 43
Figure 1.10: A model of the dimeric form of the extracellular CaSR. 44
Figure 1.11: Ca^{2+} binding sites on the CaSR. 45
Figure 1.12: Functioning of the calcium-sensing receptor in the parathyroid in response to Ca^{2+}. 47
Figure 1.13: Schematic view of Ca2+ homeostasis controlled by parathyroid hormone. 48
Figure 2.1: Assembly of blotting sandwich in submerged transfer apparatus. 69
Figure 3.1: Details of plasmid pcCaSR-FLAG. 78
Figure 3.2: Details of plasmid pcDNA3-CaSR. 79
Figure 3.3: Schematic representation of the CaSR immunoprecipitation assay. 83
Figure 3.4: Details of plasmid pCMV6-XL5-NALP5. 86
Figure 3.5: Schematic diagram of the NALP5 radioligand binding assay. 89
Figure 3.6: Summary of disease components in APS1 patients. 93
Figure 3.7: *AIRE* genotypes of APS1 patients. 95
Figure 3.8: Interleukin (IL)-22, IL-17F and IL-17A antibody indices of APS1 patient and control sera. 97
Figure 3.9: Interferon (IFN)-omega, IFN-alpha2A and IFN-lambda1 antibody indices of APS1 patient and control sera. 98
Figure 3.10: Western blot of detection of CaSR and CaSR-FLAG proteins in HEK293 cell extracts 103
Figure 3.11: CaSR antibody indices of APS1 patient and control sera. 104
Figure 3.12: Western blot for detection of CaSR-FLAG protein following immunoprecipitation with APS1 patient and control sera. 105
Figure 3.13: SDS-PAGE and autoradiography of [^{35}S]-NALP5. 108
Figure 3.14: NALP5 antibody indices of APS1 patient and control sera. 109
Figure 3.15: SDS-PAGE and autoradiography of immunoprecipitated [^{35}S]-NALP5 following NALP5 radioligand binding assays with APS1 patient and control sera. 110
Figure 3.16: Correlation of CaSR antibody index with APS1 disease duration. 115
Figure 4.1: Schematic representation of a filamentous phage particle 125
Figure 4.2: The pComb3 phage-display system. 129
Figure 4.3: Enrichment of phage displaying IgG binding CaSR peptides on their surface. 130
Figure 4.4: Position of previously identified CaSR epitopes. 133
Figure 4.5: Panning experiments of the CaSR peptide phage-display library with APS1 patient sera and anti-CaSR antibody ab79829. 143
Figure 4.6: Antibody indices of APS1 patient and control sera in CaSR peptide ELISAs 149
Figure 4.7: Position of identified epitopes on the linear sequence of the CaSR extracellular domain. 157
Figure 4.8: 3D representation of the CaSR extracellular domain showing antibody binding sites. 158
Figure 4.9: Antigenicity predictions within the CaSR extracellular domain. 159
Figure 5.1: Schematic representation of the activation of the CaSR and accumulation of inositol-1-phosphate. 184
Figure 5.2: Schematic representation of the IP-One ELISA. 185

Figure 5.3: Titration of APS1 patient CaSR antibodies against CaSR 41-69 peptide. 187
Figure 5.4: Titration of APS1 patient CaSR antibodies against the CaSR 114-126 peptide. 188
Figure 5.5: Titration of APS1 patient CaSR antibodies against the CaSR 171-195 peptide. 189
Figure 5.6: Titration of APS1 patient CaSR antibodies against the CaSR 260-340 peptide. 190
Figure 5.7: Absorption of APS1 patient CaSR antibodies with CaSR peptides prior to analysis in CaSR peptide 41-69 ELISA. 193
Figure 5.8: Absorption of APS1 patient CaSR antibodies with CaSR peptides prior to analysis in CaSR peptide 114-126 ELISA. 194
Figure 5.9: Absorption of APS1 patient CaSR antibodies with CaSR peptides prior to analysis in CaSR peptide 171-195 ELISA. 195
Figure 5.10: Absorption of APS1 patient CaSR antibodies with CaSR peptides prior to analysis in CaSR peptide 260-340 ELISA. 196
Figure 5.11: Functional affinity of APS1 patient CaSR antibodies against CaSR peptide 41-69. 198
Figure 5.12: Functional affinity of APS1 patient CaSR antibodies against CaSR peptide114-126. 199
Figure 5.13: Functional affinity of APS1 patient CaSR antibodies against CaSR peptide 171-195. 200
Figure 5.14: Functional affinity of APS1 patient CaSR antibodies against CaSR peptide 260-340. 201
Figure 5.15: IgG subclass of APS1 patient CaSR antibodies against CaSR peptides 204
Figure 5.16: Measuring the effect of Ca^{2+}-stimulation on the CaSR. 208
Figure 5.17: Effect of APS1 patient and control IgG on the response of the CaSR to Ca^{2+}-stimulation-1. 209
Figure 5.18: Effect of APS1 patient and control IgG on the response of the CaSR to Ca^{2+}-stimulation-2. 210
Figure 5.19: Effect of APS1 patient and control IgG on the response of the CaSR to Ca^{2+}-stimulation-3. 211
Figure 5.20: Effect of APS1 patient and control IgG on the response of the CaSR to Ca^{2+}-stimulation-4. 212
Figure 6.1: Plasmid vector pET14b. 226
Figure 6.2: Expression of target genes in the pET14b expression system. 227
Figure 6.3: Details of plasmid pPROEX-HTb-CaSREx. 228
Figure 6.4: A map of the pDEST14-CaSR plasmid. 231
Figure 6.5: Agarose gel of PCR amplification product amplified from pDEST14-CaSR. 232
Figure 6.6: Plasmid vector pCR®2.1-TOPO®. 233
Figure 6.7: Agarose gel of plasmids prepared from *E. coli* TOP10F' clones. 234
Figure 6.8: Schematic diagram of plasmid pCR®2.1-TOPO®-CaSR-ECD. 235
Figure 6.9: Agarose gel of PCR amplification products arising from the screening of *E. coli* JM109 clones isolated from the pET14b/CaSR-ECD cDNA cloning experiment. 238
Figure 6.10: Agarose gel of recombinant plasmids from the pET14b/CaSR-ECD cDNA cloning experiment. 239
Figure 6.11: Schematic diagram of plasmid pET14b-CaSR-ECD. 241
Figure 6.12: SDS-PAGE and Coomassie blue staining of gels containing cell extracts of *E. coli* BL21 (DE3)/pET14b-CaSR-ECD and *E. coli* BL21 (DE3)/pET14b strains 244
Figure 6.13: SDS-PAGE and Coomassie blue staining of gels containing cell extracts of *E. coli* BL21/pET14b-CaSR-ECD strains. 245
Figure 6.14: Western blotting of cell extracts of *E. coli* BL21 CODONPLUS (DE3)-RIPL/pET14b-CaSR-ECD. 247
Figure 6.15: Solubility of the His-tagged CaSR-ECD. 250
Figure 6.16: SDS-PAGE analysis of the preparation of inclusion bodies of the His-tagged CaSR-ECD. 252
Figure 6.17: The elution of protein by gel-filtration chromatography. 257

Figure 6.18: Western blotting of fractions eluted from the gel-filtration column during the purification of His-tagged CaSR-ECD expressed in *E. coli* BL21 CODONPLUS (DE3)-RIPL/pPROEX-HTb-CaSREx. 258
Figure 6.19: CaSR antibody indices of APS1 patient and control sera. 262

List of Tables

Table 1.1: Examples of *AIRE* mutations identified in APS1 patients 10
Table 1.2: Examples of autoantibody targets in APS1 16
Table 1.3: Prevalence of autoantibodies against cytokines in APS1 patients 19
Table 1.4: Clinical manifestations in APS1 patients 23
Table1.5: Prevalence of CaSR autoantibodies in idiopathic and APS1-associated hypoparathyroidism 40
Table 2.1: Bacterial strains 53
Table 2.2: Plasmid vectors and recombinant plasmids 54
Table 2.3: Restriction enzymes and buffers 58
Table 2.4: Oligonucleotide PCR amplification primers 60
Table 2.5: Oligonucleotide sequencing primers 64
Table 2.6 : Antibodies 68
Table 3.1: APS1 patient demographic and clinical characteristics and *AIRE* genotypes 91
Table 3.2: Summarised results of cytokine ELISAs 99
Table 3.3: Summary of APS1 patient antibody reactivities 100
Table 3.4: Prevalence of CaSR and NALP5 antibodies in APS1 patients with and without disease components 113
Table 3.5: Comparison of demographic and clinical characteristics of APS1 patients with and without CaSR or NALP5 antibodies 114
Table 4.1: Methods used for identifying B cell epitopes 124
Table 4.2: Identification of B cell epitopes using phage-display technology 126
Table 4.3: Previously reported CaSR antibody binding sites on the CaSR 131
Table 4.4: CaSR peptides used in ELISAs 132
Table 4.5: Amino acid sequences of translated CaSR cDNA fragments contained in the unpanned CaSR peptide phage-display library 142
Table 4.6: CaSR peptide sequences displayed on the surface of phage enriched by panning of the CaSR peptide phage-display library with anti-CaSR antibody ab79829 145
Table 4.7: CaSR peptide consensus sequences from panning experiments with APS1 patient sera 146
Table 4.8: Summary of data from CaSR peptide ELISAs 150
Table 4.9: Antibody indices of APS1 patient sera in CaSR peptide ELISAs 151
Table 4.10: CaSR epitope domains identified by phage display and/or CaSR peptide ELISA 153
Table 4.11: Summary of epitopes recognised by CaSR antibodies in APS1 patients 154
Table 4.12: Summary of APS1 patient details and CaSR epitopes 155
Table 4.13: Comparison of predicted antigenic peptides on the CaSR extracellular domain to the CaSR epitopes determined experimentally 160
Table 5.1: Properties of IgG subclasses 170
Table 5.2: Summary of APS1 patients analysed 174
Table 5.3: CaSR peptides used in ELISAs 175
Table 5.4: Non-saturating dilutions of APS1 patient sera used in absorption and functional affinity experiments 178
Table 5.5: Details of peptides used in absorption and functional affinity experiments 179
Table 5.6: Summary of titration of APS1 patient autoantibodies against CaSR epitopes 191
Table 5.7: Functional affinity of APS1 patient CaSR antibodies 202
Table 5.8: Summary of data from CaSR peptide IgG subclass ELISAs 205
Table 5.9: IgG subclasses of APS1 patient CaSR antibodies 206
Table 5.10: Summary of APS1 patient CaSR antibody titres, specificity, functional affinity, and IgG subclass-1 214
Table 5.11: Summary of APS1 patient CaSR antibody titres, specificity, functional affinity, and IgG subclass-2 215
Table 6.1: Summary of CaSR antibody detection methods 222

List of Abbreviations

AIRE	Autoimmune regulator gene
AIRE	Autoimmune regulator protein
APECED	Autoimmune polyendocrinopathy candidiasis ectodermal dystrophy
APS1	Autoimmune polyendocrine syndrome type 1
APS2	Autoimmune polyendocrine syndrome type 2
BAFF	B cell-activating factor
BPIFB1	Lung-specific protein bactericidal/permeability-increasing fold-containing B1
CARD	Caspase-recruitment domain
CaSR	Calcium-sensing receptor
cfu	Colony-forming units
cpm	Counts per min
DCs	Dendritic cells
ECD	Extracellular domain
EDTA	Ethylenediaminetetraacetic acid
ELISA	Enzyme-linked immunosorbent assay
EBI-EMBL	European Bioinformatics Institute-European Molecular Biology Laboratory
HEK293	Human embryonic kidney 293
FcγR	Fc receptors
HLA	Human leukocyte antigens
HRP	Horse-radish peroxidase
IFN	Interferon
IgG	Immunoglobulin G
IL	Interleukin
IP1	Inositol-1-phosphate
IP3	Inositol 1,4,5-trisphosphate
IPTG	Isopropyl β-D-1-thiogalactopyranoside
LB	Luria Bertani
MAP	Mitogen-activated protein
MCHR1	Melanin-concentrating hormone receptor 1
MHC	Major histocompatibility complex
MOPS	3-[N-morpholino]propanesulphonic acid
mTEC	Medullary thymic epithelial cells
NALP5	NACHT leucine-rich-repeat protein 5
NCIB	National Center for Biotehnology Information
PBS	Phosphate-buffered saline
PCR	Polymerase chain reaction
Phyre	Protein Homology/Analogy Recognition Engine
PRR	Proline-rich region
PTH	Parathyroid hormone
PVDF	Polyvinylidene difluoride
RLBAs	Radioligand binding assays
rpm	Revolutions per minute
SDS	Sodium dodecyl sulphate
SDS-PAGE	Sodium dodecyl sulphate-polyacrylamide gel electrophoresis
TEMED	N, N, N, N'-tetramethylethylenediamine
Th17	T helper type 17
Tregs	Regulatory T cells

List of Permissions

The following copyrighted material was used with permission from:

1. John Wiley & Sons Ltd., The Atrium, Southern Gate, Chichester, West Sussex, PO19 8SQ, UK.

Chapter 1 - Figure 1.1, Figure 1.2, Figure 1.3, Figure 1.4 and Figure 1.9

Chapter 4 - Figure 4.2

2. The Endocrine Society, 2055 L Street NW, Suite 600, Washington, DC 20036, USA.

Chapter 1 - Figure 1.1

Chapter 3 - Figure 3.12 Figure 3.15, Table 3.4, Table 3.5

3. Springer Science and Business Media, Van Godewijckstraat 30, P.O. Box 17, 3300 AA Dordrecht, The Netherlands.

Chapter 1 - Figure 1.2, Figure 1.8

4. Nature Publishing Group, 25 First Street, Suite 104, Cambridge, MA 02141, USA.

Chapter 1 - Figure 1.10

Chapter 4 - Figure 4.3

5. NRC Research Press, 65 Auriga Drive, Suite 203, Ottawa, ON K2E 7W6, Canada.

Chapter 4 - Figure 4.1

6. © EMD Millipore Corporation.

Chapter 6 - Figure 6.2

List of Publications

Original paper

Kemp EH, Habibullah M, Kluger N, Ranki A, Sandhu HK, Krohn KJ, Weetman AP. Prevalence and clinical associations of calcium-sensing receptor and NALP5 autoantibodies in Finnish APECED patients. J Clin Endocrinol Metab 2014;99:1064-1071.

Conference Presentations

Habibullah M, Sandhu HK, Krohn KJE, Weetman AP, Kemp EH (2013). An investigation of associations of calcium-sensing receptor autoantibodies with clinical manifestations and other autoantibody specificities in patients with autoimmune polyendocrine syndrome type 1. Yorkshire Immunology Group Symposium, Sheffield, UK.

Habibullah M, Kluger N, Ranki A, Sandhu HK, Krohn KJE, Weetman AP, Kemp EH (2014). Prevalence and clinical associations of calcium-sensing receptor autoantibodies in Finnish APECED patients. Society for Endocrinology BES Meeting, Liverpool, UK. Endocrine Abstracts 2014; 34:P382. Featured Poster Presentation.

Habibullah M, Kluger N, Ranki A, Krohn KJE, Weetman AP, Kemp EH (2015). Epitopes, specificity, functional effects and immunoglobulin G subclasses of calcium-sensing receptor autoantibodies in patients with autoimmune polyendocrine syndrome type 1. The Endocrine Society's 97th Annual Meeting and Expo (ENDO 2015), San Diego, CA, USA. Endocrine Reviews 2015; 36:OR29-2. Oral Presentation. Outstanding Abstract Award.

Habibullah M, Kluger N, Ranki A, Krohn KJE, Weetman AP, Kemp EH (2015). Prevalence and clinical associations of calcium-sensing receptor and NALP5 autoantibodies in Finnish patients with autoimmune polyendocrine syndrome type 1. Annual Meeting of the Association of Physicians of Great Britain and Ireland, Sheffield, UK.

Habibullah M, Kluger N, Ranki A, Krohn KJE, Weetman AP, Kemp EH (2015). Prevalence and clinical associations of calcium-sensing receptor and NALP5 autoantibodies in patients with autoimmune polyendocrine syndrome type 1. European Congress of

Endocrinology, Dublin, Ireland. Endocrine Abstracts 2015; 37:GP.28.08. Guided Poster Presentation.

Habibullah M, Kluger N, Ranki A, Krohn KJE, Weetman AP, Kemp EH (2015). Epitopes, specificity, functional effects and immunoglobulin G subclasses of anti-calcium-sensing receptor autoantibodies in patients with autoimmune polyendocrine syndrome type 1. Society for Endocrinology BES Meeting, Edinburgh, UK. Endocrine Abstracts 2015; 38:P436.

Chapter 1

Review of the Literature

1 Review of the Literature

1.1 Autoimmune polyendocrine syndromes

Autoimmune polyendocrine syndromes are a group of diseases caused by autoimmune activity against body organs (Kahaly, 2009). Usually, these disorders are characterised by at least two endocrine disease components, but affected individuals may also have non-endocrine manifestations (Kahaly, 2009, Cutolo, 2014). Patients have a lymphocytic infiltrate in their affected glands and organ-specific autoantibodies in their serum (Kisand and Peterson, 2011, Kahaly, 2012). Autoimmune polyendocrine syndromes have been classified into four main types (Kahaly, 2012, Cutolo, 2014).

Autoimmune polyendocrine syndrome type 1 (APS1) is a rare disease due to mutations in the autoimmune regulator (*AIRE*) gene which impair the development of immune tolerance leading to autoimmunity (Nagamine et al., 1997). The disease is also called autoimmune polyendocrinopathy candidiasis ectodermal dystrophy (APECED). Onset of APS1 usually occurs during childhood (Perheentupa, 2006), and, clinically, the disease is characterised by at least two of the following manifestation; chronic mucocutaneous candidiasis, hypoparathyroidism, and Addison's disease (Perheentupa, 2006). Other diseases can be present including hypothyroidism, vitiligo, alopecia areata and type 1 diabetes mellitus (Perheentupa, 2006). As patients with this syndrome are analysed in this thesis, the disease will be discussed in more detail in **Section 1.2**.

Autoimmune polyendocrine syndrome type 2 (APS2) or Schmidt's syndrome is the commonest autoimmune polyendocrine syndrome with a prevalence of 1:20,000 (Kahaly, 2012). There is a higher prevalence in women, and the disease usually presents in adulthood, although children can be affected (Kahaly, 2012, Betterle et al., 2002). It is characterised by the presence of Addison's disease, which is the main component, thyroid autoimmunity (Graves' disease or hypothyroidism), and/or type 1 diabetes mellitus (Neufeld et al., 1981, Kahaly, 2012, Cutolo, 2014). In addition, APS2 can involve non-endocrine conditions such as myasthenia gravis, celiac disease, vitiligo, stiff-man syndrome, alopecia areata, and pernicious anaemia (Kahaly, 2012, Cutolo, 2014). In common with many autoimmune diseases, the primary genetic association of

APS2 is with alleles of class II human leukocyte antigens (HLA), notably with haplotypes DR3/DQ2 and DR4/DQ8 (Kahaly, 2012, Cutolo, 2014).

Autoimmune polyendocrine syndrome type 3 is defined by the presence of autoimmune thyroid disease and autoimmune disorders other than Addison's disease and hypoparathyroidism (Kahaly, 2012). Type 4 APS is defined by a combination of autoimmune endocrine disorders that does not fulfil the markers of the other three types (Cutolo, 2014). Other diseases outside of this autoimmune polyendocrine syndrome classification, but which nevertheless include polyendocrinopathy, are immune dysfunction polyendocrinopathy X-linked (IPEX), POEMS (polyneuropathy, organomegaly, endocrinopathy, M-protein, skin changes) disease, and Kearns–Sayre syndrome (Cutolo, 2014).

1.2 Autoimmune polyendocrine syndrome type 1: aetiology and pathogenesis

1.2.1 The *AIRE* gene and AIRE protein

Autoimmune polyendocrine syndrome type 1 arises from mutations in the autoimmune regulator (*AIRE*) gene which are deleterious to the functioning of the autoimmune regulator (AIRE) protein (Nagamine et al., 1997). The *AIRE* gene is located on chromosome 21 at position q22.3. The gene is 13-kilobase, is composed of 14 exons (Nagamine et al., 1997), and encodes the 58-kDa AIRE transcription factor which is composed of 545 amino acids (Peterson et al., 2008). The AIRE protein is composed of several domains (**Figure 1.1**) including a central putative DNA-binding domain called the SAND (Sp100, AIRE1, Nuc P41/75, DEAF1) domain, a proline-rich region (PRR) which is suggested to be involved in transcription, a caspase-recruitment domain (CARD) which is a six-helix structure located at the N-terminal and is required for AIRE oligomerisation, and two plant homeodomains PHD1 and PHD2 which take part in protein-protein and protein-DNA interactions (Peterson et al., 2008). At the N-terminal, there is a nuclear localisation signal, and the C-terminal is also required for activation of the transcription process.

In the cell, the AIRE protein is located in nuclear bodies, which are the sites of chromatin-associated, transcriptionally active proteins (Bjorses et al., 2000, Gaetani et al., 2012). Moreover, recent studies have shown that AIRE promotes transcription

'non-classically' through interacting with chromatin in complexes with the transcriptional regulator CREB-binding protein, the positive transcription-elongation factor b, RNA polymerase II, DNA-dependent protein kinase, and topoisomerase 2 (**Figure 1.2**) (Pitkanen et al., 2005, Abramson et al., 2010, Gaetani et al., 2012).

1.2.2 AIRE function in promoting central and peripheral tolerance

Mainly, the *AIRE* gene is expressed in medullary thymic epithelial cells (mTEC) where the AIRE transcription factor promotes the expression of tissue-specific antigens (Heino et al., 1999, Peterson et al., 2008). Via major histocompatibility complex (MHC) class II antigens, mTECs then present tissue-restricted antigens to developing thymocytes (precursor immune cells) causing their apoptosis so that potentially autoreactive T cells are eliminated by negative selection enabling self-tolerance to be established (Anderson et al., 2002, Liston et al., 2003) (**Figure 1.2 and 1.3**). In addition to its role in affecting negative selection, there is now evidence that AIRE-driven expression of tissue-specific antigens also supports the generation of naturally occurring regulatory T cells (Tregs) (Malchow et al., 2013, Yang et al., 2015). The action of the AIRE transcription factor has also been shown to be required for the maturation of mTECs (Matsumoto, 2011, Wang et al., 2012), and for the regulation of intra-thymic chemokines that are needed for the correct localisation of thymocytes and dendritic cells (DCs) so that proper antigen presentation in the thymus is ensured (Kurobe et al., 2006, Lei et al., 2011). Although several of these proposed functions require more detailed study, ultimately, they may all contribute to the development of central tolerance.

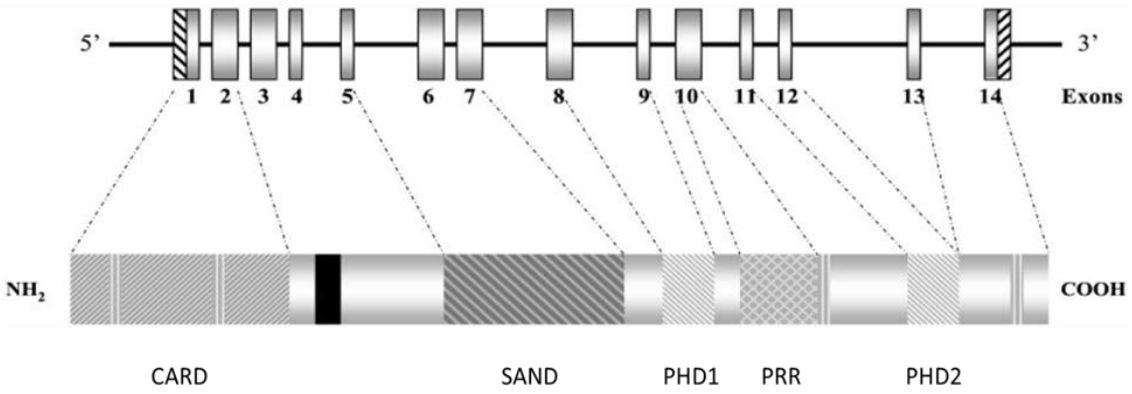

Figure 1.1: Schematic representation of the human AIRE protein.

The AIRE protein is composed of several domains including a central putative DNA-binding domain called the SAND (Sp100, AIRE1, Nuc P41/75, DEAF1) domain, a proline-rich region (PRR) which is suggested to be involved in transcription, a caspase-recruitment domain (CARD) which is a six-helix structure located at the N-terminal and is required for AIRE oligomerisation, and two plant homeodomains PHD1 and PHD2 which take part in protein-protein and protein-DNA interactions. The image, from a paper (Meloni et al., 2002), was used with kind permission from Endocrine Society.

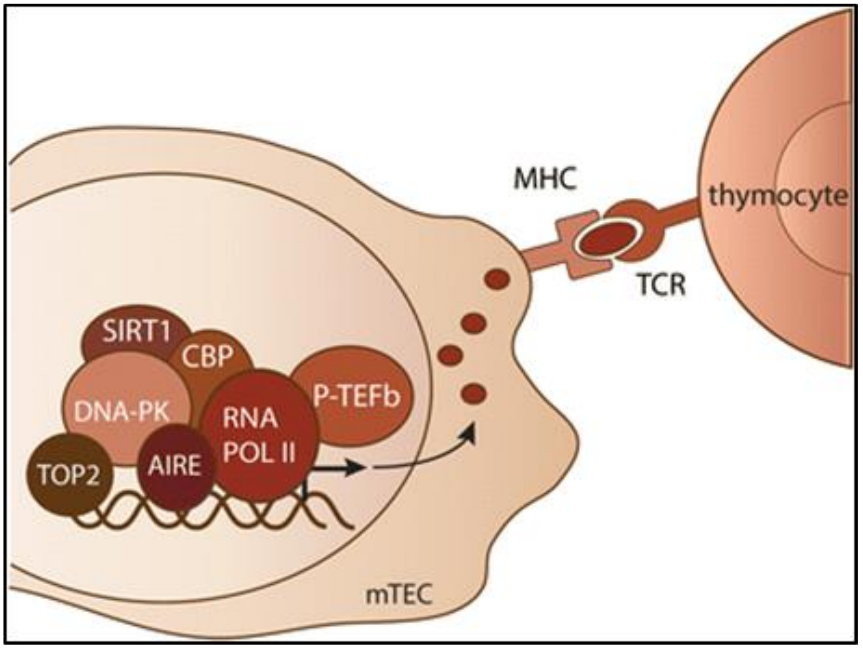

Figure 1.2: AIRE interaction with transcriptional partners

In medullary thymic epithelial cells (mTEC), AIRE transcription factor drives expression of tissue-specific antigens through interaction with chromatin in complexes with DNA-dependent protein kinase (DNA-PK), topoisomerase 2 (TOP2), positive transcription elongation factor (P-TEFb), CREB-binding protein (CBP) and Sirtuin 1 (SIRT1). The expressed antigens are processed within the cell and presented by major histocompatibility complex (MHC) antigens to developing thymocytes. Those thymocytes which express T cell receptors (TCR) with high affinity towards self-peptides are deleted or are selected for development as regulatory T cells. The image, from a paper by (Kisand and Peterson, 2015), was used with kind permission from Springer.

The role of AIRE in establishing central tolerance has been well-studied. Nevertheless, central tolerance alone does not remove entirely mature T cells which have the potential to react against self-antigens. Peripheral mechanisms are therefore required to ensure immune responses against tissues are negated. However, AIRE's possible function in peripheral tolerance, which includes mechanisms such as the induction of functional energy in autoreactive T lymphocytes, the deletion of self-reactive T cells through apoptosis, and the suppressive action of Tregs, is not as well-defined (Metzger and Anderson, 2011). There is evidence that extra-thymic AIRE-expressing cells present in secondary lymphoid tissue (Poliani et al., 2010) have the capacity to present peripheral tissue antigens to autoreactive T cells ultimately causing their deletion (**Figure 1.3**) (Gardner et al., 2008). Interestingly, the self-antigens were different from those presented in the thymus (Eldershaw et al., 2011). In mice, Aire protein has been detected in the spleen and lymph nodes (Adamson et al., 2004).

1.2.3 *AIRE* gene mutations in APS1

In 1997, mutations in the *AIRE* gene were first identified as the cause of APS1 (Nagamine et al., 1997). Since then, over 100 *AIRE* mutations have been found (**Table 1.1**) (Heino et al., 2001, Michels and Eisenbarth, 2009, Kisand and Peterson, 2011). Examples include the common 967-979del13bp and R257X mutations (**Table 1.1**) which are present in more than 95% of APS1 patients (Nagamine et al., 1997). Particularly, R257X is present in 83% of patients of Finnish origin (Nagamine et al., 1997). Among Sardinians (Rosatelli et al., 1998) and Iranian Jews (Zlotogora and Shapiro, 1992), the R139X and Y85C mutations (**Table 1.1**), respectively, are more common.

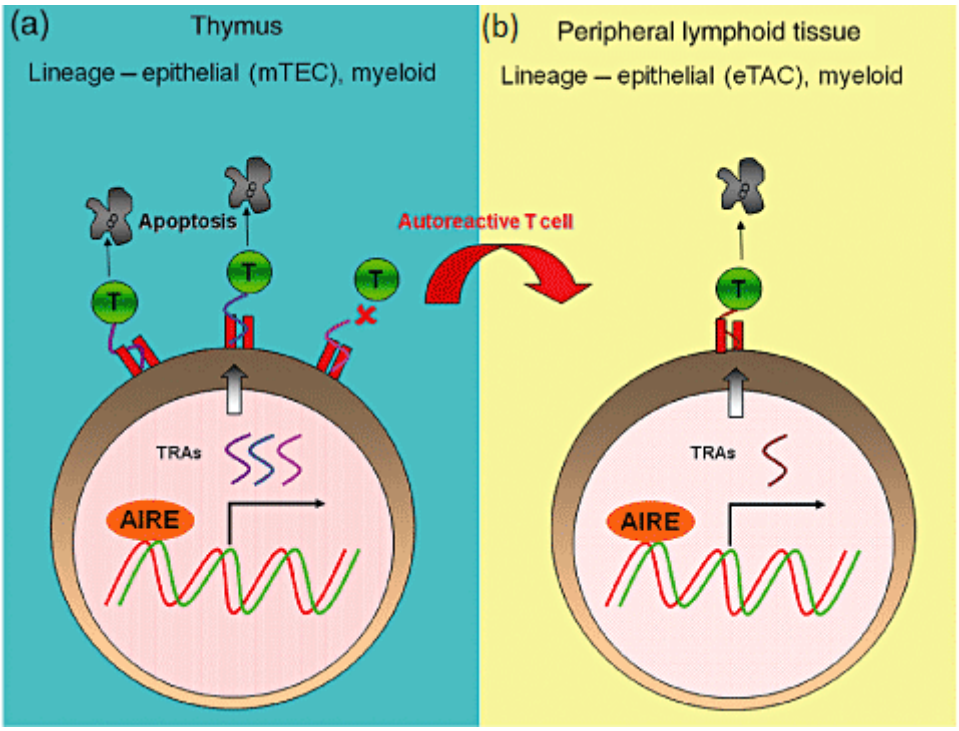

Figure 1.3: AIRE function in promoting central and peripheral tolerance

(a) Tissue-specific antigens are expressed by medullary thymic epithelial cells (mTECs) and myeloid cells under the control of AIRE. T cells which recognise these tissue-specific antigens with high affinity are eliminated by apoptosis. AIRE-driven expression of tissue-specific antigens also supports the generation of naturally occurring regulatory T cells in the thymus. **(b)** Any self-reactive T cells that do not interact with their cognate antigen and escape to the periphery are eliminated following exposure to tissue-specific antigens displayed in the peripheral lymphoid tissue by extra-thymic AIRE-expressing cells (eTAC). In the periphery, the suppressive action of regulatory T cells can also help in the establishment of self-tolerance. AIRE expressed in the periphery may control the expression of different tissue-specific antigens to those under AIRE control in the thymus. The image, from a paper by (Eldershaw et al., 2011), was used with kind permission from John Wiley and Sons.

The mutations are distributed throughout the coding region of *AIRE*, and they are either nonsense or frame-shift mutations that result in deletion of part of the protein, or are missense mutations that result in a single amino acid change (Peterson and Peltonen, 2005). For example, Y85C is a missense mutation located in the CARD domain (**Figure 1.1**) which disrupts AIRE multimerisation or localisation to nuclear bodies (Ferguson et al., 2008). The G228W mutation (**Table 1.1**) is found within the SAND domain (**Figure 1.1**) and impedes AIRE localisation to nuclear bodies and severely affects the transcriptional activity of the AIRE protein (Ilmarinen et al., 2005). Several mutations such as the 967-979del13bp deletion (**Table 1.1**) occur in the PHD domains (**Figure 1.1**), and so reduce AIRE's transcriptional functionality (Chignola et al., 2009).

The majority of *AIRE* mutations such as the R257X and 967-979del13bp are homozygous recessive, although they can occur as compound heterozygotes resulting in APS1 (Cervato et al., 2009). The G228W variant has been reported as a dominant mutation (Ilmarinen et al., 2005). In a recent study, the C311Y mutation (**Table 1.1**) was identified in AIRE's PHD1 domain (**Figure 1.1**) and was shown to be heterozygous dominant (Oftedal et al., 2015). The APS1 phenotypes of these patients were typically characterised by a later onset of autoimmune disorders and milder disease manifestations (Oftedal et al., 2015). Chronic *Candida* infection appears to be most prevalent in patients with the nonsense genotypes R257X or R139X, with 100% of individuals affected (Kisand et al., 2011, Kisand et al., 2010). This disease component occurs with less prevalence in APS1 patients with the 967-979del13bp mutation, and in those with *AIRE* missense genotypes such as Y85C (Kisand et al., 2011, Kisand et al., 2010, Zlotogora and Shapiro, 1992). Otherwise, there are no significant correlations with particular *AIRE* mutations and many of the clinical phenotypes (**Section1.3.3**) of APS1 patients (Halonen et al., 2002).

Table 1.1: Examples of *AIRE* mutations identified in APS1 patients

Mutation	Exon	Effect on coding sequence	Population	References
30-52dup23bp	E1	R15fsX19	Hungarian, Austrian	(Cihakova et al., 2001)
47C>T	E1	T16M	Russian	(Cihakova et al., 2001)
191-226del36bp	E2	del64-75 and D76Y	American, Caucasian	(Nagamine et al., 1997)
254A>G	E2	Y85C	Iranian Jewish	(Zlotogora and Shapiro, 1992)
415C>T	E3	R139X	Sardinian	(Rosatelli et al., 1998)
508^509ins13bp	E4	A170fsX219	German	(Nagamine et al., 1997)
607C>T	E5	R203X	Italian	(Scott et al., 1998)
769C>T	E6	R257X	Italian, Finnish	(Nagamine et al., 1997)
809G>T	E6	G228W	Italian	(Cetani et al., 2001)
969^970insCCTG	E8	L323fsX372	Italian	(Rosatelli et al., 1998, Bjorses et al., 2000)
967-979del13bp	E8	C322fsX372	Finnish, British, Dutch, German, Canadian, Swedish	(Nagamine et al., 1997, Rosatelli et al., 1998)
923G>A	E8	C311Y	Finnish	(Bjorses et al., 2000, Oftedal et al., 2015)
1072C>T	E9	Q358X	Italian	(Meloni et al., 2002)
Ains1283–1284	E10	P422fsX	Finnish	(Bjorses et al., 2000)
C1309del	E10	P436fsX478	French	(Bjorses et al., 2000)
1296delGinsAC	E11	R433fsX502	American Caucasian	(Heino et al., 1999)
1344delCinsTT	E11	C449fsX502	Japanese	(Heino et al., 2001)
1638A>T	E14	X564C+59aa	Finnish	(Bjorses et al., 2000)

1.2.4 Models of pathogenesis in APS1

Given AIRE's role in promoting central tolerance (**Section 1.2.2**), there has been much research into the exact mechanism by which *AIRE* mutations result in APS1. The simplest model of APS1 pathogenesis, which has been suggested from the study of *AIRE* knock-out mice (Anderson et al., 2002, Ramsey et al., 2002, Jiang et al., 2005, Niki et al., 2006), is one of deficient negative selection in the thymus due to the inability of mutant AIRE transcription factor to promote tissue-specific antigen expression (**Figure 1.4a**) (Kisand and Peterson, 2011). Consequently, naive autoreactive T cells are allowed to escape to the periphery where T helper cells become activated on antigen recognition producing pro-inflammatory cytokines and promoting the activation of autoreactive B lymphocytes (Devoss et al., 2008). These actions result in organ destruction, autoantibody production and, ultimately, the autoimmune diseases which are seen in APS1 (**Sections 1.3.3**).

Although it is highly likely that the first model has a part to play in APS1 development, in humans, this model does not explain the existence of autoantibodies against type I interferons and T helper 17 cell-related cytokines (**Section 1.2.6**) (Meager et al., 2006) which can predate the onset of any clinical symptoms and the appearance of tissue-specific autoantibodies. AIRE does not regulate the expression of these cytokines in the thymus, so it is difficult to see how the loss of antigen expression alone can account for this particular immune response. There are also findings that naïve CD8+ T lymphocytes are pre-activated in the thymus of APS1 patients (Laakso et al., 2011). These observations have led to the suggestion that in the AIRE-deficient thymus of APS1 patients, in addition to defective negative selection, the development of tertiary lymphoid tissue occurs, where pre-activated autoreactive T cells, and B cells that produce cytokine-targeting autoantibodies, are generated and exported (**Figure 1.4b**) (Kisand and Peterson, 2011). However, the mechanisms that are involved in such a process have yet to be defined.

Whatever the exact mechanism of dysregulation in the thymus in APS1, the autoimmune diseases found in the syndrome are thought to result from T cell-mediated damage of the specific organs. This has been supported by the examination of available tissue samples from various endocrine glands which show lymphocytic infiltration (Betterle and Zanchetta, 2003). In a study of an ASP1 patient with alopecia,

in addition to other diseases, a biopsy of the affected scalp showed a significant infiltration of T cells in the hair follicles (**Figure 1.5**) (Faiyaz-Ul-Haque et al., 2009).

A number of studies have examined different T cell subsets within APS1 patients. There are alterations in the CD4+ T lymphocyte population of APS1 patients with an increased frequency of activated cells being reported in one study (Perniola et al., 2005). However, this observation does conflict with other reports which indicate normal CD4+ T cell numbers (Wolff et al., 2010). Notably, the analysis of T helper 17 cell subsets has shown a diminution of them, and thus a concomitant reduction in the expression of the protective cytokines interleukin (IL)-22 and IL-17 (Wolff et al., 2010, Laakso et al., 2014). Likewise, there is an increased frequency of highly differentiated CD8+ T lymphocytes in APS1 patients which express the cytolytic mediator perforin (Laakso et al., 2011). To date, however, the targets of cytotoxic T cells in APS1 patients have not been studied extensively, but there are some examples such as aromatic L-amino acid decarboxylase (Kluger et al., 2015). This autoantigen was recognised by cytotoxic T cells in 43% of APS1 patients with gastrointestinal dysfunction (Kluger et al., 2015).

Concomitant to thymic defects in the control of autoreactive effector T cells, the defective development of Tregs in the AIRE-deficient thymus may also lead to inadequate suppression of autoreactive T lymphocytes in the periphery (Laakso et al., 2010, Malchow et al., 2013). Indeed, defects in Tregs have been reported in several studies. A reduction in the number of CD4+ CD25+ T cells was found in APS1 patients when compared with healthy controls (Ryan et al., 2005, Wolff et al., 2010). In addition, the frequency of FOXP3+ Tregs was reported to be decreased in patients with APS1, and the cells themselves expressed lower levels of FOXP3, the key Tregs key regulator, when compared with Tregs from individuals without disease (Kekalainen et al., 2007, Miyara et al., 2009, Laakso et al., 2010). The suppressive function of Tregs from APS1 patients against effector T lymphocytes is also impaired (Kekalainen et al., 2007). However, as yet, it has not been clarified as to whether Tregs defects in APS1 patients are due to defective selection events in the thymus or to altered homeostasis of Tregs in the periphery (Metzger and Anderson, 2011).

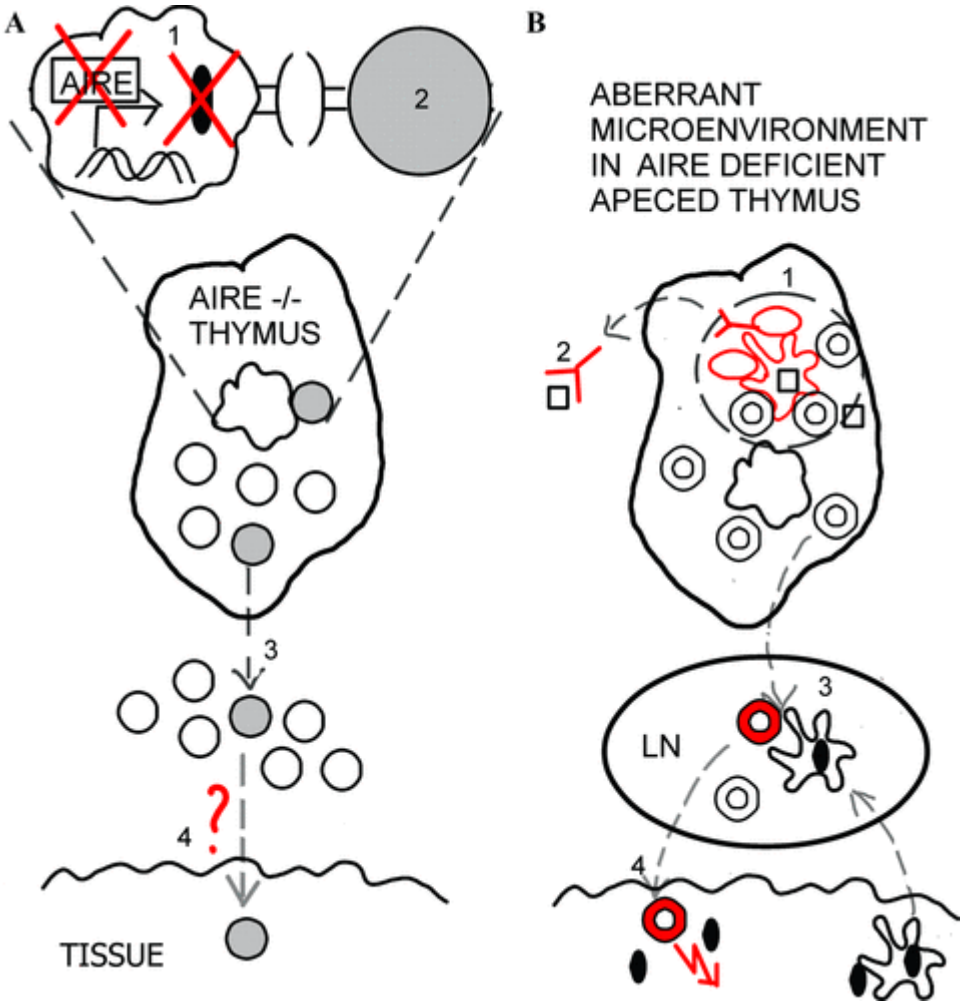

Figure 1.4: Current and alternative model of AIRE deficiency

(a) The current model of deficient negative selection. **(1)** In medullary thymic epithelial cells, AIRE deficiency leads to down-regulation of the expression of tissue-specific autoantigens (dark oval) that are not presented to thymocytes. **(2)** Self-reactive thymocytes (grey circles) are not negatively selected. **(3)** They are exported to the periphery together with non-self-reactive thymocytes (white circles). **(4)** Naive autoreactive T cells become activated on antigen recognition causing tissue destruction, the production of pro-inflammatory cytokines, and the activation of autoreactive B lymphocytes. **(b)** The alternative model of an aberrant microenvironment in the thymus. **(1)** Tertiary lymphoid tissue is formed where cytokines (rectangles) are presented in an immunogenic manner to T and B cells. **(2)** Neutralising anti-cytokine autoantibodies are released directly from the thymus. **(3)** CD8+ thymocytes are exported to the periphery and are activated after tissue-specific antigen (dark oval) is released and presented by dendritic cells. **(4)** Immune attack toward tissues. The image, taken from a paper by (Kisand and Peterson, 2011), is used with kind permission from John Wiley and Sons.

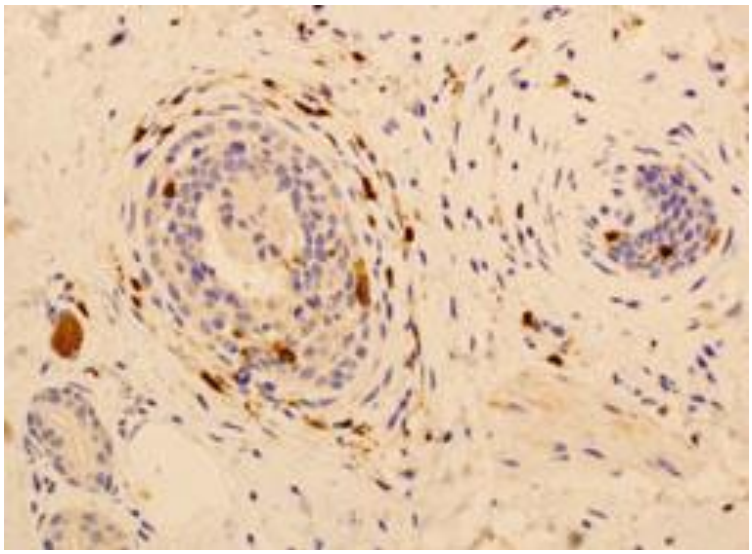

Figure 1.5: Immunohistochemistry staining of the hair follicles from an APS1 patient.

The image shows T cell infiltration of the hair follicle. The image, taken from a paper by (Faiyaz-Ul-Haque et al., 2009), is used with kind permission from John Wiley and Sons.

1.2.5 Organ-specific autoantibodies in APS1

Organ-specific autoantibodies (**Table 1.2**) are a hallmark of APS1 (Peterson and Peltonen, 2005). Many tissue-specific autoantibody targets are intracellular enzymes involved in the synthesis of hormones or neurotransmitter biosynthesis (Gylling et al., 2000). It has been suggested, therefore, that the humoral immune response against such autoantigens results from the release of the proteins upon organ destruction mostly likely as a result of autoreactive T cell activity (Kisand and Peterson, 2015). Another theory proposed to explain the presence of autoantibodies in APS1 also comes from the *Aire*-deficient mouse model (Lindh et al., 2008). Here, the production of autoantibodies by B cells in the spleen was reported to be independent of activation by T cells and linked to the overproduction of B cell-activating factor (BAFF) by DCs (**Figure 1.6**) (Lindh et al., 2008). Although this mechanism has not been analysed in relation to APS1, patients have do have elevated levels of BAFF (Lindh et al., 2008).

Many of the autoantibodies found in APS1 patients are considered unlikely to have a pathogenic role *in vivo* (Kisand and Peterson, 2015). However, autoantibodies against some autoantigens such as the calcium-sensing receptor (CaSR) have been shown to have stimulatory activity (Kemp et al., 2009), which might prevent parathyroid hormone (PTH) secretion leading to clinical hypoparathyroidism (**Section 1.3.3.2**). In addition, anti-parietal cell autoantibodies have cytolytic activity and contribute to the destruction of gastric parietal cells in APS1 (Perniola et al., 2000). Autoantibodies against secreted intrinsic factor can render it unable to bind vitamin B12 resulting in autoimmune gastritis (**Section 1.3.3.8**) (Proust-Lemoine et al., 2010, Betterle et al., 1998).

Associations exist between the presence of certain autoantibodies and the occurrence of a particular APS1 clinical manifestation. For example, humoral immune responses against steroid 21-hydroxylase, tyrosine phosphatase-like protein IA-2, and cytochrome P450 1A2 are diagnostic for Addison's disease, type 1 diabetes mellitus, and hepatitis, respectively (**Table 1.2**) (Soderbergh et al., 2004). However, many organ-specific autoantibodies can occur in patients regardless of their disease manifestations, so are not useful in making an exact diagnosis (**Table 1.2**) (Soderbergh et al., 2004).

Table 1.2: Examples of autoantibody targets in APS1

Autoantibody target	Prevelance of autoantibodies in APS1 (%)	Reported association with APS1 disease component	Reference
NACHT leucine-rich-repeat protein 5	32-49	Hypoparathyroidism	(Alimohammadi et al., 2008, Meloni et al., 2012)
Calcium-sensing receptor	12-86	Association with hypoparathyroidism contraversial	(Gylling et al., 2003, Gavalas et al., 2007)
Steroid 21-hydroxylase[1]	55-69	Addison's disease	(Wolff et al., 2007, Meloni et al., 2012)
Steroid 17α-hydroxylase	24-58	Addison's disease; premature ovarian failure	(Soderbergh et al., 2004, Meloni et al., 2012)
Side-chain cleavage enzyme	36-68	Premature ovarian failure	(Soderbergh et al., 2004, Wolff et al., 2007)
Thyroglobulin	15-21	Hypothyroidism	(Proust-Lemoine et al., 2010, Meloni et al., 2012)
Thyroid peroxidase	15-21	Hypothyroidism	(Proust-Lemoine et al., 2010, Meloni et al., 2012)
Tyrosine phosphatase-like protein IA-2[1]	7	Type 1 diabetes mellitus	(Soderbergh et al., 2004, Proust-Lemoine et al., 2010)
Tudor domain-containing protein 6	49	Not associated with hypopituitarism	(Bensing et al., 2007)
49-kDa pituitary enolase	68	Not associated with hypopituitarism	(O'Dwyer et al., 2007)
Intrinsic factor[1]	15-30	Chronic atrophic gastritis	(Betterle et al., 1998, Proust-Lemoine et al., 2010)
Gastric parietal cell proton pump	24	Chronic atrophic gastritis	(Perniola et al., 2000)
Glutamic acid decarboxylase 65	27-42	Gastro-intestinal dysfunction	(Wolff et al., 2007, Proust-Lemoine et al., 2010, Meloni et al., 2012)
Tryptophan hydroxylase	28-61	Intestinal dysfunction	(Ekwall et al., 1998, Dal Pra et al., 2004)
Histidine decarboxylase	37	Intestinal dysfunction	(Skoldberg et al., 2003)
Alpha 5 defensin of Paneth cells	27	Intestinal dysfunction	(Dobes et al., 2015)
Cytochrome P450 1A2[1]	6-8	Hepatitis	(Clemente et al., 1997, Gebre-Medhin et al., 1997, Obermayer-Straub et al., 2001)
Cytochrome P450 2A6	6-8	Hepatitis	(Clemente et al., 1998, Obermayer-Straub et al., 2001)
Tyrosine hydroxylase	44-50	Alopecia areata; dental enamel dysplasia	(Hedstrand et al., 2000, Soderbergh et al., 2004, Bratland et al., 2013)
SOX9 transcription factor	15	Vitiligo	(Hedstrand et al., 2001)
SOX10 transcription factor	22	Vitiligo	(Hedstrand et al., 2001)
Aromatic L-amino acid decarboxylase	39-68	Vitiligo; hepatitis	(Husebye et al., 1997, Soderbergh et al., 2004)

[1]Autoantibodies with good predictive value for a specific disease manifestation in APS1.

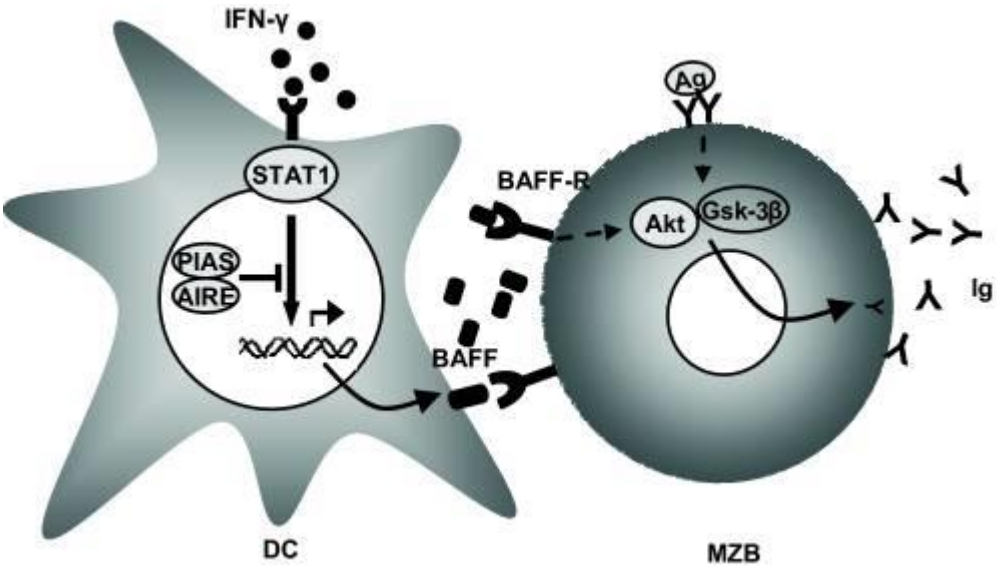

Figure 1.6: Schematic picture of the possible role for AIRE in interferon-γ receptor signaling.

In the absence of AIRE, the transcriptional co-activator protein inhibitor of activated STAT1 (PIAS1) cannot mediate inhibition of STAT1 signaling upon interferon (IFN)-γ receptor stimulation, resulting in excessive B cell-activating factor (BAFF) production by dendritic cells (DC). Subsequently, the increased levels of BAFF result in overly activated B cells (MZB) that produce autoantibodies (IgG) against a specific antigen (Ag). Thus, BAFF contributes to the phenotype seen in Aire-deficient mice and possibly in APS1 patients. From a paper by (Lindh et al., 2008), this figure did not require permission for use in this thesis.

1.2.6 Anti-cytokine autoantibodies in APS1

Anti-cytokine autoantibodies are highly prevalent in APS1 patients (**Table 1.3**). Interferon (IFN)-ω autoantibodies have been reported in 100% of APS1 cases. Autoantibodies against IFN-α and IFN-β have been detected at a lower prevalence of 95% and 22%, respectively (Meager et al., 2006). Autoantibodies against IFN-ω and IFN-α present as early as the first year of age and, in some APS1 cases, can be detected prior to the onset of clinical manifestation or the appearance of organ-specific autoantibodies (Toth et al., 2010, Wolff et al., 2013). Due to their prevalence and high titres, IFN-ω and IFN-α autoantibodies are considered appropriate serum markers for APS1 (Husebye et al., 2009). In terms of activity, autoantibodies against type I interferons (IFN-ω and IFN-α) are able to neutralise the effects of their target cytokine (Meager et al., 2006), and have also been shown to reduce the expression of genes that are normally stimulated by interferons (Kisand et al., 2008).

In more recent studies, autoantibodies that specifically neutralise the activity of either interleukin (IL)-22, IL-17F or IL-17A have been identified in APS1 patients (**Table 1.3**) (Kisand et al., 2010, Puel et al., 2010). High titre autoantibodies against IL-22 can be detected very early, within months after birth (Wolff et al., 2013), and are the most prevalent humoral immune response against T helper 17 cell-related cytokines (Kisand et al., 2010, Puel et al., 2010). Usually, autoantibodies against IL-17 cytokines appear later and are less prevalent (Kisand et al., 2010, Puel et al., 2010). The correlations of IL-22, IL-17F and IL-17A autoantibodies with the development of candidiasis in APS1 are detailed in **Section 1.3.3.1.**

Table 1.3: Prevalence of autoantibodies against cytokines in APS1 patients

Cytokine target[1]	Prevalence of autoantibodies in APS1 (%)	Reference
IFN-ω	100	(Meager et al., 2006)
IFN-α	95	(Meager et al., 2006)
IFN-β	22	(Meager et al., 2006)
IFN-λ	14	(Meager et al., 2006)
IL-22	91	(Kisand et al., 2010, Puel et al., 2010)
IL-17F	75	(Kisand et al., 2010, Puel et al., 2010)
IL-17A	41	(Kisand et al., 2010, Puel et al., 2010)

[1]IFN, interferon; IL, interleukin.

1.3 Autoimmune polyendocrine syndrome type 1: diagnosis, epidemiology and clinical features

1.3.1 Diagnosis

Although, the clinical diagnosis of APS1 is normally based upon at least two of the characteristic triad of major disease components of chronic mucocutaneous candidiasis (*Candida* infection), hypoparathyroidism (low serum PTH and calcium levels), and Addison's disease (adrenal insufficiency) (Perheentupa, 2006), when a sibling is affected, the presence of only one of these manifestations is enough to justify diagnosis (Husebye et al., 2009). In cases with an atypical presentation, the confirmation of *AIRE* gene mutations will aid in clinical diagnosis (Husebye et al., 2009). Finally, autoantibodies against IFN-ω and IFN-α are detectable in the majority of patients (Meager et al., 2006), so they are now included in the diagnostic criteria of APS1 (Husebye et al., 2009).

1.3.2 Epidemiology

Autoimmune polyendocrine syndrome type 1 is found worldwide with small numbers of patients (1:10,000,000) reported in Japan (Sato et al., 2002), India (Zaidi et al., 2009), and the USA (Wang et al., 1998). However, by far, the greatest concentration of APS1 cases is found in Europe where the disease affects approximately 1:100,000 individuals in the Irish, Norwegian and Polish populations (Dominguez et al., 2006, Stolarski et al., 2006), and 1:500,000 French (Proust-Lemoine et al., 2012). In some European ethnicities APS1 is even more prevalent. For example, 1:25,000 in Finnish (Perheentupa, 2006), 1:14,000 in Sardinians (Rosatelli et al., 1998), and 1:35,000 in Apulians (Meloni et al., 2002). A high number of Iranian Jews in Israel also suffer from APS1 with a prevalence of 1:9,000 (Zlotogora and Shapiro, 1992). Depending on the population, some reports suggest a different in the prevalence of APS1 between men and women, with a female:male ratio ranging from 0.81:1 to 2.4:1 (Kahaly, 2009).

1.3.3 Clinical manifestations

Mostly, APS1 becomes apparent during childhood or in adolescence (Husebye et al., 2009), although, rarely, the disease has been reported to initially manifest in young adults between the ages of 18 and 25 years (Magitta et al., 2008). The classic disease

triad is usually in evidence by the third decade of life, but there are cases where not all three diseases develop (Husebye et al., 2009). Albeit with less frequency, several other disease manifestations can be present including hypothyroidism, type 1 diabetes mellitus, hepatitis, alopecia and vitiligo (Perheentupa, 2006). Notably, the number of diseases afflicting patients can vary considerably ranging from one to 10 (Perheentupa, 2006). The various clinical manifestations of APS1 are detailed in the next sections and are summarised for different populations in **Table 1.4**.

1.3.3.1 Chronic mucocutaneous candidiasis

Chronic mucocutaneous candidiasis (**Figure 1.7a**) is most usually the first clinical sign to appear in those affected by APS1, although in some cases, it can appear after the main endocrinopathies of hypoparathyroidism and Addison's disease (Ahonen et al., 1990). The prevalence of chronic mucocutaneous candidiasis in APS1 varies between 70-100% depending on patient ethnicity (**Table 1.4**) (Myhre et al., 2001), although exceptionally, this falls to 18% in Iranian APS1 patients (Zlotogora and Shapiro, 1992). Typically, chronic mucocutaneous candidiasis manifests in APS1 patients within the first decade of life (Husebye et al., 2009), and the development of chronic mucocutaneous candidiasis is rarer once APS1 patients have reached adulthood (Ahonen et al., 1990, Meloni et al., 2012). For example, chronic mucocutaneous candidiasis is present in 26% of Finnish APS1 patients within the first year after birth, and in over 50% by the age of five years (Ahonen et al., 1990). A report on Sardinians indicated appearance of chronic mucocutaneous candidiasis at a median age of three years in 86% of patients (Meloni et al., 2012).

The severity of *Candida* infection can vary between patients. Generally, infection starts with oral thrush with symptoms such as ulceration, redness and soreness at the corners of the mouth (Husebye et al., 2009). However, it can be life-threatening, as the initial mouth infection can become chronic and may progress to oral mucous squamous cell carcinoma (Husebye et al., 2009, Kluger et al., 2012). Candida oesophagitis has also been reported in APS1 patients resulting in pain while swallowing, retrosternal pain, and dysphagia (Collins et al., 2006, Perheentupa, 2006). This can progress to local stricture and, exceptionally, to oesophageal cancer (Rosa et al., 2008, Koch et al., 2009). Moreover, chronic mucocutaneous candidiasis affecting

the intestinal tract can lead to chronic diarrhoea (Kluger et al., 2013), and infection of the fingernails to chronic paronychia (Collins et al., 2006). It is noteworthy that chronic mucocutaneous candidiasis can be present in the oesophagus and the intestine without any signs of oral candidiasis (Husebye et al., 2009, Kluger et al., 2012).

The basis for the extensive *Candida* infection in APS1 is thought to be impaired responses by T helper 17 cells. These cells normally produce the protective cytokines IL-17A, IL-17F, and IL-22 (Kisand et al., 2011, Lindh et al., 2013), which induce the synthesis of anti-microbial peptides (Liang et al., 2006). However, the T helper 17 lymphocytes of APS1 patients are unable to produce IL-17F and IL-22 (Laakso et al., 2014). In addition, high levels of autoantibodies against the IL-17 family of cytokines are detected in patients with APS1 (**Section 1.2.6; Table 1.3**), and these are thought to predispose individuals to candidiasis by virtue of their neutralising activities (Kisand et al., 2010). Correlating with this, APS1 patients with no or mild candidiasis have low or undetectable levels of autoantibodies against IL-17A, IL-17F, and IL-22 (Kisand et al., 2010, Sarkadi et al., 2014).

Table 1.4: Clinical manifestations in APS1 patients

Clinical manifestation	Prevalence (%)	Studies included[1]
Chronic mucocutaneous candidiasis	70-100	1-20
Hypoparathyroidism	50-100	1-20
Addison's disease	22-100	1-20
Hypothyroidism	0-50	1-20
Type 1 diabetes mellitus	0-18	1, 3, 4, 6-9, 11-13, 15-22
Gonadal insufficiency - male	0-40	2-4, 16, 20
Gonadal insufficiency - female	7-71	2-4, 7, 16-20
Hypopituitarism	0-7	3, 7, 12, 13,16, 18, 19
Chronic atrophic gastritis	0-33	1-4, 6-12, 15-17, 19, 20
Intestinal dysfunction malabsorption	5-27	1-3, 5,6, 8-11, 13, 16-20
Hepatitis	18	1-3, 5-11, 15-20
Alopecia areata	13-50	1-5, 6-20
Vitiligo	0-33	1-3, 5, 7-13, 15-20
Ocular abnormalities - keratitis	0-37	2-4, 7-9, 11-13, 15-19
Nail dystrophy	0-50	2, 3, 12
Dental enamel dysplasia	25-77	2, 7, 9-12, 14, 16, 18
Lung disease	6-7	23, 24
Kidney impairment	2-9	3, 17, 18, 20
Asplenia	2-9	3, 7, 17

[1] **[1]** North American (Neufeld et al., 1981); **[2]** Finnish (Ahonen et al., 1990); **[3]** Finnish, (Perheentupa, 2006); **[4]** Iranian (Zlotogora and Shapiro, 1992); **[5]** North American (Wang et al., 1998); **[6]** Italian, (Perniola et al., 2000); **[7]** Sardinian (Meloni et al., 2012); **[8]** Italian (Betterle et al., 2002); **[9]** Norwegian (Myhre et al., 2001); **[10]** Slovenian (Podkrajsek et al., 2005); **[11]** Slovenian (Podkrajsek et al., 2008); **[12]** Irish, (Collins et al., 2006); **[13]** Polish, (Stolarski et al., 2006); **[14]** Slovakian(Magitta et al., 2008); **[15]** Italian (Mazza et al., 2011); **[16]** French, (Proust-Lemoine et al., 2010); **[17]** Russian (Orlova et al., 2010); **[18]** Norwegian (Wolff et al., 2007); **[19]** Italian, (Betterle et al., 1998); **[20]** Italian (Cervato et al., 2009); **[21]** Finnish (Tuomi et al., 1996); **[22]** Finnish (Gylling et al., 2000); **[23]** European (Alimohammadi et al., 2009); **[24]** Swedish (Shum et al., 2013).

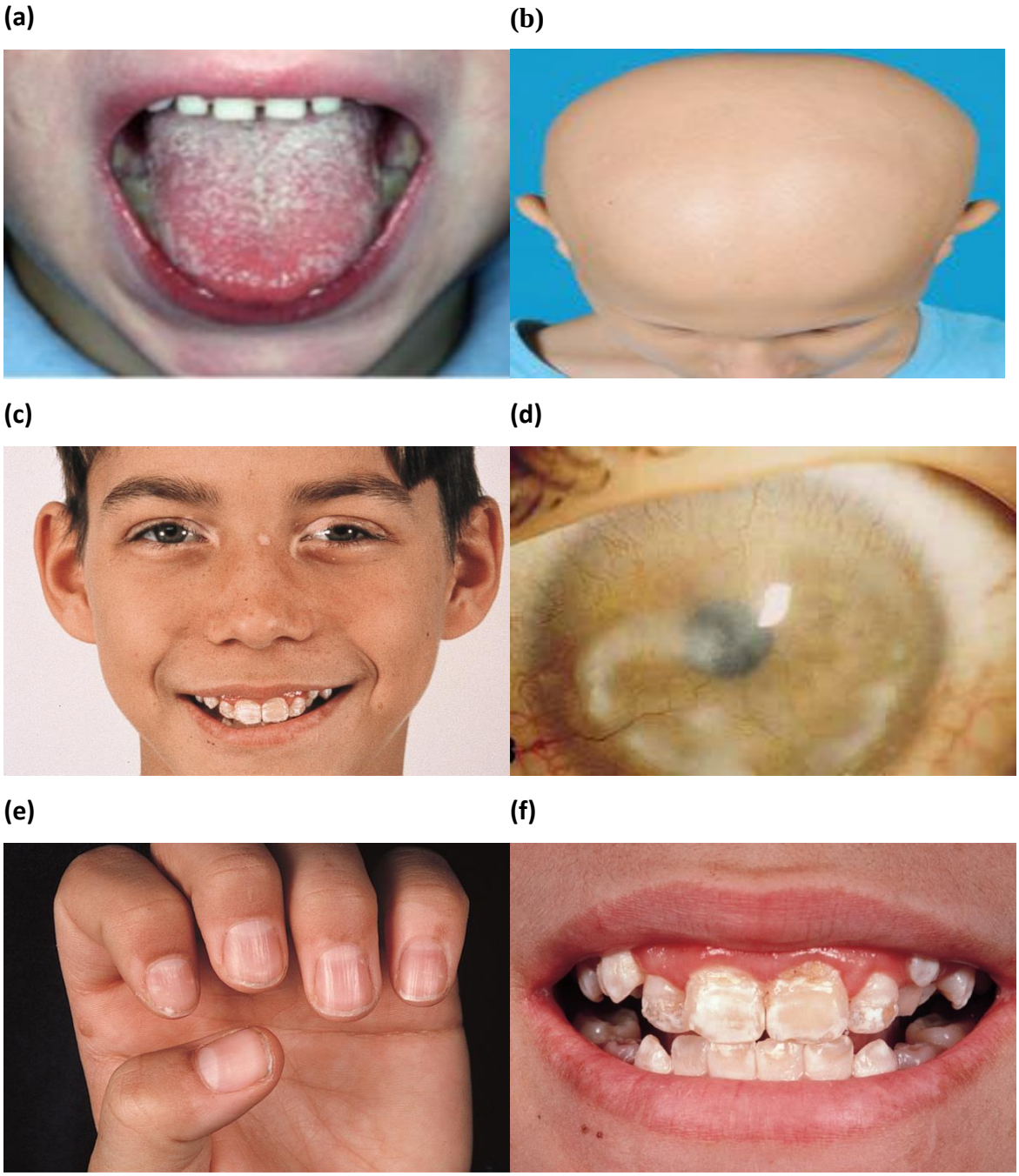

Figure 1.7: Clinical manifestations of APS1.

The following clinical manifestations of APS1 are shown **(a)** chronic mucocutaneous candidiasis **(b)** alopecia areata, **(c)** vitiligo, **(d)** keratitis, **(e)** nail dystrophy, and **(f)** dental enamel dysplasia. Images (a), taken from a paper by (Collins et al., 2006), (b), taken from a paper by (Faiyaz-Ul-Haque et al., 2009), and (d), taken from a paper by (Merenmies and Tarkkanen, 2000), are used with kind permission from John Wiley and Sons. Images (c), (e) and (f), taken from a paper by (Walter, 2000), are used with kind permission from the American Medical Association.

1.3.3.2 Hypoparathyroidism

Hypoparathyroidism is the most common endocrine abnormality associated with APS1 affecting 50-100% of patients, depending on the population (**Table 1.4**) (Perheentupa, 2006). In most cases, it is the first endocrine disease to appear and manifests between the ages of four and five years (Perheentupa, 2006). By the age of 30 years, up to 85% of APS1 patients are affected by parathyroid dysfunction (Husebye et al., 2009), although it can be diagnosed in later adulthood (Gylling et al., 2003, Zlotogora and Shapiro, 1992). Of interest, the presence of hypoparathyroidism shows a distinct gender difference affecting 98% of females compared with 71% of males (Perheentupa, 2006).

Patients with this particular endocrinopathy present with normal or low levels of PTH, hypocalcaemia and high serum phosphate concentrations (Husebye et al., 2009). Symptoms are related to hypoparathyroidism include clumsiness, seizures, diarrhoea, muscle cramps, and paraesthesia (Husebye et al., 2009). The manifestation is thought to be caused by aberrant autoimmune responses against the parathyroid glands (Brandi et al., 1986). Autoantibodies against proteins highly expressed in the parathyroid (**Table 1.2**), including the NACHT leucine-rich-repeat protein 5 (NALP5) and the CaSR have been reported in APS1 patients (**Table 1.2**) (Gavalas et al., 2007). As it is relevant to this thesis, parathyroid autoimmunity including autoantibodies against the glands will be discussed in more detail in **Section 1.4.**

1.3.3.3 Addison's disease

Addison's disease is the second most common endocrine manifestation of APS1 with a prevalence of between 22% and 100% (**Table 1.4**) (Neufeld et al., 1981, Perniola et al., 2000, Meloni et al., 2012). It usually appears subsequent to chronic mucocutaneous candidiasis and hypoparathyroidism (Perheentupa, 2006). The age of onset of Addison's disease in APS1 patients varies widely. In the Finnish population, the disease begins after three years of age (Perheentupa, 2006). By the end of first decade, 40% of patients present with adrenal insufficiency (Perheentupa, 2006). This rises to just under three-quarters of patients by the second decade, and to almost all cases by the fourth decade (Perheentupa, 2006). A median age of 10 years was reported in the same study (Perheentupa, 2006).

Due to low levels of cortisol and aldosterone, patients suffer from low blood pressure, weight loss, general fatigue, and significant pigmentation of the skin (Husebye et al., 2009). In terms of pathogenicity, Addison's disease in APS1 is suggested to result from destructive autoimmune reactivity against the adrenal glands (Bratland et al., 2009, Rottembourg et al., 2010, Dawoodji et al., 2014). There is a close association in APS1 patients between Addison's disease and autoantibodies against several targets related to the adrenal glands, including steroid 17α-hydroxylase, steroid 21-hydroxylase, and side-chain cleavage enzyme (**Table 1.2**) (Soderbergh et al., 2004, Wolff et al., 2010). Autoantibodies can be detected years before the symptoms of Addision's disease presents, so they are an early marker of adrenal insufficiency in APS1 (Soderbergh et al., 2004, Wolff et al., 2010). This enables Addison's disease to be diagnosed and monitored to avoid a life-threatening adrenal crisis.

1.3.3.4 Hypothyroidism

Unlike the common endocrine diseases which appear in APS1 patients, thyroid autoimmunity affects a minority ranging from 0-50% (**Table 1.4**) (Wolff et al., 2007). Graves' disease or hyperthyroidism is not usually a feature of APS1, and very few cases have been reported (Pelletier-Morel et al., 2008). Hypothyroidism usually manifests following puberty and, in one-third of patients, an underactive thyroid is detectable by middle-age (Perheentupa, 2006). The age range of presenting with hypothyroidism is 4.7–45 years, with a median age of 26.5 years (Perheentupa, 2006). The symptoms of hypothyroidism in APS1 are similar to those of isolated autoimmune hypothyroidism including enlargement of the thyroid glands, thyroid failure, high levels of thyroid-stimulating hormone and low levels of free thyroxine (Perniola et al., 2008, Weetman, 2004). The thyroid gland is targeted and damaged by infiltrating T lymphocytes (Weetman, 2004), resulting in high titres of thyroid peroxidase and thyroglobulin autoantibodies which serve as markers for this disease component (**Table 1.2**) (Perniola et al., 2000, Perniola et al., 2008).

1.3.3.5 Type 1 diabetes mellitus

The prevalence type 1 diabetes mellitus in APS1 varies between populations ranging from 0-18% (**Table 1.4**) (Tuomi et al., 1996). Typically, the age of onset lies between 30

and 50 years (Husebye et al., 2009, Perheentupa, 2006). The disease is caused by autoimmune destruction of pancreatic islet cells which results in a lack of insulin production and high blood glucose levels, both hallmarks of type 1 diabetes mellitus not associated with APS1 (Nokoff et al., 2012). In APS1, type 1 diabetes mellitus is associated with autoantibodies that target tyrosine phosphatase-like protein IA-2 (**Table 1.2**) (Soderbergh et al., 2004, Van den Driessche et al., 2009, Boitard, 2012).

1.3.3.6 Gonadal insufficiency

Hypogonadism caused causes premature ovarian insufficiency in women and testicular insufficiency in men. Premature ovarian failure is one of the more common endocrinopathies (**Table 1.4**) (Ahonen et al., 1990, Zlotogora and Shapiro, 1992, Meloni et al., 2012), with approximately two-thirds of female APS1 patients eventually developing this feature by the third decade of life (Perheentupa, 2006). High levels of follicle-stimulating hormone and luteinising hormone, in addition to a reduction in oestrogen levels, are characteristic, and the result is arrested or interrupted pubertal development or premature menopause (Husebye et al., 2009). Patients may also suffer from amenorrhea, infertility, and psychological stress (Dragojević-Dikić et al., 2010). Testicular insufficiency is rare in male APS1 patients, occurring in 0-40% of cases (**Table 1.4**) (Ahonen et al., 1990, Zlotogora and Shapiro, 1992, Cervato et al., 2009). Generally, the condition develops in adulthood (Perheentupa, 2006). Again, high follicle-stimulating hormone and luteinising hormone levels are definitive, along with low testosterone (Husebye et al., 2009).

Most of the patients with gonadal insufficiency also have Addison's disease and, therefore, they present with autoantibodies against several steroid-producing organs including the adrenal cortex, testes, placenta and ovary (Dragojević-Dikić et al., 2010, Husebye et al., 2009). The presence of anti-side-chain cleavage enzyme autoantibodies correlates significantly with premature ovarian failure (**Table 1.2**) (Soderbergh et al., 2004).

1.3.3.7 Hypopituitarism

Hypopituitarism has been reported only in a minority of APS1 patients ranging from 0-7% of cases (**Table 1.4**) (Betterle et al., 1998, Stolarski et al., 2006, Meloni et al., 2012).

This clinical feature usually has an early onset (Perheentupa, 2006). Affected individuals display growth hormone, gonadotropin or adrenocorticotropic hormone deficiency (Husebye et al., 2009, Perheentupa, 2006). Autoimmune responses against the pituitary are thought to be responsible for this particular disease manifestation. However, although autoantibodies against the pituitary (**Table 1.2**), such as against tudor domain-containing protein 6 (Bensing et al., 2007) and pituitary enolase (O'Dwyer et al., 2007), have been shown in APS1 patients with pituitary failure, there is as yet no clear marker to predict hypopituitarism.

1.3.3.8 Chronic atrophic gastritis

By middle-age, up to 33% of APS1 patients are affected by chronic atrophic gastritis (**Table 1.2**) (Perheentupa, 2006), which is also referred to as pernicious anaemia. The condition normally presents in early adulthood (Betterle et al., 1998), although some cases have been reported in children with APS1 (Oliva-Hemker et al., 2006). Symptoms may include atrophic glossitis, diarrhoea, anaemia, leukopenia, thrombopenia, and pancytopenia peripheral neuropathy which are due to a chronic deficiency in vitamin B12 resulting from gastric atrophy (Husebye et al., 2009). Histopathology of gastric tissue has revealed an infiltration of T lymphocytes which eventually leads to gastric gland destruction (Skoldberg et al., 2003). Autoantibodies against the gastric parietal cell protein pump have also been implicated in the destruction of gastric parietal cells (Perniola et al., 2000). As a consequence, the level of intrinsic factor is diminished and because this is required for the uptake of vitamin B12, there is a concomitant development of pernicious anaemia. In addition, patients have autoantibodies against vitamin B12 binding protein (**Table 1.2**) which prevent the normal uptake of vitamin B12 (Toh et al., 1997).

1.3.3.9 Intestinal dysfunction

Intestinal dysfunction can manifest with different several symptoms (Kluger et al., 2013). Chronic diarrhoea occurs in 5% of APS1 cases (Perheentupa, 2006). Less frequently, constipation is found in 2% of patients (Perheentupa, 2006). Malabsorption is more prevalent, affecting 5-27% of APS1 patients depending on the series (**Table 1.4)** (Betterle et al., 1998). In some cases of APS1, the symptoms may result from

Candida infection of the gut (Gianani and Eisenbarth, 2003, Kluger et al., 2013), and chronic diarrhoea has also been linked to the hypocalcaemia associated hypoparathyroidism (Kluger et al., 2013). With respect to autoimmunity, there doesn't appear to be appreciable lymphocyte infiltration in intestinal biopsies (Kluger et al., 2013), although gastrointestinal endocrine cells can be targeted by autoimmune responses (Gianani and Eisenbarth, 2003). The presence of autoantibodies against tryptophan hydroxylase (Ekwall et al., 1998), and Paneth cell-specific alpha 5 defensin (Dobes et al., 2015) has been associated with intestinal dysfunction in APS1 (**Table 1.2**).

1.3.3.10 Hepatitis

Hepatitis develops in 5-36% of APS1 patients (**Table 1.4**) (Betterle et al., 1998, Perheentupa, 2006), and is usually present before the age of 20 years (Betterle et al., 1998, Perheentupa, 2006). Clinical symptoms can range from asymptomatic to mild, but in severe cases the disease can be fatal as a result of liver necrosis (Obermayer-Straub et al., 2001). APS1-associated hepatitis is considered to be caused by autoimmune reactivity and there has been much research to identify and characterise autoantibody targets which could act as markers for the disease (**Table 1.2**). These include cytochromes P450 1A2 and P450 2A6 (Obermayer-Straub et al., 2001), and aromatic L-amino acid decarboxylase (Soderbergh et al., 2004) Of these, anti-cytochrome P450 1A2 autoantibody levels have been found to correlate with the presence and severity of hepatitis (Obermayer-Straub et al., 2001).

1.3.3.11 Alopecia areata

In APS1, the hair loss disease alopecia areata (**Figure 1.7b**) is present in 13-50% of patients (**Table 1.4**) (Neufeld et al., 1981, Zlotogora and Shapiro, 1992, Betterle et al., 2002), and is the most common ectodermal feature (Perheentupa, 2006). Normally, the onset occurs during adulthood and alopecia areata is not usually an initial clinical sign of APS1 (Perheentupa, 2006). There is evidence that autoimmune attack of the hair follicles is responsible for patchy or total hair loss. For example, histopathological examination of alopecia areata scalp lesions shows an intra-follicular and peri-follicular infiltration of T cells, Langerhans cells and macrophages (Perret et al., 1984, Todes-

Taylor et al., 1984). In addition, autoantibodies against hair follicle components have been detected in APS1 patients with alopecia areata (Hedstrand et al., 2000). More specifically, anti-tyrosine hydroxylase autoantibodies have been found to correlate significantly with alopecia areata in APS1 (**Table 1.2**) (Hedstrand et al., 2000). However, further investigations are required to determine any significance of tyrosine hydroxylase autoantibodies in relation to the pathogenesis of alopecia areata.

1.3.3.12 Vitiligo

Vitiligo (**Figure 1.7c**), characterised by the loss of cutaneous melanocytes, can become extensive and affects from 0-33% of APS1 patients depending on the patient series (**Table 1.4**) (Perheentupa, 2006). The disorder can present not only in the first month after birth up to the second decade of life, but it can appear at later ages (Betterle et al., 1998, Perheentupa, 2006). As in isolated vitiligo, destruction of pigment-producing cells is mediated via cytotoxic T cells which target melanocyte-specific proteins such as tyrosinase (van den Boorn et al., 2009). In addition, several proteins have been identified as autoantibody targets in APS1 patient with vitiligo (**Table 1.2**), including the melanocyte-specific transcription factors SOX9 and SOX10 (Hedstrand et al., 2001).

1.3.3.13 Ocular abnormalities

Ocular abnormalities can affect the eyelashes, cornea, retina and optic nerve (Wolff et al., 2013). Symptoms normally appear as early as two years of age (Mezgueldi et al., 2015), but the onset can also occur in adults (Perheentupa, 2006). The predominant eye manifestation is keratitis (**Figure 1.7d**) which occurs in APS1 with a large variation in prevalence ranging from 0-37% of patients (**Table 1.4**) (Proust-Lemoine et al., 2010). Keratitis in APS1 begins with indicators such as intense photophobia, a feeling of sand in the eyes, blepharospasm, and a reduction in lacrimation (Husebye et al., 2009). More serious effects can ensue including corneal scarring and perforation which can lead to sight loss (Yeh and Matoba, 2007). Although the aetiology of keratitis remains obscure, it has been suggested to arise from an autoimmune response against the corneal/conjunctival epithelium. Indeed, in APS1 patients, the progression of epithelial edema and superficial opacity can be reversed under topical steroid therapy (Tarkkanen and Merenmies, 2001).

1.3.3.14 Nail dystrophy

Nail dystrophy (**Figure 1.7e**) is frequently evident in patients with up to 50% of individuals being affected (**Table 1.4**) (Ahonen et al., 1990, Perheentupa, 2006). The aetiology of nail dystrophy, however, remains controversial. In one study of Irish APS1 patients, all nail changes were related to infection by *Candida* and did not display the characteristic nail pitting associated with nail dystrophy (Collins et al., 2006). In contrast, approximately 50% of the cases of distinctive nail dystrophy in a Finnish APS1 patient series were not related to *Candida* or other fungal infections (Ahonen et al., 1990, Perheentupa, 2006).

1.3.3.15 Dental enamel dysplasia

Approximately 25-77% of APS1 patients are affected by dental enamel dysplasia (**Figure 1.7f**) (**Table 1.4**) (Perheentupa, 2006). The presentation varies between patients, some cases present with mild symptoms like transverse grooves in the enamel, while others present with rows of pits of inconstant size alternating with zones of well-formed enamel (Perheentupa, 2006). In severe forms of disease, all permanent teeth have hypoplastic enamel (Perheentupa, 2006). The cause of enamel dysplasia in APS1 has yet to be established. A study of Norwegian APS1 patients found a significant correlation between dental disease and autoantibodies against tyrosine hydroxylase, these being present in 70% (7/10) of patients with enamel dysplasia and 22% (4/18) of those without (Bratland et al., 2013). However, it was not explained how tyrosine hydroxylase autoantibodies could instigate disease pathogenesis (Bratland et al., 2013), although it has been suggested that immune responses which adversely affecting ameloblasts may play a part (Pavlic and Waltimo-Siren, 2009).

1.3.3.16 Lung disease

Involvement of the respiratory system in APS1 is quite rare with a prevalence of 6-7% (**Table 1.4**) (Alimohammadi et al., 2009). Symptoms can vary from airway hyper-responsiveness, lower respiratory infections, and chronic cough. Progressive worsening of the symptoms over time can result in chronic respiratory failure which can be fatal (Alimohammadi et al., 2009). Autoantibodies against a potassium channel regulating protein, a protein expressed in the epithelial cells of terminal bronchioles,

have been identified in 88% (7/8) of cases with respiratory problems, but less than 1% (1/102) of those without lung involvement (Alimohammadi et al., 2009). In addition, the lung-specific protein bactericidal/permeability-increasing fold-containing B1 (BPIFB1) was identified as an autoantibody target in 100% (6/6) of APS1 patients with respiratory problems, the majority of whom also had bronchiolar inflammation (Shum et al., 2013). However, anti-BPIFB1 autoantibodies were found in only 4% (4/98) of APS1 cases where no lung disease was evident (Shum et al., 2013). The immune responses against lung tissue indicate a possible role for autoimmunity in the development of respiratory disease in some APS1 patients.

1.3.3.17 Kidney impairment

Kidney disease has not been noted as a common problem in APS1, being reported in 2-9% of patients albeit in a limited number of studies (**Table 1.4**) (Wolff et al., 2007, Cervato et al., 2009, Orlova et al., 2010). Kidney manifestations include renal tubular acidosis, nephrocalcinosis, and in later stages chronic renal failure. Indeed, half of those patients affected develop renal failure by their third decade of life (Perheentupa, 2006), and this can prove fatal (Betterle et al., 1998). Renal biopsies from patients have shown lymphocytic infiltration and deposition of complement components (Al-Owain et al., 2010), and anti-proximal renal tubular autoantibodies have been detected in some cases (Ulinski et al., 2006) Both observations suggest the involvement of autoimmune pathogenic mechanisms in the development of renal complications, at least in some APS1 patients.

1.3.3.18 Asplenia

Asplenia in APS1 (Parker et al., 1990, Pollak et al., 2009) is rare with a prevalence of 2-9% (**Table 1.4**) (Perheentupa, 2006, Orlova et al., 2010, Meloni et al., 2012), although this has been reported at 19% in adult patients (Perheentupa, 2006). The decrease in spleen size makes patients vulnerable to bacterial infections, so vaccination of APS1 patients with asplenia against *Streptococcus pneumoniae* and *Haemophilus influenzae* may be required (Husebye et al., 2009). Although autoimmune destruction of the spleen has been proposed (Friedman et al., 1991), the pathogenic mechanisms involved in the development of asplenia are still unclear.

1.4 Hypoparathyroidism in APS1

Since APS1 is due to a defect in the *AIRE* gene, the diseases that form part of the clinical picture are assumed to be autoimmune in origin. For example, as is the case for the isolated form of the disease not in the context of APS1, Addison's disease and type 1 diabetes mellitus are caused by autoimmunity against the affected gland. Consequently, there has been some study to characterise autoimmunity against the parathyroid.

1.4.1 Animal models of autoimmunity against the parathyroid

Establishing animal models that replicate the disease in humans is an important piece of evidence that suggests autoimmunity. Although this has not been thoroughly investigated, hypoparathyroidism has indeed been induced in rats and dogs after immunisation with parathyroid tissue (Lupulescu et al., 1968a). In these animals, a infiltration of lymphocytes into the parathyroid was noted, along with the presence of serum autoantibodies against the gland (Lupulescu et al., 1968b) In addition, the immunisation of rabbits with homogenised parathyroid tissue originating from rats or cows resulted in the production of parathyroid tissue-specific autoantibodies (Altenahr and Jenke, 1974). Furthermore, passive immunisation of rats with the serum from the immunised rabbits caused a very severe infiltration of lymphocytes into the parathyroid, although hypoparathyroidism was not evident in the animals (Altenahr and Jenke, 1974).

1.4.2 T cells in hypoparathyroidism

The presence of a lymphocytic infiltration in the target tissue and the demonstration of T cell reactivity to putative tissue antigens are indicative of autoimmunity (Rose and Bona, 1993). There have been case reports of histological changes in the parathyroid in idiopathic hypoparathyroidism including T and B lymphocyte infiltration (**Figure 1.8**) (Kossling and Emmrich, 1971, Vandecas and Gepts, 1973). In a study of idiopathic hypoparathyroid patients, an increase in circulating activated T cells compared to controls has been reported (Wortsman et al., 1992). However, so far, T cell reactivity against antigens of the parathyroid has not been shown convincingly.

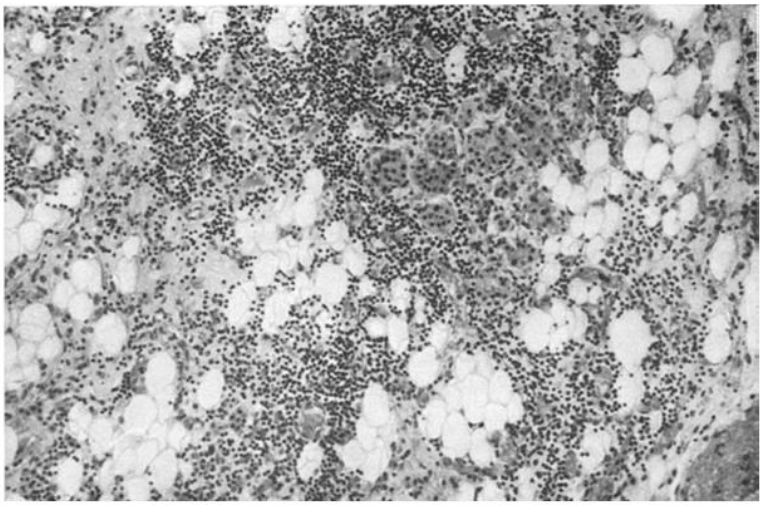

Figure 1.8: Infiltration of the parathyroid with lymphocytes.

Lymphocyte infiltration can be seen in the parathyroid glands of a patient with autoimmune hypoparathyroidism. The image, from a paper by (Vandecas and Gepts, 1973), was used with kind permission from Springer.

1.4.3 Anti-parathyroid autoantibodies

Many early studies revealed autoantibodies against the parathyroid glands in patients with hypoparathyroidism (Blizzard et al., 1966, Irvine and Scarth, 1969, Betterle et al., 1985, Brandi et al., 1986, Fattorossi et al., 1988). However, none of these reported the exact antigen specificity of the antibodies, and the cellular components the antibodies reacted against differed between each of the studies. Better evidence in support of humoral immune responses against the parathyroid came from the analysis of isolated parathyroid cells by measuring inhibition of PTH-secretion as an index of autoantibody binding (Posillico et al., 1986). In this study of 23 sera from patients with idiopathic hypoparathyroidism, three inhibited the secretion of PTH. In one patient, a reduction in antibody levels along with spontaneous improvement of the disease was found over time. Such findings suggested an aetiological role for autoantibodies against the parathyroid in some patients suffering from hypoparathyroidism. However, additional characterisation of parathyroid autoantigens was not undertaken for a considerable period of time.

1.4.4 Autoantibodies against NACHT leucine-rich-repeat protein 5

Antibody reactivity against the NACHT leucine-rich-repeat protein 5 (NALP5) was initially discovered during the immunoscreening of a human parathyroid cDNA library with an APS1 patient's serum (Alimohammadi et al., 2008). A subsequent evaluation using a radioligand binding assay showed that NALP5 autoantibodies were detectable in 41% of 87 patients with APS1 (Alimohammadi et al., 2008). Furthermore, immunostaining of human parathyroid gland tissue using sera from the APS1 patients who had NALP5 autoantibodies identified antibody reaction towards parathyroid chief cells (Alimohammadi et al., 2008). Absorption of the serum with recombinant NALP5 protein blocked the parathyroid staining, which suggested the antibody reactivity was against NALP5 (Alimohammadi et al., 2008). In addition, no staining of parathyroid tissue was found when using APS1 patient sera without NALP5 autoantibodies (Alimohammadi et al., 2008). Interestingly, NALP5 autoantibodies were not detected in 20 patients with idiopathic hypoparathyroidism, indicating that autoimmunity against NALP5 might be specific for APS1 (Alimohammadi et al., 2008).

Subsequently, the association of NALP5 autoantibodies with APS1 was established in a report of 147 patients who had idiopathic hypoparathyroidism. A single case showed reactivity against NALP5 autoantibodies (Tomar et al., 2012). Further genetic and serological analysis confirmed that this patient had occult APS1. Autoantibodies against NALP5 have also been detected in a patient with thymoma who had acquired APS1 and hypoparathyroidism (Cheng et al., 2010), and in an APS1 patient who was suffering from chronic hypoparathyroidism (Cervato et al., 2010).

In the study of Alimohammadi and colleagues, even though all 14 APS1 patients presenting without hypoparathyroidism were negative for NALP5 autoantibodies, the usefulness of NALP5 autoantibodies as a marker for APS1-associated hypoparathyroidism is open to question, as 51% of patients with parathyroid underactivity were not positive for NALP5 autoantibodies (Alimohammadi et al., 2008). In addition, two further cases of APS1 with hypoparathyroidism were also negative for antibody reactivity against NALP5 (Tomar et al., 2012).

1.4.5 Autoantibodies against the calcium-sensing receptor

The calcium-sensing receptor (**Section 1.4.6**) has a prominent role in controlling PTH-secretion in response to the concentration of extracellular calcium (Brown et al., 1993, Brown et al., 1995). It was first identified as a potential parathyroid autoantigen by Li and co-workers (Li et al., 1996). Antibody reactivity against the CaSR was found in 14/25 (56%) of sera from patients with hypoparathyroidism using a radioligand binding assay (**Table 1.5**). With regard to the 14 patients who were CaSR antibody-positive, six had APS1 and eight had adult-onset hypoparathyroidism. Interestingly, there was a reduced chance of finding positivity for CaSR if the patient had had hypoparathyroidism for more than five years. In an independent study, an attempt to confirm these results using a radioligand binding assay was not successful (Gylling et al., 2003). Furthermore, of 60 APS1 patients (17% of whom were studied within a year of diagnosis), only 12% showed reactivity against the CaSR using a radioligand binding assay, while 4% of the control sera were also positive (Gylling et al., 2003). This study did not report an obvious difference between the APS1 patients with and without hypoparathyroidism in term of the presence of CaSR autoantibodies (**Table 1.5**).

In contrast, other studies were able to demonstrate CaSR autoantibodies in patients with hypoparathyroidism. For instance, a study of 147 idiopathic hypoparathyroid patients, showed one-quarter of the patients had CaSR autoantibodies (**Table 1.5**) (Tomar et al., 2013). In another study, the extracellular domain of the CaSR was expressed in *E. coli* and then used in immunoblotting experiments to detect CaSR autoantibodies (Mayer et al., 2004). Just below one-third of the patients with idiopathic hypoparathyroidism were positive for CaSR autoantibodies. Also, autoantibodies against the receptor were detected in one out of eight APS1 patients with hypoparathyroidism and one out of six APS2 patients with hypoparathyroidism using the same detection method (**Table 1.5**) (Mayer et al., 2004).

Autoantibodies that affected the function of the receptor were first recognised in a study of four patients with hypocalciuric hypercalcemia (Kifor et al., 2003). Anti-parathyroid antibodies were identified in these patients by immunofluorescence, while CaSR autoantibodies were identified using an immunoprecipitation method (**Table 1.5**). The functional effects of the autoantibodies on the receptor were revealed by demonstrating that patient IgG could increase the secretion of PTH from human parathyroid cells in culture. The activating effect could be blocked by pre-absorption of the patient sera with extracts of HEK293 cells containing expressed CaSR. In two cases, affinity-purified patient antibodies inhibited CaSR-mediated accumulation of inositol-phosphate and activation of mitogen-activated protein (MAP)-kinase activity in response to high extracellular Ca^{2+}. Later, two patients with idiopathic hypoparathyroidism were described by Kifor and colleagues (Kifor et al., 2004). In both patients, CaSR-stimulating antibodies could be detected using the same methods as in their previous study (Kifor et al., 2003). One patient had Graves' disease, but had undamaged parathyroid glands. The second patient had Addison's disease and spontaneously remitting hypoparathyroidism. In both patients, the fact that the parathyroid glands showed no structural abnormalities suggested that their hypoparathyroidism was due to autoantibodies against the CaSR which induced abnormal receptor function (Kifor et al., 2003).

More recently, using an immunoprecipitation assay with CaSR expressed in HEK293 cells, 86% (12/14) of the APS1 patients that participated in the study were found to be positive for CaSR autoantibodies, whereas all control sera showed a negative result

(**Table 1.5**) (Gavalas et al., 2007). Surprisingly, the same sera were negative when a radioligand binding assay was used as the CaSR antibody detection method. This highlighted the importance of the choice of assay employed to detect the autoantibodies (Gavalas et al., 2007). The prevalence of CaSR autoantibodies was significantly increased in APS1 patients compared with controls (**Table 1.5**). Although 12 of 13 patients with APS1-related hypoparathyroidism were positive for CaSR autoantibodies, the availability of only one patient without hypoparathyroidism meant it was not possible to conclude firmly that autoantibodies against the receptor were a serological marker for low parathyroid function (Gavalas et al., 2007).

In a later study, phage-display technology was applied to the analysis of the binding sites of CaSR autoantibodies in the 12 CaSR antibody-positive APS1 patients (Kemp et al., 2010). This study identified amino acids between residues 41-69 in the extracellular domain of the CaSR as the major epitope recognised by the CaSR autoantibodies in APS1 patients. Other epitopes identified were amino acids between residues 114-126 and 171-195 (Kemp et al., 2010). Further studies on the same 12 APS1 patients revealed that IgG samples from two of the patients (both with hypoparathyroidism) with CaSR autoantibodies elevated both Ca^{2+}-dependent inositol-phosphate accumulation and MAP-kinase phosphorylation in HEK293 cells expressing the CaSR, indicating a stimulatory effect on the receptor (Kemp et al., 2009). While the majority of APS1 patients in this study did not have detectable CaSR-stimulating autoantibodies, the study highlighted a small minority of patients whose hypoparathyroidism was the result of functional suppression of the parathyroid glands rather than their irreversible destruction.

Overall, a number of aspects of CaSR autoantibodies in idiopathic hypoparathyroidism and APS1 need to be investigated. Firstly, the variability of their prevalence (**Table 1.5**) could be due to differences in the type of measurement method employed, as no gold standard test for CaSR autoantibodies is currently available. Importantly, the CaSR antigen (used to detect reactivity) can have a major impact on the frequency of autoantibody detection (Gylling et al., 2003, Gavalas et al., 2007). In addition, the ethnicity and size of the patient and control groups, as well as the criteria to identify positivity may affect the reported prevalence of CaSR autoantibodies. Secondly, while they might just be markers for parathyroid gland destruction resulting from the action

of cytotoxic T cells (Wortsman et al., 1992), the effects of CaSR autoantibodies on receptor function, which could lead to the development hypoparathyroidism, needs further investigation. Although only a small number of cases have been reported of CaSR-activating autoantibodies (Kifor et al., 2004, Kemp et al., 2009), it could be that CaSR autoantibodies have effects such as complement-fixation or antibody-dependent cellular cytotoxicity, processes that could lead to parathyroid destruction (Brandi et al., 1986). Finally, the question as to the correlation of CaSR autoantibodies and hypoparathyroidism in APS1 requires clarification.

Table1.5: Prevalence of CaSR autoantibodies in idiopathic and APS1-associated hypoparathyroidism

Method of CaSR autoantibody detection	Number of participants with CaSR autoantibodies (%)		*P* value[2]	*P* value[3]	Reference
Radioligand binding assay with *in vitro* translated CaSR	APS1 with HP[1] HP Controls	6/17 (35) 8/8 (100) 0/22 (0)	0.004 < 0.0001	-	(Li et al., 1996)
Radioligand binding assay with *in vitro* translated CaSR	APS1 with HP APS1 no HP Controls	6/50 (12) 1/10 (10) 8/192 (4)	0.044 0.370	1.000	(Gylling et al., 2003)
Radioligand binding assay with *in vitro* translated CaSR	APS1 with HP APS1 no HP Controls	0/73 (0) 0/17 (0) 0/100 (0)	- -	-	(Soderbergh et al., 2004)
Immunoblotting of the CaSR expressed in *Escherichia coli*	APS1 with HP HP APS2 with HP APS2 no HP Controls	1/8 (13) 5/17 (29) 1/6 (17) 0/27 (0) 0/32 (0)	0.200 0.003 0.162 -	- - 0.182	(Mayer et al., 2004)
Immunoprecipitation of the CaSR expressed in HEK293 cells	HP Controls	2/2 (100) 0/5 (0)	0.048	-	(Kifor et al., 2003)
Immunoprecipitation of the CaSR expressed in HEK293 cells	APS1 with HP APS1 no HP Controls	12/13 (92) 0/1 (0) 0/28 (0)	< 0.0001 -	0.143	(Gavalas et al., 2007)
Immunoblotting of the CaSR expressed in HEK293 cells	HP Controls	36/147 (25) 27/199 (14)	0.011	-	(Tomar et al., 2013)

[1]HP, hypoparathyroidism.
[2]Patients compared with controls.
[3]APS1 or APS2 patients with hypoparathyroidism compared to those without hypoparathyroidism.

1.4.6 The calcium-sensing receptor

Since the CaSR has been identified as a target of autoantibodies in APS1 and these are analysed in this thesis, the structure and the functioning of the receptor in the parathyroid are summarised in the next sections.

1.4.6.1 Structure of the calcium-sensing receptor

The gene encoding the G-protein-coupled CaSR is located on the long arm of chromosome 3, and is composed of seven exons, six of which encode the extracellular domain and one of which encodes both the transmembrane and intracellular domains (Brown and MacLeod, 2001). The CaSR is 120 kDa in size, is composed of 1,078 amino acids, and consists of three different parts (**Figure 1.9**). The extracellular N-terminal domain, which is composed of 612 amino acids, contains all the Ca^{2+}-binding sites (Brauner-Osborne et al., 1999). All CaSR agonists and antagonists also act on this domain (Brauner-Osborne et al., 1999). The second part of the CaSR is a 250-amino acid seven transmembrane domain. Finally, the C-terminal intracellular domain is composed of 216 amino acids (Brown et al., 1998, Garrett et al., 1995). From the high resolution crystal structure of the related metabotropic glutamate receptor type 1 (Kunishima et al., 2000), a conformational structure for the CaSR has been suggested (**Figure 1.10**). The CaSR is proposed to exist as a dimer (Gama et al., 2001) with the paired extracellular domains assuming a bi-lobed, venus-flytrap structure (Hermans and Challiss, 2001).

The extracellular domain contains a cysteine-rich region which connects the venus-flytrap structure of the CaSR with the transmembrane domain (**Figure 1.10**), and which appears to be necessary for signalling between these two parts of the protein (Hu et al., 2000). It has been reported that mutations in the cysteine-rich region which change the cysteine residues lead to abnormalities in expression and function of the receptor (Fan et al., 1998). Furthermore, deletion of this region adversely affects CaSR function, even though it does not bind Ca^{2+} directly (Hu et al., 2000). Biochemical studies of several other cysteine residues within the extracellular domain, for example C129 and C131 (**Figure 1.9**), have found that they are important in ensuring the correct receptor conformation (Bai, 2004).

Further analysis of the extracellular domain shows it contains 11 N-linked glycosylation sites which have a role in the folding and export of the CaSR, but not in its function (**Figure 1.9**) (Ray et al., 1998). This extracellular domain contains four loop structures (**Figure 1.9**), three of which have been shown by mutational analysis to have a critical role in CaSR function (Reyes-Cruz et al., 2001). For example, mutations in loop 1 (G39-G67) and loop 4 (C437-C449) lead to a reduction in the receptor's response to Ca^{2+}, and deletion of loop 2 (Q117-S137) can obliterate receptor function. Mutations in loop 3 (F356-I416) have not been found mutations to affect receptor function (Reyes-Cruz et al., 2001).

The Ca^{2+}-binding sites in the extracellular domain of the CaSR have not been defined exactly due to the lack of a crystal structure for the receptor and the limitation of methods used to measure direct binding of Ca^{2+}. The current identified sites are predicted based on the crystal structures of metabotropic glutamate receptor type 1 (Kunishima et al., 2000, Zhang et al., 2015). Ca^{2+}-binding site 1 is a pocket involving amino acids S147, S170, D190, Y218 and E297, and is located between loops 1 and 2 (Silve et al., 2005, Huang et al., 2007) (**Figure 1.11**). Mutating any of these amino acid residues causes abnormalities in receptor function (Silve et al., 2005, Huang et al., 2007). Site 1 is the most convincing as a Ca^{2+}-binding site compared to the four other sites that have been proposed (Zhang et al., 2015).

In the CaSR, 250 amino acids form the transmembrane domain consisting of seven membrane-spanning regions which connect the extracellular and intracellular parts of the receptor (**Figure 1.9 and Figure 1.10**) (Brown and MacLeod, 2001). The transmembrane domain is involved in phospholipase C activation and thus receptor activity (Chang et al., 2000). The inner C-terminal domain of the receptor is crucial for signalling and contains two protein kinase A and five protein kinase C phosphorylation sites which are involved in CaSR activity (**Figure 1.9 and Figure 1.10**) (Bai et al., 1997, Jiang et al., 2002).

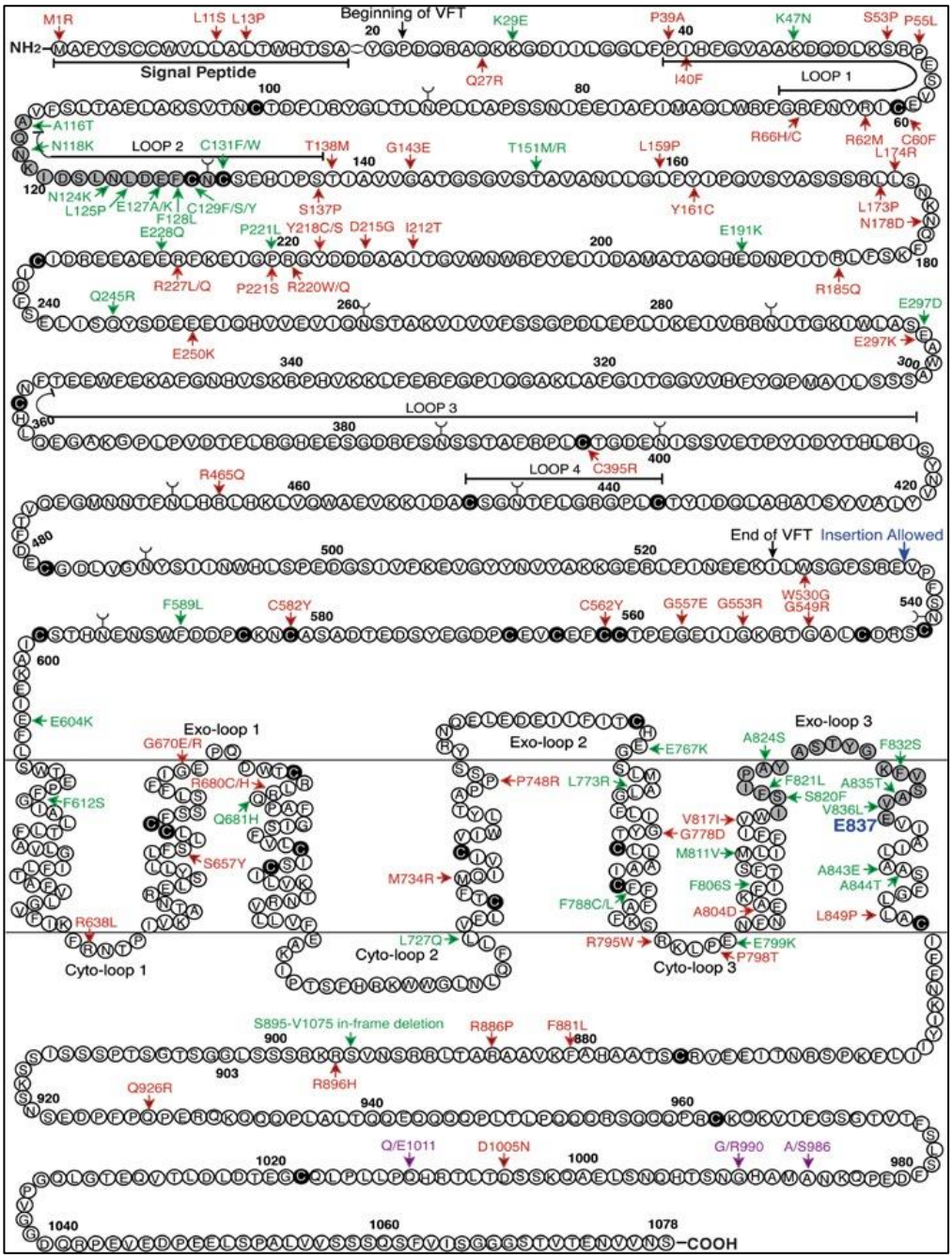

Figure 1.9: Schematic representation of the calcium-sensing receptor

The amino acid sequence of the calcium-sensing receptor is shown with the single letter code. The following are features are shown: cysteine residues in black, amino (N)-linked glycosylation sites indicated by the Y symbol, the beginning and end of the venus-flytrap (VFT) region in the extracellular domain, loops 1-4 of the extracellular domain, and the cysteine-rich region that connects the VFT region to the transmembrane domain. The image, from a paper by (Hu and Spiegel, 2007), is used with kind permission from John Wiley and Sons.

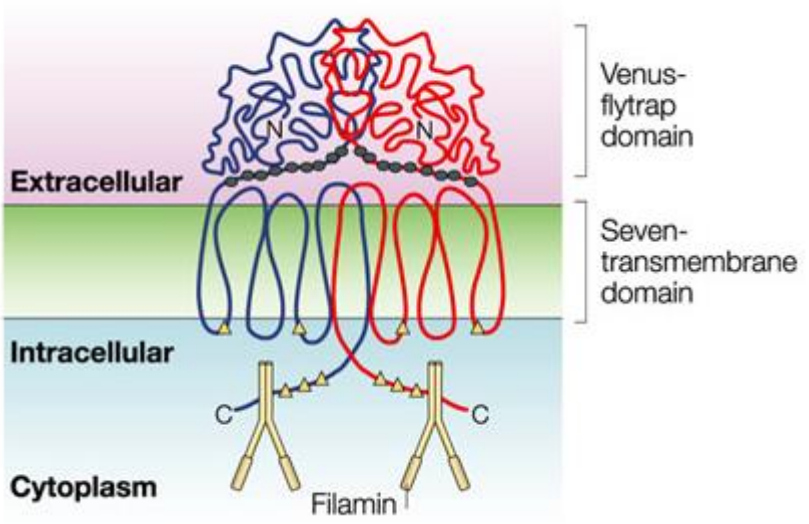

Figure 1.10: A model of the dimeric form of the extracellular CaSR.

The CaSR is composed of a dimer pair, which is shown in red and blue. The extracellular domains assume a bi-lobed, venus-flytrap modelled on the known crystal structure of the metabotropic glutamate receptor type 1 (Kunishima et al., 2000). Each amino (N)-terminal extracellular domain is composed of 612 amino acids. Each CaSR monomer has a 250-amino acid seven transmembrane domain. The cysteine residues that comprise the cysteine-rich domain between the extracellular domain and the transmembrane domain are indicated as grey circles. The carboxy (C)-terminal intracellular domain is composed of 216 amino acids. The locations of the internal putative protein kinase C phosphorylation sites are indicated as yellow triangles. The image, from a paper by (Hofer and Brown, 2003), is used with kind permission from Nature Publishing Group.

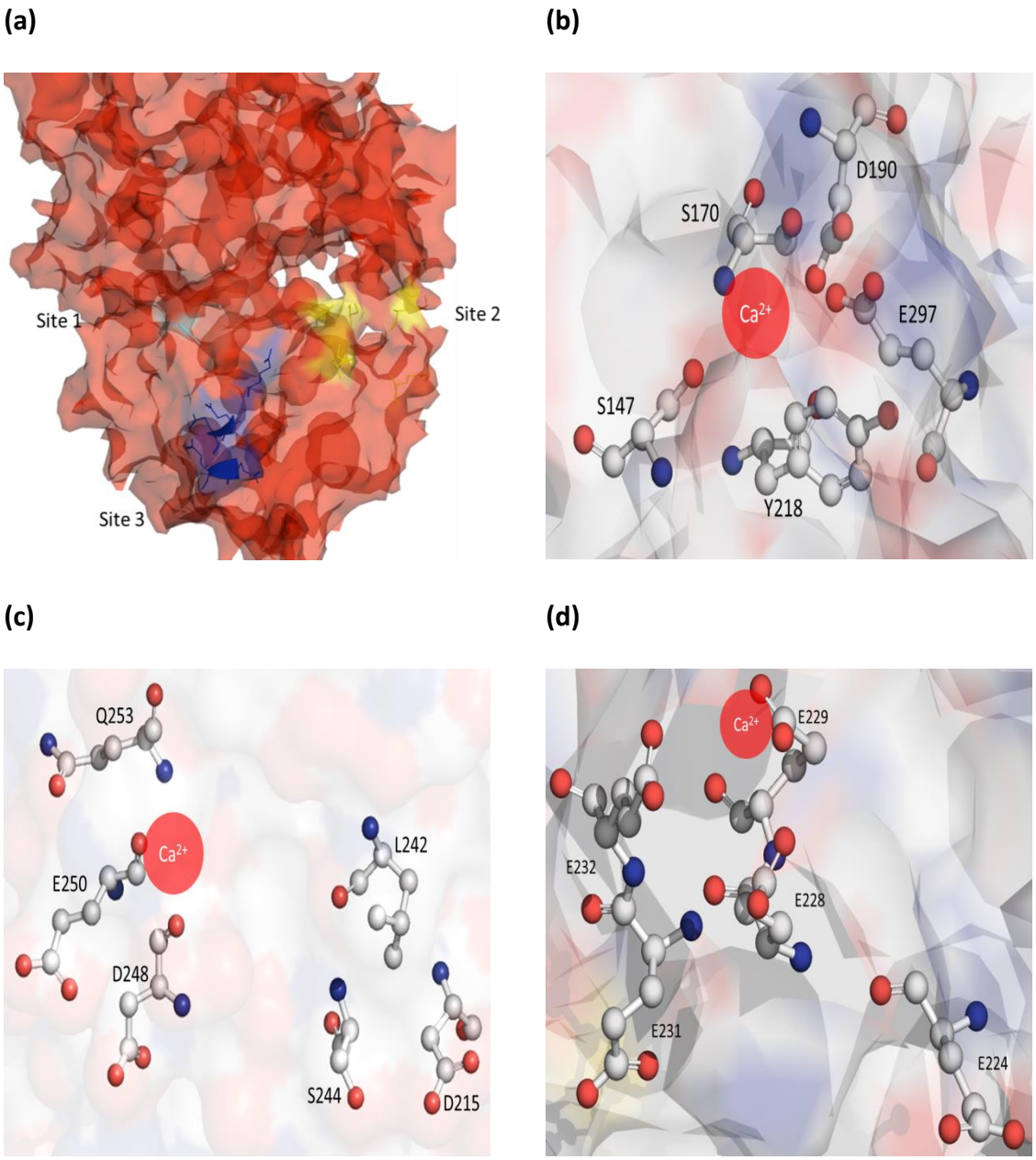

Figure 1.11: Ca^{2+} binding sites on the CaSR.

The predicted Ca^{2+} binding sites were taken from Huang et al., 2010. **(a)** The location of Ca^{2+} binding sites with respect to the CaSR are site 1 in cyan, site 2 in yellow and site 3 in blue; **(b)** Site 1 showing the amino acid residues involved; **(c)** Site 2 showing the amino acid residues involved; and **(d)** Site 3 showing the amino acid residues involved. These figures were generated by PyMol software.

1.4.6.2 Functioning of the CaSR in the parathyroid in response to Ca^{2+}

The CaSR is predominantly expressed in the parathyroid gland (Brown and MacLeod, 2001) where it controls the release of PTH in order to maintain blood calcium levels within strict limits 2.25-2.5 mmol/L (Brown et al., 1993). The receptor is activated by direct contact of Ca^{2+} at the Ca^{2+}-binding sites in the extracellular domain (**Figure 1.12**). The presence of high Ca^{2+} concentrations stimulates the CaSR triggering a Gq-protein-mediated activation of phospholipase C (**Figure 1.12**). Activated phospholipase C hydrolyses phosphatidylinositol-4,5-bisphosphate to inositol 1,4,5-trisphosphate, which in turn evokes the release of Ca^{2+} from cytosolic stores (Squires, 2000). In addition, Ca^{2+} can enter the cellular space by tissue-specific voltage dependent Ca^{2+} channels (Scherubl et al., 1991) and/or non-selective cation channels (Silva et al., 1994). The elevation of intracellular Ca^{2+} inhibits the exocytosis of PTH and, therefore, a return to normal blood calcium concentrations is achieved (Chattopadhyay et al., 1996).

Conversely, when low serum Ca^{2+} concentrations are detected by the CaSR, the secretion of PTH from the parathyroid is initiated (Brown et al., 1995). As a consequence, uptake of Ca^{2+} by the intestine is increased as PTH induces the production of 1,25-dihydroxyvitamin D (**Figure 1.13**) (Brown, 1999). Higher PTH levels also cause the release of Ca^{2+} from bone tissue and re-absorption of Ca^{2+} by the kidneys (**Figure 1.13**) (Kurokawa, 1994, Manolagas and Jilka, 1995). As a consequence, serum Ca^{2+} levels are returned to a normal baseline value.

Abnormally elevated activity of the CaSR in the presence of low serum Ca^{2+} can be caused by activating mutations or stimulating autoantibodies results in lowering of PTH-secretion. Mutations that activate the CaSR are associated with autosomal dominant hypocalcemia (Pollak et al., 1994, Pearce et al., 1996, Lienhardt et al., 2001). In patients with this disease, the receptor gains high sensitivity to serum Ca^{2+} (Brown, 2007) leading to the clinical symptoms of low PTH levels, hypocalcemia, hypercalciuria, and hyperphosphatemia (Winter et al., 1983). Autoantibodies that stimulate the receptor have an analogous effect upon PTH secretion and thus autoimmune hypoparathyroidism can result (**Section 1.4.5**) (Kifor et al., 2004, Kemp et al., 2009).

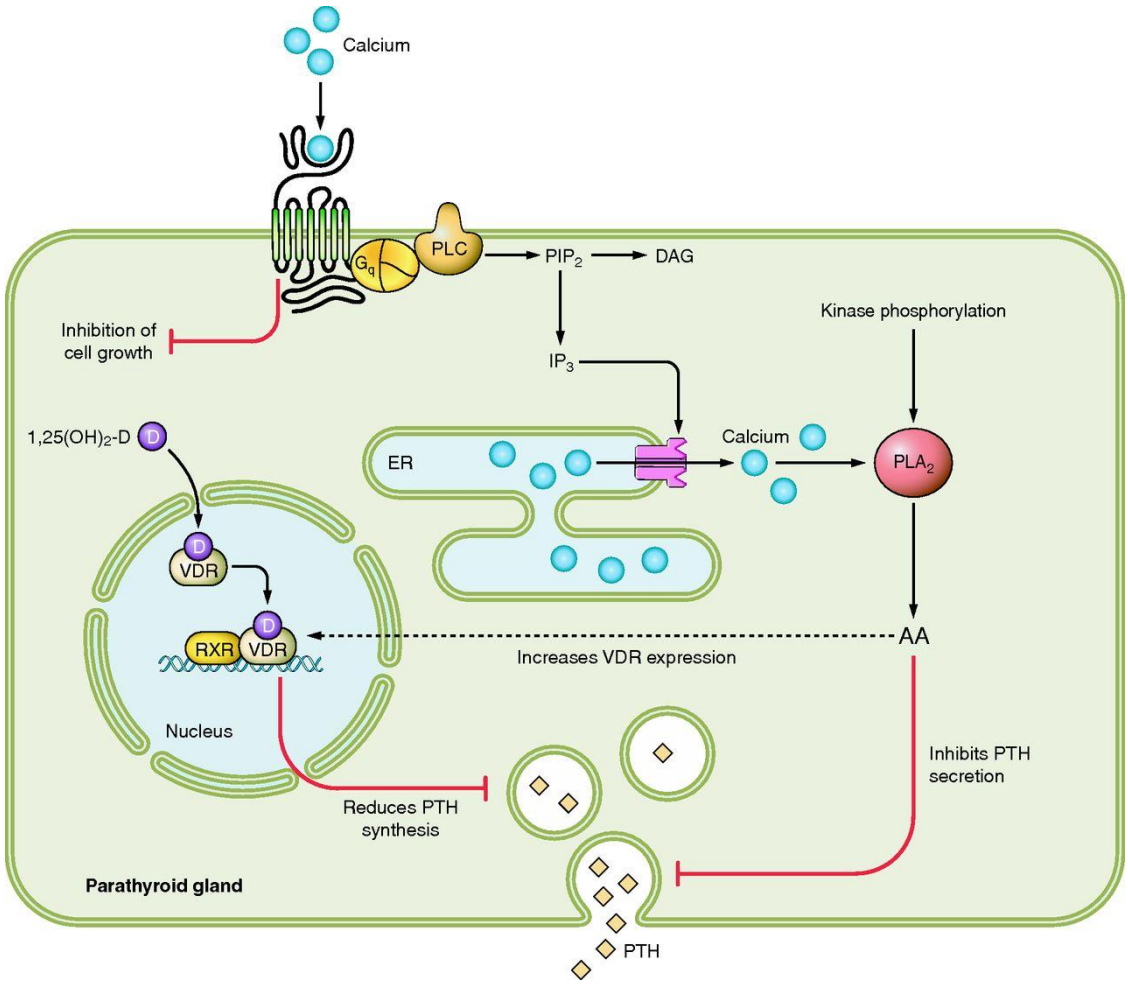

Figure 1.12: Functioning of the calcium-sensing receptor in the parathyroid in response to Ca^{2+}.

High serum Ca^{2+} concentrations stimulate, via the calcium-sensing receptor on parathyroid chief cells, a Gq-protein-mediated activation of phospholipase C (PLC). The resulting formation of inositol 1,4,5-trisphosphate (IP3) evokes an increase in Ca^{2+} from cytosolic stores in the endoplasmic reticulum (ER). Activation of CaSR leads to production of arachidonic acid (AA) metabolites, which inhibit the release of parathyroid hormone (PTH) and increase the expression of vitamin D receptor (VDR), which in addition to the elevation of intracellular Ca^{2+} inhibits the exocytosis of PTH. A return to normal blood calcium concentrations is therefore achieved. Conversely, a low serum Ca^{2+} concentration leads to PTH release which causes uptake of Ca^{2+} by the intestine, release of Ca^{2+} from bone tissue and re-absorption of Ca^{2+} by the kidneys. Consequently, serum Ca^{2+} levels are returned to a normal baseline level. The image, from a paper by (Kopic and Geibel, 2013), did not require permission for use in this thesis.

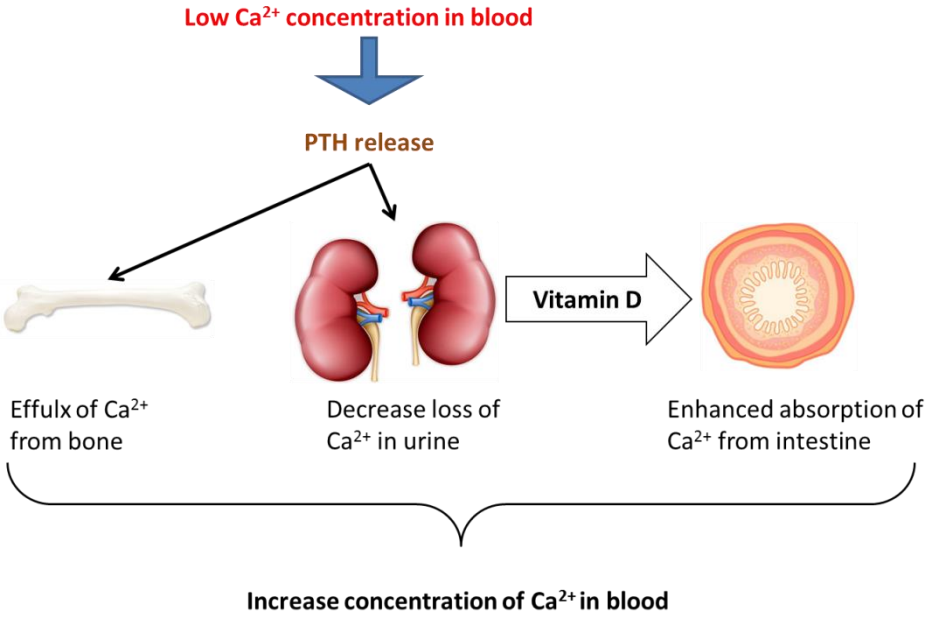

Figure 1.13: Schematic view of Ca2+ homeostasis controlled by parathyroid hormone.

Reduced serum Ca^{2+} concentrations activate the calcium-sensing receptor causing secretion of parathyroid hormone (PTH) from the parathyroid. In consequence, higher PTH levels cause the release of Ca^{2+} from bone tissue and re-absorption of Ca^{2+} by the kidneys, also uptake of Ca^{2+} by the intestine is increased as PTH induces the production of 1,25-dihydroxyvitamin D. As a consequence, serum Ca^{2+} levels are returned to a normal baseline value.

1.5 Project Aims

Previous work in our laboratory detected CaSR autoantibodies in 12/14 of patients with APS1 using CaSR expressed in mammalian cells in an immunoprecipitation assay (Gavalas et al., 2007). In addition, CaSR autoantibodies that stimulate the CaSR have been found in a small minority (2/14) of APS1 patients (Kemp et al., 2009). Further studies have identified the binding sites (epitopes) of the CaSR autoantibodies in APS1 patients. The epitopes were mapped to amino acid residues 41-69 (12/14 patients), 114-126 (5/14 patients) and 171-195 (4/14 patients) at the amino-terminal of the extracellular domain of the receptor (Kemp et al., 2010). The current project will aim to investigate further the properties of and the role of CaSR autoantibodies in APS1 patients. The specific aims will be:

- To investigate the prevalence of CaSR autoantibodies in a larger cohort of APS1 patients.
- To investigate the association of CaSR autoantibodies with the clinical manifestations, particularly hypoparathyroidism.
- To examine any adverse functional affects upon the CaSR of any detected CaSR autoantibodies.
- To determine the binding sites of any newly detected CaSR autoantibodies.
- To determine the IgG subclasses of CaSR autoantibodies.
- To develop a convenient ELISA format using recombinant CaSR for detecting CaSR autoantibodies in patient sera.

Chapter 2

General Materials and Methods

2 General Materials and Methods

2.1 Reagents

The majority of reagents, including chemicals, buffers, solvents, acids and media components were purchased from Sigma-Aldrich (Poole, UK), Melford Laboratories (Ipswich, UK) or Fisher Scientific UK Ltd. (Loughborough, UK), and were of analytical or molecular biology grade. The source of some reagents is indicated in the text.

2.2 Plasticware

Plasticware including: 90-mm petri-dishes, 96-well microtitre plates, 6-well plates, 0.5-ml and 1.5-ml tubes, universal tubes, pipette tips, pipettes, and Oak Ridge centrifuge tubes, cell culture flasks and dishes were from either Sarstedt Ltd. (Numbrecht, Germany), Starlab (UK) Ltd. (Milton Keynes, UK), Corning Incorporated (Corning, NY, USA), Nalgene Nunc International (Rochester, NY, USA) or Bibby Sterilin Ltd. (Bargoed, UK).

2.3 Bacterial growth medium

Luria Bertani (LB) medium was prepared in deionised water and contained: 1% (w/v) tryptone, 0.5% (w/v) yeast extract, and 1% (w/v) sodium chloride. Medium 2YT was also made in deionised water and was composed of: 1.6% (w/v) tryptone, 1% (w/v) yeast extract, and 0.5% (w/v) sodium chloride. Media were sterilised by autoclaving at 121°C for 20 min. Solid media were prepared by adding 1.5% (w/v) agar to the appropriate liquid medium before sterilisation. After autoclaving, the agar was left to cool to about 40-45°C before adding any required antibiotic(s). The cooled agar was poured into 90-mm petri-dishes and allowed to set. Plates were then dried and stored at 4°C until required.

Antibiotics were prepared as 1000x concentrated stocks. Ampicillin (sodium salt) and kanamycin sulphate were prepared in deionised water, chloramphenicol in 100% ethanol, and tetracycline hydrochloride in 50% (w/v) ethanol. Solutions were sterilised by filtration through 0.22 micron Millex® Filter Units (Millipore Corp., Bedford, MA, USA). Antibiotic solutions were stored at –20°C and used in culture medium and agar

plates when required at the following concentrations: ampicillin (sodium salt), 100 μg/ml; kanamycin sulphate, 50 μg/ml; chloramphenicol, 30 μg/ml; tetracycline hydrochloride, 10 μg/ml.

2.4 Bacterial strains

The bacterial strains used in this study were derivatives of *Escherichia coli* and are given in **Table 2.1.** Derivatives of bacterial strains carrying plasmid vectors or recombinant plasmids were constructed by transformation (**Section 2.13**). All *E. coli* strains were routinely grown from frozen stocks by initially streaking onto LB agar plates (**Section 2.3**), containing selective antibiotic(s) where required (**Section 2.3**). Plates were then incubated at 37°C overnight. A single colony of the desired bacterial strain was then inoculated into LB medium with the appropriate antibiotic supplementation, and incubated at 37°C overnight in a rotary incubator shaking at 250 revolutions per minute (rpm). For long-term storage at -80°C, 0.7-ml aliquots of an overnight-grown bacterial culture were mixed with 0.3-ml aliquots of sterile 50% (v/v) glycerol.

2.5 Plasmids

The plasmids used in this study are listed in **Table 2.2.** They were stored at -20°C in sterile TE buffer (10 mM Tris-hydrochloride; 1 mM ethylenediaminetetraacetic acid (EDTA); pH 8.0) (Promega, Southampton, UK). Diagrams of plasmids pDEST14-CaSR (Source BioScience imaGenes, Berlin, Germany), pCR®2.1-TOPO® (Life Technologies Ltd., Paisley, UK), pET14b (Novagen/Merck KgaA, Darmstadt, Germany) are shown in **Figures 6.4, 6.6 and 6.1**, respectively.

Table 2.1: Bacterial strains

Strain	Details	Source
JM109	Used for the propagation of plasmid vectors and recombinant plasmids.	Promega (Southampton, UK)
BL21 (DE3)	Used for the expression of cloned DNA.	Agilent Technologies Inc. (Santa Clara, CA, USA)
BL21 (DE3)pLysS	Used for the expression of cloned DNA. Chloramphenicol resistant.	Agilent Technologies Inc.
BL21 GOLD (DE3)	Used for the expression of cloned DNA. Tetracyline resistant.	Agilent Technologies Inc.
BL21 GOLD (DE3)pLysS	Used for the expression of cloned DNA. Chloramphenicol and tetracycline resistant.	Agilent Technologies Inc.
BL21 CODONPLUS (DE3)-RIPL	Used for the expression of cloned DNA. Chloramphenicol, tetracycline and streptomycin resistant.	Agilent Technologies Inc.
TOP10F'	Used for recovery of cloned PCR amplification products from TOPO® cloning reactions.	Life Technologies Ltd. (Paisley, UK)
JM109/pCMV6-XL5-NALP5	Carries recombinant plasmid pCMV6-XL5-NALP5 (**Table 2.2**)	Dr. Helen Kemp (Department of Oncology and Metabolism, University of Sheffield, Sheffield, UK)
JM109/pcCaSR-FLAG	Carries recombinant plasmid pcCaSR-FLAG (**Table 2.2**)	Dr. Helen Kemp
JM109/pDEST14-CaSR	Carries recombinant plasmid pDEST14-CaSR (**Table 2.2**).	This study (Chapter 6)
JM109/pET14b	Carries plasmid vector pET14b (**Table 2.2**).	This study (Chapter 6)
JM109/pET14b-CaSRECD	Carries recombinant plasmid pET14b-CaSRECD (**Table 2.2**).	This study (Chapter 6)
TOP10F'/pCR2.1-TOPO-CaSRECD	Carries recombinant plasmid pCR2.1-TOPO-CaSRECD (**Table 2.2**).	This study (Chapter 6)
BL21 (DE3)/pET14b-CaSRECD	Carries recombinant plasmid pET14b-CaSRECD (**Table 2.2**).	This study (Chapter 6)
BL21 (DE3)pLysS /pET14b-CaSRECD	Carries recombinant plasmid pET14b-CaSRECD (**Table 2.2**).	This study (Chapter 6)
BL21 GOLD (DE3)/pET14b-CaSRECD	Carries recombinant plasmid pET14b-CaSRECD (**Table 2.2**).	This study (Chapter 6)
BL21 GOLD (DE3)pLysS /pET14b-CaSRECD	Carries recombinant plasmid pET14b-CaSRECD (**Table 2.2**).	This study (Chapter 6)
BL21 CODONPLUS (DE3)-RIPL/ pET14b-CaSRECD	Carries recombinant plasmid pET14b-CaSRECD (**Table 2.2**).	This study (Chapter 6)
BL21 (DE3)/pET14b	Carries plasmid vector pET14b (**Table 2.2**).	This study (Chapter 6)
BL21 (DE3)pLysS /pET14b	Carries plasmid vector pET14b (**Table 2.2**).	This study (Chapter 6)
BL21 GOLD (DE3)/pET14b	Carries plasmid vector pET14b (**Table 2.2**).	This study (Chapter 6)
BL21 GOLD (DE3)pLysS /pET14b	Carries plasmid vector pET14b (**Table 2.2**).	This study (Chapter 6)
BL21 CODONPLUS (DE3)-RIPL/ pET14b	Carries plasmid vector pET14b (**Table 2.2**).	This study (Chapter 6)
BL21 CODONPLUS (DE3)-RIPL/ pPROEX-HTb-CaSREx	Carries plasmid vector pPROEX-HTb (**Table 2.2**).	This study (Chapter 6)

Table 2.2: Plasmid vectors and recombinant plasmids

Plasmid	Details	Source
pDEST14-CaSR	Plasmid vector pDEST14 containing full-length Calcium-sensing receptor (CaSR) cDNA (3.2-kilobase). Selectable marker is ampicillin resistance (**Figure 6.4**).	Source BioScience imaGenes (Berlin, Germany)
pCR®2.1-TOPO®	A 3.9-kilobase vector for cloning PCR products. Contains binding sites for T7 Promoter and M13 Reverse primers flanking the cloning site. Selectable markers are ampicillin and kanamycin resistance (**Figure 6.6**).	Life Technologies Ltd. (Paisley, UK)
pCR2.1-TOPO-CaSRECD	Plasmid vector pCR®2.1-TOPO® containing CaSR-extracellular domain cDNA (base pairs 1-1800). Selectable markers are ampicillin and kanamycin resistance.	This study (Chapter 6)
pET14b	A 4.7-kilobase expression vector with a selectable resistance marker to ampicillin. Contains binding sites for T7 Promoter and T7 Terminator primers flanking a multiple cloning site (**Figure 6.1**).	Novagen/Merck KgaA (Darmstadt, Germany)
pET14b-CaSRECD	Plasmid vector pET14b containing CaSR extracellular domain cDNA (base pairs 1-1800) cloned into the *Xho*I restriction site. Selectable marker is ampicillin resistance.	This study (Chapter 6)
pCMV6-XL5-NALP5	Plasmid vector pCMV-XL5 containing NACHT leucine-rich-repeat protein 5 (NALP5) cDNA (3.6-kilobase). Selectable marker is ampicillin resistance (**Figure 3.4**).	Professor Olle Kampe (Department of Medical Sciences, Uppsala University Hospital, Uppsala, Sweden)
pcCaSR-FLAG	Plasmid vector pcDNA3 containing full-length CaSR cDNA (3.2-kilobase) with a FLAG tag. Selectable marker is ampicillin resistance (**Figure 3.1**).	Dr. Helen Kemp (Department of Oncology and Metabolism, University of Sheffield, Sheffield, UK)
pcDNA3-CaSR	Plasmid vector pcDNA3 containing full-length CaSR cDNA (3.2-kilobase). Selectable marker is ampicillin resistance (**Figure 3.2**).	Dr. Helen Kemp
pPROEX-HTb-CaSREx	Plasmid vector pPROEX-HTb containing CaSR extracellular domain cDNA (base pairs 58-1800) cloned into the *XhoI* restriction site. Selectable marker is ampicillin resistance (**Figure 6.3**).	Professor Ravinder Goswami (Department of Endocrinology and Metabolism, All India Institute of Medical Sciences, New Delhi, India).

2.6 Small-scale plasmid preparations

This method was carried out according to the protocol of Dr Helen Kemp (Department of Oncology and Metabolism, University of Sheffield, Sheffield, UK). The Wizard® *Plus* SV Minipreps DNA Purification System (Promega) was used to purify plasmid DNA from a 5-ml or 10-ml overnight culture of the required bacterial strain, according to the manufacturer's protocol. Briefly, a single colony of the desired bacterial strain was isolated by streaking out 20 µl of frozen bacterial stock onto LB agar containing the appropriate antibiotic(s). A single colony from the selective plate was then used to inoculate 10 ml of LB medium containing the relevant antibiotic(s) which was subsequently shaken in a rotary incubator at 250 rpm at 37°C overnight. The bacterial cell pellet was obtained by centrifugation at 10,000 *g* for 10 min and resuspended in 250 µl of Cell Resuspension Solution (50 mM Tris-hydrochloride, pH 7.5; 10 mM EDTA; 100 µg/ml RNase A). The cells were lysed by the addition of 250 µl of Cell Lysis Solution (200 mM sodium hydroxide; 1% (w/v) sodium dodecyl sulphate (SDS)). The cell extract was then neutralised by the addition of 350 µl of Neutralisation Solution (759 mM potassium acetate; 4.09 M guanidine hydrochloride; 2.12 M glacial acetic acid; pH 4.2), mixed gently and centrifuged at 10,000 *g* for 10 min at room temperature. The cleared lysate was then loaded on to a Wizard® SV Minicolumn which was centrifuged at 10,000 *g* for 1 min at room temperature and the flow- through discarded. The Minicolumn was washed with 750 µl of Column Wash Solution (60% (v/v) ethanol; 60 mM potassium acetate; 8.3 mM Tris-hydrochloride; 0.04 mM EDTA) and then with 250 µl of Column Wash Solution with centrifugation at for 2 min at room temperature each time. To recover the DNA bound to the column, 100 µl of nuclease-free water was added to the column and this was centrifuged at 10,000 *g* for 1 min at room temperature. The concentration of the DNA was measured by spectrophotometry at 260 nm using a NanoDrop ND-1000 Spectrometer (Labtech, Wilmington, DE, USA) and NanoDrop Software (Labtech). Plasmids were checked qualitatively by agarose gel electrophoresis (**Section 2.8**).

2.7 Large-scale plasmid preparations

This method was carried out according to the protocol of Dr Helen Kemp (Department of Oncology and Metabolism, University of Sheffield, Sheffield, UK). A large-scale

culture of the bacterial strain carrying the desired plasmid was prepared by inoculation of 0.5-1 litres of LB medium containing the appropriate antibiotic(s), with a 10-ml starter culture. This was followed by incubation overnight with shaking at 37°C. The culture was then centrifuged at 4,000 *g* for 30 min and plasmid extracted from the cell pellet using a Qiagen Plasmid DNA Maxiprep Kit (Qiagen Ltd., Crawley, UK) as directed in the manufacturer's protocol. The bacterial cell pellet was resuspended in 10 ml of P1 Buffer (50 mM Tris-hydrochloride, pH 8.0; 10 mM EDTA; 100 µg/ml RNase A) in a 50-ml Oak Ridge centrifuge tube. An equal volume of P2 Buffer (200 mM sodium hydroxide; 1% (w/v) SDS) was then added to the resuspended cells and mixed by gentle inversion, followed by incubation at room temperature for 5 min. After the addition of 10 ml of P3 Buffer (1.32 M potassium acetate, pH 5.5), the lysed cells were mixed gently but thoroughly and incubated on ice for 20 min. The cell extract was subsequently centrifuged at 20,000 *g* for 30 min at 4°C resulting in a clear supernatant. A Qiagen column was equilibrated by adding QBT Buffer (750 mM sodium chloride; 50 mM 3-[N-morpholino]propanesulphonic acid (MOPS), pH 7.0; 15% (v/v) isopropanol; 0.15% (v/v) Triton X-100) and was allowed to empty by gravity flow. The clear supernatant was then loaded onto the column and left to flow through before washing the column twice with 30 ml of QC Buffer (1 M sodium chloride; 50 mM MOPS, pH 7.0; 15% (v/v) isopropanol). Subsequently, plasmid DNA was eluted with 15 ml of QF Buffer (1.25 M sodium chloride; 50 mM Tris-hydrochloride, pH 8.5; 15% (v/v) isopropanol) and precipitated by the addition of 10.5 ml of 100% isopropanol and centrifugation at 15,000 *g* for 30 min at 4°C. The resulting DNA pellet was washed with 70% (v/v) ethanol, centrifuged at 15,000 *g* for 10 min at 4°C and finally resuspended in 300 µl of TE buffer. The concentration of the DNA was measured by spectrophotometry (**Section 2.6**). Plasmids were also checked qualitatively by agarose gel electrophoresis (**Section 2.8**).

2.8 Agarose gel electrophoresis

This method was carried out according to the protocol of Dr Helen Kemp (Department of Oncology and Metabolism, University of Sheffield, Sheffield, UK). For analysis of DNA, agarose gels, 0.8-1% (w/v), were prepared by boiling molecular biology grade agarose in TAE electrophoresis buffer (40 mM Tris-acetate; 1 mM EDTA; pH 8.3) (Promega) for 1-2 min in a microwave oven. For every 50 ml of the gel solution, 1 µl of

ethidium bromide solution (10 mg/ml) (Promega) The molten agarose was cooled and poured into the casting deck of a Sub-Cell® Horizontal Electrophoresis System (Bio-Rad Laboratories Ltd., Hemel Hempstead, UK). After the gel had set, the combs were removed and the gel placed in the electrophoresis tank with TAE as the running buffer. Blue/Orange Loading Dye 6x (0.4% (w/v) orange G; 0.03% (w/v) bromphenol blue; 0.03% (w/v) xylene cyanol FF; 15% (w/v) Ficoll® 400; 10 mM Tris-hydrochloride, pH 7.5; 50 mM EDTA, pH 8.0) (Promega) was added to the DNA sample at 1/6th of the volume, and the sample was then loaded into a gel slot. To size DNA products after they had migrated through the gel, a 'marker' lane was included which contained a 0.5-1.0-µg sample of either *Hin*dIII-restricted bacteriophage λ DNA (125-23,130-bp DNA fragments) (Promega) or 1-kb DNA Ladder (500-10,000-bp DNA fragments) (New England Biolabs®, Hitchin, UK). Gels were run in a Sub-Cell® Horizontal Electrophoresis System (Bio-Rad Laboratories Ltd.) at 50-70 volts using a PowerPac Basic Power Supply (Bio-Rad Laboratories Ltd.), and subsequently viewed and recorded using a GBOX Gel Documentation System (Syngene, Cambridge, UK) and GeneSnap Image Acquisition Software (Syngene).

2.9 Restriction enzyme digests

This method was carried out according to the protocol of Dr Helen Kemp (Department of Oncology and Metabolism, University of Sheffield, Sheffield, UK). Restriction enzymes **(Table 2.3)** and restriction enzyme buffers **(Table 2.3)** were supplied by Promega. Restriction enzyme digests of plasmids and polymerase chain reaction (PCR) amplification products were carried out in 0.5-ml tubes in a volume not normally exceeding 25 µl and contained up to 1 µg of DNA, 10 units of enzyme(s) and 0.1 volumes of the appropriate 10x restriction enzyme buffer. Each reaction proceeded for 90 min at 37°C, unless otherwise stated. Restriction digests were analysed by agarose gel electrophoresis (**Section 2.8**).

Table 2.3: Restriction enzymes and buffers

Enzyme[1]	Buffer (10x concentration)[1]	Restriction site
*Xho*I	Buffer D: 60 mM Tris-HCl, pH 7.9; 1.5 M NaCl; 60 mM $MgCl_2$; 10 mM dithiothreitol.	5'-CTCGAG-3'

[1]Enzymes and buffers were supplied by Promega (Southampton, UK).

2.10 Polymerase chain reaction amplification

This method was carried out according to the protocol of Dr Helen Kemp (Department of Oncology and Metabolism, University of Sheffield, Sheffield, UK). For polymerase chain reaction (PCR) amplification, forward and reverse oligonucleotide primers were appropriately designed to amplify the required regions of a DNA fragment. Primers were synthesised to order by Eurofins Genetic Services Ltd. (London, UK) and were stored at -40°C in sterile, nuclease-free water at a concentration of 100 pmol/µl. The PCR primers used in this study are listed in **Table 2.4.** The exact primers used for PCR amplification of a particular DNA are given at the relevant points in the Results Chapters. Reactions were carried out in 0.5-ml tubes in 50-µl volumes comprising, unless otherwise indicated: 50 ng of template DNA, 0.01-1 µM of each required (forward and reverse) primer, 1.25 units of GoTaq® Flexi DNA polymerase (Promega), 0.2 mM deoxynucleotides (dATP, dGTP, dCTP and dTTP) (Promega), 1.5 mM magnesium chloride (Promega) and 0.2 volumes of 5x GoTaq® Flexi Buffer (50 mM Tris-hydrochloride, pH 8.5; 0.05% (w/v) gelatine; 250 mM potassium chloride; 0.5% (v/v) Tween 20; 0.5% (v/v) Nonidet P-40) (Promega). Reactions without template DNA were included as controls. Each reaction was overlaid with mineral oil (Sigma-Aldrich) to prevent evaporation during heating, and was then subjected to PCR amplification in a DNA Thermal Cycler (Perkin-Elmer/Cetus, Norwalk, CT, USA). Unless stated otherwise, the cycling conditions were denaturation at 95°C for 1 min, annealing at 55°C for 1 min and extension at 72°C for 2 min for 30 cycles. The reactions were completed by a final extension at 72°C for 10 min, followed by a soak at 4°C. Amplification products were analysed by agarose gel electrophoresis (**Section 2.8)**

Table 2.4: Oligonucleotide PCR amplification primers

Primer	Sequence[1]	Source
CASR-ECD-F	5'-ttctcgagatggcattttatagc-3'	Eurofins Genetic Services Ltd. (London, UK)
CASR-ECD-R	5'-aactcgagcgcctatcaggcaatgcaggaggt-3'	Eurofins Genetic Services Ltd.

[1]The *Xho*I restriction sites are underlined in the forward (F) and reverse (R) primers.

2.11 Extraction and purification of DNA fragments from agarose gels

When electrophoresis was performed to purify a required DNA fragment, generated either from a PCR amplification reaction or a restriction enzyme digest, the DNA fragment was recovered from an agarose gel using a Wizard® PCR Preps DNA Purification Kit (Promega). Briefly, the area of the gel containing the relevant band of DNA was visualised using an ultra-violet transilluminator, excised using a clean scalpel and placed in a 1.5-ml tube. The gel slice was dissolved in 1 ml of Wizard® PCR Preps DNA Purification Resin and applied to a Wizard® Minicolumn. The column was washed with 2 ml of 80% (v/v) isopropanol and then was centrifuged at 10,000 *g* for 2 min. The DNA was eluted in 30 µl of sterile TE buffer and stored at -20°C until required. Purified DNA fragments were analysed by agarose gel electrophoresis (**Section 2.8)** and the concentration of the DNA was measured by spectrophotometry (**Section 2.6**).

2.12 DNA ligations

This method was carried out according to the protocol of Dr Helen Kemp (Department of Oncology and Metabolism, University of Sheffield, Sheffield, UK). Ligation of plasmid vector and DNA fragments was performed using T4 DNA ligase (Promega) in in a 0.5-ml tube in a reaction volume of 10-20 µl. Reactions usually contained 20-100 ng of plasmid vector. The amount of insert DNA was calculated as: ng vector x size of insert (kilobase)/size of vector (kilobase) x molar ratio of insert to vector. Vector and insert DNA were usually at a molar ratio of between 1 and 3. The following were then added: 1-2 units of T4 DNA ligase (Promega), 0.1 volumes of 10x DNA ligase buffer (300 mM Tris-hydrochloride, pH 7.8; 100 mM magnesium chloride; 100 mM dithiothreitol; 10 mM adenosine triphosphate) (Promega) and the required volume of nuclease-free water. The reaction was subsequently incubated at 15°C overnight before using in the transformation of bacterial cells (**Section 2.14**).

2.13 Bacterial transformation

When required, a 50-100-µl aliquot of chemically competent *E. coli* JM109 cells (Promega) was thawed from storage at -80°C. The appropriate DNA sample (plasmid DNA or DNA in a ligation reaction) was gently mixed with the cells which were incubated on ice for 5-10 min. The cells were then heat shocked at exactly 42°C for 45

sec and returned to ice. After 2 min, the cells were transferred to a culture tube containing 900-950 µl of chilled SOC medium (2% (w/v) tryptone; 0.5% (w/v) yeast extract; 10 mM sodium chloride; 2.5 mM potassium chloride; 10 mM magnesium chloride; 10 mM magnesium sulphate; 20 mM glucose) (Life Technologies Ltd.). The culture tube was placed in the rotary incubator shaking at 150 rpm and grown for 1 h, to allow expression of the antibiotic resistance genes carried by the transforming plasmid DNA. A 100-µl aliquot of undiluted transformed cells, and of 1:10 and 1:100 dilutions, were then spread on agar plates containing the appropriate antibiotic(s), and the plates incubated at 37°C overnight. As a control in each transformation experiment, an aliquot of untransformed cells was also plated on to selective medium. Individual colonies were subsequently purified by streaking onto fresh LB agar plates with selective antibiotic(s) for growth overnight at 37°C.

For *E. coli* BL21 strains **(Table 2.1),** a 100-µl aliquot of chemically competent cells (Agilent Technologies Inc., Santa Clara, CA, USA) was thawed from storage at -80°C. β-mercaptoethanol was added to a final concentration of 24 mM and 28 mM to BL21 (DE3) and BL21 CODONPLUS (DE3)-RIPL cells, respectively. The appropriate DNA sample was gently mixed with the cells which were then incubated on ice for 30 min. BL21(DE3) and BL21(DE3)pLysS cells were subsequently heat shocked at exactly 42°C for 45 sec and returned to ice. BL21 Gold (DE3), BL21 Gold (DE3)pLysS and BL21 CODONPLUS (DE3)-RIPL cells were heat shocked at exactly 42°C for 20 sec and returned to ice. After 2 min, the cells were transferred to a culture tube containing 900 µl of chilled SOC medium and the protocol continued as above.

2.14 TOPO® cloning reactions

TOPO® cloning reactions were used to directly clone PCR amplification products into plasmid vector pCR®2.1-TOPO® (**Figure 6.6**) (Life Technologies Ltd.) according to a TOPO® TA Cloning Kit (Life Technologies Ltd.). Each 6-µl reaction was set up in a 0.5-ml tube with: 2 µl of fresh PCR amplification product, 1 µl of reaction buffer (1.2 M sodium chloride; 60 mM magnesium chloride), 1 µl of pCR®2.1-TOPO® linearised vector, and 2 µl of nuclease-free water. The reaction was mixed gently and incubated at the room temperature for 15 min and then placed on ice. To recover cloned PCR amplification products, 2 µl of the TOPO® cloning reaction were added into a vial of

One Shot® Chemically Competent *E. coli* TOP10F' cells (Life Technologies Ltd.) and mixed gently. The cells were incubated on ice for 5 min and then heat-shocked for 30 sec at 42°C without shaking. The cells were immediately transferred to ice and 250 µl of room temperature SOC medium were added. The cells were then incubated at 37°C in a rotary incubator shaking at 200 rpm. After 1 h, 10-50 µl of the culture were plated onto LB agar containing kanamycin at 50 µg/ml, and the plates incubated at 37°C overnight. Individual colonies were then purified by streaking onto fresh LB agar plates with kanamycin at 50 µg/ml and growing overnight at 37°C.

2.15 DNA sequencing

Automated DNA sequencing was carried out by the Genetics Core Facility of the Medical School at the University of Sheffield, Sheffield, UK. DNA templates (plasmids or PCR amplification products) and oligonucleotide sequencing primers were provided to the service at 50-100 ng/µl and 1 pmol/µl, respectively. Sequencing primers M13 Reverse and T7 promoter (**Table 2.5**) were purchased from Promega. Primer T7 Terminator was from Novagen/Merck KgaA. Other primers (**Table 2.5)** were synthesised to order by Eurofins Genetic Services Ltd. Sequencing reactions were performed using a BigDye® Terminator Cycle Sequencing Kit Version 3.1 (Applied Biosystems, Foster City, CA, USA) and an ABI 3730 Capillary Sequencer (Applied Biosystems).

2.16 DNA and protein analyses

Analyses of DNA and protein sequences were carried out using Lasergene Core Suite sequence analysis software (DNASTAR, Inc. Madison, WI, USA) and the network facilities of the European Bioinformatics Institute-European Molecular Biology Laboratory (EBI-EMBL) (http://www.ebi.ac.uk/) (Cambridge, UK), and the ExPASy Bioformatics Resources Portal (http://web.expasy.org) (*SIB Swiss Institute of Bioinformatics, Switzerland*). Protein and DNA homology searches against the GenBank database were performed using the BLAST service of the National Center for Biotechnology Information (NCIB) (http://www.ncbi.nlm.nih.gov/) (Bethesda, MD, USA).

Table 2.5: Oligonucleotide sequencing primers

Primer	Sequence	Source
T7 Promoter	5’-taatacgactcactataggg-3’	Promega (Southampton, UK)
T7 Terminator	5'-gctagttattgctcagcgg-3'	Novagen/Merck KgaA (Darmstadt, Germany)
M13 Reverse	5’-caggaaacagctatgac-3’	Promega
CASR-646F	5’-gccatggcagacatc-3’	Eurofins Genetic Services Ltd. (London, UK)
pc3prim1	5’-gtggcggccgcaaattc-3’	Eurofins Genetic Services Ltd.
CaSR-451	5’-acggcagtggcaaatctg-3’	Eurofins Genetic Services Ltd.
CaSR-951	5’-cattggattcgctct-3’	Eurofins Genetic Services Ltd.
CaSR-1151	5’-ttagcaacagctcga-3’	Eurofins Genetic Services Ltd.

2.17 Sodium dodecyl sulphate-polyacrylamide gel electrophoresis

This method was carried out according to the protocol of Dr Helen Kemp (Department of Oncology and Metabolism, University of Sheffield, Sheffield, UK). Sodium dodecyl sulphate-polyacrylamide gel electrophoresis (SDS-PAGE) of proteins was performed in 7.5, 8, 10% (w/v) polyacrylamide gels. Resolving gels consisted of: 7.5, 8, or 10% (v/v) ProtoGel (37.5:1 acrylamide:bisacrylamide) (GeneFlow, Lichfield, UK), 375 mM Tris-hydrochloride (pH8.8), 0.1% (w/v) SDS, 0.1% (w/v) ammonium persulphate and 0.1% (v/v) N, N, N, N'-tetramethylethylenediamine (TEMED). Stacking gels contained: 4% (v/v) ProtoGel, 125 mM Tris-hydrochloride (pH6.8), 0.1% (w/v) SDS, 0.05% (w/v) ammonium persulphate and 0.1% (v/v) TEMED.

The gels were created using a Bio-Rad Mini-Protean Tetra Cell apparatus (Bio-Rad Laboratories Ltd.). Briefly, glass plates and spacers were assembled using the dedicated equipment according to the manufacturer's instructions. The resolving gel solution was poured into the space between the plates and overlaid with 100 µl of butan-1-ol. After the gel had polymerized, the butan-1-ol was poured off and a gel comb was inserted before the solution for the stacking gel was poured in on top. Then, the gel comb was removed and the full apparatus assembled into the gel running tank. Laemmli buffer (25 mM Tris-base; 0.1% (w/v) SDS; 192 mM glycine; pH 8.3) (GeneFlow) was poured into the tank until the bottom of the plates was covered and the top buffer reservoir was full.

Prior to loading, protein samples were mixed with SDS-sample buffer (2% (w/v) SDS; 25% (v/v) glycerol; 0.01% (w/v) bromophenol blue; 2% (v/v) 2-mercaptoethanol; 62.5 mM Tris-hydrochloride, pH 6.8) (Bio-Rad Laboratories Ltd.) and heated at 95°C for 5 min. Samples were then loaded into the gel wells. Protein size markers were Prestained SDS-PAGE Standards, Low Range (20-104 kDa) (Bio-Rad Laboratories Ltd.) or Precision Plus Protein All Blue Standards (10-250 kDa) (Bio-Rad Laboratories Ltd.). Gels were run at 35 milli-amperes for 3-5 h or until the visible dye front had reached the bottom of the plates. The apparatus was subsequently dismantled and, when staining was required, the gel transferred to a plastic tray and stained with Coomassie® Blue stain (0.05% (w/v) Coomassie® Brilliant Blue (Bio-Rad Laboratories Ltd.); 10% (v/v) glacial acetic acid; 25% (v/v) isopropanol) on a rocking platform. After a minimum of 30 min of staining, the gel was destained by repeated fresh additions of destain solution

(10% (v/v) glacial acetic acid; 25% (v/v) isopropanol), until the protein markers were clearly visible.

2.18 Antibodies

The antibodies used in this study are listed in **Table 2.6.** These were stored in accordance with the manufacturers' instructions at 4°C or -20°C.

2.19 Western blotting

Proteins separated in SDS-polyacrylamide gels by SDS-PAGE (**Section 2.18**) were transferred to Whatman™ Westran® Clear Signal polyvinylidene difluoride (PVDF) blotting membrane (GE Healthcare Life Sciences, Little Chalfont, UK) using a Bio-Rad Mini Trans-Blot Cell (Bio-Rad Laboratories Ltd.). Before transfer, membranes were soaked in 100% methanol for 30 sec, and then in transfer buffer (25 mM Tris-base; 192 mM glycine; pH 8.3) for 5 min. SDS-polyacrylamide gels, 3 MM Whatman paper (Whatman International Ltd., Maidstone, UK) and sponges needed for the blotting sandwich were also soaked in transfer buffer for 5 min. After assembly, the blotting sandwich was placed into a Bio-Rad Mini Trans-Blot Cell and subjected to 100 volts for 1 h (**Figure 2.1).**

Following transfer, the membrane was incubated in phosphate-buffered saline (137 mM sodium chloride; 2.7 mM potassium chloride; 8.1 mM disodium hydrogen phosphate; 1.5 mM Potassium dihydrogen phosphate; pH 7.4) (PBS) (Sigma-Aldrich)/1 % (v/v) Blocking Reagent (Roche Diagnostics, Mannheim, Germany) at room temperature with shaking for 60 min, or overnight at 4°C. The membrane was then washed for 15 min with PBS/0.1% (v/v) Tween-20 (washing buffer). Primary antibody was applied to the membrane at the required dilution in PBS/0.5 % (v/v) Blocking Reagent and incubated with shaking at room temperature for 1.5 h. Subsequently, the membrane was washed with washing buffer for 3 x 10 min. The appropriate secondary antibody conjugated to horseradish peroxidase **(Table 2.6)** was applied to the membrane at the required dilution in PBS/0.5 % (v/v) Blocking Reagent and incubated for 1 h at room temperature with shaking. Afterwards, the membrane was washed with washing buffer for 3 x 15 min. Excess buffer was drained from the membrane and the binding of the secondary antibody conjugated to horseradish peroxidase was

detected by enhanced chemiluminescence using a BM Chemiluminescence Blotting Substrate (POD) Kit (Roche Diagnostics) and as explained in the manufacturer's manual. The detection reagent system consisted of luminol, hydrogen peroxide and 4-iodophenol and was applied to the membrane for 1 min before draining and wrapping the membrane in Saran Wrap (Baco professional, Telford, UK). The membrane was placed into a Hypercassette™ (GE Healthcare Life Sciences, Little Chalfont, UK) with Fuji Medical X-Ray Film (FujiFilm Europe GmbH, Dusseldorf, Germany). After exposure of the film for the required time, it was developed using Photosol CD18 x-ray developer (Photosol Ltd., Basildon, UK), rinsed in water and then fixed in Photosol CF40 fixer (Photosol Ltd.).

Table 2.6 : Antibodies

Antibody	Details	Source
Anti-His-tag	Mouse monoclonal antibody against six histidine residues (6xHis epitope tag).	Life Technologies Ltd. (Paisley, UK)
Anti-FLAG-HRP	Mouse monoclonal antibody against the FLAG epitope (DYKDDDDK) conjugated to horseradish peroxidase (HRP).	Sigma-Aldrich (Poole, UK)
Anti-CaSR (ab79829)	Rabbit polyclonal antibody against the amino acid residues 47-69 of the calcium-sensing receptor (CaSR).	Abcam, Inc. (Cambridge, MA, USA)
Anti-CaSR (ab19347)	Mouse monoclonal antibody against the amino acid residues 214-235 of the CaSR	Abcam
Anti-CaSR11-S	Rabbit polyclonal antiserum against a C-terminal peptide of the CaSR.	Alpha Diagnostics (International, San Antonio, TX, USA)
Anti-NALP5	Goat polyclonal antibody against an internal peptide of NACHT leucine-rich-repeat protein 5 (NALP5).	Santa Cruz Biotechnology, Inc. (Santa Cruz, CA, USA)
Anti-mouse IgG-HRP	Goat polyclonal antibody against mouse IgG conjugated to HRP.	Life Technologies Ltd.
Anti-rabbit IgG-HRP	Goat polyclonal antibody against rabbit IgG conjugated to HRP.	Sigma-Aldrich
Anti-human IgG-AP	Goat polyclonal antibody against human IgG (γ-chain-specific) conjugated to alkaline phosphatase (AP).	Sigma-Aldrich
Anti-rabbit IgG-AP	Goat polyclonal antibody against rabbit IgG conjugated to alkaline phosphatase (AP).	Sigma-Aldrich

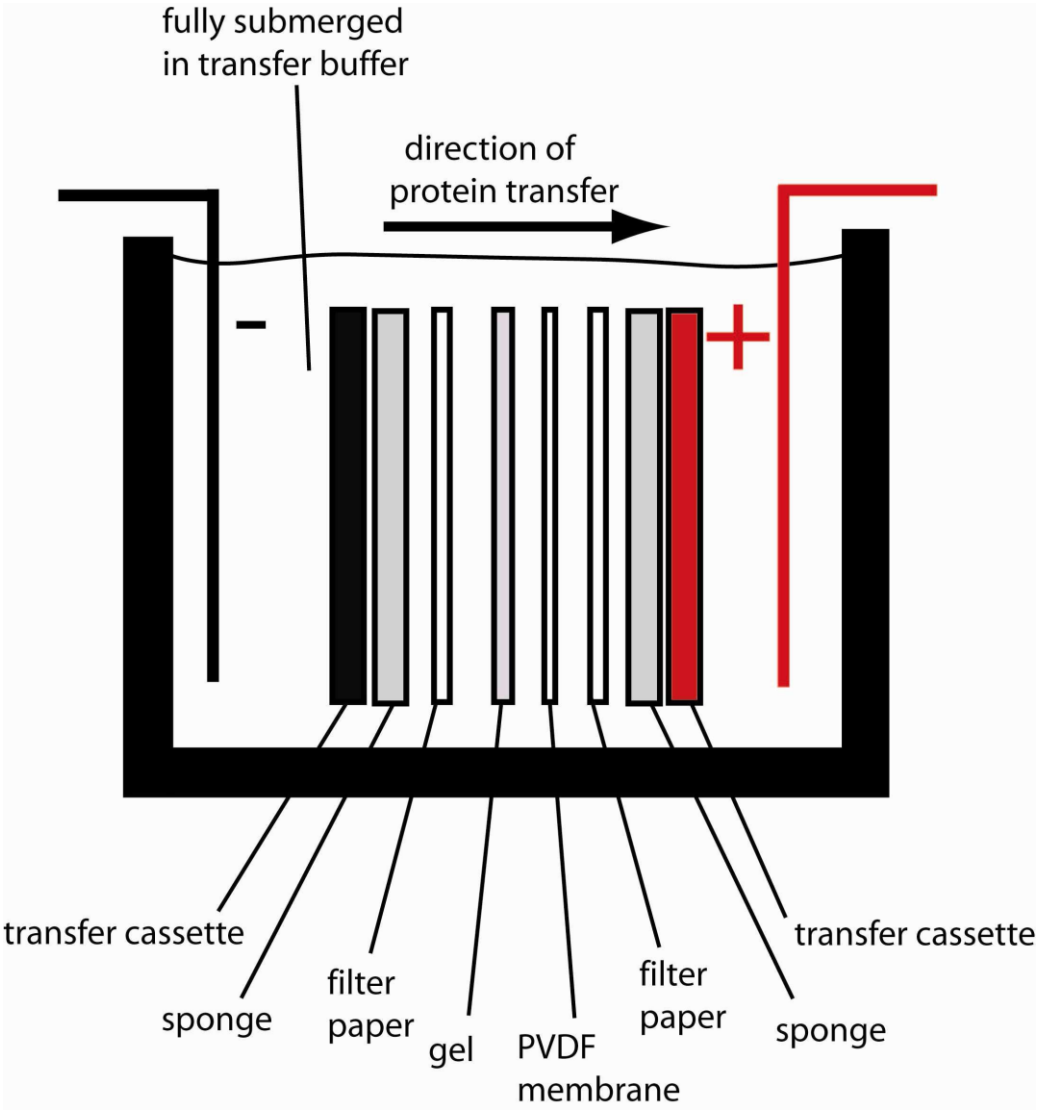

Figure 2.1: Assembly of blotting sandwich in submerged transfer apparatus.

Chapter 3

Prevalence and Clinical Associations of Calcium-Sensing Receptor and NALP5 Autoantibodies in Finnish Patients with Autoimmune Polyendocrine Syndrome Type 1

3 Prevalence and Clinical Associations of Calcium-Sensing Receptor and NALP5 Autoantibodies in Finnish Patients with Autoimmune Polyendocrine Syndrome Type 1

3.1 Introduction

The autoimmune regulator transcription factor encoded by *AIRE* is mainly expressed in medullary thymic epithelial cells (mTEC) where it regulates expression of peripheral tissue-specific antigens in order to establish self-tolerance in developing T lymphocytes (Zuklys et al., 2000). Mutations in the *AIRE* gene (Finnish-German, 1997, Nagamine et al., 1997) cause the development of autoimmune polyendocrine syndrome type 1 (APS1) also referred to as autoimmune polyendocrinopathy-candidiasis-ectodermal dystrophy (APECED) (Perheentupa, 2006). The majority of APS1 patients have high IgG antibody titers against type I interferons (IFN) and T helper type 17 (Th17) cell-related cytokines (Kisand et al., 2008, Puel et al., 2010), and these represent useful diagnostic markers for APS1 due to their early appearance and long persistence (Kisand et al., 2008, Puel et al., 2010).

Clinically, APS1 is characterised in the majority of cases by the presence of chronic mucocutaneous candidiasis, hypoparathyroidism and Addison's disease (adrenal insufficiency) (Perheentupa, 2006). Occurring less frequently are hypothyroidism, type 1 diabetes mellitus, vitiligo, alopecia areata, hepatitis and pernicious anaemia (Perheentupa, 2006). Patients suffer from chronic inflammation of their internal organs due to infiltrating autoreactive T lymphocytes, and usually have variety of autoantibodies against the affected tissue (Soderbergh et al., 2004). In many cases, a correlation between a disease component and an autoantibody target is observed (Soderbergh et al., 2004). Examples include tyrosine hydroxylase and alopecia, tryptophan hydroxylase and intestinal dysfunction, and side-chain cleavage enzyme and ovarian insufficiency, in each case, the autoantigen being expressed in the affected tissue (Soderbergh et al., 2004). Likewise, antibodies against parathyroid-expressed NALP5 have been associated with the

clinical and biochemical manifestations of hypoparathyroidism, which include hypocalcemia, hyperphosphatemia and low serum levels of PTH (Alimohammadi et al., 2008). In addition, the CaSR, which plays a critical role in keeping calcium homeostasis by sensing serum calcium levels and regulating PTH production and secretion, also represents a parathyroid-expressed antibody target in APS1 (Li et al., 1996, Gylling et al., 2003, Mayer et al., 2004, Gavalas et al., 2007), although this has not been a consistent finding (Soderbergh et al., 2004). However, it is unclear as to whether or not CaSR antibodies are a specific or sensitive marker for hypoparathyroidism in patients with this autoimmune syndrome (Gylling et al., 2003, Gavalas et al., 2007).

3.2 Aims

The aims of this part of the project were:

- To determine the *AIRE* genotypes and cytokine antibody profiles of the APS1 patient group in order to confirm the clinical diagnosis of APS1.
- To investigate the prevalence of CaSR and NALP5 antibodies in the APS1 patients.
- To assess associations between the presence of CaSR and NALP5 antibodies and APS1 disease components and patient demographic characteristics.

3.3 Materials and Methods

3.3.1 Patients and controls

The study was approved by the Medical Ethics Committee of Helsinki University Central Hospital, and was performed in accordance with the Declaration of Helsinki. Informed written consent was obtained from all participants or their parents prior to inclusion in the study. The APS1 patients were under the care of Professor Annamari Ranki and Dr Nicolas Kluger at the Department of Dermatology, Allergology and Venereology, Institute of Clinical Medicine, University of Helsinki and Helsinki University Central Hospital, Helsinki, Finland. Forty-four unrelated Finnish APS1 patients were included and were 18 males and 26 females with a mean age of 33 years (range: 8-67 years). Individual patient sex and age details are given in **Table 3.1**. The diagnostic criteria for the various endocrine, ectodermal and other disease components have been detailed previously (Ahonen et al., 1990), and the diagnosis of APS1 was based upon the presence of at least two of the three classical clinical criteria of chronic mucocutaneous candidiasis, hypoparathyroidism and Addison's disease (Ahonen et al., 1990). Thirty eight healthy blood donors to the Finnish Red Cross Blood Service, who had no clinical signs or a family history of APS1 or of other autoimmune disease, served as controls and included 16 males and 22 females with a mean age of 36 years (range: 19-64 years). Serum samples obtained from participants were stored at -80^{o}C until required for analysis.

3.3.2 *AIRE* gene genotyping

The *AIRE* genotypes of the APS1 patients were determined by Professor Annamari Ranki and Dr Nicolas Kluger by PCR amplification and DNA sequencing of the 14 *AIRE* exons, as detailed previously (Wolff et al., 2007).

3.3.3 Cytokine enzyme-linked immunosorbent assays

Antibodies against cytokines were detected in enzyme-linked immunosorbent assays (ELISAs). Interleukin (IL)-22, IL-17A, IL-17F (all from R and D Systems, Minneapolis, MN, USA), interferon (IFN)-omega, IFN-alpha2A and IFN-lambda1 (IL-29) (all from Sigma-

Aldrich) were received dried and were solubilised and stored according to the manufacturer's instructions. For ELISAs, the required cytokine was diluted in PBS to 100 ng/ml and 100-µl samples used to coat the wells of a 96-well microtitre plate. An equivalent number of wells were coated with 100 µl of 0.1% (w/v) bovine serum albumin for the measurement of non-specific binding of the sera. The plates were then incubated overnight at 4°C.

Excess cytokine was removed by decanting and all the wells were blocked with blocking buffer (PBS/ 0.1% (w/v) Tween-20/3% (w/v) bovine serum albumin) for 30 min at 37°C. Plates were washed four times with washing buffer (PBS/0.1% (v/v) Tween-20). Aliquots (100 µl) of APS1 patient or control sera at a 1:100 dilution in blocking buffer were added to the wells. PBS was applied as a control to measure any non-specific binding of the secondary antibody. The plates were incubated at room temperature for 1 h and then washed four times with washing buffer. A 100-µl aliquot of goat anti-human IgG polyclonal antibody conjugated to alkaline phosphatase (Sigma-Aldrich) diluted to 1:2000 in blocking buffer was added to each well for 1 h at room temperature. After washing five times with washing buffer, 100 µl of alkaline phosphatase substrate Sigma Fast p-nitrophenyl phosphate (Sigma-Aldrich) were applied to each well and plates incubated at room temperature to allow colour development. A LabSystems Integrated EIA Management System spectrophotometer (Life Sciences International, Basingstoke, UK) was used to read absorption of the wells at 405 nm. All sera were tested in duplicate and the mean OD_{405} value taken. Each mean OD_{405} value was corrected for background binding of the sera to the well without antigen.

The binding reactivity of each patient and control sera to the cytokine was expressed as an antibody index calculated as: mean OD_{405} of tested serum/mean OD_{405} of a population of healthy control sera. Each serum was tested in at least two experiments and the mean cytokine antibody index calculated. The upper limit of normal for each cytokine ELISA was calculated using the mean antibody index + 3SD of a population of healthy control sera. Sera with a cytokine antibody index greater than the upper limit of normal were regarded as positive for cytokine antibodies.

3.3.4 Detection of CaSR antibodies

As detailed below, antibodies against the CaSR were detected using CaSR immunoprecipitation assays with CaSR-FLAG protein expressed in human embryonic kidney 293 (HEK293) cells.

3.3.4.1 Culture and maintenance of HEK293 cells

Human embryonic kidney 293 cells (ECACC, Public Health England, Salisbury, UK) were cultured in DMEM medium (25 mM D-glucose; 1 mM sodium pyruvate; 2 mM L-glutamine; 10% (v/v) fetal calf serum; 100 units/ml penicillin G; 100 μg/ml streptomycin) (all from Life Technologies Ltd., Paisley, UK) in T75 tissue culture flasks at 37°C in a 95% humidified atmosphere of 5% CO_2. Cells were passaged by trypsin digestion when 70-100% confluent. At each passage, the culture medium was removed from the cells which were then washed in phosphate-buffered saline (137 mM sodium chloride; 2.7 mM potassium chloride; 8.1 mM disodium hydrogen phosphate; 1.5 mM potassium dihydrogen phosphate; pH 7.4) (PBS) (Sigma-Aldrich, Poole, UK). Subsequently, the cells were incubated in trypsin solution (0.05% (w/v) trypsin; 0.53 mM ethylenediaminetetraacetic acid) (Life Technologies Ltd.) for 2-3 min at 37°C. The cells were then resuspended in culture medium prior to centrifuging for 5 min. The cell pellet was resuspended in culture medium and cells were counted in a haemocytometer before plating out at the required cell density.

3.3.4.2 Transfection of HEK293 cells

For transfections, HEK293 cells were plated at 1 x 10^6 cells in 100-mm dishes in 10 ml of culture medium and grown to 50-60% confluence. The cells were then incubated with 10 ml of fresh culture medium for 6 h at 37°C before transfection with either plasmid pcCaSR-FLAG (Kemp et al., 2007) or pcDNA3-CaSR (Kemp et al., 2014) using a Calcium Phosphate Transfection System (Life Technologies Ltd.) according to the manufacturer's protocol. Plasmids were a gift from Dr. Helen Kemp (Department of oncology and Metabolism, University of Sheffield, Sheffield, UK). Plasmid pcCaSR-FLAG was vector pcDNA3 (Life

Technologies Ltd.) containing full-length CaSR cDNA (3,234-basepairs) with an inserted nucleotide sequence (21-basepairs) encoding part of a FLAG epitope (YKDDDDK) for expression immediately after the CaSR amino acid residue aspartate-371 (**Figure 3.1**). Plasmid pcDNA3-CaSR was pcDNA3 containing full-length CaSR cDNA without an incorporated FLAG epitope (**Figure 3.2**). Briefly, 20 µg of plasmid DNA were mixed with 300 µl of sterile water and 36 µl of 2 M calcium chloride. This solution was added drop-wise into 300 µl of HEPES-buffered saline whilst passing air through the latter. The resulting precipitate was left at room temperature for 20 min. The precipitate was added to the HEK293 cells which were then incubated for 16 h at 37°C. Transfected cells were washed twice in PBS and incubated in serum-free culture medium for a further 48 h at 37°C to allow expression of the encoded CaSR protein. Untransfected HEK293 cells were also included for use as a control.

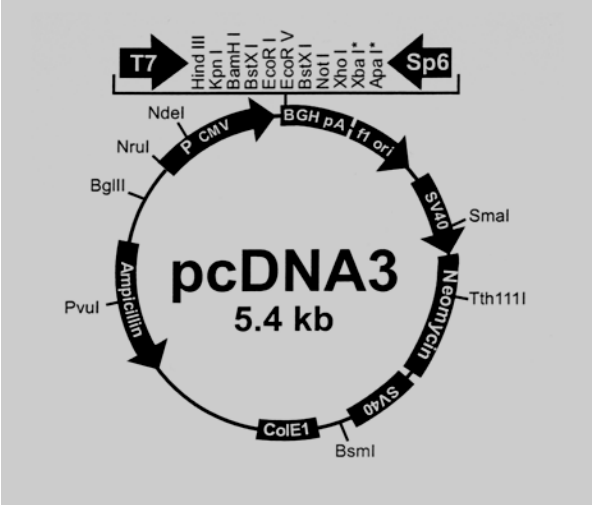

Amino acid sequence of cDNA-encoded CaSR-FLAG protein

MAFYSCCWVLLALTWHTSAYGPDQRAQKKGDIILGGLFPIHFGVAAKDQDLKSR
PESVECIRYNFRGFRWLQAMIFAIEEINSSPALLPNLTLGYRIFDTCNTVSKAL
EATLSFVAQNKIDSLNLDEFCNCSEHIPSTIAVVGATGSGVSTAVANLLGLFYI
PQVSYASSSRLLSNKNQFKSFLRTIPNDEHQATAMADIIEYFRWNWVGTIAADD
DYGRPGIEKFREEAEERDICIDFSELISQYSDEEEIQHVVEVIQNSTAKVIVVF
SSGPDLEPLIKEIVRRNITGKIWLASEAWASSSLIAMPQYFHVVGGTIGFALKA
GQIPGFREFLKKVHPRKSVHNGFAKEFWEETFNCHLQEGAKGPLPVD**YKDDDDK**
TFLRGHEESGDRFSNSSTAFRPLCTGDENISSVETPYIDYTHLRISYNVYLAVY
SIAHALQDIYTCLPGRGLFTNGSCADIKKVEAWQVLKHLRHLNFTNNMGEQVTF
DECGDLVGNYSIINWHLSPEDGSIVFKEVGYYNVYAKKGERLFINEEKILWSGF
SREVPFSNCSRDCLAGTRKGIIEGEPTCCFECVECPDGEYSDETDASACNKCPD
DFWSNENHTSCIAKEIEFLSWTEPFGIALTLFAVLGIFLTAFVLGVFIKFRNTP
IVKATNRELSYLLLFSLLCCFSSSLFFIGEPQDWTCRLRQPAFGISFVLCISCI
LVKTNRVLLVFEAKIPTSFHRKWWGLNLQFLLVFLCTFMQIVICVIWLYTAPPS
SYRNQELEDEIIFITCHEGSLMALGFLIGYTCLLAAICFFFAFKSRKLPENFNE
AKFITFSMLIFFIVWISFIPAYASTYGKFVSAVEVIAILAASFGLLACIFFNKI
YIILFKPSRNTIEEVRCSTAAHAFKVAARATLRRSNVSRKRSSSLGGSTGSTPS
SSISSKSNSEDPFPQPERQKQQQPLALTQQEQQQQPLTLPQQQRSQQQPRCKQK
VIFGSGTVTFSLSFDEPQKNAMAHRNSTHQNSLEAQKSSDTLTRHQPLLPLQCG
ETDLDLTVQETGLQGPVGGDQRPEVEDPEELSPALVVSSSQSFVISGGGSTVTE
NVVNS

Nucleotide sequence of CaSR-FLAG cDNA

atggcattttatagctgctgctgggtcctcttggcactcacctggcacacctctgcctacgggccagaccagcgagcccaaaagaaggggacattatccttgggggctctttcctattcattttg
gagtagcagctaaagatcaagatctcaaatcaaggccggagtctgtggaatgtatcaggtataatttccgtgggtttcgctggttacaggctatgatatttgccatagaggagataaacagcagccc
agcccttcttcccaacttgacgctgggatacaggatatttgacacttgcaacaccgtttctaaggccttggaagccaccctgagttttgttgctcaaaacaaaattgattctttgaaccttgatgag
ttctgcaactgctcagagcacattccctctacgattgctgtggtgggagcaactggctcaggcgtctccacggcagtggcaaatctgctggggctcttctacattccccaggtcagttatgcctcct
ccagcagactcctcagcaacaagaatcaattcaagtctttcctccgaaccatccccaatgatgagcaccaggccactgccatggcagacatcatcgagtatttccgctggaactgggtgggcacaat
tgcagctgatgacgactatgggcggccggggattgagaaattccgagaggaagctgaggaaagggatatctgcatcgacttcagtgaactcatctcccagtactctgatgaggaagagatccagcat
gtggtagaggtgattcaaaattccacggccaaagtcatcgtggttttctccagtggcccagatcttgagcccctcatcaaggagattgtccggcgcaatatcacgggcaagatctggctggccagcg
aggcctgggccagctcctccctgatcgccatgcctcagtacttccacgtggttggcggcaccattggattcgctctgaaggctgggcagatcccaggcttccgggaattcctgaagaaggtccatcc
caggaagtctgtccacaatggttttgccaaggagttttgggaagaaacatttaactgccacctccaagaaggtgcaaaaggacctttacctgtggactacaaggatgacgatgacaagacctttctg
agaggtcacgaagaaagtggcgacaggtttagcaacagctcgacagcctccgaccccctctgtacaggggatgagaacatcagcagtgtcgagaccccttacatagattacacgcatttacggatat
cctacaatgtgtacttagcagtctactccattgcccacgccttgcaagatatatatacctgcttacctgggagagggctcttcaccaatggctcctgtgcagacatcaagaaagttgaggcgtggca
ggtcctgaagcacctacggcatctaaactttacaaacaatatgggggagcaggtgacctttgatgagtgtggtgacctggtggggaactattccatcatcaactggcacctctccccagaggatggc
tccatcgtgtttaaggaagtcgggtattacaacgtctatgccaagaagggagaaagactcttcatcaacgaggagaaaatcctgtggagtgggttctccagggaggtgcccttctccaactgcagcc
gagactgcctggcagggaccaggaaagggatcattgaggggagcccacctgctgctttgagtgtgtggagtgtcctgatggggagtatagtgatgagacagatgccagtgcctgtaacaagtgccc
agatgacttctggtccaatgagaaccacacctcctgcattgccaaggagatcgagtttctgtcgtggacggagccctttgggatcgcactcaccctctttgccgtgctgggcattttcctgacagcc
tttgtgctgggtgtgtttatcaagttccgcaacacacccattgtcaaggccaccaaccgagagctctcctacctcctcctcttctccctgctctgctgcttctccagctccctgttcttcatcgggg
agccccaggactggacgtgccgcctgcgccagccggcctttggcatcagcttcgtgctctgcatctcatgcatcctggtgaaaaccaaccgtgtcctcctggtgtttgaggccaagatccccaccag
cttccaccgcaagtggtgggggctcaacctgcagttcctgctggttttcctctgcaccttcatgcagattgtcatctgtgtgatctggctctacaccgcgccccctcaagctaccgcaaccaggag
ctggaggatgagatcatcttcatcacgtgccacgagggctccctcatggccctgggcttcctgatcggctacacctgcctgctggctgccatctgcttcttctttgccttcaagtcccggaagctgc
cggagaacttcaatgaagccaagttcatcaccttcagcatgctcatcttcttcatcgtctggatctccttcattccagcctatgccagcacctatggcaagtttgtctctgccgtagaggtgattgc
catcctggcagccagctttggcttgctggcgtgcatcttcttcaacaagatctacatcattctcttcaagccatcccgcaacaccatcgaggaggtgcgttgcagcaccgcagctcacgctttcaag

Figure 3.1: Details of plasmid pcCaSR-FLAG.

Plasmid pcCaSR-FLAG is vector pcDNA3 containing full-length CaSR cDNA (3,234-basepairs) with an inserted nucleotide sequence (21-basepairs) encoding part of a FLAG epitope (YKDDDDK) for expression immediately after CaSR amino acid residue aspartate-371. The CaSR cDNA was cloned between the *KpnI* and *XbaI* restriction sites and was in the correct orientation for expression in mammalian cells from the cytomegalovirus (CMV) promoter present in pcDNA3. The selectable marker for propagation in bacteria was ampicillin resistance.

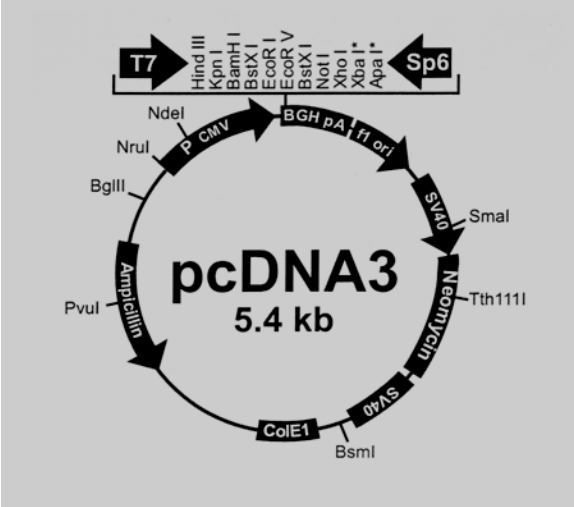

Amino acid sequence of cDNA-encoded CaSR protein

MAFYSCCWVLLALTWHTSAYGPDQRAQKKGDIILGGLFPIHFGVAAKDQDLKSRPE
SVECIRYNFRGFRWLQAMIFAIEEINSSPALLPNLTLGYRIFDTCNTVSKALEATL
SFVAQNKIDSLNLDEFCNCSEHIPSTIAVVGATGSGVSTAVANLLGLFYIPQVSYA
SSSRLLSNKNQFKSFLRTIPNDEHQATAMADIIEYFRWNWVGTIAADDDYGRPGIE
KFREEAEERDICIDFSELISQYSDEEEIQHVVEVIQNSTAKVIVVFSSGPDLEPLI
KEIVRRNITGKIWLASEAWASSSLIAMPQYFHVVGGTIGFALKAGQIPGFREFLKK
VHPRKSVHNGFAKEFWEETFNCHLQEGAKGPLPVDTFLRGHEESGDRFSNSSTAFR
PLCTGDENISSVETPYIDYTHLRISYNVYLAVYSIAHALQDIYTCLPGRGLFTNGS
CADIKKVEAWQVLKHLRHLNFTNNMGEQVTFDECGDLVGNYSIINWHLSPEDGSIV
FKEVGYYNVYAKKGERLFINEEKILWSGFSREVPFSNCSRDCLAGTRKGIIEGEPT
CCFECVECPDGEYSDETDASACNKCPDDFWSNENHTSCIAKEIEFLSWTEPFGIAL
TLFAVLGIFLTAFVLGVFIKFRNTPIVKATNRELSYLLLFSLLCCFSSSLFFIGEP
QDWTCRLRQPAFGISFVLCISCILVKTNRVLLVFEAKIPTSFHRKWWGLNLQFLLV
FLCTFMQIVICVIWLYTAPPSSYRNQELEDEIIFITCHEGSLMALGFLIGYTCLLA
AICFFFAFKSRKLPENFNEAKFITFSMLIFFIVWISFIPAYASTYGKFVSAVEVIA
ILAASFGLLACIFFNKIYIILFKPSRNTIEEVRCSTAAHAFKVAARATLRRSNVSR
KRSSSLGGSTGSTPSSSISSKSNSEDPFPQPERQKQQQPLALTQQEQQQQPLTLPQ
QQRSQQQPRCKQKVIFGSGTVTFSLSFDEPQKNAMAHRNSTHQNSLEAQKSSDTLT
RHQPLLPLQCGETDLDLTVQETGLQGPVGGDQRPEVEDPEELSPALVVSSSQSFVI
SGGGSTVTENVVNS

Nucleotide sequence of CaSR cDNA

atggcattttatagctgctgctgggtcctcttggcactcacctggcacacctctgcctacgggccagaccagcgagcccaaaagaaggggagcattatccttgggggctctttcctattcatttt
ggagtagcagctaaagatcaagatctcaaatcaaggccggagtctgtggaatgtatcaggtataatttccgtgggtttcgctggttacaggctatgatatttgccatagaggagataaacagcagc
ccagcccttcttcccaacttgacgctgggatacaggatatttgacacttgcaacaccgtttctaaggccttggaagccaccctgagttttgttgctcaaaacaaaattgattctttgaaccttgat
gagttctgcaactgctcagagcacattccctctacgattgctgtggtgggagcaactggctcaggcgtctccacggcagtggcaaatctgctggggctcttctacattccccaggtcagttatgcc
tcctccagcagactcctcagcaacaagaatcaattcaagtctttcctccgaaccatccccaatgatgagcaccaggccactgccatggcagacatcatcgagtatttccgctggaactgggtgggc
acaattgcagctgatgacgactatgggcggccggggattgagaaattccgagaggaagctgaggaaagggatatctgcatcgacttcagtgaactcatctcccagtactctgatgaggaagagatc
cagcatgtggtagaggtgattcaaaattccacggccaaagtcatcgtggttttctccagtggcccagatcttgagcccctcatcaaggagattgtccggcgcaatatcacgggcaagatctggctg
gccagcgaggcctgggccagctcctccctgatcgccatgcctcagtacttccacgtggttggcggcaccattggattcgctctgaaggctgggcagatcccaggcttccgggaattcctgaagaag
gtccatcccaggaagtctgtccacaatggttttgccaaggagttttgggaagaaacatttaactgccacctccaagaaggtgcaaaaggacctttacctgtggacacctttctgagaggtcacgaa
gaaagtggcgacaggtttagcaacagctcgacagccttccgaccccctctgtacaggggatgagaacatcagcagtgtcgagacccccttacatagattacacgcatttacggatatcctacaatgtg
tacttagcagtctactccattgcccacgccttgcaagatatatatacctgcttacctgggagagggctcttcaccaatggctcctgtgcagacatcaagaaagttgaggcgtggcaggtcctgaag
cacctacggcatctaaactttacaaacaatatgggggagcaggtgacctttgatgagtgtggtgacctggtggggaactattccatcatcaactggcacctctccccagaggatggctccatcgtg
tttaaggaagtcgggtattacaacgtctatgccaagaagggagaaagactcttcatcaacgaggagaaaatcctgtggagtgggttctccagggaggtgcccttctccaactgcagccgagactgc
ctggcagggaccaggaaagggatcattgaggggagcccacctgctgctttgagtgtgtggagtgtcctgatggggagtatagtgatgagacagatgccagtgcctgtaacaagtgcccagatgac
ttctggtccaatgagaaccacacctcctgcattgccaaggagatcgagtttctgtcgtggacggagccctttgggatcgcactcaccctctttgccgtgctgggcattttcctgacagcctttgtg
ctgggtgtgtttatcaagttccgcaacacacccattgtcaaggccaccaaccgagagctctcctacctcctcctcttctccctgctctgctgcttctccagctccctgttcttcatcggggagccc
caggactggacgtgccgcctgcgccagccggcctttggcatcagcttcgtgctctgcatctcatgcatcctggtgaaaaccaaccgtgtcctcctggtgtttgaggccaagatccccaccagcttc
caccgcaagtggtgggggctcaacctgcagttcctgctggttttcctctgcaccttcatgcagattgtcatctgtgtgatctggctctacaccgcgccccctcaagctaccgcaaccaggagctg
gaggatgagatcatcttcatcacgtgccacgagggctccctcatggccctgggcttcctgatcggctacacctgcctgctggctgccatctgcttcttctttgccttcaagtcccggaagctgccg
gagaacttcaatgaagccaagttcatcaccttcagcatgctcatcttcttcatcgtctggatctccttcattccagcctatgccagcacctatggcaagtttgtctctgccgtagaggtgattgcc
atcctggcagccagctttggcttgctggcgtgcatcttcttcaacaagatctacatcattctcttcaagccatcccgcaacaccatcgaggaggtgcgttgcagcaccgcagctcacgctttcaag

Figure 3.2: Details of plasmid pcDNA3-CaSR.

Plasmid pcDNA3-CaSR is vector pcDNA3 containing full-length CaSR cDNA (3,234-basepairs). The CaSR cDNA was cloned between the *KpnI* and *XbaI* restriction sites and was in the correct orientation for expression in mammalian cells from the cytomegalovirus (CMV) promoter present in pcDNA3. The selectable marker for propagation in bacteria was ampicillin resistance.

3.3.4.3 Preparation of cell extracts and protein determination

This method was carried out according to the protocol of Dr Helen Kemp (Department of Oncology and Metabolism, University of Sheffield, Sheffield, UK). For cell extract preparation, untransfected and transfected HEK293 cells were transferred into PBS containing Protease Inhibitor Cocktail (Sigma-Aldrich) and washed three times. The cell pellet was resuspended in immunoprecipitaion buffer (150 mM sodium chloride; 25 mM sodium phosphate (pH 6.9); 1% (v/v) Triton X-100; 0.5% (v/v) Nonidet P40; Protease Inhibitor Cocktail), sonicated four times for 20 sec on ice and then centrifuged. The total protein content of cell extracts was determined using a Bio-Rad Protein Assay Kit (Bio-Rad Laboratories Ltd., Hemel Hempstead, UK) according to the manufacturer's instructions. A protein standard curve was prepared using bovine serum albumin (Sigma-Aldrich) standards (0.1 mg/ml, 0.08 mg/ml, 0.06 mg/ml, 0.04 mg/ml, and 0.02 mg/ml), 100 µl of which were added to 200 µl of Bradford Reagent plus 700 µl of distilled water in a plastic 0.1-cm cuvette. Readings were taken for all samples at OD_{595} in a LabSystems Integrated EIA Management System spectrophotometer. The reading values were then plotted against the protein concentration to create a protein standard curve. Every cell extract sample to be measured was mixed with 200 µl Bradford reagent plus the necessary amount of distilled water to make up a volume of 1 ml in a plastic 0.1-cm cuvette. The protein concentration in each sample was determined by direct comparison of the OD_{595} reading against the standard curve values. Cell extracts were stored at -80°C at a protein concentration of 10 mg/ml.

3.3.4.4 Detection of CaSR expression

Human embryonic kidney 293 cell extracts were analysed for the presence of expressed CaSR-FLAG or CaSR by western blotting (**Section 2.19**). Aliquots of cell extract containing 10 µg of protein were added to 20 µl of sodium dodecyl sulphate (SDS)-sample buffer (2% (w/v) SDS; 25% (v/v) glycerol; 0.01% (w/v) bromophenol blue; 2% (v/v) 2-mercaptoethanol; 62.5 mM Tris-hydrochloride, pH 6.8) (Bio-Rad Laboratories Ltd.) and heated at 95°C for 5 min. Proteins were subjected to SDS-PAGE in 7.5% (w/v)

polyacrylamide gels along with Precision Plus Protein All Blue Standards (10-250 kDa) (Bio-Rad Laboratories. Ltd.), as described in **Section 2.17.**

The separated proteins were transferred onto Whatman™ Westran® Clear Signal polyvinylidene difluoride (PVDF) blotting membrane (GE Healthcare Life Sciences), as detailed in **Section 2.19.** The membranes were subjected to western blotting with either rabbit anti-CaSR (C-terminal peptide) polyclonal antiserum used at 1:100 dilution (anti-CASR11-S antiserum; Alpha Diagnostics, International, San Antonio, TX, USA) and goat anti-rabbit IgG polyclonal antibody conjugated to horseradish peroxidase used at a dilution of 1:1000 (anti-rabbit IgG antibody-HRP; Sigma-Aldrich) or mouse anti-FLAG epitope (DYKDDDDK) monoclonal antibody conjugated to horseradish peroxidase used at a dilution of 1:1000 (anti-FLAG antibody-HRP; Sigma-Aldrich). Blots were developed using enhanced chemiluminescence (**Section 2.19)** and then exposed to Fuji Medical X-Ray Film (FujiFilm Europe GmbH, Dusseldorf, Germany) for 5-min periods in a Hypercassette™ (GE Healthcare Life Sciences) at room temperature. Exposed films were subsequently developed using Photosol CD18 x-ray developer (Photosol Ltd., Basildon, UK), rinsed in water and then fixed in Photosol CF40 fixer (Photosol Ltd.).

3.3.4.5 CaSR immunopreciptation assays

For each CaSR immunoprecipitation assay (**Figure 3.3**), a 50-µl aliquot of pre-washed GammaBind® G Sepharose beads (GE Healthcare Life Sciences, Little Chalfont, UK) was incubated with a 1:50 dilution of APS1 patient or control serum in 1 ml of immunoprecipitation buffer for 1 h at 4°C. As a positive control, anti-CaSR11-S antiserum was used in the assay at a 1:100 dilution. Assays without serum were used as controls for non-specific binding of the CaSR-FLAG protein to the beads. Bead-IgG complexes were then collected by centrifugation and subsequently incubated in 1 ml of immunoprecipitation buffer with an aliquot of HEK293-CaSR-FLAG cell extract containing 500 µg of total protein at 4°C for 16 h. Subsequently, the bead-IgG-protein complexes were collected by centrifugation and washed three times for 15 min at 4°C with immunoprecipitation buffer. Finally, 20 µl of SDS-sample buffer were added to the bead-

IgG-protein complexes and the sample heated at 95°C for 5 min. Immunoprecipitated proteins were subjected to SDS-PAGE and western blotting exactly as described above (**Section 3.3.4.4**). Densitometry of the bands on exposed film was carried out in a Bio-Rad GS 690 Scanning Densitometer with Multi-Analyst Version 1.1 Software (Bio-Rad Laboratories Ltd.), which produced a densitometry value for each individual band. Sera were always tested in duplicate and the mean densitometry value was calculated from the two samples.

A CaSR antibody index for each serum was calculated as: densitometry value of tested serum/mean densitometry value of a population of healthy control sera. Each serum was tested in at least two experiments and the mean CaSR antibody index calculated. The upper limit of normal for the CaSR immunoprecipitation assay was calculated using the mean CaSR antibody index + 3SD of a population of healthy individuals. Any serum with a CaSR antibody index above the upper limit of normal was designated as positive for CaSR antibodies.

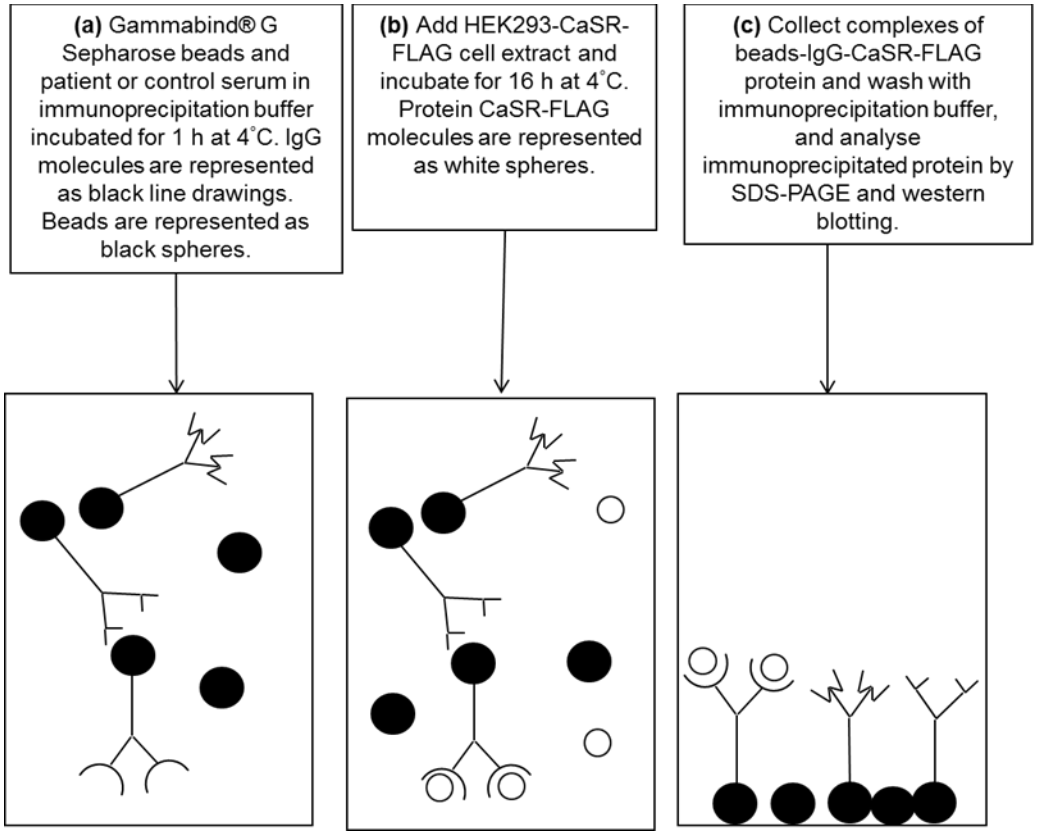

Figure 3.3: Schematic representation of the CaSR immunoprecipitation assay.

The stages of the assay are **(a)** Gammabind® G Sepharose beads bind to APS1 patient's IgG, **(b)** CaSR-FLAG protein in the HEK293 cell extract binds to specific anti-CaSR antibodies if there are any present in the APS1 patient's serum, and **(c)** the complexes of the beads-IgG-CaSR-FLAG protein are collected and analysed by SDS-PAGE and western blotting to determine if the CaSR has been immunoprecipitated.

3.3.5 Detection of NALP5 antibodies

As detailed below, NALP5 antibodies were detected using radioligand binding assays (RLBAs) with *in vitro* translated radiolabelled NALP5 as the ligand.

3.3.5.1 *In vitro* translation of NALP5 cDNA

A TnT® T7-Coupled Reticulocyte Lysate System (Promega, Southampton, UK) was used to produce NALP5 labelled with [^{35}S]-methionine, as detailed previously (Alimohammadi et al., 2008) The plasmid pCMV6-XL5-NALP5 (**Figure 3.4**) was vector pCMV6-XL5 (OriGene Technologies Inc., Rockville, MD, USA) containing NALP5 cDNA (3,600-basepairs) and was a gift from Professor Olle Kampe (Department of Medical Sciences, Uppsala University Hospital, Uppsala, Sweden). *In vitro* translation reactions were set up in 0.5 ml tubes in 50-µl volumes containing: 0.5 µg of plasmid pCMV6-XL5-NALP5, 0.5 volumes of TnT® Rabbit Reticulocyte Lysate, 10 units of TnT® T7 RNA Polymerase, 0.02 mM amino acid mixture minus methionine, 0.04 volumes of 25x TnT® Reaction Buffer, 40 units of RNasin® Ribonuclease Inhibitor (Promega) and 0.04 volumes of 10 mCi/ml translation-grade [^{35}S]-methionine (1,000 Ci/mmol) (Perkin-Elmer LAS UK Ltd., Beaconsfield, UK). Reactions were incubated at 30°C for 120 min and then stored at -40°C until needed.

The percentage incorporation of [^{35}S]-methionine into the translated NALP5 protein was determined by trichloroacetic acid-precipitation, as detailed by the manufacturer (Promega). In brief, 2 µl of the *in vitro* translation reaction were added to 98 µl of 1 M sodium hydroxide/2% (v/v) hydrogen peroxide and incubated at 37°C for 10 min. Subsequently, 900 µl of ice-cold 25% (w/v) trichloroacetic acid/2% (w/v) casamino acids (Difco, Detroit, MI, USA) were added and the reaction incubated on ice for 30 min. To collect the precipitated translation products, 250 µl of the trichloroacetic acid reaction mixture were vacuum filtered onto a Whatman GF/A glass fibre filter (Whatman International Ltd., Maidstone, UK) pre-wetted with cold 5% (w/v) trichloroacetic acid. The filter was rinsed three times with 1 ml of ice-cold 5% (w/v) trichloroacetic acid, once with 1 ml of acetone and then allowed to dry at room temperature before immersing in 3 ml of Ultima-Gold® XR scintillation fluid (Packard Bioscience, Groningen, The Netherlands) and

counting in a Beckman LS 6500 Multi-Purpose Scintillation Counter (Beckman Coulter, Inc., Fullerton, CA, USA). To determine total counts per min (cpm) present in the reaction, a 5-µl aliquot of the trichloroacetic acid reaction mixture was spotted directly on to a filter. This was dried for 10 min before counting as above. The percent incorporation of [^{35}S]-methionine was determined as: 100 x (cpm of washed filter/cpm of unwashed filter x 50), and this ranged from 7-15%.

For qualitative analysis of radiolabelled NALP5 protein, a 5-µl aliquot of the *in vitro* translation reaction containing [^{35}S]-NALP5 was added to 20 µl of SDS-sample buffer and heated at 95°C for 5 min prior to SDS-PAGE in an 8% (w/v) polyacrylamide gel, as detailed in **Section 2.17.** Precision Plus Protein All Blue Standards (10-250 kDa) were also loaded onto the gel as protein size markers. After running, the gel was treated with Coomassie Blue® stain (0.05% (w/v) Coomassie® Brilliant Blue (Bio-Rad Laboratories Ltd.); 10% (v/v) glacial acetic acid; 25% (v/v) isopropanol) and then destain solution (10% (v/v) glacial acetic acid; 25% (v/v) isopropanol) before soaking for 30 min in Amersham Amplify™ Fluorographic Reagent (GE Healthcare Life Sciences), before drying for 2 h at 60°C on to 3MM Whatman paper (Whatman International Ltd.) in a Bio-Rad Gel Dryer 583 (Bio-Rad Laboratories Ltd.). The dried gel was subjected to autoradiography by exposure to Fuji Medical X-Ray Film in a Hypercassette™ at room temperature for 24 h. Exposed film was subsequently developed using Photosol CD18 x-ray developer, rinsed in water and then fixed in Photosol CF40 fixer.

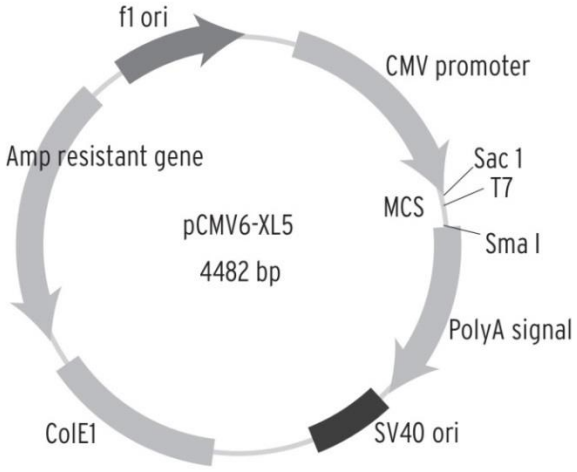

.

Amino acid sequence of NALP5 protein

MKVAGGLELGAAALLSASPRALVTLSTGPTCSILPKNPLFPQNLSSQPCIKMEG
DKSLTFSSYGLQWCLYELDKEEFQTFKELLKKKSSESTTCSIPQFEIENANVEC
LALLLHEYYGASLAWATSISIFENMNLRTLSEKARDDMKRHSPEDPEATMTDQG
PSKEKVPGISQAVQQDSATAAETKEQEISQAMEQEGATAAETEEQEISQAMEQE
GATAAETEEQGHGGDTWDYKSHVMTKFAEEEDVRRSFENTAADWPEMQTLAGAF
DSDRWGFRPRTVVLHGKSGIGKSALARRIVLCWAQGGLYQGMFSYVFFLPVREM
QRKKESSVTEFISREWPDSQAPVTEIMSRPERLLFIIDGFDDLGSVLNNDTKLC
KDWAEKQPPFTLIRSLLRKVLLPESFLIVTVRDVGTEKLKSEVVSPRYLLVRGI
SGEQRIHLLLERGIGEHQKTQGLRAIMNNRELLDQCQVPAVGSLICVALQLQDV
VGESVAPFNQTLTGLHAAFVFHQLTPRGVVRRCLNLEERVVLKRFCRMAVEGVW
NRKSVFDGDDLMVQGLGESELRALFHMNILLPDSHCEEYYTFFHLSLQDFCAAL
YYVLEGLEIEPALCPLYVEKTKRSMELKQAGFHIHSLWMKRFLFGLVSEDVRRP
LEVLLGCPVPLGVKQKLLHWVSLLGQQPNATTPGDTLDAFHCLFETQDKEFVRL
ALNSFQEVWLPINQNLDLIASSFCLQHCPYLRKIRVDVKGIFPRDESAEACPVV
PLWMRDKTLIEEQWEDFCSMLGTHPHLRQLDLGSSILTERAMKTLCAKLRHPTC
KIQTLMFRNAQITPGVQHLWRIVMANRNLRSLNLGGTHLKEEDVRMACEALKHP
KCLLESLRLDCCGLTHACYLKISQILTTSPSLKSLSLAGNKVTDQGVMPLSDAL
RVSQCALQKLILEDCGITATGCQSLASALVSNRSLTHLCLSNNSLGNEGVNLLC
RSMRLPHCSLQRLMLNQCHLDTAGCGFLALALMGNSWLTHLSLSMNPVEDNGVK
LLCEVMREPSCHLQDLELVKCHLTAACCESLSCVISRSRHLKSLDLTDNALGDG
GVAALCEGLKQKNSVLARLGLKACGLTSDCCEALSLALSCNRHLTSLNLVQNNF
SPKGMMKLCSAFACPTSNLQIIGLWKWQYPVQIRKLLEEVQLLKPRVVIDGSWH
SFDEDDRYWWKN

Nucleotide sequence of NALP5 cDNA

atgaaggttgcaggaggacttgaacttggagctgctgctctgctctcagcatcaccacgtgctcttgtcactctttccacaggtcctacttgctctatattaccaaagaatccacttttccccc
aaaacctgagctctcagccttgtatcaagatggaaggagacaaatcgctcacctttttccagctacgggctgcaatggtgtctctatgagctagacaaggaagaatttcagacattcaaggaatt
actaaagaagaaatcttcagaatcgaccacatgctctattccacagtttgaaatcgagaatgccaacgtggaatgtctggcactcctcttgcatgagtattatggagcatcgctggcctgggct
acgtccattagcatctttgaaaacatgaacctgcgaaccctctcggagaaggcacgggatgacatgaaaagacattcaccagaagatcctgaagcaacgatgactgaccaaggaccaagcaagg
aaaaagtgccaggaatttcacaagctgtgcaacaagatagtgccacagctgcagagacaaaagaacaagaaatttcacaagctatggaacaagaaggtgccacagcagcagagacagaagaaca
agaaatttcacaagctatggaacaagaaggtgccacagcagcagagacagaagaacaaggacatggaggtgacacatgggactacaagagtcacgtgatgaccaaattcgctgaggaggaggat
gtacgtcgtagttttgaaaacactgctgctgactggccggaaatgcaaacgttggctggtgcttttgattcagaccggtggggcttccggcctcgcacggtggttctgcacggaaagtcaggaa
ttgggaaatcggctctagccagaaggatcgtgctgtgctgggcgcaaggtggactctaccagggaatgttctcctacgtcttcttcctccccgttagagagatgcagcggaagaaggagagcag
tgtcacagagttcatctccagggagtggccagactcccaggctccggtgacggagatcatgtcccgaccagaaaggctgttgttcatcattgacggtttcgatgacctgggctctgtcctcaac
aatgacacaaagctctgcaaagactgggctgagaagcagcctccgttcaccctcatacgcagtctgctgaggaaggtcctgctcccctgagtccttcctgatcgtcaccgtcagagacgtgggca
cagagaagctcaagtcagaggtcgtgtctccccgttacctgttagttagaggaatctccggggaacaaagaatccacttgctccttgagcgcgggattggtgagcatcagaagacacaaggggtt
gcgtgcgatcatgaacaaccgtgagctgctcgaccagtgccaggtgcccgccgtgggctctctcatctgcgtggccctgcagctgcaggacgtggtgggggagagcgtcgccccccttcaaccaa
acgctcacaggcctgcacgccgctttttgtgtttcatcagctcacccctcgaggcgtggtccggcgctgtctcaatctggaggaaagagttgtcctgaagcgcttctgccgtatggctgtggagg
gagtgtggaataggaagtcagtgtttgacggtgacgacctcatggttcaaggactcggggagtctgagctccgtgctctgtttcacatgaacatccttctcccagacagccactgtgaggagta
ctacaccttcttccacctcagtctccaggacttctgtgccgccttgtactacgtgttagagggcctggaaatcgagccagctctctgccctctgtacgttgagaagacaaagaggtccatggag
cttaaacaggcaggcttccatatccactcgctttggatgaagcgtttcttgtttggctcgtgagcgaagacgtaaggaggccactggaggtcctgctgggctgtcccgttcccctgggggtga
agcagaagcttctgcactgggtctctctgttgggtcagcagcctaatgccaccaccccaggagacaccctggacgccttccactgtcttttcgagactcaagacaaagagtttgttcgcttggc
attaaacagcttccaagaagtgtggcttccgattaaccagaacctggacttgatagcatcttccttctgcctccagcactgtccgtatttgcggaaaattcgggtggatgtcaaagggatcttc
ccaagagatgagtccgctgaggcatgtcctgtggtccctctatggatgcgggataagaccctcattgaggagcagtgggaagatttctgctccatgcttggcacccacccacacctgcggcagc
tggacctgggcagcagcatcctgacagagcgggccatgaagaccctgtgtgccaagctgaggcatcccacctgcaagatacagaccctgatgtttagaaatgcacagattacccctggtgtgca
gcacctctggagaatcgtcatggccaaccgtaacctaagatccctcaacttgggaggcacccacctgaaggaagaggatgtaaggatggcgtgtgaagccttaaaacacccaaaatgtttgttg
gagtctttgaggctggattgctgtggattgacccatgcctgttacctgaagatctcccaaatccttacgacctcccccagcctgaaatctctgagcctggcaggaaacaaggtgacagaccagg
gagtaatgcctctcagtgatgccttgagagtctcccagtgcgcccgcagaagctgatactggaggactgtggcatcacagccacgggttgccagagtctggcctcagccctcgtcagcaaccg
gagcttgacacacctgtgcctatccaacaacagcctggggaacgaaggtgtaaatctactgtgtcgatccatgaggcttccccactgtagtctgcagaggctgatgctgaatcagtgccacctg
gacacggctggctgtggttttcttgcacttgcgcttatgggtaactcatggctgacgcacctgagccttagcatgaaccctgtggaagacaatggcgtgaagcttctgtgcgaggtcatgagag
aaccatcttgtcatctccaggacctggagttggtaaagtgtcatctcaccgccgcgtgctgtgagagtctgtcctgtgtgatctcgaggagcagacacctgaagagcctggatctcacggacaa
tgccctgggtgacggtggggttgctgcgctgtgcgaggactgaagcaaaagaacagtgttctggcgagactcgggttgaaggcatgtggactgacttctgattgctgtgaggcactctccttg
gcctttcctgcaaccggcatctgaccagtctaaacctggtgcagaataacttcagtcccaaaggaatgatgaagctgtgttcggcctttgcctgtcccacgtctaacttacagataattgggc
tgtggaaatggcagtaccctgtgcaaataaggaagctgctggaggaagtgcagctactcaagccccgagtcgtaattgacggtagttggcattcttttgatgaagatgaccggtactggtggaa
aaac

Figure 3.4: Details of plasmid pCMV6-XL5-NALP5.

Plasmid pCMV6-XL5-NALP5 is vector pCMV6-XL5 containing full-length NALP5 cDNA (3,600-basepairs) cloned in the *EcoRI* and *SalI* restriction sites of the multi-cloning site (MCS) and was in the correct orientation for expression from the T7 promoter present in the pCMV6-XL5. The selectable marker for propagation in bacteria was ampicillin resistance.

3.3.5.2 NALP5 radioligand binding assays

This method was carried out according to the protocol of Dr Helen Kemp (Department of Oncology and Metabolism, University of Sheffield, Sheffield, UK). For each NALP5 RLBA (**Figure 3.5**), a 1 to 2-µl aliquot of the required *in vitro* translation reaction (equivalent to 50,000-100,000 cpm of trichloroacetic acid-precipitable material) was suspended in 50 µl of immunoprecipitation buffer (20 mM Tris-hydrochloride, pH 8.0; 150 mM sodium chloride; 1% (v/v) Triton X-100; 10 mg/ml aprotinin (Bayer, Newbury, UK)) in a 1.5-ml tube. An APS1 patient or control serum was added to a tube at a 1:100 dilution. As a positive control, goat anti-NALP5 (internal peptide) polyclonal antibody (anti-NALP5 antibody) (Santa Cruz Biotechnology, Inc., Santa Cruz, CA, USA) was added to a tube at a 1:200 dilution. Assay tubes without serum were also included as controls for non-specific binding of radiolabelled NALP5 protein to protein G Sepharose™ 4 Fast Flow (GE Healthcare Life Sciences). The assay tubes were incubated overnight with shaking at 4°C. Subsequently, 50 µl of protein G Sepharose™ 4 Fast Flow, prepared according to the manufacturer, were added to each of the tubes, which were then incubated for a further 90 min at 4°C. Subsequently, the protein G Sepharose-antibody-antigen complexes were collected by centrifugation at 5,000 *g* and washed six times for 15 min in immunoprecipitation buffer at 4°C. The complexes were then transferred to 1 ml of Ultima-Gold® XR scintillation fluid contained in a 10-ml scintillation vial (Molecular Devices, Sunnyvale, CA, USA). Immunoprecipitated radioactivity in cpm was evaluated in a Beckman LS 6500 Multi-Purpose Scintillation Counter. Sera were always tested in duplicate and the mean cpm was calculated from the two samples.

Antibody levels were expressed as a NALP5 antibody index. This was calculated for each serum tested as: cpm immunoprecipitated by tested serum/mean cpm immunoprecipitated by the population of healthy control sera. Each serum was tested in at least two experiments and the mean NALP5 antibody index calculated. The upper limit of normal for the NALP5 RLBA was calculated using the mean NALP5 antibody index + 3SD of a population of healthy controls. Any serum sample with a NALP5 antibody index above the upper limit of normal was designated as NALP5 antibody-positive.

For qualitative analysis of immunoprecipitated NALP5 protein, the protein G Sepharose™-antibody-antigen complexes were resuspended in 100 µl of SDS-sample buffer, heated at 95°C for 5 min, centrifuged, and the supernatants recovered for SDS-PAGE and autoradiography as described in **Section 3.3.5.1**.

3.3.6 Statistical analyses

As appropriate, Fisher's exact test for 2 x 2 contingency tables for comparing categorical data, non-parametric Mann-Whitney tests for comparing two unpaired groups of continuous data, non-parametric Spearman's rank (r) correlation test to measure the statistical dependence between two variables, and multiple regression analysis for estimating the relationship between a dependent variable and one or more independent variables, were carried out using GraphPad Instat 3 software (GraphPad Software, La Jolla, CA, USA). In all tests, *P* values (two-tailed) < 0.05 were regarded as significant.

Antibody assay precision was evaluated by calculating the intra-assay coefficient of variation (expressed as a percentage) for a series of different serum samples that were measured in duplicate within the same assay run. Antibody assay reproducibility was evaluated by calculating the inter-assay coefficient of variation (expressed as a percentage) for a series of different serum samples that were measured in several consecutive assay runs.

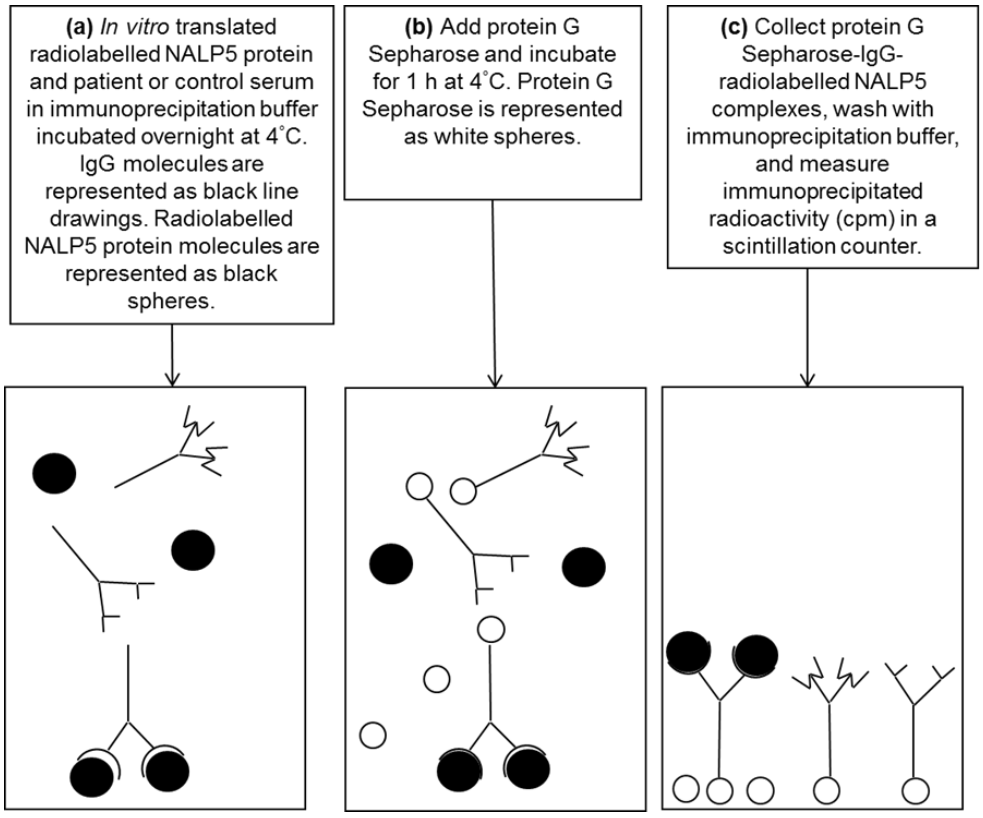

Figure 3.5: Schematic diagram of the NALP5 radioligand binding assay.

The stages of the assay are **(a)** *in vitro* translated NALP5 binds to specific anti-NALP5 antibodies if there are any present in the APS1 patient's serum, **(b)** protein G Sepharose binds to IgG molecules, and **(c)** the protein G Sepharose-IgG-radiolabelled NALP5 complexes are collected and analysed in a scintillation counter to determine if the NALP5 protein has been immunoprecipitated.

3.4 Results

3.4.1 Clinical characteristics of APS1 patients

The clinical profile of each of the APS1 patients is given in **Table 3.1.** The mean age at APS1 presentation was five years (range: 0-18 years) and the mean APS1 duration was 28 years (range: 5.5-53 years). Of the 44 patients, 43 (98%) had either two or three of the major APS1 clinical manifestations of chronic mucocutaneous candidiasis, hypoparathyroidism and Addison's disease. The remaining patient had chronic mucocutaneous candidiasis, no hypoparathyroidism nor Addison's disease, but had five other APS1 component diseases. Thirty eight of the 44 patients (86%) had at least one other disease component outside of the classic APS1 triad, four patients had seven (16%), with the median being five. The number and percentage of the 44 APS1 patients with the various endocrine, ectodermal and other disease manifestations are summarised in **Figure 3.6.**

Excluding premature ovarian failure and male hypogonadism, there were no significant differences between the sexes with regard to the presence of the APS1 component diseases, except in the case of hypoparathyroidism. This disease manifestation was present in 25 out of 26 (96%) females and 13 out of 18 (72%) males (P = 0.034, Fisher's exact test for 2 x 2 contingency tables). The mean age at hypoparathyroidism presentation was seven years (range: 1.5-19 years) and the mean duration of hypoparathyroidism was 25 years (range: 0-54 years).

Table 3.1: APS1 patient demographic and clinical characteristics and *AIRE* genotypes

Patient	Sex[1]	Age (years)	Age at APS1 onset (years)	Age at HP onset (years)[2]	APS1 duration (years)	HP duration (years)[2]	Disease components[3]	*AIRE* genotype
APS1-1	F	46	2	1.9	44	44.1	CMC; HP; AD; HT; POF; AA; AS; TIN	c.769C>T /c.769C>T
APS1-2	M	46	7	6.7	39	39.3	CMC; HP; AD; HT; HG; AA; V; T1D; AS; K	c.769C>T /c.967-979del13bp
APS1-3	F	51	3	3.1	48	47.9	CMC; AD; HP; POF; T1D; AS; OBS	c.769C>T /c.769C>T
APS1-4	M	37	2	2	35	35	CMC; AD; HP; T1D;	c.769C>T /c.769C>T
APS1-5	F	10	5	5.3	5	4.7	CMC; HP; AD	c.769C>T /c.769C>T
APS1-6	F	12	3	4.5	9	7.5	CMC; HP; AD; POF; GHD	c.769C>T /c.769C>T
APS1-7	M	9	4	4	5	5	CMC; HP; AD; K	c.769C>T /c.769C>T
APS1-8	M	13	5	15.5	8	0	CMC; HP; AD; K; V; CD; AS	c.769C>T /c.769C>T
APS1-9	M	30	7	7.3	21	22.7	CMC; HP; AD; T1D	c.769C>T /c.769C>T
APS1-10	M	47	15	NA	32	NA	CMC; AD; PA; AA	c.769C>T /c.769C>T
APS1-11	F	16	4	6.5	12	9.5	CMC; HP; AD; H; POF; OBS	c.769C>T /c.769C>T
APS1-12	F	27	2	6.8	25	20.2	CMC; HP; AD; K; AA; POF; OBS	c.769C>T /c.769C>T
APS1-13	M	25	4	15	21	10	CMC; HP; AD; K; AA; V; OBS; AS; HG	c.769C>T /c.769C>T
APS1-14	F	43	5	5	38	38	CMC; HP; AD; POF; AA; V; CD	c.769C>T /c.769C>T
APS1-15	M	9	5	7.5	4	1.5	CMC; HP; AD	c.769C>T /c.769C>T
APS1-16	F	11	5	8.5	6	2.5	CMC; HP; AD	c.769C>T /c.769C>T
APS1-17	M	12	7	7.7	5	4.3	CMC; HP; AD	c.769C>T /c.769C>T
APS1-18	F	26	1	1.6	25	24.4	CMC; HP; AD; POF; PA; AA; EPA; T1D; AS; V	c.769C>T /c.769C>T
APS1-19	M	23	1	1.5	22	21.5	CMC; HP; AD; AA; V; T1D; HT; AS; AT	c.769C>T /c.769C>T
APS1-20	F	46	2	6.8	44	39.2	CMC; HP; AD; POF; AA; K;OBS	c.769C>T /c.769C>T
APS1-21	F	43	5	4.2	38	38.8	CMC; HP; AD; POF; PA; AA; V; T1D; AS; OBS	c.769C>T /c.769C>T
APS1-22	M	67	18	NA	49	NA	CMC; AD; T1D	c.769C>T /c.769C>T
APS1-23	M	32	3	18.9	29	13.1	CMC; AD; HP; AA	c.769C>T /c.769C>T
APS1-24	F	32	6	6.5	26	25.5	CMC; AD; HP; POF; OBS	c.769C>T /c.769C>T
APS1-25	F	56	4	2.5	51	53.5	CMC; AD; HP; HT; POF ; K; OBS	c.769C>T /c.769C>T
APS1-26	F	32	7	8	25	24	CMC; HP; HT; OBS	c.769C>T/1163^1164insA
APS1-27	F	25	10	10.9	15	14.1	CMC; HP; POF; TIN; OBS	c.769C>T /c.769C>T
APS1-28	F	46	5	4.9	41	41.1	CMC; HP; AD; POF; AS; OBS	c.769C>T /c.923G>A
APS1-29	F	50	8	NA	42	NA	CMC; AD; HT; AA; AS	c.769C>T /c.923G>A
APS1-30	M	43	0	15	28	28	CMC; HP; AD; HT; AA; V; AS ; K; OBS	c.769C>T /c.1638A>T
APS1-31	F	17	4	4.2	13	12.8	CMC; HP; AD; POF; GHD	c.769C>T /c.967-979del13bp
APS1-32	M	17	2	4.4	15	12.6	CMC; HP; AD; V; AA; HT; GHD; H; K; OBS	c.769C>T /c.769C>T
APS1-33	F	52	3	14.2	49	37.8	CMC; HP	c.769C>T /c.769C>T
APS1-34	M	18	2	NA	16	NA	CMC; V; AA; HG; TIN; OBS	c.769C>T /c.967-979del13bp
APS1-35	F	54	6	2.0	48	54	CMC; HP; HT; K	c.769C>T /c.769C>T
APS1-36	F	58	5	4.5	53	53.5	CMC; AD; HP; AA;V; POF;	c.769C>T /c.769C>T

APS1-37	F	8	2.5	2.5	5.5	5.5	CMC; AD; HP; OBS	c.769C>T /c.1638A>T
APS1-38	F	35	2	2.9	33	32.1	CMC; HP; HT; OBS	c.769C>T /c.769C>T
APS1-39	M	30	1	6.1	29	23.9	CMC; AD; HP; AA; V; GHD; H; OBS	c.769C>T /c.769C>T
APS1-40	M	41	5	NA	36	NA	CMC; AD; AA	c.769C>T /c.769C>T
APS1-41	F	44	2	3.6	42	40.4	CMC; AD; HP; HT; POF; AS; AA; PA; K	c.769C>T /c.769C>T
APS1-42	M	44	6	NA	38	NA	CMC; AD; AA	c.769C>T /c.769C>T
APS1-43	F	20	3	3.5	17	16.5	CMC; AD; HP; HT; AA; POF; AS	c.769C>T /c.769C>T
APS1-44	F	56	10	10	46	46	CMC; AD; HP	c.769C>T /c.769C>T

[1]F, female; M, male.
[2]NA, not applicable.
[3]AA, alopecia areata; AD, Addison's disease; AT, arterial hypertension; AS, asplenia; CD, chronic diarrhoea; CMC, chronic mucocutaneous candidiasis; EPA, exocrine pancreatic atrophy; GHD, growth hormone deficiency; H, hepatitis; HG, hypogonadism (male); HP, hypoparathyroidism; HT, hypothyroidism; K, keratoconjunctivitis; OBS, chronic obstipation; PA, pernicious anaemia; POF, premature ovarian failure; T1D, type 1 diabetes mellitus; TIN, tubulonephritis; V, vitiligo.

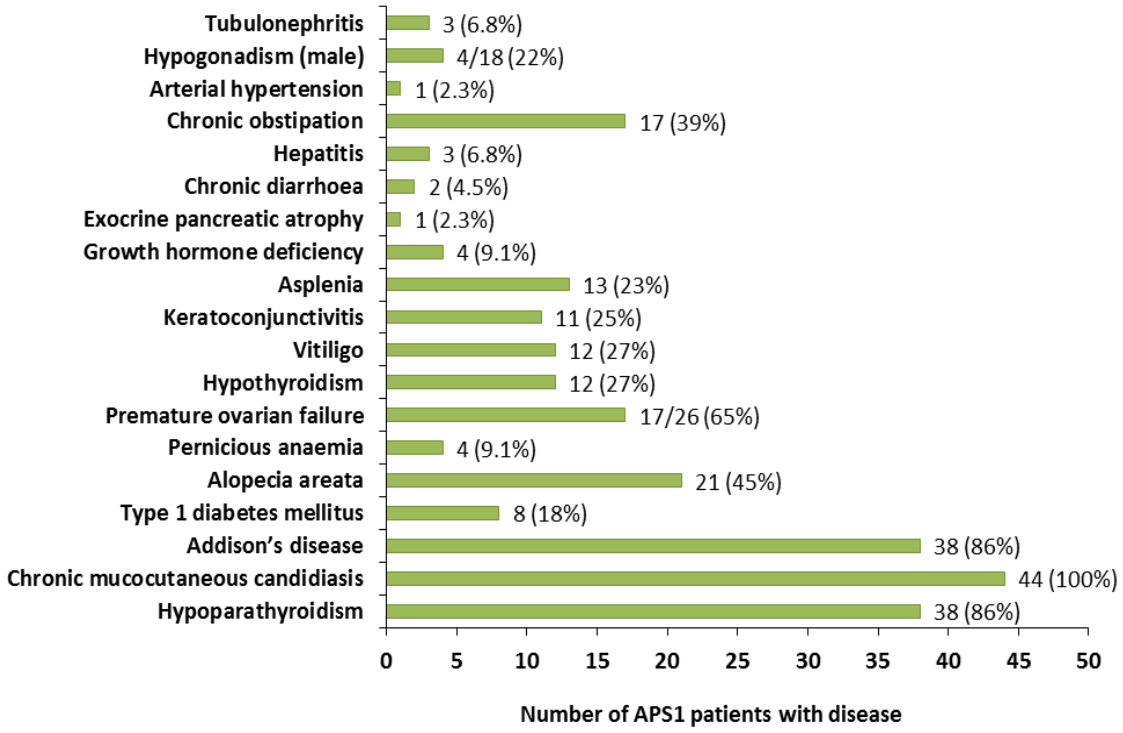

Figure 3.6: Summary of disease components in APS1 patients.

The number and percentage of the 44 APS1 patients with various endocrine, ectodermal and other disease manifestations are shown.

3.4.2 *AIRE* genotypes of the APS1 patients

To confirm the clinical diagnosis of APS1, the *AIRE* gene of each patient was analysed for the presence of mutations by DNA sequencing. The *AIRE* genotypes of the individual APS1 patients are given in **Table 3.1**. The exon 6 *AIRE* mutation c.769C>T (R257X) was found in all 44 (100%) patients, with 36 (82%) homozygous for this mutation. The remaining eight patients were compound heterozygotes with the c.769C>T mutation at one allele. The number and percentage of the 44 APS1 patients with different *AIRE* genotypes are summarised in **Figure 3.7**.

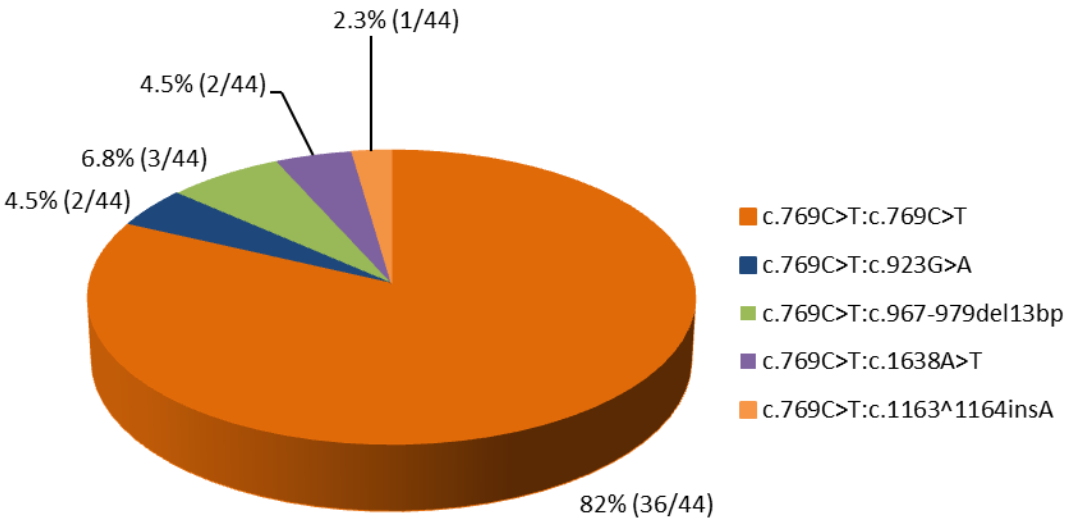

Figure 3.7: *AIRE* genotypes of APS1 patients.

The number and percentage of the 44 APS1 patients with each *AIRE* genotype are shown. The effect of each *AIRE* gene mutation on the amino acid sequence of the protein is given in parentheses. c.769C>T (R257X) is in exon 6; c.967-979del13bp (C322fsX372) is in exon 8; c.923G>A (C311Y) is in exon 8; c.1638A>T (X546C) is in exon 14; and c.1163^1164insA (M388fsX422) is in exon 10.

3.4.3 Detection of cytokine antibodies in APS1 patients and controls

To detect the presence of antibodies against IL-22, IL-17A, IL-17F, IFN-omega, IFN-alpha2A, and IFN-lambda1, serum samples from 44 APS1 patients and 18 healthy controls were analysed in an ELISA format carried out as detailed in **Section 3.3.3**. The results are shown in **Figures 3.8 and 3.9**. For each cytokine ELISA, the mean antibody index of the APS1 patient and control groups, and the antibody index range of the APS1 patient and control groups are summarised in **Table 3.2**. In all cases, except in the IFN-lambda1 ELISA, there was a significant difference between the antibody indices of the APS1 patient and control groups (*P* values were < 0.0001, Mann-Whitney test). In the IFN-lambda1 ELISA, there was no significant different between the antibody indices of the APS1 patients and controls (*P* = 0.052, Mann-Whitney test). The intra- and inter-assay coefficients of variation for each of the ELISAs are given in **Table 3.2**.

The upper limits of normal (mean antibody index + 3SD of 18 healthy individuals) for the cytokine ELISAs were antibody indices of 1.29 for the IL-22 ELISA; 1.29 for the IL-17F ELISA; 1.29 for the IL-17A ELISA; 1.84 for the IFN-omega ELISA; 2.83 for the IFN-alpha2A ELISA; and 1.59 for the IFN-lambda1 ELISA. All control sera were negative for antibodies against all the cytokines tested, as their antibody indices (**Table 3.2)** were below the upper limit of normal. In the APS1 patient group, antibody indices above the upper limit of normal (**Table 3.3**), indicated that the prevalence of antibody-positivity against each cytokine was 44/44 (100%) for IL-22; 41/44 (93%) for IL-17F; 25/44 (57%) for IL-17A; 29/44 (66%) for IFN-omega; 40/44 (91%) for IFN-alpha2A; and 5/44 (11%) for IFN-lambda1. With the exception of IFN-lambda1, antibody positivity was significantly more frequent in the APS1 patient group than in the healthy controls: All *P* values were < 0.0001 (Fisher's exact test for 2 x 2 contingency tables). In contrast, the antibody response against IFN-lambda1 was not elevated to statistical significance in the APS1 patient group when compared with healthy controls (*P* = 0.309, Fisher's exact test for 2 x 2 contingency tables).

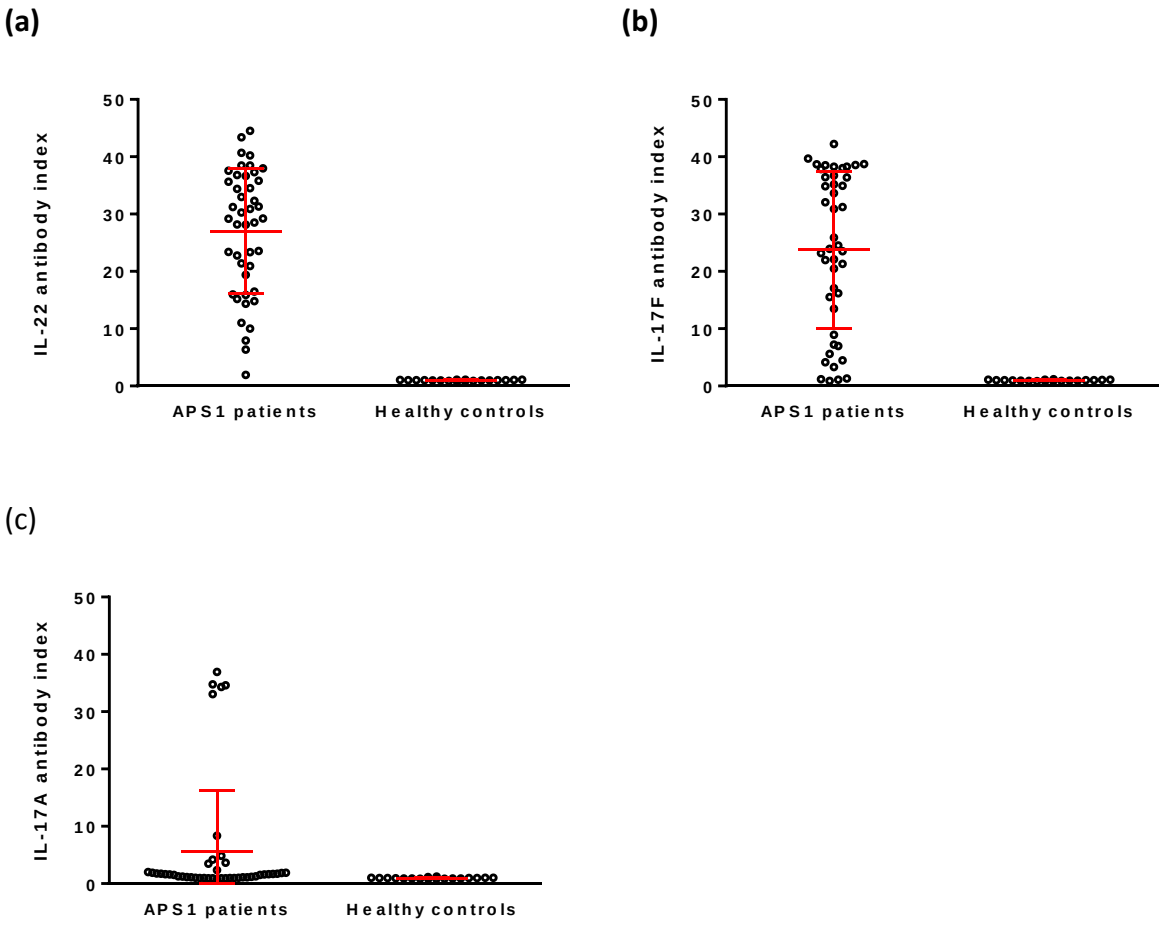

Figure 3.8: Interleukin (IL)-22, IL-17F and IL-17A antibody indices of APS1 patient and control sera.

Sera from 44 APS1 patients and 18 healthy controls were evaluated for **(a)** IL-22, **(b)** IL-17F, and **(c)** IL-17A antibodies using ELISAs. The antibody index is shown for each APS1 patient and control serum and is the mean antibody index of at least two experiments. The mean antibody index ± SD for the APS1 patient group and the control group was, respectively, 27.0 ± 10.9 (range: 1.94-44.5) and 0.99 ± 0.10 (range: 0.88-1.11) in the IL-22 ELISA; 23.8 ± 13.7 (range: 1.12-42.2) and 0.99 ± 0.10 (range: 0.87-1.19) in the IL-17F ELISA; and 5.56 ± 10.7 (range: 0.77-36.9) and 0.96 ± 0.11 (range: 0.83-1.24) in the IL-17A ELISA. In all three ELISAs, there was a significant difference between the antibody indices of the APS1 patient and control groups (*P* values were < 0.0001, Mann-Whitney test).

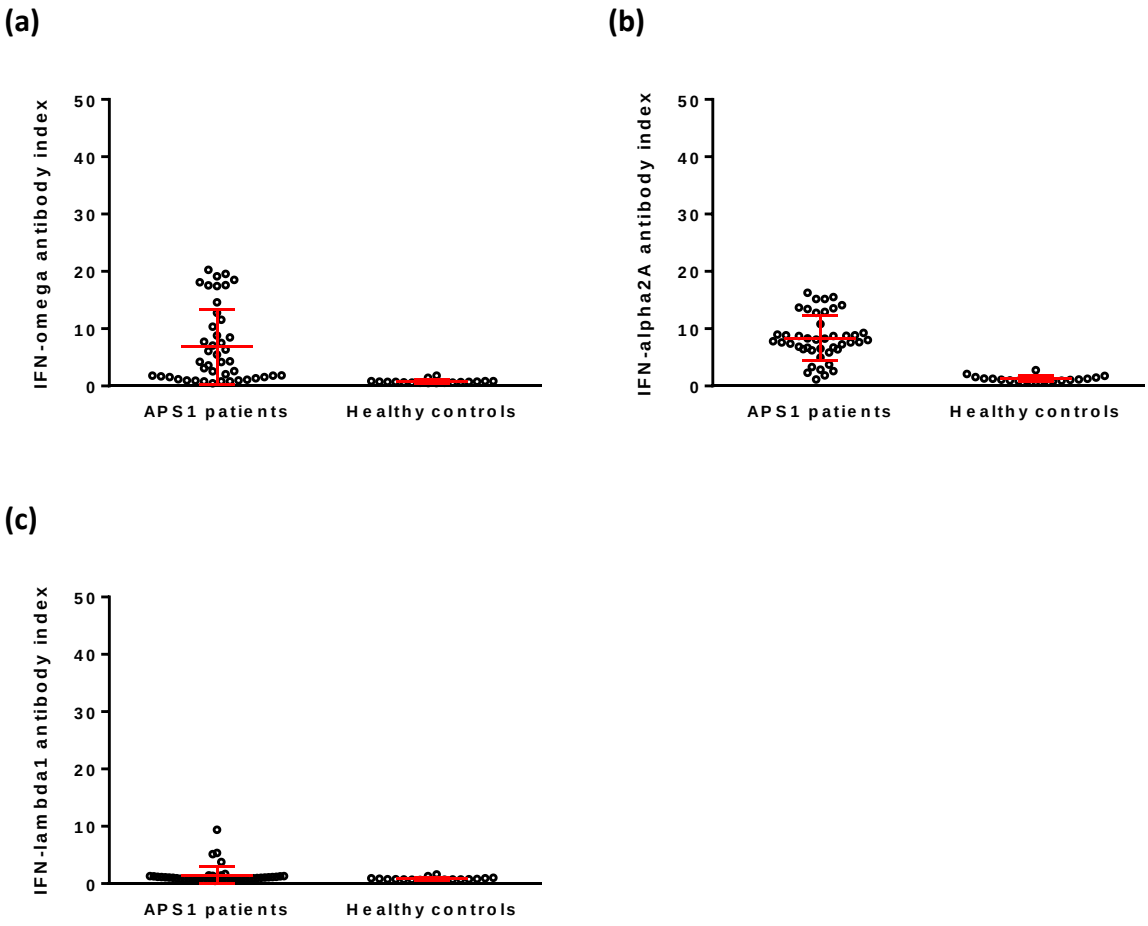

Figure 3.9: Interferon (IFN)-omega, IFN-alpha2A and IFN-lambda1 antibody indices of APS1 patient and control sera.

Sera from 44 APS1 patients and 18 healthy controls were evaluated for **(a)** IFN-omega, **(b)** IFN-alpha2A, and **(c)** IFN-lambda1 antibodies using ELISAs. The antibody index is shown for each APS1 patient and control serum and is the mean antibody index of at least two experiments. The mean antibody index ± SD for the APS1 patient group and the control group was, respectively, 6.85 ± 6.56 (range: 0.47-20.2) and 0.79 ± 0.35 (range: 0.51-1.80) in the IFN-omega ELISA; 8.37 ± 3.90 (range: 1.15-16.2) and 1.26 ± 0.52 (range: 0.76-2.75) in the IFN-alpha2A ELISA; and 1.41 ± 1.60 (range: 0.48-9.38) and 0.84 ± 0.25 (range: 0.64-1.60) in the IFN-lambda1 ELISA. In the IFN-omega and IFN-alpha2A ELISAs, there was a significant difference between the antibody indices of the APS1 patient and control groups (*P* values were < 0.0001, Mann-Whitney test). In the IFN-lambda1 ELISA, there was no significant different between the antibody indices of the APS1 patients and controls (P = 0.052, Mann-Whitney test).

Table 3.2: Summarised results of cytokine ELISAs

ELISA detail	Result
IL-22 ELISA	
Mean antibody index ± SD of APS1 patients	27.0 ± 10.9
Antibody index range of APS1 patients	1.94-44.5
Mean antibody index ± SD of healthy controls	0.99 ± 0.10
Antibody index range of healthy controls	0.88-1.11
Intra-assay coefficient of variation	4.3%
Inter-assay coefficient of variation	10.7%
IL-17F ELISA	
Mean antibody index ± SD of APS1 patients	23.8 ± 13.7
Antibody index range of APS1 patients	1.12-42.2
Mean antibody index ± SD of healthy controls	0.99 ± 0.10
Antibody index range of healthy controls	0.87-1.19
Intra-assay coefficient of variation	4.0%
Inter-assay coefficient of variation	4.8%
IL-17A ELISA	
Mean antibody index ± SD of APS1 patients	5.56 ± 10.7
Antibody index range of APS1 patients	0.77-36.9
Mean antibody index ± SD of healthy controls	0.96 ± 0.11
Antibody index range of healthy controls	0.83-1.24
Intra-assay coefficient of variation	4.1%
Inter-assay coefficient of variation	6.1%
IFN-omega ELISA	
Mean antibody index ± SD of APS1 patients	6.85 ± 6.56
Antibody index range of APS1 patients	0.47-20.2
Mean antibody index ± SD of healthy controls	0.79 ± 0.35
Antibody index range of healthy controls	0.51-1.80
Intra-assay coefficient of variation	3.0%
Inter-assay coefficient of variation	12.8%
IFN-alpha2A ELISA	
Mean antibody index ± SD of APS1 patients	8.37 ± 3.90
Antibody index range of APS1 patients	1.15-16.2
Mean antibody index ± SD of healthy controls	1.26 ± 0.52
Antibody index range of healthy controls	0.76-2.75
Intra-assay coefficient of variation	3.2%
Inter-assay coefficient of variation	10.8%
IFN-lambda1 ELISA	
Mean antibody index ± SD of APS1 patients	1.41 ± 1.60
Antibody index range of APS1 patients	0.48-9.38
Mean antibody index ± SD of healthy controls	0.84 ± 0.25
Antibody index range of healthy controls	0.64-1.60
Intra-assay coefficient of variation	2.7%
Inter-assay coefficient of variation	5.2%

Table 3.3: Summary of APS1 patient antibody reactivities

Patient	Antibody index in each antibody assay[1]							
	CaSR	NALP5	IL-22	IL-17F	IL-17A	IFN-omega	IFN-alpha2A	IFN-lambda1
APS1-1	**2.63**	0.57	**31.2**	**6.98**	1.29	**6.09**	**8.97**	0.70
APS1-2	**2.83**	0.61	**23.4**	**38.3**	**36.9**	0.82	**4.99**	0.72
APS1-3	**4.59**	1.35	**22.8**	**22.1**	**4.86**	**4.23**	**7.40**	**3.76**
APS1-4	**8.64**	1.25	**19.4**	**3.32**	**8.37**	**8.82**	**7.59**	**5.15**
APS1-5	**33.2**	1.09	**15.2**	**1.30**	0.98	0.80	**5.84**	0.87
APS1-6	**16.5**	**121.7**	**38.5**	**15.5**	**34.3**	**3.09**	**14.1**	1.31
APS1-7	**21.7**	**32.5**	**10.0**	1.12	**1.84**	**14.6**	**13.0**	1.25
APS1-8	**4.25**	1.41	**38.0**	**22.0**	**2.01**	**7.06**	**13.7**	1.09
APS1-9	**52.4**	1.11	**40.2**	**37.9**	**1.73**	1.83	**16.2**	1.11
APS1-10	**42.3**	0.62	**1.94**	**4.13**	**2.37**	**10.4**	**12.8**	1.44
APS1-11	**8.50**	1.14	**43.4**	**38.6**	**3.64**	**5.47**	**13.4**	1.15
APS1-12	**21.2**	19.3	**15.9**	**30.9**	**1.52**	0.99	**3.74**	0.95
APS1-13	**4.22**	0.65	**38.5**	**38.7**	**1.88**	**11.6**	**15.2**	1.04
APS1-14	**49.1**	0.87	**36.6**	**38.0**	**1.65**	**19.6**	**13.6**	1.08
APS1-15	**77.9**	**3.45**	**28.5**	**33.6**	**1.54**	0.97	1.85	0.69
APS1-16	**120.2**	0.84	**14.8**	1.19	0.77	0.47	**3.33**	0.48
APS1-17	1.03	0.86	**35.8**	**5.60**	**1.76**	1.83	**10.8**	1.30
APS1-18	1.98	28.5	**37.6**	**38.7**	**1.68**	**8.49**	**15.2**	1.36
APS1-19	1.00	0.89	**44.5**	**38.5**	**3.49**	**20.2**	**15.5**	1.07
APS1-20	0.74	1.40	**16.5**	**23.9**	0.95	1.18	2.60	0.64
APS1-21	1.10	0.63	**40.7**	**31.2**	1.24	0.93	**2.87**	0.73
APS1-22	1.65	**3.59**	**29.2**	**16.2**	**1.61**	**2.57**	**6.67**	0.93
APS1-23	0.96	1.20	**23.3**	**23.5**	0.98	**17.6**	**6.23**	0.63
APS1-24	0.59	**8.98**	**32.3**	**39.7**	**1.71**	**2.05**	**7.29**	0.79
APS1-25	0.64	1.41	**34.4**	**42.2**	1.11	**3.62**	**7.66**	0.60
APS1-26	1.19	1.16	**30.3**	**13.5**	**4.18**	**7.51**	**6.73**	0.77
APS1-27	0.76	1.04	**37.3**	**23.2**	1.09	1.69	**8.77**	1.18
APS1-28	0.73	**39.5**	**31.3**	**17.1**	0.94	1.36	1.15	0.64
APS1-29	0.68	**12.4**	**11.0**	**7.22**	1.04	1.56	2.31	0.59
APS1-30	0.71	0.90	**36.8**	**36.4**	1.16	**6.36**	**8.87**	0.72
APS1-31	1.11	0.82	**6.36**	**24.5**	1.18	**7.72**	**8.25**	**5.37**
APS1-32	0.77	**36.0**	**34.5**	**36.4**	1.09	**18.1**	**8.74**	1.19
APS1-33	1.42	0.92	**23.6**	**4.48**	**1.61**	**1.86**	**8.73**	1.44
APS1-34	1.95	1.13	**28.2**	**34.9**	**34.6**	**19.1**	**8.10**	**9.38**
APS1-35	0.81	0.91	**33.0**	**8.95**	1.02	**4.18**	**8.84**	0.76
APS1-36	0.53	0.70	**28.1**	**25.9**	**34.8**	0.82	**6.53**	0.58
APS1-37	1.35	6.72	**29.2**	**36.7**	**33.1**	**17.6**	**9.27**	0.79
APS1-38	0.93	1.25	**14.4**	**35.2**	**1.90**	**12.8**	**7.82**	0.99
APS1-39	1.04	**37.8**	**35.7**	**38.3**	1.29	**17.4**	**8.30**	**1.67**
APS1-40	0.64	**25.4**	**21.4**	**21.3**	0.92	1.56	**7.59**	1.01
APS1-41	0.75	0.92	**7.93**	0.91	0.99	**4.30**	**6.41**	0.83
APS1-42	1.27	1.37	**21.0**	**32.1**	**1.66**	**2.62**	**8.03**	1.14
APS1-43	0.95	1.19	**30.9**	**34.9**	0.94	1.11	**6.85**	0.85
APS1-44	0.78	0.64	**16.0**	**20.5**	0.98	**18.5**	**6.42**	1.25

[1]Bold type-face indicates antibody-positive APS1 patient serum.

3.4.4 Detection of CaSR antibodies in APS1 patients and controls

3.4.4.1 Expression of CaSR-FLAG in HEK293 cells

The CaSR-FLAG protein expressed in HEK293 cells was detected as a 140-kDa band on western blots using anti-FLAG antibody-HRP or anti-CASR11-S antiserum plus anti-rabbit IgG antibody-HRP (**Figure 3.10**). No binding of the anti-FLAG antibody-HRP was observed on western blots containing extracts of HEK293 cells expressing CaSR without a FLAG epitope or extracts of untransfected HEK293 cells (**Figure 3.10**), indicating that the anti-FLAG antibody-HRP did not bind non-specifically to other peptide sequences.

3.4.4.2 Results of CaSR immunoprecipitation assays

To detect the presence of antibodies against the CaSR, serum samples from 44 APS1 patients and 23 healthy controls were analysed in CaSR immunoprecipitation assays, as detailed in **Section 3.3.4.** The results are shown in **Figure 3.11.** The mean CaSR antibody index of the APS1 patient group, the healthy control group and the anti-CASR11-S antiserum was, respectively, 11.3 ± 23.8 (range: 0.59-120.2), 1.00 ± 0.39 (range: 0.62-1.93), and 31.6 ± 1.66 (range: 29.9-33.2). There was a significant difference between the CaSR antibody indices of the APS1 patient and control groups (P = 0.034, Mann-Whitney test). The intra- and inter-assay coefficients of variation for the CaSR immunoprecipitation assay were, respectively, 3.5% and 14.9%.

The upper limit of normal for the CaSR immunoprecipitation assay was a CaSR antibody index of 2.17 (mean CaSR antibody index + 3SD of 23 healthy individuals). As expected, the CaSR was immunoprecipitated by the anti-CASR11-S antiserum which had a CaSR antibody index of 31.6, this being above the upper limit of normal. All healthy controls were CaSR antibody-negative as their CaSR antibody indices (range: 0.62-1.93) were below the upper limit of normal. Of the 44 APS1 patient sera, 16 (36%) were considered CaSR antibody-positive, as their CaSR antibody index was above the upper limit of normal value of 2.17 (**Table 3.3**). Compared with controls, the prevalence of CaSR antibodies was significantly

elevated in the APS1 patient group (P = 0.0001, Fisher's exact test for 2 x 2 contingency tables).

Figure 3.12 illustrates western blotting for the detection of CaSR-FLAG protein with anti-FLAG antibody-HRP following immunoprecipitation with patient sera, control sera or anti-CASR11-S antiserum. In the absence of serum or anti-CASR-S11 antiserum in the CaSR immunoprecipitation assay reaction, the CaSR-FLAG protein could not be detected on the subsequent western blots with anti-FLAG antibody-HRP, indicating that there were no detectable levels of CaSR-FLAG binding to GammaBind® G Sepharose beads.

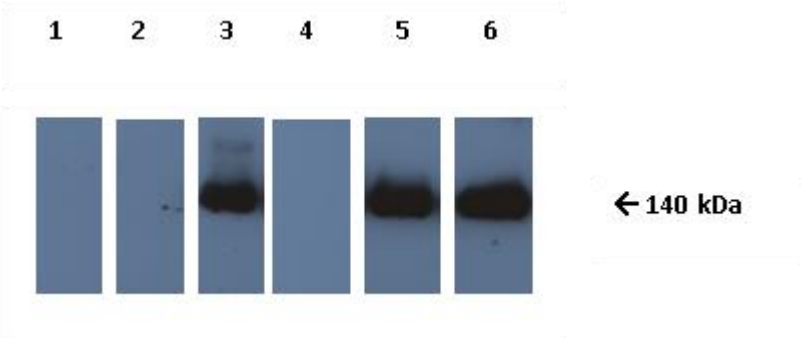

Figure 3.10: Western blot of detection of CaSR and CaSR-FLAG proteins in HEK293 cell extracts

Cell extracts from untransfected HEK293 cells and HEK293 cells transfected with either pcCaSR-FLAG or pCDNA3-CaSR were subjected to SDS-PAGE in 7.5% (w/v) polyacrylamide gels and transferred to Whatman™ Westran® Clear Signal PVDF blotting membrane. Proteins were detected on the blots by enhanced chemiluminescence following probing with anti-CASR11-S antiserum plus anti-rabbit IgG antibody-HRP, or with anti-FLAG antibody-HRP. The CaSR protein appears as a 140-kDa band. The results are shown for: untransfected HEK293 cell extract probed with anti-CASR11-S antiserum plus anti-rabbit IgG antibody-HRP (lane 1); untransfected HEK293 cell extract probed with anti-FLAG antibody-HRP (lane 2); pcDNA3-CaSR-transfected HEK293 cell extract probed with anti-CASR11-S antiserum plus anti-rabbit IgG antibody-HRP (lane 3); pcDNA3-CaSR-transfected HEK293 cell extract probed with anti-FLAG antibody-HRP (lane 4); pcCaSR-FLAG-transfected HEK293 cell extract probed with anti-CASR11-S antiserum plus anti-rabbit IgG antibody-HRP (lane 5); pcCaSR-FLAG-transfected HEK293 cell extract probed with anti-FLAG antibody-HRP (lane 6).

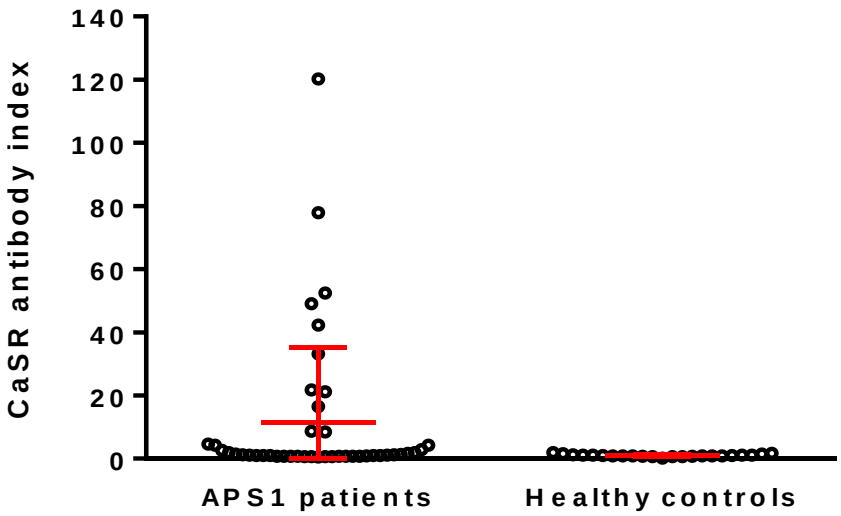

Figure 3.11: CaSR antibody indices of APS1 patient and control sera.

Sera from 44 APS1 patients and 23 healthy controls were evaluated for CaSR antibodies using CaSR immunoprecipitation assays. The CaSR antibody index is shown for each APS1 patient and control serum and is the mean antibody index of at least two experiments. The mean CaSR antibody index ± SD for the APS1 patient group and for the control group was, respectively, 11.3 ± 23.8 (range: 0.59-120.2) and 1.00 ± 0.39 (range: 0.62-1.93). There was a significant difference between the CaSR antibody indices of the APS1 patient and control groups (P = 0.034, Mann-Whitney test).

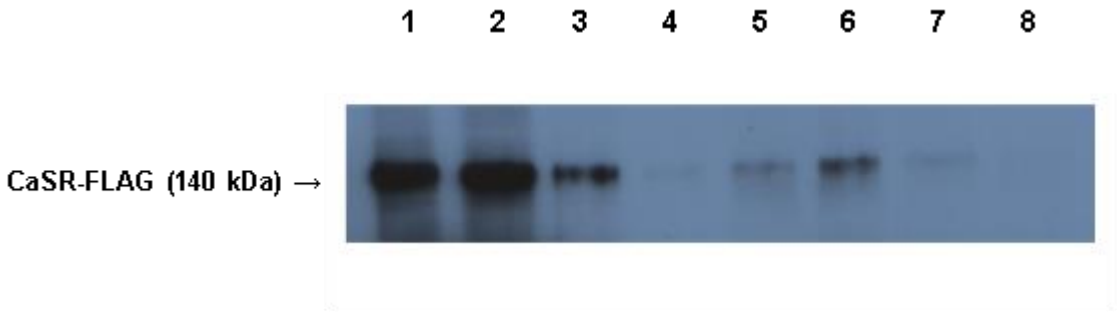

Figure 3.12: Western blot for detection of CaSR-FLAG protein following immunoprecipitation with APS1 patient and control sera.

APS1 patient and control sera, and anti-CASR11-S antiserum, were analysed for CaSR-FLAG binding in CaSR immunoprecipitation assays. Proteins immunoprecipitated from the HEK293 cell extract containing expressed CaSR-FLAG protein were separated by SDS-PAGE in 7.5% (w/v) polyacrylamide gels and transferred to Whatman™ Westran® Clear Signal PVDF blotting membrane. The CaSR-FLAG protein was detected on the blots using anti-FLAG antibody-HRP and enhanced chemiluminescence. The results are shown for immunoprecipitation of CaSR-FLAG by: anti-CASR11-S antiserum (lane 1); CaSR antibody-positive APS1 patient sera (lanes 2, 3 and 6); control sera (lanes 4, 5 and 7); GammaBind® G Sepharose beads alone (no serum or anti-CASR11-S antiserum) (lane 8). The image is from an article by Kemp et al, 2014, and is taken with kind permission from The Endocrine Society (2055 L Street NW, Suite 600, Washington, DC 20036, USA).

3.4.5 Detection of NALP5 antibodies in APS1 patients and controls

3.4.5.1 *In vitro* translation of NALP5

In vitro translation of NALP5 cDNA in plasmid pCMV6-XL5-NALP5 (**Figure 3.5**) produced a protein product with an estimated molecular weight of approximately 134 kDa (**Figure 3.13**), which agreed well with the molecular weight of 132 kDa predicted from the amino acid sequence of the protein with 1201 residues (Brown et al., 1993).

3.4.5.2 Results of NALP5 radioligand binding assays

Forty-four APS1 patient and 38 control sera were tested for the presence of NALP5 antibodies using NALP5 RLBAs, as detailed in **Section 3.3.5**. The results are shown in **Figure 3.14.** The mean NALP5 antibody index of the APS1 patient group, the healthy control group, and the anti-NALP5 antibody was, respectively, 9.24 ± 20.7 (range: 0.57-121.7), 1.01 ± 0.24 (range: 0.57-1.38), and 28.9 ± 0.35 (range: 28.6-29.3). There was a significant difference between the NALP5 antibody indices of the APS1 patient and control groups (P = 0.038, Mann-Whitney test). The intra- and inter-assay coefficients of variation for the NALP5 RLBA were, respectively, 5.4% and 5.5%.

The upper limit of normal for the NALP5 RLBA was an NALP5 antibody index of 1.73 (mean NALP5 antibody index + 3SD of 38 healthy individuals). As expected, NALP5 was immunoprecipitated by the anti-NALP5 antibody which had a NALP5 antibody index of 28.9, this being above the upper limit of normal. Healthy controls were all NALP5 antibody-negative, each with a NALP5 antibody index (range: 0.57-1.38) below the upper limit of normal. Of the 44 APS1 patient sera, 13 (30%) were considered NALP5 antibody-positive, as their NALP5 antibody index was above the upper limit of normal value of 1.73 (**Table 3.3**). Compared with controls, the prevalence of NALP5 antibodies was significantly elevated in the APS1 patient group (P = 0.0001, Fisher's exact test for 2 x 2 contingency tables).

Qualitative analysis of the proteins immunoprecipitated in the NALP5 RLBA by APS1 patient and control sera indicated that all of the 13 NALP5 antibody-positive APS1 patient

sera tested immunoprecipitated a protein band of 134 kDa, which is of the expected size for NALP5 in SDS-polyacrylamide gels. This is illustrated in **Figure 3.15,** for three APS1 patients, one healthy control, and the anti-NALP5 antibody. There was no detectable binding of [^{35}S]-NALP5 to protein G Sepharose^{TM} 4 Fast Flow in the absence of serum or anti-NALP5 antibody (**Figure 3.15**).

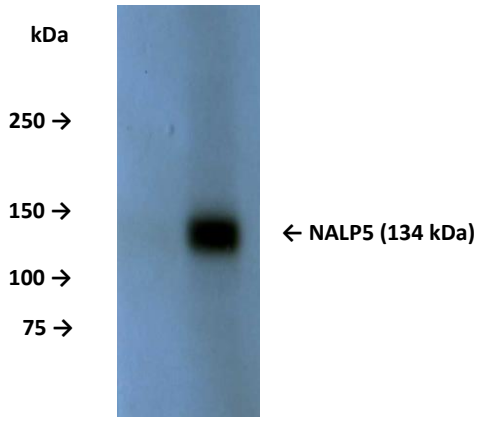

Figure 3.13: SDS-PAGE and autoradiography of [^{35}S]-NALP5.

Radiolabelled NALP5 was produced *in vitro* in a TnT® T7-Coupled Reticulocyte Lysate System using plasmid pCMV6-XL5-NALP5. [^{35}S]-labelled NALP5 protein was analysed by SDS-PAGE in an 8% (w/v) SDS-polyacrylamide gel followed by autoradiography. Precision Plus Protein All Blue Standards (10-250 kDa) are indicated.

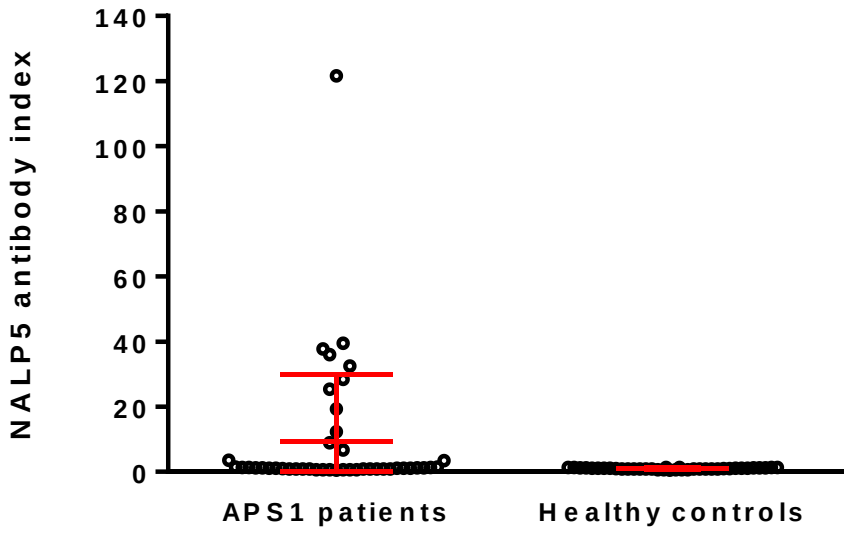

Figure 3.14: NALP5 antibody indices of APS1 patient and control sera.

Sera from 44 APS1 patients and 38 healthy controls were evaluated for NALP5 antibodies using NALP5 RLBAs. The NALP5 antibody index is shown for each APS1 patient and control serum and is the mean NALP5 antibody index of at least two experiments. The mean NALP5 antibody index ± SD for the APS1 patient group and the control group was, respectively, 9.24 ± 20.7 (range: 0.57-121.7) and 1.01 ± 0.24 (range: 0.57-1.38). There was a significant difference between the NALP5 antibody indices of the APS1 patient and control groups (P = 0.038, Mann-Whitney test).

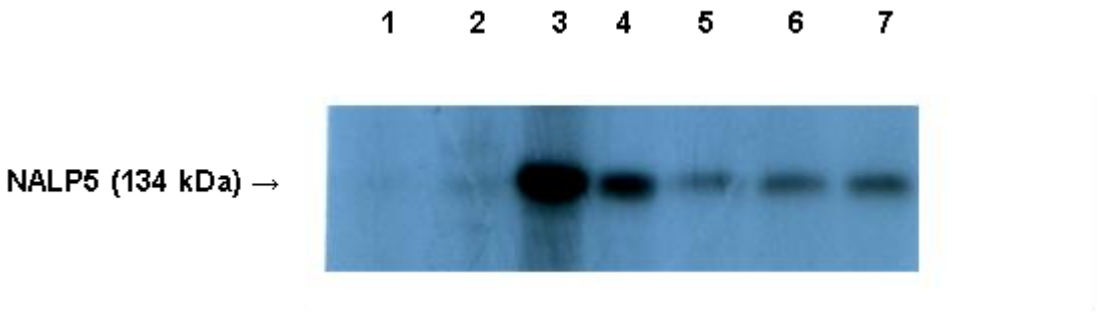

Figure 3.15: SDS-PAGE and autoradiography of immunoprecipitated [^{35}S]-NALP5 following NALP5 radioligand binding assays with APS1 patient and control sera.

Radiolabelled NALP5 was produced *in vitro* in a TnT® T7-Coupled Reticulocyte Lysate System and then used in NALP5 RLBAs with APS1 patient and control sera, and anti-NALP5 antibody. Immunoprecipitation of [^{35}S]-labelled NALP5 protein was analysed by SDS-PAGE in 8% (w/v) polyacrylamide gels followed by autoradiography. The results are shown for: [^{35}S]-NALP5 with protein G SepharoseTM 4 Fast Flow alone (no serum or anti-NALP5 antibody) (lane 1); [^{35}S]-NALP5 immunoprecipitated with a NALP5 antibody-negative control serum (lane 2); *in vitro* translated [^{35}S]-NALP5 (without immunoprecipitation) (lane 3); [^{35}S]-NALP5 immunoprecipitated with anti-NALP5 antibody (lane 4); [^{35}S]-NALP5 immunoprecipitated with NALP5 antibody-positive APS1 patient sera (lanes 5-7). The image is from an article by Kemp et al, 2014, and is taken with kind permission from The Endocrine Society (2055 L Street NW, Suite 600, Washington, DC 20036, USA).

3.4.6 Associations of CaSR and NALP5 antibodies with the clinical and demographic characteristics and *AIRE* genotypes of APS1 patients

No statistically significant associations were found between the presence of CaSR or NALP5 antibodies and the disease components of APS1, including hypoparathyroidism (**Table 3.4**) With respect to hypoparathyroidism diagnosis, the detection of CaSR and NALP5 antibodies had specificities (percentage of patients correctly identified with no hypoparathyroidism and calculated as: 100 x true negatives/true negatives + false positives) of 83% and 50%, and sensitivities (percentage of patients correctly diagnosed with hypoparathyroidism and calculated as: 100 x true positives/true positives + false negatives) of 39% and 26%, respectively (**Table 3.4**) In addition, there was no significant difference between the combined prevalence of CaSR and NALP5 antibodies (whether occurring alone or together) in patients with (21/38 = 55%) or without (4/6 = 66%) hypoparathyroidism (P = 0.68, Fisher's exact test). Furthermore, the frequencies of CaSR and NALP5 antibodies were not significantly greater in females with APS1-associated hypoparathyroidism when compared with males with APS1-associated hypoparathyroidism (**Table 3.5**).

There were no significant associations between the presence of CaSR or NALP5 antibodies and either the sex or age of the patients (**Table 3.5**). A significant association between a shorter APS1 duration (< 10 years) and positivity for CaSR antibodies was revealed, although this was not the case for NALP5 antibodies (**Table 3.5**). Furthermore, higher CaSR antibody indices correlated with a shorter duration of APS1 (Spearman's r = -0.44 with 95% confidence intervals: -0.66 to -0.16; P = 0.0027) (**Figure 3.16**). Multiple regression analysis indicated that the correlation of higher CaSR antibody indices with shorter APS1 duration was not independent of age (P = 0.099), but was independent of sex (P = 0.010). In contrast, there was no significant correlation between higher NALP5 antibody indices and the duration of APS1 (Spearman's r = -0.16 with 95% confidence intervals: -0.44 to 0.15; P = 0.30).

No significant associations were found with the *AIRE* genotypes of the APS1 patients and the presence of antibodies against the CaSR or NALP5. Fifteen patients were homozygous

for the c.769C>T mutation. The remaining patient had a c.769C>T/c.967-979del13bp genotype. Amongst the 13 patients with NALP5 antibodies, there were 10 c.769C>T homozygotes, two c.769C>T/c.923G>A heterozygotes, and one c.769C>T/ c.1638A>T heterozygote.

Table 3.4: Prevalence of CaSR and NALP5 antibodies in APS1 patients with and without disease components

Disease component	Number of APS1 patients with disease component (%)	Number of patients with disease component and CaSR antibodies (%)	Number of patients without disease component and CaSR antibodies (%)	*P* value[1]	Number of patients with disease component and NALP5 antibodies (%)	Number of patients without disease component and NALP5 antibodies (%)	*P* value[1]
Hypoparathyroidism	38/44 (86)	15/38 (39)	1/6 (17)	0.39	10/38 (26)	3/6 (50)	0.34
Chronic mucocutaneous candidiasis	44/44 (100)	16/44 (36)	0/0 (0)	ND[2]	13/44 (30)	0/0 (0)	ND[2]
Addison's disease	38/44 (86)	16/38 (42)	0/6 (0)	0.072	13/38 (34)	0/6 (0)	0.16
Type 1 diabetes mellitus	8/44 (18)	4/8 (50)	12/36 (33)	0.43	2/8 (25)	11/36 (31)	1.00
Alopecia areata	21/44 (45)	6/21 (29)	10/23 (43)	0.36	6/21 (29)	7/23 (30)	1.00
Pernicious anaemia	4/44 (9.1)	1/4 (25)	15/40 (38)	1.00	1/4 (25)	12/40 (30)	1.00
Premature ovarian failure	17/26 (65)	6/17 (35)	2/9 (22)	0.67	5/17 (29)	2/9 (22)	1.00
Hypothyroidism	12/44 (27)	2/12 (17)	14/32 (44)	0.16	2/12 (17)	11/32 (34)	0.46
Vitiligo	12/44 (27)	4/12 (33)	12/32 (38)	1.00	3/12 (25)	10/32 (31)	1.00
Keratoconjunctivitis	11/44 (25)	5/11 (45)	11/33 (30)	0.49	3/11 (27)	10/33 (30)	1.00
Asplenia	13/44 (23)	5/13 (38)	11/31 (35)	1.00	3/13 (23)	10/31 (32)	0.72
Growth hormone deficiency	4/44 (9.1)	1/4 (25)	15/40 (38)	1.00	3/5 (60)	10/39 (26)	0.14
Exocrine pancreatic atrophy	1/44 (2.3)	0/1 (0)	16/43 (37)	1.00	1/1 (100)	12/43 (30)	0.30
Chronic diarrhoea	2/44 (4.5)	2/2 (100)	14/42 (33)	0.13	0/2 (0)	13/42 (31)	1.00
Hepatitis	3/44 (6.8)	1/3 (33)	15/41 (37)	1.00	2/3 (67)	11/41 (27)	0.20
Chronic obstipation	17/44 (39)	4/17 (24)	12/27 (44)	0.21	6/17 (35)	7/27 (26)	0.52
Arterial hypertension	1/44 (2.3)	0/1 (0)	16/43 (37)	1.00	0/1 (0)	13/43 (30)	1.00
Hypogonadism (male)	4/18 (22)	2/4 (50)	6/14 (43)	1.00	1/4 (25)	5/14 (36)	1.00
Tubulonephritis	3/44 (6.8)	1/3 (33)	15/41 (37)	1.00	0/3 (0)	13/41 (32)	0.54

[1]*P* values were calculated using 2 x 2 contingency tables and Fisher's exact test for comparing the prevalence of CaSR or NALP5 antibodies in APS1 patients with or without disease components. *P* values < 0.05 were considered significant.
[2]ND, not determined.
The table is from an article by Kemp et al, 2014, and is taken with kind permission from The Endocrine Society (2055 L Street NW, Suite 600, Washington, DC 20036, USA).

Table 3.5: Comparison of demographic and clinical characteristics of APS1 patients with and without CaSR or NALP5 antibodies

Demographic/clinical characteristic	Number of CaSR antibody-positive APS1 patients with characteristic (%) (except detail of the whole group[1])	Number of CaSR antibody-negative APS1 patients with characteristic (%) (except detail of the whole group[1])	*P* value	Number of NALP5 antibody-positive APS1 patients with characteristic (%) (except detail of the whole group[1])	Number of NALP5 antibody-negative APS1 patients with characteristic (%) (except detail of the whole group[1])	*P* value
Sex						
All APS1 patients (n = 44)						
Male	8/16 (50)	10/28 (36)	0.53[2]	6/13 (46)	12/31 (39)	0.74[2]
Female	8/16 (50)	18/28 (64)		7/13 (54)	19/31 (61)	
APS1 patients with hypoprathyroidism (n =38)						
Male	7/15 (47)	6/23 (26)	0.30[2]	4/10 (40)	9/28 (32)	0.71[2]
Female	8/15 (53)	17/23 (74)		6/10 (60)	19/28 (68)	
Age						
Mean (years) ± SD of the group (n = 44)	27.0 ± 15.9[1]	36.7 ± 15.6[1]	0.067[3]	28.8 ± 18.3[1]	35.0 ± 15.3[1]	0.18[3]
< 10 years	3/16 (19)	1/28 (4)	0.13[2]	3/13 (23)	1/31 (3)	0.071[2]
> 10 years	13/16 (81)	27/28 (96)		10/13 (77)	30/31 (97)	
APS1 duration						
Mean (years) ± SD of the group (n = 44)	22.0 ± 15.5[1]	31.4 ± 14.2[1]	0.044[3]	23.9 ± 15.3[1]	29.7 ± 15.1[1]	0.26[3]
< 10 years	6/16 (38)	2/28 (7)	0.019[2]	4/13 (31)	4/31 (13)	0.21[2]
> 10 years	10/16 (62)	26/28 (93)		9/13 (69)	27/31 (87)	

[1]Mean age or disease duration and SD of the APS1 patient group.

[2]*P* value calculated using Fisher's exact test for 2 x 2 contingency tables for comparing the prevalence of demographic and clinical characteristics in CaSR or NALP5 antibody-positive and antibody-negative patient groups. *P* values < 0.05 were considered significant.

[3]*P* value calculated using the Mann-Whitney test for comparing demographic and clinical characteristics in CaSR or NALP5 antibody-positive and antibody-negative patient groups. *P* values < 0.05 were considered significant.

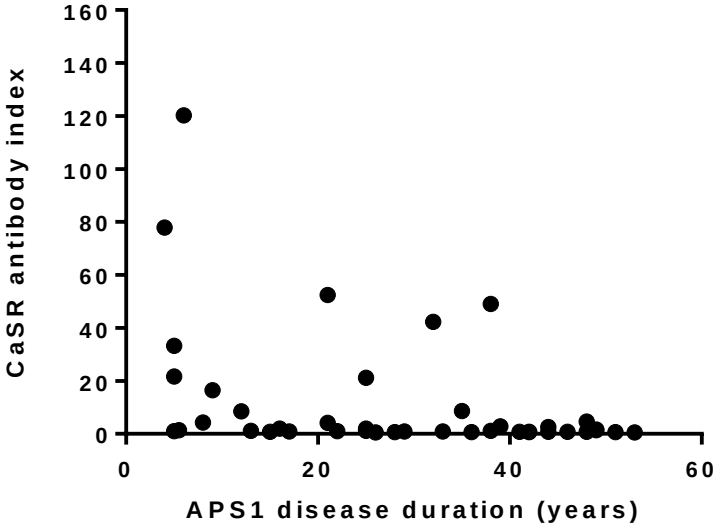

Figure 3.16: Correlation of CaSR antibody index with APS1 disease duration.

Higher CaSR antibody indices correlated with a shorter duration of APS1 (Spearman's r = -0.44 with 95% confidence intervals: -0.66 to -0.16; P = 0.0027).

3.5 Discussion

Patient clinical details Clinically, 43 patients in the current cohort of 44 displayed at least two of the major APS1 disease manifestations of chronic mucocutaneous candidiasis, hypoparathyroidism and Addison's disease (Perheentupa, 2006). Hypoparathyroidism was present in 86% of patients and had a significantly greater prevalence in females (96%) than in males (72%). Both observations concur with previous reports that hypoparathyroidism affects more than 80% of APS1 patients (Perheentupa, 2006), and is the only disease component that has a difference in prevalence between males and females (Gylling et al., 2003). The other APS1 disease manifestations were also found at a similar prevalence to previous studies (Soderbergh et al., 2004, Perheentupa, 2006).

AIRE genotype and cytokine antibodies To further confirm the clinical diagnosis of APS1, each patient's *AIRE* gene was analysed for the presence of mutations. The predominant Finnish *AIRE* mutation c.769C>T was evident in 100% of the individuals (Perheentupa, 2006), and the majority (82%) were homozygous for this *AIRE* genotype. Eight patients were compound heterozygotes with one c.769C>T mutated allele and a second well-known mutation occurring elsewhere in their *AIRE* gene coding region. Serologically, antibodies against cytokines are extremely useful as diagnostic markers for APS1 and, indeed, antibodies against type I IFNs (IFN-alpha2, IFN-omega and IFN-lambda1), and IL-22 and Th17 cell-related cytokines (IL-17A and IL-17F) were found in our patients at a similar prevalence to earlier reports (Meager et al., 2006, Cervato et al., 2010).

Prevalence of CaSR and NALP5 antibodies Previous studies on APS1 patients have identified the CaSR (Li et al., 1996, Gylling et al., 2003, Mayer et al., 2004, Gavalas et al., 2007) and NALP5 (Alimohammadi et al., 2008, Cervato et al., 2010, Tomar et al., 2012) as autoantibody targets, both of which are expressed to a high level in the parathyroid gland (Brown et al., 1993, Alimohammadi et al., 2008). Here, NALP5 antibodies were detected at a slightly lower prevalence to that already reported: 30% of APS1 patients were NALP5 antibody-positive in this study *versus* 40% of patients in the analysis by Alimohammadi and colleagues (Alimohammadi et al., 2008). Depending on the study, antibodies against the CaSR have been documented to occur in 0-86% of APS1 patients (Li et al., 1996, Gylling et al., 2003, Mayer et al., 2004, Soderbergh et al.,

2004, Gavalas et al., 2007). In the present analysis, the receptor was confirmed as an autoantigen, although CaSR antibodies were detected at a lower prevalence (36%) than found earlier by our group (86%) (Gavalas et al., 2007). The variability of CaSR and NALP5 antibody prevalence in APS1 cohorts could be due to differences in the size and origin of the patient and control groups, the criteria used to define positivity or the type of antibody assay employed (Li et al., 1996, Gylling et al., 2003, Mayer et al., 2004, Soderbergh et al., 2004, Gavalas et al., 2007, Alimohammadi et al., 2008, Tomar et al., 2013). For example, the previous report of NALP5 antibodies included APS1 patients of several origins (Alimohammadi et al., 2008), whereas only Finnish patients were recruited for the present study. Indeed, in the case of the frequency of antibodies against tryptophan hydroxylase, there is variation between APS1 patients from different countries in that 100%, 37% and 22% of Swedish, Finnish and Norwegian patients, respectively, were positive (Ekwall et al., 1998). Although the type of assay employed can have an effect upon the detection rate of CaSR antibodies (Gavalas et al., 2007, Tomar et al., 2013), it is most likely that the lower frequency found in the present study, compared with a previous report (Gavalas et al., 2007), is due to the difference in cohort size (44 patients *versus* 14 patients), as the same CaSR immunoprecipitation assay was used with APS1 patients of the same origin (Finnish) (Gavalas et al., 2007).

Association of CaSR and NALP5 antibodies with hypoparathyroidism Since the clinical manifestations in APS1 have been associated with specific autoantibodies (Soderbergh et al., 2004), it is not unreasonable to assume there is a parathyroid autoantigen(s) which could act as an independent marker for hypoparathyroidsim. Therefore, the main aim of the present study was to investigate any potential association between clinical hypoparathyroidism and the presence of CaSR and NALP5 antibodies. However, although CaSR antibodies were detected in a higher percentage (15/38 = 39%) of patients with hypoparathyroidism compared to those without (1/6 = 17%), the difference in their frequency did not reach statistical significance (P = 0.392). In contrast to a previous study (Alimohammadi et al., 2008), NALP5 antibodies did not have 100% specificity for the diagnosis of hypoparathyroidism in this APS1 patient cohort since immunoreactivity against NALP5 was detected too in three out of six (50%) patients without hypoparathyroidism. Again, this contrast could be due to the somewhat different origins of the populations included in this and the previous study

(Alimohammadi et al., 2008). Indeed, tryptophan hydroxylase antibodies have been reported to significantly associate with intestinal dysfunction in APS1 in a mixed population of Scandinavian background (Ekwall et al., 1998), but this was not the case for Italian APS1 patients (Dal Pra et al., 2004). Furthermore, there is also the issue of the very small numbers of APS1 patients without hypoparathyroidism that are available for testing. Between studies, this rarity can have a significant impact on the reported specificity of CaSR and NALP5 antibodies for diagnosing hypoparathyroidism in APS1. Interestingly, the combined prevalence of CaSR and NALP5 antibodies (whether occurring alone or together) also did not significantly differ between patients with (21/38 = 55%) and without (4/6 = 66%) hypoparathyroidism (P = 0.684). Furthermore, despite earlier reports that CaSR antibodies were more prevalent in females than in males with APS1-associated hypoparathyroidism (72% *versus* 14%, respectively) (Li et al., 1996), the frequency of CaSR and NALP5 antibodies was not significantly greater in our female patient group with hypoparathyroidism, even though the disease was more common in our female APS1 patients than in the males.

The absence of both CaSR and NALP5 antibodies in a high percentage of APS1 patients with hypoparathyroidism (17/38 = 45% in this study) could be explained by the existence in some patients of autoantibodies against different parathyroid antigens or that some patients simply never develop autoantibodies against the parathyroid gland. Alternatively, the absence of NALP5 and CaSR antibodies could be due to loss of the antigen required to drive their production before they could be studied. Indeed, with type 1 diabetes mellitus, antibodies against islet cells are not longer detectable after the clinical onset of disease when the pancreatic ß cells have been destroyed and the islet cell autoantigen has disappeared (Hermitte et al., 1998). In keeping with this, Li and colleagues (Li et al., 1996) reported there was significantly less chance of detecting CaSR antibodies in APS1 patients if hypoparathyroidism had been present for more than five years. Likewise, we found a significant association between a shorter APS1 duration (< 10 years) and CaSR sero-positivity, although this was not the case for NALP5 antibodies.

Aetiology and pathogenesis of hypoparathyroidism in APS1 Since other APS1 endocrinopathies are typical autoimmune diseases with T cell infiltration of the affected organ and circulating tissue-specific autoantibodies, there is an assumption

that hypoparathyroidism has a similar pathogenesis. Cases of idiopathic hypoparathyroidism with lymphocytic infiltration of the parathyroid gland have been reported (Vandecas and Gepts, 1973) and, in one case, this was accompanied by a positive leukocyte migration inhibition test (Vandecas and Gepts, 1973). However, T cell reactivity against specific parathyroid antigens has not been convincingly demonstrated, although in one study of patients with idiopathic hypoparathyroidism, there was an increase in activated T lymphocytes in the circulation compared to controls (Wortsman et al., 1992). In APS1, autoreactive T lymphocytes which have escaped clonal deletion due to the lack of AIRE expression in thymic medullary epithelial cells (Zuklys et al., 2000) may target and damage the parathyroid leading to hypoparathyroidism and the secondary development of autoantibodies such as those against the CaSR and NALP5.

In organ-specific autoimmune disorders like type 1 diabetes mellitus and Hashimoto's thyroiditis, autoimmune destruction of tissue is provoked by T cells, and autoantibodies have a limited pathogenic role (Liblau et al., 1995). Therefore, CaSR and NALP5 antibodies and other humoral immune responses against the parathyroid (Betterle et al., 1985, Brandi et al., 1986, Posillico et al., 1986, Fattorossi et al., 1988) may just represent an epiphenomenon with T lymphocytes being primarily responsible for parathyroid damage. Conversely, due to their cell surface target, CaSR antibodies could destroy parathyroid cells through the fixing of complement or through antibody-dependent cellular cytotoxicity. Indeed, Brandi and colleagues (Brandi et al., 1986) have demonstrated antibody-mediated cellular cytotoxicity against cultured bovine parathyroid cells when exposed to serum from patients with idiopathic hypoparathyroidism. Alternatively, CaSR antibodies might lead to a decline in PTH-release essentially by acting as an agonist for binding to the CaSR expressed on the surface of parathyroid chief cells. Well-known examples of the organ-specific autoantigens that are extracellular receptors include the thyrotropin receptor in Graves' hyperthyroidism and the acetylcholine receptor in myasthenia gravis (Morgenthaler et al., 2007, Jacob et al., 2012). Initial evidence in support of a functional humoral immune response against the parathyroid gland came from the inhibition of PTH secretion from dispersed human parathyroid cells by three patients with idiopathic hypoparathyroidism (Posillico et al., 1986). So far, however, few patients have been identified with CaSR-activating antibodies that could potentially

reduce PTH secretion (Kifor et al., 2004, Kemp et al., 2009). IgG from two patients with APS1 (both with hypoparathyroidism) activated the receptor expressed in HEK293 cells (Kemp et al., 2009), and sera from two patients with idiopathic hypoparathyroidism inhibited PTH-secretion from human parathyroid cells (Kifor et al., 2004). Of the two idiopathic hypoparathyroid patients, one had transient hypoparathyroidism and the second had a morphologically intact parathyroid gland, despite many years of hypoparathyroidism, suggesting that CaSR-activating antibodies need not irreversibly destroy the parathyroid (Kifor et al., 2004).

Conclusions To conclude, neither CaSR nor NALP5 antibodies were found to be specific or sensitive markers for hypoparathyroidism in APS1. Finding a parathyroid-specific antigen which can be associated with hypoparathyroidism to allow serologic diagnosis of the disease is therefore still necessary. The discovery of novel parathyroid antibody targets, even if they are just markers of disease, are likely also to reveal important T cell autoantigens in an analogous way to thyroid peroxidase antibodies in autoimmune thyroid disease. Further investigations are also required to determine the exact role of the autoimmune response against both the CaSR and NALP5 in the pathogenesis of APS1. Particularly, the identification of T cells against both autoantigens and the detailed characterisation of potential CaSR antibody effects will allow insights into possible pathogenic processes that might lead to impaired parathyroid function in APS1.

Chapter 4

Mapping of autoantibody binding sites on the calcium-sensing receptor

4 Mapping of autoantibody binding sites on the calcium-sensing receptor

4.1 Introduction

4.1.1 Antibody-antigen interactions

The term epitope is used to describe the exact region on an antigen that is recognised by an antibody. The part of the antibody that interacts with the epitope is referred to as the paratope. Although antigenic epitopes vary enormously in terms of size, primary amino acid sequence, secondary structure, and post-translational modifications (Westwood and Hay, 2001), they are usually defined as either linear or conformational. Linear epitopes are distinguished by their amino acid sequence and can range from 5-6 amino acid residues (Roitt and Delves, 1997) to 15-22 amino acid residues (von Mikecz et al., 1995). In contrast, conformational epitopes are distinguished by the secondary or tertiary structure of the antigen (Roitt and Delves, 1997). Usually, antibodies recognise epitopes that depend on the structure of a native antigen, so B cell epitopes are often hydrophilic and exposed on the antigen surface (Westwood and Hay, 2001). This knowledge does allow the prediction of antibody binding sites, but their identification ultimately requires confirmation by experimental methods (Westwood and Hay, 2001).

4.1.2 B cell epitope mapping techniques

Several different approaches are available for mapping antibody epitopes and these are summarised in **Table 4.1.** X-ray crystallography and nuclear magnetic resonance are powerful techniques for studying antigen-antibody interactions, particularly in relation identifying to conformational epitopes (Amit et al., 1986, Morris, 2001, Hore, 2015). A second methodology uses the manipulation of cDNA to create substitutions and/or deletions in the primary sequence of the antigen molecule (Pettersson, 1992, Westwood and Hay, 2001). The immunoreactivity of the altered protein can then be tested in ELISAs, immunoblots or by immunoprecipitation. Thirdly, antibody reactivity can be analysed directly against synthetic peptides or enzymatically digested protein fragments (Pettersson, 1992). The latter two techniques can only identify linear

epitopes which may or may not be part of a conformational epitope, although, more recently, the creation of chimeric antigens has been applied with these methods to characterise antibody binding sites which are structure dependent (Hu et al., 2007). Finally, phage-display technology has proved useful for identifying linear and conformational epitopes (Williams et al., 2001).

4.1.3 Phage-display technology

Filamentous bacteriophage particles comprise of a single-stranded DNA genome enclosed in a tube of major phage coat protein pVIII. At either end of the tube there are 4-5 copies of each of four species of minor phage coat proteins (**Figure 4.1**) (Wilson and Finlay, 1998, Russel et al., 2004, Bazan et al., 2012). The development of phage-display technology stemmed from the finding that inserting DNA fragments into gene *gIII* of the phage genome resulted in the expression of the encoded peptide as a fusion protein with the minor phage coat protein pIII, and the 'display' of the fusion on the surface of the phage particle (Smith, 1985). Subsequently, phage libraries displaying an array of fusion proteins can be screened rapidly in panning experiments to identify peptides with the required binding activities. That the selected peptides are linked to the DNA that encodes them is a major advantage of the technology.

Phage-display has a variety of applications including the analysis of the interactions of transcription factors and receptors with their ligand (Bass et al., 1990, Butteroni et al., 2000), enzymes with their substrate (Redl et al., 1999), and antibodies with their recognised antigen (Barbas, 1993, Kemp et al., 2002). Phage-display technology has also been utilised to identify autoantigenic epitopes by screening phage libraries displaying random peptide sequences generated from a selected antigen with autoimmune disease patient sera (**Table 4.2**).

Table 4.1: Methods used for identifying B cell epitopes

Method	Type of epitope	Reference
X-ray crystallography Allows direct analysis of the 3-dimensional structure of an antigen-antibody complex.	Linear; conformational	(Amit et al., 1986)
Nuclear magnetic resonance	Linear; conformational	(Hore, 2015)
Mass spectrometry	Conformational; post-translationally modified	(Hager-Braun and Tomer, 2005)
Phage-display technology Epitopes are determined by affinity selection screening with monoclonal antibody or polyclonal.	Linear; conformational	(Williams et al., 2001)
Synthetic peptides or peptide fragments Can be used in a number of different assay systems including enzyme-linked immunosorbent assay (ELISA) and immunoprecipitation using monoclonal antibody or polyclonal sera.	Linear	(Pettersson, 1992, Westwood and Hay, 2001)
Recombinant proteins Sub-cloning and expression of cDNA encoding antigen peptide fragments generated by naturally occurring restriction sites, exonuclease digestion, polymerase chain reaction or site-directed mutagenesis. Can be used in a number of different assay systems including immunoblotting, ELISA, immunoprecipitation and radiobinding assays using monoclonal antibody or polyclonal sera.	Linear	(Pettersson, 1992, Westwood and Hay, 2001)

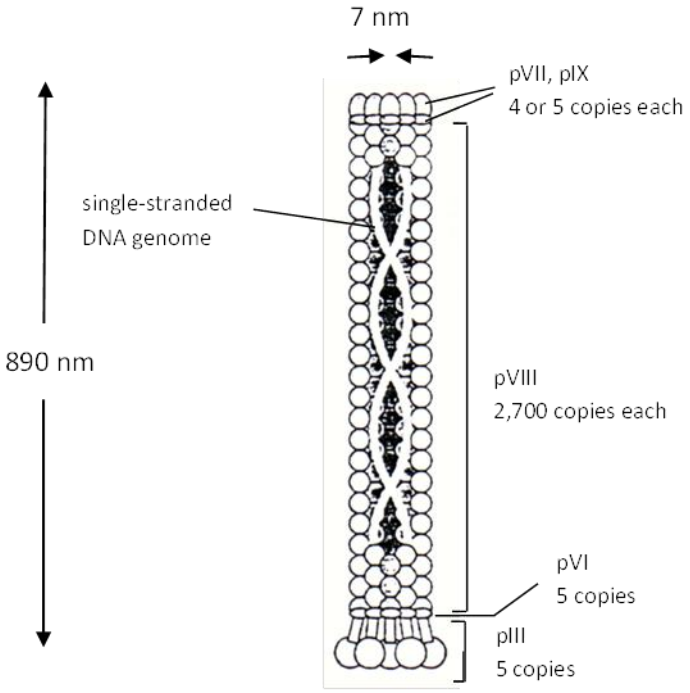

Figure 4.1: Schematic representation of a filamentous phage particle.

A single-stranded circular DNA genome is encased in 2,700 copies of the major coat protein pVIII, and four or five copies of each of four types of minor coat proteins, including pIII. The figure was used with kind permission from NRC Research Press from a paper by Wilson and Finlay, 1998.

Table 4.2: Identification of B cell epitopes using phage-display technology

Autoantigen	Autoimmune disease	Epitope type identified	Reference
Glutamic acid decarboxylase	Autoimmune polyendocrine syndrome type 2; Stiffman syndrome	Linear	(Al-bukhari et al., 2002)
Glutamic acid decarboxylase	Type 1 diabetes mellitus	Linear	(Myers et al., 2000)
Tyrosinase phosphatase-like protein IA-2/ICA512bdc	Type 1 diabetes mellitus	Linear	(Farilla et al., 2002, Dromey et al., 2004)
Smith autoantigen	Systemic lupus erythematosus	Linear	(del Rincon et al., 2000)
Gliadin	Celiac disease	Linear	(Osman et al., 2000)
Pyruvate dehydrogenase complex E2	Primary biliary cirrhosis	Conformational	(Rowley et al., 2000)
Platelet autoantigen	Autoimmune thrombocytopenic purpura	Conformational	(Gevorkian et al., 1998)
Melanin-concentrating hormone receptor 1	Vitiligo	Linear	(Gavalas et al., 2009)
Calcium-sensing receptor	Autoimmune polyendocrine syndrome type 1	Linear	(Kemp et al., 2010)

4.1.4 Identification of antibody binding sites on the CaSR

Several techniques have been used to map epitopes on the CaSR. Previously, a CaSR cDNA fragment library was constructed in the phage-display vector pComb3 (Kemp et al., 2010). In this library, peptides encoded by cloned CaSR cDNA fragments were expressed from the *lacZ* gene promoter as fusions at the amino terminus with the PelB leader sequence and at the carboxy terminus with phage coat protein pIII (**Figure 4.2**). Subsequently, the expressed CaSR peptides were exposed on the surface of phage particles (**Figure 4.2**). The CaSR peptide phage-display library was used in panning experiments as detailed in **Figure 4.3** to map the epitopes of CaSR antibodies found in 12 APS1 patients (Kemp et al., 2010). The identified antibody binding sites are listed in **Table 4.3,** In addition, peptide ELISAs (**Table 4.4**) have been used both to identify and to confirm epitopes recognised by CaSR antibodies found in patients with APS1 (Kemp et al., 2010), autoimmune hypoparathyroidism (Kifor et al., 2004) and autoimmune hypocalciuric hypercalcaemia (Kifor et al., 2003, Pallais et al., 2004, Kemp et al., 2010) (**Table 4.3**). The positions of the epitopes identified on the CaSR are shown in **Figure 4.4.**

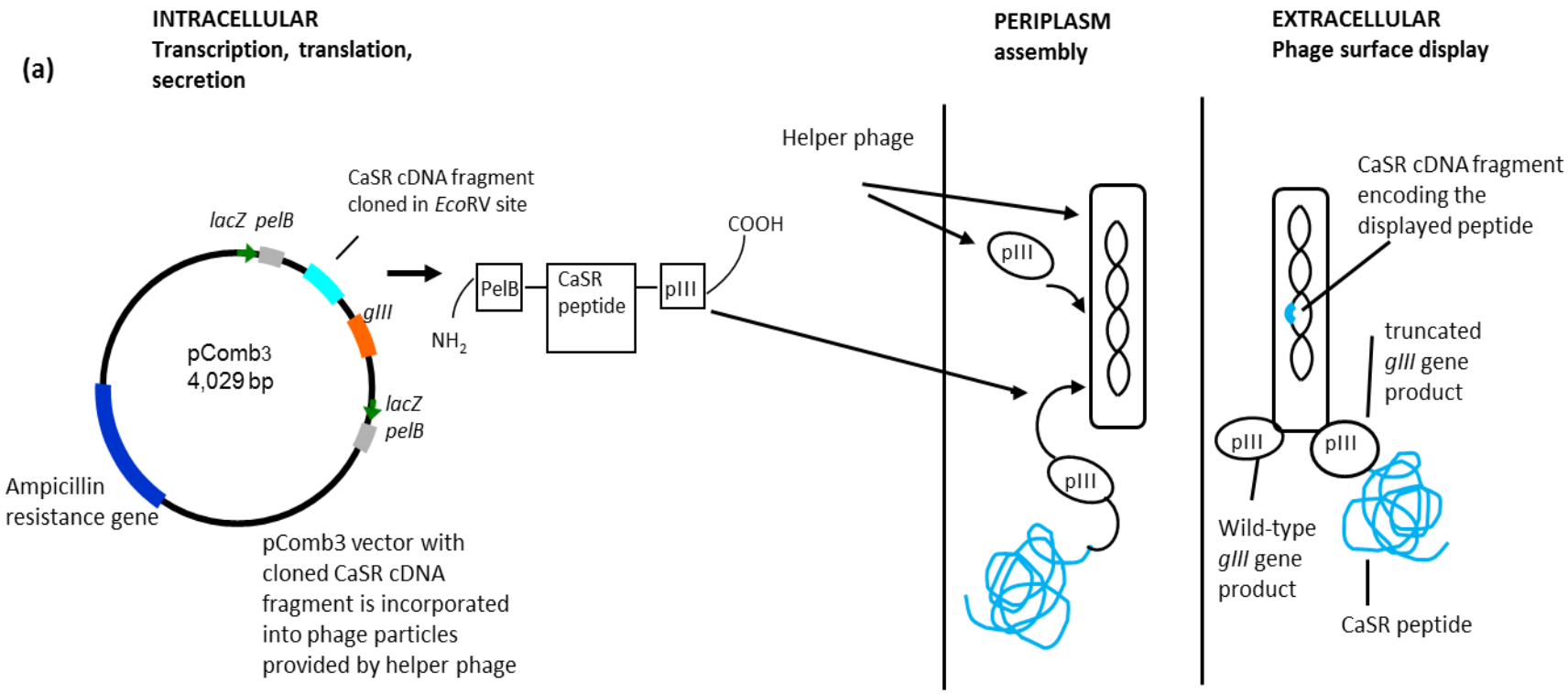
(a)
INTRACELLULAR
Transcription, translation, secretion
PERIPLASM
assembly
EXTRACELLULAR
Phage surface display
CaSR cDNA fragment cloned in EcoRV site
lacZ pelB
gIII
pComb3
4,029 bp
lacZ
pelB
Ampicillin resistance gene
pComb3 vector with cloned CaSR cDNA fragment is incorporated into phage particles provided by helper phage
NH2
PelB
CaSR peptide
pIII
COOH
Helper phage
pIII
pIII
CaSR cDNA fragment encoding the displayed peptide
truncated gIII gene product
pIII
pIII
Wild-type gIII gene product
CaSR peptide

(b)

GGTGGCGGCCGCAAATTCTATTTCAAGGAGACAGTCATAATGAAATACCTATTGCCTACGGCAGCCGCTGGATTG
G G G R K F Y F K E T V I M K Y L L P T A A A G L
TTATTACTCGCTGCCCAACCAGCCATGGCCCAGGTGAAACTGCTCGAGGTCGACGGTATCGATAAGCTTGATCAT
L L L A A Q P A M A Q V K L L E V D G I D K L D H
TTTGGAGTAGCAGCTAAAGATCAAGATCTCAAATCAAGGCCGGAGTCTGTGGAATGTATCAGGTATAATTTCCGT
F G V A A K D Q D L K S R P E S V E C I R Y N F R
GGGTTTCGCTGGTTACAGGCTATGATCGAATTCCTGCAGCCCGGGGGATCCACTAGTGGTGGCGGTGGCTCTCCA
G F R W L Q A M I E F L Q P G G S T S G G G G S P
TTCGTTTGTGAATATCAAGGCCAATCGTCTGACCTGCCTCAA
F V C E Y Q G Q S S D L P Q

Figure 4.2: The pComb3 phage-display system.

(a) The expression of CaSR peptides, from cDNA fragments cloned into the *Eco*RV site of pComb3 (highlighted in yellow), as fusion proteins to coat protein pIII (highlighted in red and encoded by *gIII*) is controlled by the *lacZ* gene promoter. The PelB leader sequence (highlighted in grey and encoded by *pelB*) allows the secretion of the CaSR peptide fusion proteins into the periplasm of the bacterial cell. Subsequently, the CaSR peptide fusion proteins are assembled into phage particles and displayed on the surface of the phage by virtue of coat protein pIII. Sequencing primer pc3prim1 (highlighted in green) anneals prior to the *pelB* gene sequence. The figure was used with kind permission from John Wiley and Sons from a paper by (Crameri et al., 1994). **(b)** An example of a CaSR peptide cloned in the +1 frame with respect the PelB leader sequence and in-frame with coat protein pIII is shown in turquoise.

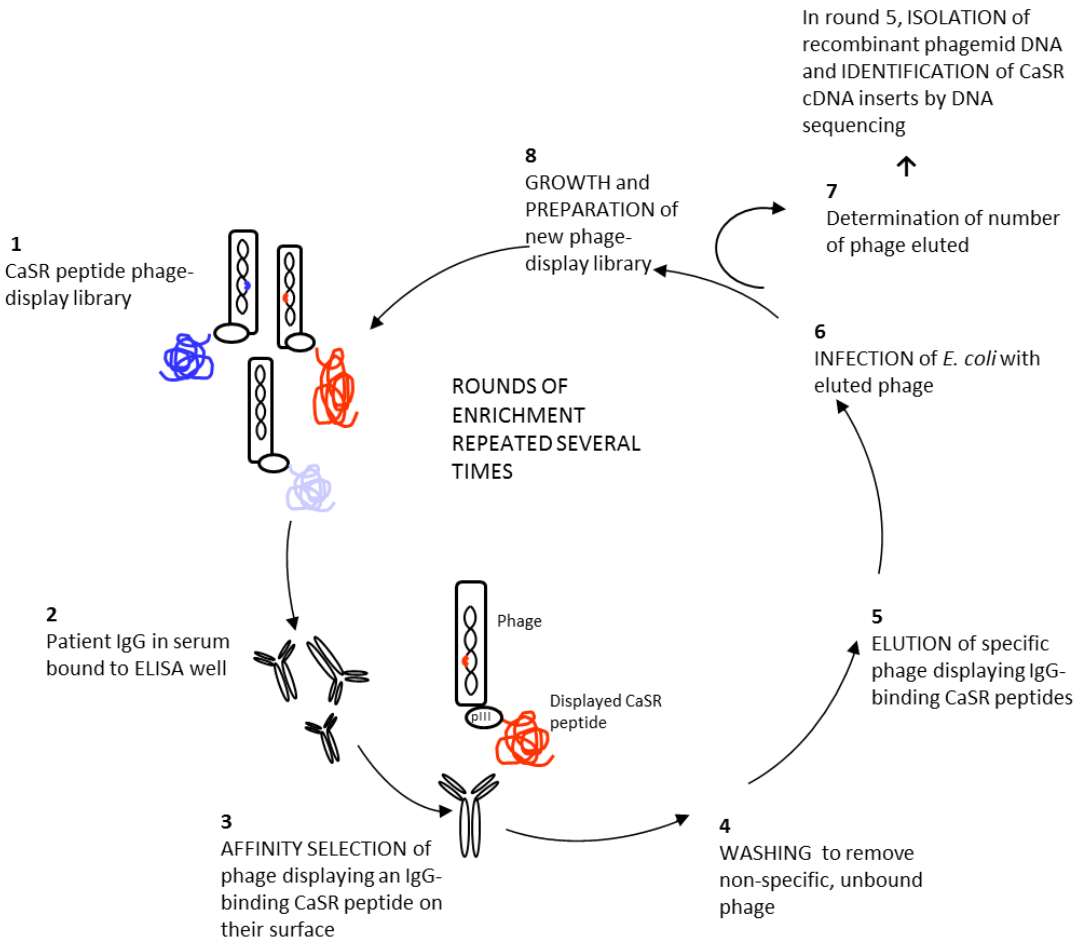

Figure 4.3: Enrichment of phage displaying IgG binding CaSR peptides on their surface.

1. Phage expressing immunoreactive CaSR peptides from cloned CaSR cDNA fragments. **2.** IgGs in patient serum. **3.** IgGs capture phage expressing immunoreactive CaSR peptides. **4.** Non-specifically bound phage are removed by washing. **5.** Phage displaying peptides that bind specifically to IgG molecules are eluted with acidified glycine. **6.** The eluted phage are infected into *E. coli* to enrich specifically-bound phage. **7.** The number of phage eluted is determined and, in round five of panning, phagemid DNA is isolated from infected cells and analysed by sequencing to identify CaSR cDNA inserts. **8.** The eluted phage are grown and a new phage display library then prepared for further rounds of panning. The figure was used with kind permission from the Nature Publishing Group from a paper by (Waterman et al., 2010).

Table 4.3: Previously reported CaSR antibody binding sites on the CaSR

CaSR epitope[1]	Patient detail	Number of patients	Technique	Reference
41-69	APS1	12	Phage-display and CaSR peptide ELISAs	(Kemp et al., 2010)
	Autoimmune hypocalciuric hypercalcemia	1		(Kemp et al., 2010)
114-126	APS1	5	Phage-display and CaSR peptide ELISAs	(Kemp et al., 2010)
171-195	APS1	4		(Kemp et al., 2010)
214-236	Autoimmune hypocalciuric hypercalcaemia	1	CaSR peptide ELISAs	(Pallais et al., 2004)
	Autoimmune hypocalciuric hypercalcaemia	4		(Kifor et al., 2003)
	Autoimmune hypoparathyroidism	2		(Kifor et al., 2004)
344-358	Autoimmune hypocalciuric hypercalcaemia	1	CaSR peptide ELISAs	(Pallais et al., 2004)
	Autoimmune hypocalciuric hypercalcaemia	4		(Kifor et al., 2003)
	Autoimmune hypoparathyroidism	2		(Kifor et al., 2004)
374-391	Autoimmune hypocalciuric hypercalcaemia	1	CaSR peptide ELISAs	(Pallais et al., 2004)
	Autoimmune hypocalciuric hypercalcaemia	4		(Kifor et al., 2003)
	Autoimmune hypoparathyroidism	2		(Kifor et al., 2004)

[1]Amino acid residues are numbered according to CaSR peptide sequence with the ATG initiation codon as residue number 1.

Table 4.4: CaSR peptides used in ELISAs

CaSR peptide[1]	Number of amino acids	Amino acid sequence of peptide
41-69	38	HFGVAAKDQDLKSRPESVECIRYNFRGFR
75-115	41	IFAIEEINSSPALLPNLTLGYRIFDTCNTVSKALEATLSFV
114-126	13	FVAQNKIDSLNLD
138-170	33	TIAVVGATGSGVSTAVANLLGLFYIPQVSYASS
171-195	25	SRLLSNKNQFKSFLRTIPNDEHQAT
214-238	25	ADDDYGRPGIEKFREEAEERDICID
260-340	81	QNSTAKVIVVFSSGPDLEPLIKEIVRRNITGKIWLASEAWASSSLI AMPQYFHVVGGTIGFALKAGQIPGFREFLKKVHPR
344-358	15	HNGFAKEFWEETFNC
374-391	18	LRGHEESGDRFSNSSTAF

[1]Amino acid residues are numbered according to CaSR peptide sequence with the ATG initiation codon as residue number 1.

MAFYSCCWVLLALTWHTSAYGPDQRAQKKGDIILGGLFPIHFGVAAKDQDLKSRPESVE
CIRYNFRGFRWLQAMIFAIEEINSSPALLPNLTLGYRIFDTCNTVSKALEATLSFVAQN
KIDSLNLDEFCNCSEHIPSTIAVVGATGSGVSTAVANLLGLFYIPQVSYASSSRLLSNK
NQFKSFLRTIPNDEHQATAMADIIEYFRWNWVGTIAADDDYGRPGIEKFREEAEERDIC
IDFSELISQYSDEEEIQHVVEVIQNSTAKVIVVFSSGPDLEPLIKEIVRRNITGKIWLA
SEAWASSSLIAMPQYFHVVGGTIGFALKAGQIPGFREFLKKVHPRKSVHNGFAKEFWEE
TFNCHLQEGAKGPLPVDTFLRGHEESGDRFSNSSTAFRPLCTGDENISSVETPYIDYTH
LRISYNVYLAVYSIAHALQDIYTCLPGRGLFTNGSCADIKKVEAWQVLKHLRHLNFTNN
MGEQVTFDECGDLVGNYSIINWHLSPEDGSIVFKEVGYYNVYAKKGERLFINEEKILWS
GFSREVPFSNCSRDCLAGTRKGIIEGEPTCCFECVECPDGEYSDETDASACNKCPDDFW
SNENHTSCIAKEIEFLSWTEPFGIALTLFAVLGIFLTAFVLGVFIKFRNTPIVKATNRE
LSYLLLFSLLCCFSSSLFFIGEPQDWTCRLRQPAFGISFVLCISCILVKTNRVLLVFEA
KIPTSFHRKWWGLNLQFLLVFLCTFMQIVICVIWLYTAPPSSYRNQELEDEIIFITCHE
GSLMALGFLIGYTCLLAAICFFFAFKSRKLPENFNEAKFITFSMLIFFIVWISFIPAYA
STYGKFVSAVEVIAILAASFGLLACIFFNKIYIILFKPSRNTIEEVRCSTAAHAFKVAA
RATLRRSNVSRKRSSSLGGSTGSTPSSSISSKSNSEDPFPQPERQKQQQPLALTQQEQQ
QQPLTLPQQQRSQQQPRCKQKVIFGSGTVTFSLSFDEPQKNAMAHRNSTHQNSLEAQKS
SDTLTRHQPLLPLQCGETDLDLTVQETGLQGPVGGDQRPEVEDPEELSPALVVSSSQSF
VISGGGSTVTENVVNS

Figure 4.4: Position of previously identified CaSR epitopes.

Epitopes are shown at amino acid residues 41-69 (red), 114-126 (yellow), 171-195 (pink), 214-236 (grey), 344-358 (green), and 374-391 (purple).

4.2 Aim

The aim of this part of the project was to identify the binding sites on the CaSR recognised by APS1 patient CaSR antibodies. This information could help in **(a)** understanding how CaSR antibodies can adversely affect the function of the receptor (Kemp et al, 2009; Kifor et al, 2004) if they bind at functionally relevant sites, **(b)** developing new and more specific CaSR antibody assays. For example, if the epitope of a pathogenic antibody can be defined exactly, recombinant proteins containing only the epitope site could be used in the titration of pathogenic antibodies within a patient's heterogeneous antibody population, **(c)** providing insights into the initiation of the autoimmune process. For example by molecular mimicry, if epitopes on the CaSR are recognised by antibodies arising from the immune response against infecting microbes (Wucherpfennig, 2001a), **(d)** characterising the light chain usage of CaSR antibodies, as in the case of thyroid peroxidase antibodies in autoimmune thyroid disease (McIntosh et al., 1997), and **(e)** engineering specific functional monoclonal antibodies, for instance for treatment of hypercalcaemia.

The specific objectives of this part of the project were:

- To use panning experiments with a CaSR peptide phage display library and APS1 patient sera to identify consensus peptides representing potential CaSR epitopes.
- To verify potential CaSR epitopes by analysing the reactivity of APS1 patient and control sera in CaSR peptide ELISAs.

4.3 Materials and Methods

4.3.1 Patient and control sera

The clinical and demographic details of the 44 APS1 patients (16 CaSR antibody-positive and 28 CaSR antibody-negative) and 16 healthy controls used in this part of the study are given in Chapter 3 (**Section 3.3.1 and Table 3.1**).

4.3.2 CaSR peptide phage-display library

The CaSR peptide phage-display library made in pComb3 (**Figure 4.2**) (Kemp et al., 2010) was provided by Dr Helen Kemp (Department of Oncology and Metabolism, University of Sheffield, Sheffield, UK) and was stored at -80°C. To determine the phage titre of the library, *Escherichia coli* XL1-Blue MRF' (Agilent Technologies, Wokingham, UK) was grown to exponential phase at 37°C with shaking in 0.5 ml of LB medium (**Section 2.3**) with tetracycline at 10 µg/ml. The culture was then infected with a 2-µl aliquot of a 10^{-4} dilution of the phage-display library and incubated at room temperature for 15 min. Samples (1, 10 and 100-µl) of the culture were plated onto LB agar containing 100 µg/ml ampicillin (**Section 2.3**). An uninfected 100-µl sample of the culture was plated as a negative control. Plates were incubated at 37°C overnight, the colonies counted, and the phage titre as colony-forming units (cfu) per ml was determined.

To check that the library contained random CaSR cDNA fragments, 20 randomly selected bacterial colonies isolated in the titration experiment were firstly purified by streaking onto fresh LB agar with ampicillin at 100 µg/ml, and then later inoculated into 10 ml of LB medium with ampicillin at 100 µg/ml and grown overnight at 37°C. Subsequently, phagemid DNA was extracted from the cells using a Wizard® Plus SV Minipreps DNA Purification System (**Section 2.6**) and sequenced (**Section 2.16**) with pComb3-specific primer pc3prim1 (5'-GGTGGCGGCCGCAAATTC-3') (Eurofins Genetic Services Ltd., London, UK) (**Figure 4.2**). Each cloned DNA fragment was translated and then analysed for matches to the CaSR amino acid sequence (**Section 4.3.6**). The reading frame of each cloned DNA fragment with respect to the PelB leader sequence and phage coat protein pIII was also determined.

4.3.3 Enrichment of the CaSR peptide phage-display library (panning experiments)

Panning experiments were carried out according to the protocol of Dr Helen Kemp (Department of Oncology and Metabolism, University of Sheffield, Sheffield, UK) (Kemp et al., 2010). For panning experiments (**Figure 4.3**), 10-µl aliquots of APS1 patient sera or rabbit anti-CaSR (amino acid residues 47-69) polyclonal antibody ab79829 (anti-CaSR antibody ab79829) (Abcam, Cambridge, UK) were applied to the wells of 96-well microtitre plates in 50 µl of coating buffer (1.5 mM sodium carbonate; 3.5 mM sodium hydrogen carbonate; pH 9.2). Plates were incubated at room temperature for 2 h to allow antibody-binding before washing with PBS/0.05% (w/v) Tween 20 (PBS/Tween). To block any non-specific phage binding later in the procedure, 400 µl of 2% (w/v) bovine serum albumin in PBS were added to the wells and incubation at room temperature continued for 2 h. The wells were again rinsed with PBS/Tween before the addition of a 100-µl sample of phage display library containing an estimated 10^9 to 10^{10} phage (depending on the exact phage display library used). Plates were incubated overnight at 4^oC to allow the interaction of CaSR antibodies with peptides displayed on the surface of the phage particles. The wells were washed extensively with PBS/Tween to remove unbound phage. Bound phage were then eluted with 150 µl of 100 mM hydrochloric acid (adjusted to pH 2.2 with glycine) and then neutralised with 9 µl of 2 M Tris-base. The phage suspension was subsequently used to infect 2 ml of exponentially growing *E. coli* XL1-Blue MRF' for 15 min at room temperature. Aliquots (10 and 100-µl) of the infected cells were then plated onto LB agar containing 10 µg/ml tetracycline and 100 µg/ml ampicillin and the plates incubated overnight at 37°C. This allowed the assessment of the total number of eluted phage in each round of panning.

A phage-display library for the next round of panning was then generated. The *E. coli* XL1-Blue MRF' culture infected with eluted phage was made up to 10 ml with LB medium and incubated for 1 h with shaking at 37°C before superinfection with of 1 x 10^{11} plaque-forming units of VCS-M13 helper phage (Agilent Technologies). Following incubation at room temperature for 30 min, the cells were transferred to 100 ml of LB medium containing 10 µg/ml tetracycline, 100 µg/ml ampicillin and 10 µg/ml kanamycin (**Section 2.3**) and grown overnight with shaking at 37°C. The 100-ml culture was centrifuged at 2,000 *g* for 15 min to remove all bacterial cells. Phage particles

were precipitated from the supernatant with 15 ml of 40% (w/v) polyethylene glycol 4000 and 15 ml of 5 M sodium chloride per 100 ml. Following overnight incubation at 4°C, the phage were harvested by centrifugation at 2,000 *g* for 30 min and the pellet resuspended in 1-2 ml of PBS before storage at -20°C. This first round phage-display library, enriched in phage particles displaying IgG-binding peptides, was titrated as detailed above (**Section 4.3.2**), and was then used in a second round of panning in the same way as the original library. In all, five rounds of panning were undertaken for each sample.

In each round, the ratio of the number of phage eluted to the number of phage applied initially to the ELISA plate well was determined. Compared to the ratio found in the round one of panning, the fold increase in this ratio in each subsequent panning round was calculated.

4.3.4 Analysis of the panned phage-display library

After the fifth round of panning, 10-16 randomly selected bacterial colonies, isolated by plating out the culture infected with eluted phage, were purified by streaking onto fresh LB agar containing ampicillin at 100 µg/ml. The bacterial clones were then grown overnight with shaking at 37°C in 10 ml of LB medium containing 100 µg/ml ampicillin. Subsequently, phagemid DNA was prepared from each culture using a Wizard® Plus SV Minipreps DNA Purification System. In order to identify any immunoreactive CaSR peptides that had been enriched during the panning procedure, each phagemid DNA sample was subjected to sequencing using primer pc3prim1. This allowed the sequence of the cloned DNA fragments to be determined. As detailed in **Section 4.3.6**, each cloned DNA fragment was translated and then analysed for matches to the CaSR amino acid sequence. The reading frame of each cloned DNA fragment with respect to the PelB leader sequence and phage coat protein pIII was also determined.

4.3.5 CaSR peptide ELISAs

Antibodies against CaSR peptides were detected in ELISAs as previously described (Kemp et al., 2010). All CaSR peptides (**Table 4.4**) were received dried and were solubilised and stored according to the manufacturer's instructions (Cambridge Peptides Ltd., Birmingham, UK). For ELISAs, the required peptide was diluted in PBS to

200 ng/ml and 100-µl samples used to coat the wells of a 96-well microtitre plate. An equivalent number of wells were coated with 100 µl of 0.1% (w/v) bovine serum albumin for the measurement of non-specific binding of the sera. The plates were then incubated overnight at 4°C.

Excess peptide was removed by decanting and the wells were blocked with blocking buffer (PBS; 0.1% (w/v) Tween-20; 3% (w/v) bovine serum albumin) for 30 min at 37°C. Plates were washed four times with washing buffer (PBS/0.1% (v/v) Tween-20). Aliquots (100 µl) of serum at a 1:100 dilution in blocking buffer were added to the wells. PBS was applied as a control to measure any non-specific binding of the secondary antibody. Positive control antibodies were: anti-CaSR antibody ab79829 and mouse anti-CaSR (amino acid residues 214-235) monoclonal antibody ab19347 (anti-CaSR antibody ab19347) (Abcam, Cambridge, UK), and were used at a 1:500 dilution. The plates were incubated at room temperature for 1 h and then washed four times with washing buffer. A 100-µl of goat anti-human IgG polyclonal antibody conjugated to alkaline phosphatase (Sigma-Aldrich) diluted to 1:2000 in blocking buffer was added to each well for 1 h at room temperature. To detect the positive control antibodies, goat anti-rabbit IgG or goat anti-mouse IgG polyclonal antibodies conjugated to alkaline phosphatase (Sigma-Aldrich) were used at a 1:2000 dilution. After washing five times with washing buffer, 100 µl of alkaline phosphatase substrate Sigma Fast *p*-nitrophenyl phosphate (Sigma-Aldrich) were applied to each well and plates incubated at room temperature to allow colour development. A LabSystems Integrated EIA Management System spectrophotometer was used to read absorption of the wells at 405 nm. All sera were tested in duplicate and the average OD_{405} value taken. Each mean OD_{405} value was corrected for background binding of the sera to the well without antigen.

The binding reactivity of each patient and control sera to the peptide was expressed as an antibody index calculated as: mean OD_{405} of tested serum/mean OD_{405} of a population of healthy control sera. Each serum was tested in at least two experiments and the mean antibody index calculated. The upper limit of normal for each ELISA was calculated using the mean antibody index + 3SD of a population of healthy control sera. Sera with an antibody index greater than the upper limit of normal were regarded as antibody-positive.

4.3.6 Statistical analyses

Fisher's exact test for 2 x 2 contingency tables for comparing categorical data was carried out using GraphPad Instat 3 software (GraphPad Software). In all tests, *P* values (two-tailed) < 0.05 were regarded as significant. Antibody assay precision was evaluated by calculating the intra-assay coefficient of variation (expressed as a percentage) for a series of different serum samples that were measured in duplicate within the same assay run. Antibody assay reproducibility was evaluated by calculating the inter-assay coefficient of variation (expressed as a percentage) for a series of different serum samples that were measured in several consecutive assay runs.

4.3.7 DNA and protein sequences analyses

Analyses of DNA and protein sequences were carried out using Lasergene Core Suite sequence analysis software (DNASTAR, Inc., Madison, WI, USA), the network facilities of the European Bioinformatics Institute-European Molecular Biology Laboratory (www.ebi.ac.uk) (Cambridge, UK), and the ExPASy Bioformatics Resources Portal (web.expasy.org) (Swiss Institute of Bioinformatics, Switzerland). Protein and DNA homology searches against the GenBank database were performed using the BLAST service of the National Center for Biotechnology Information (www.ncbi.nlm.nih.gov) (Bethesda, MD, USA).

4.3.8 Antigenicity predictions

Antigenicity predictions on the CaSR extracellular domain were made using the Immune Epitope Database and Analysis Resource (tools.immuneepitope.org) (National Institute of Allergy and Infectious Diseases, Bethesda, MD, USA) (Kolaskar and Tongaonkar, 1990).

4.3.9 *In silico* modelling of CaSR epitopes

Since the CaSR has not been crystallised, the 3D structure of the of the CaSR extracellular domain was solved at high resolution using the web-based Protein Homology/Analogy Recognition Engine (Phyre) service (www.sbg.bio.ic.ac.uk/phyre2) (Imperial College London, UK) (Kelley and Sternberg, 2009, Kelley et al., 2015) enabling a model to be made with a high degree of confidence (90% modelled at > 90%

confidence). The positions of the epitopes identified on the modelled CaSR were visualised using PyMOL molecular graphics system software (www.pymol.org) (Schrödinger, Cambridge, UK) (DeLano et al., 2000).

4.4 Results

4.4.1 Analysis of the unpanned CaSR peptide phage-display library

The titre of the phage-display library was determined as in **Section 4.3.2,** and was estimated at 9.3 x 10^{11} cfu/ml. The results of sequencing 20 randomly selected phagemid from the titration experiment indicated that the cloned CaSR cDNA fragments were varied with respect to their encoded amino acid sequence (**Table 4.5**) showing no bias in the reading frame or for any specific part of the CaSR.

4.4.2 Panning of the CaSR peptide phage-display library with APS1 patient and anti-CaSR antibody

The CaSR peptide phage-display library was screened for immunoreactive CaSR peptides with sera from 16 CaSR antibody-positive APS1 patients and a CaSR antibody-negative APS1 patient, and with anti-CaSR antibody ab79829 as a positive control. Five rounds of panning were carried out. In each round, the ratio of the number of phage eluted to the number of phage applied initially to the ELISA plate well was determined. Compared to the ratio found in the first round of panning, the fold increase in this ratio in each subsequent panning round was calculated. The results are given in **Figure 4.5**. In most cases, an increase in the ratio of phage eluted to phage applied was observed by the third round of panning, suggesting that enrichment of phage expressing IgG-binding CaSR peptides had occurred during the successive rounds. In contrast, no increase was seen from panning of the library with the CaSR antibody-negative APS1 patient serum (**Figure 4.5**).

Table 4.5: Amino acid sequences of translated CaSR cDNA fragments contained in the unpanned CaSR peptide phage-display library

Clone number	Amino acid sequence of CaSR peptide encoded by the cloned cDNA fragment	Amino acid residues of the CaSR	Reading frame in relation to the PelB leader sequence	In-frame with coat protein pIII
1	HFGVAAKDQDLKSRPESVECIRYNFRGFRWLQA MIFAIEEINSSPALLPNLTLGYRIF	41-98	+1	Yes
2	AKEFWEETFNCHLQEGAKGPLPVDTFLRGHEES GDRFSNSSTAFRPLCTGDENISSVETPYIDY	348-411	-1	No
3	HNGFAKEFWEETFNCHLQEGAKGPLPVDTFLRG HEESGDRFSNSSTAFRPLCTG	344-397	-1	No
4	KSFLRTIPNDEHQATAMADIIEYFRWNWVGTIA ADDDYGRPGIEKFREEAEERDICIDFS	180-240	-2	No
5	AILAASFGLLACIFFNKIYIILFKPSRNTIEEV RCSTAAHAFKVAARATL	840-954	+2	No
6	FRWLQAMIFAIEEINSSPALLPNLTLGYRIFDT CNTVSKALEATLSFVAQNKIDSLNLDEFCNCSE HIPSTIAVV	68-142	-3	No
7	PSTIAVVGATGSGVSTAVANLLGLFYIPQVSYA SSSRLLSNKNQFKSF	136-183	+1	Yes
8	EDPFPQPERQKQQQPLALTQQEQQQQPLTLPQQ QRSQQQPRCKQKVIFGSGTVTFSLSFD EPQKNA	874-985	+2	No
9	GFRWLQAMIFAIEEINSSPALLPNLTLGYRIFD TCNTVSKALEAT	67-111	+2	No
10	HRNSTHQNSLEAQKSSDTLTRHQPLLPLQCGET DLDLTVQE	989-1028	+1	Yes
11	ASACNKCPDDFWSNENHTSCIAKEIEFLSWTEP FGIALTLFAVLGIFLTAFVLGVFIKFR	578-638	-2	No
12	IVVFSSGPDLEPLIKEIVRRNITGKIWLASEAW ASSSLIAMPQYF	267-311	+2	No
13	CHEGSLMALGFLIGYTCLLAAICFFFAFKSRKL PENFNEAKFITFSMLIFFIVWISFIPAYASTYG KFVSAVEVI	765-838	-3	No
14	MAFYSCCWVLLALTWHTSAYGPDQRAQKKGDII LGGLFPIHFGVAAKDQDLKSRPESVECIRYNFR GFRWLQAMIFAIEEINSSPALLPNLTLGYRIFD TCN	1-102	-1	No
15	PIVKATNRELSYLLLFSLLCCFSSSLFFIGEPQ DWTCRLRQPAFGI	639-686	+1	No
16	TIEEVRCSTAAHAFKVAARATLRRSN	868-893	-2	No
17	SNSSTAFRPLCTGDENISSVETPYIDYTHLRIS YNVYLAVYSIAHALQD	385-433	+3	No
18	FTNNMGEQVTFDECGDLVGNYSIINWHLSPEDG SIVFKEVGYYNVYA	469-515	+2	No
19	SPALVVSSSQSFVISGGGSTVTENVVNS	1068-1078	-2	No
20	RVLLVFEAKIPTSFHRKWWGLNLQFLLVFLCTF MQIVICVIWLYTAPPSSYRNQELEDEIIFITCH EGSLMALGFLIGYTCLL	701-782	+1	No

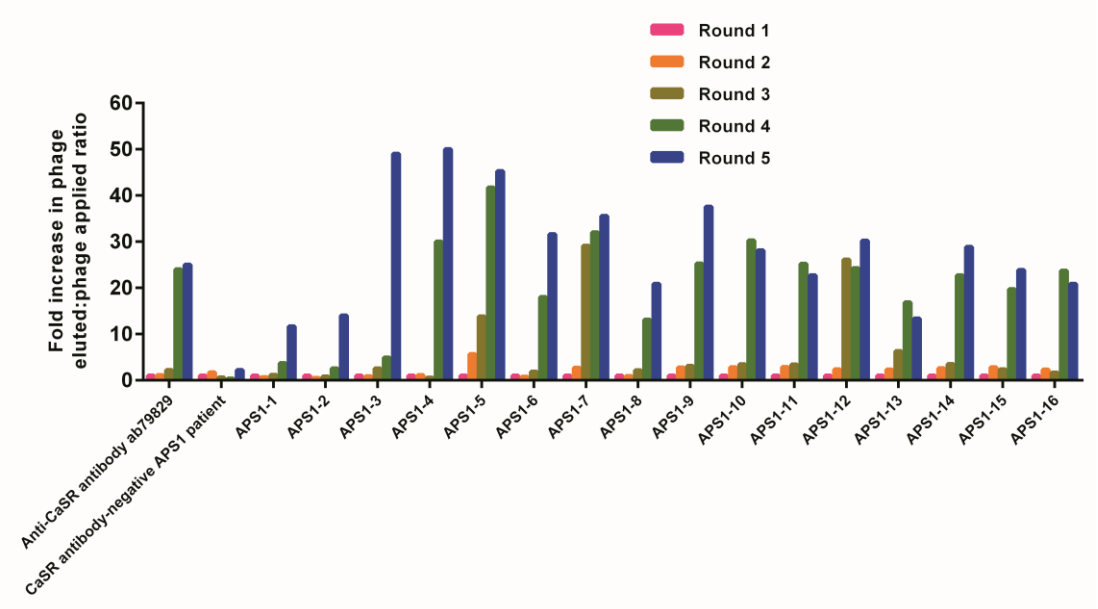

Figure 4.5: Panning experiments of the CaSR peptide phage-display library with APS1 patient sera and anti-CaSR antibody ab79829.

The results are shown as a fold increase in the ratio of phage eluted to phage applied with respect to the first round of panning.

4.4.3 Identification of CaSR peptides enriched by panning

Phagemid DNA from 10-16 randomly selected bacterial clones isolated from the fifth round of panning with APS1 patient sera and anti-CaSR antibody ab79829 was subjected to DNA sequencing in order to identify if particular CaSR peptides had been selected during the panning process. Each cloned DNA fragment was translated and then analysed for matches to the CaSR amino acid sequence. The reading frame of each cloned fragment with respect to the PelB leader sequence and phage coat protein pIII was also determined.

Table 4.6 summarises the CaSR peptide sequences encoded by 10 phagemid isolated from the fifth round of panning with anti-CaSR antibody ab79829. The results demonstrated that specific CaSR peptides were indeed enriched by panning of the phage display library with anti-CaSR antibody ab79829. Eight of the ten (80%) peptide sequences analysed included an identical CaSR peptide consensus sequence which encompassed the epitope (amino acid residues 47-69) of the anti-CaSR antibody ab79829. All eight peptide sequences were in-frame with the PelB leader sequence at the amino terminal and with the *gIII*-encoded coat protein pIII at the carboxy-terminal necessary for expression of the peptides on the surface of phage (**Figure 4.2**). The remaining two phagemid contained CaSR cDNA fragments that could not be expressed as fusion proteins as they were not in the correct reading frame with respect to the PelB leader sequence and phage coat protein pIII.

Identical analysis was repeated for the panning experiments carried out with APS1 patient sera. The CaSR peptide consensus sequences identified are given in **Table 4.7**. At least one CaSR peptide consensus sequence, assumed to represent a CaSR epitope, was identified for each CaSR antibody-positive APS1 patient. Two patients (APS1-2 and APS1-4) had each enriched one in-frame CaSR peptide (amino acids 850-909 and 260-340, respectively) that was only represented once within the set of analysed sequences. However, these could still represent CaSR antibody binding sites, since they would have been expressed on the surface of the phage by virtue of their in-frame fusion with both the PelB leader sequence and phage coat protein pIII. The CaSR antibody-negative patient did not enrich any specific CaSR peptide sequences, and the phagemid analysed carried CaSR cDNA fragment inserts that would not be expressed as fusion proteins.

Table 4.6: CaSR peptide sequences displayed on the surface of phage enriched by panning of the CaSR peptide phage-display library with anti-CaSR antibody ab79829

Sequence number	Amino acid sequence of peptides recovered following five rounds of panning[1]	Amino acid residues of the CaSR	Reading frame in relation to the PelB leader sequence	In-frame with coat protein pIII
1	AYGPDQRAQKKGDIILGGLFPIHFGVAAKDQDLKS RPXSVECIRYNFRGFRWL	**19-71**	**+1**	**Yes**
2	HTSAYGPDQRAQKKGDIILGGLFPIHFGVAAKDQD LKSRPESVECIXYNFRGFRWLQAM	**16-74**	**+1**	**Yes**
3	LTWHTSAYGPDQRAQKKGDIILGGLFPIHFGVAAK DQDLKSRXXSVECIRYNFRGFRWL	**13-71**	**+1**	**Yes**
4	LACIFFNKIYIILFKPSRNTIEEVRCSTAAHAFKV AARATLRRSNVSR	848-986	+3	No
5	SAYGPDQRAQKKGDIILGGLFPIHFGVAAKDQDLK SRPXSVECIXYNFRGFRWLQAM	**20-74**	**+1**	**Yes**
6	TGKIWLASEAWASSSLIAMPQYFHVVGGTIGFALK AGQIPGFREFLKKVHPRK	289-341	+3	No
7	YGPDQRAQKKGDIILGGLFPIHFGVAAKDQDLKSR PXSVECIXYNFRGFRWLQAM	**20-74**	**+1**	**Yes**
8	LTWHTSAYGPDQRAQKKGDIILGGLFPIHFGVAAK DQDLKSRPESVECIRYNFRGFRWL	**13-71**	**+1**	**Yes**
9	AQKKGDIILGGLFPIHFGVAAKDQDLKSRPESVEC IRYNFRGFRWLQAMI	**26-75**	**+1**	**Yes**
10	AQKKGDIILGGLFPIHFGVAAKDQDLKSRPESVEC IRYNFRGFRWLQAM	**26-74**	**+1**	**Yes**

[1]The consensus amino acid sequence (residues 26-70) is shown in red. The epitope of the anti-CaSR antibody ab79829 is between amino acid residues 41 and 69.

Table 4.7: CaSR peptide consensus sequences from panning experiments with APS1 patient sera

APS1 patient	CaSR peptide consensus sequence	Amino acid residues of CaSR[1]	Number of peptide sequences containing the in-frame CaSR peptide consensus sequence (%)[2]
APS1-1	AQKKGDIILGGLFPIHFGVAAKDQDLKSRPESVECIRYNFRGFRWL	26-71	8/16 (50)
APS1-2	HFGVAAKDQDLKSRPESVECIRYNFRGFRWL	41-71	7/16 (44)
	ACIFFNKIYIILFKPSRNTIEEVRCSTAAHAFKVAARATLRRSNVSRKRSSSLGGSTGST	850-909[3]	1/16 (6)
APS1-3	AYGPDQRAQKKGDIILGGLFPIHFGV	19-44	5/16 (31)
	TIAVVGATGSGVSTAVANLLGLFYIPQVSYASSSRLLSNKNQFKSFLRTIPND	138-190	2/16 (13)
APS1-4	DQRAQKKGDIILGGLFPIHFGVA	23-45	7/16 (44)
	QNKIDSLNLDEFCNCSEHIPSTIAVVGA	117-144	2/16 (13)
	QNSTAKVIVVFSSGPDLEPLIKEIVRRNITGKIWLASEAWASSSLIAMPQYFHVVGGTIGFALKAGQIPGFREFLKKVHPR	260-340[3]	1/16 (6)
APS1-5	QKKGDIILGGLFPIHFGVAAKDQDLKSRPESVECIRYNFRGFRWL	27-71	8/16 (50)
	KALAEATLSFVAQNKIDSLNLDEFCNC	106-131	3/16 (19)
APS1-6	HFGVAAKDQDLKSRPESVECIRYNFRGFRWL	41-71	8/16 (50)
	KALAEATLSFVAQNKIDSLNLDEFCN	106-130	2/16 (13)
APS1-7	HFGVAAKDQDLKSRPESVECIRYNFRGFRWL	41-71	3/16 (19)
	FVAQNKIDSLNLD	114-126	5/16 (31)
APS1-8	AQKKGDIILGGLFPIHFGVAAKDQDLKSRPESVECIRYNFRGFRWL	26-71	5/10 (50)
APS1-9	AQKKGDIILGGLFPIHFGVAAKDQDLKSRPESVECIRYNFRGFR	26-69	9/16 (56)
	SRLLSNKNQFKSFLRTIPNDEHQAT	171-195	2/16 (13)
APS1-10	GDIILGGLFPIHFGVAAKDQDLKSRPESVECIRYNFRGFRW	30-70	7/16 (44)
	TVSKALAEATLSFVAQNKIDSLNLDEFCNCSE	103-133	2/16 (13)
APS1-11	AQKKGDIILGGLFPIHFGVAAKDQDLKSRPESVECIRYNFRGFRWL	26-71	3/30 (10)
APS1-12	AQKKGDIILGGLFPIHFGVAAKDQDLKSRPESVECIRYNFRGFRWL	26-71	10/16 (63)
	SRLLSNKNQFKSFLRTIPNDEHQAT	171-195	3/16 (19)
APS1-13	AQKKGDIILGGLFPIHFGVAAKDQDLKSRPESVECIRYNFRGFRWL	26-71	3/16 (19)
APS1-14	HFGVAAKDQDLKSRPESVECIRYNFRGFR	41-69	8/10 (80)
	SRLLSNKNQFKSFLRTIPNDEHQAT	171-195	2/10 (20)
APS1-15	HFGVAAKDQDLKSRPESVECIRYNFRGFR	41-69	8/16 (50)
	SRLLSNKNQFKSFLRTIPNDEHQAT	171-195	3/16 (19)
APS1-16	AQKKGDIILGGLFPIHFGVAAKDQDLKSRPESVECIRYNFRGFRWL	26-71	4/16 (25)
	TVSKALAEATLSFVAQNKIDSLNLDEFCNCSE	103-133	5/16 (31)

[1]Amino acid residues are numbered according to CaSR peptide sequence with the ATG initiation codon as residue number 1.
[2]CaSR peptide consensus sequences were in-frame with the PelB leader sequence and coat protein pIII which are encoded by the pComb3 vector (**Figure 4.2**) and are required for expression of peptides on the surface of phage.
[3]Unrepeated in-frame CaSR peptides such that a CaSR peptide consensus could not be identified by comparing sequences.

4.4.4 CaSR peptide ELISAs with APS1 patient and control sera

To confirm the presence or not of antibodies against the potential epitope domains identified by phage display, serum samples from all 44 APS1 patients and 16 healthy controls were analysed in an ELISA format with specific CaSR peptides (**Table 4.4**), as detailed in **Section 4.4.5**. Positive control anti-CaSR antibodies ab79829 and ab19347 were included in ELISAs when appropriate. The peptides chosen represented potential epitopes identified in the phage display experiments and those epitopes reported previously to be recognised by CaSR antibodies in patients with either APS1 (Kemp et al, 2010), autoimmune hypoparathyroidism (Kifor et al., 2004) or autoimmune hypocalciuric hypercalcaemia (Kifor et al., 2003, Pallais et al., 2004, Kemp et al., 2010) (**Table 4.3**). Immunoreactivity against the potential epitope represented by amino acids 850-890 was not investigated in peptide ELISA experiments.

The antibody indices of the APS1 patient and control sera in the CaSR peptide ELISAs are shown in **Figure 4.6.** For each CaSR peptide ELISA, the mean antibody index of the APS1 patient and control groups, the antibody index range of the APS1 patient and control groups, the intra- and inter-assay coefficients of variation, and the upper limit of normal (mean antibody index + 3SD of 16 healthy individuals) are summarised in **Table 4.8**.

All control sera were negative for antibodies against all the CaSR peptides tested, as their antibody indices (**Table 4.8**) were below the upper limits of normal in the ELISAs. In the APS1 patient group, some antibody indices were above the upper limit of normal (**Table 4.9**). The prevalence of antibody-positivity against each CaSR peptide is summarised in **Table 4.8**. Only in the case of the 41-69 CaSR peptide was antibody positivity significantly more prevalent in the APS1 patient group than in the healthy controls: $P = 0.0032$, Fisher's exact test for 2 x 2 contingency tables. In contrast, the frequency of the antibody response against CaSR peptides 114-126, 171-195 and 260-340 was not elevated to statistical significance when comparing the APS1 patient group with healthy controls: All P values were > 0.05 in Fisher's exact test for 2 x 2 contingency tables.

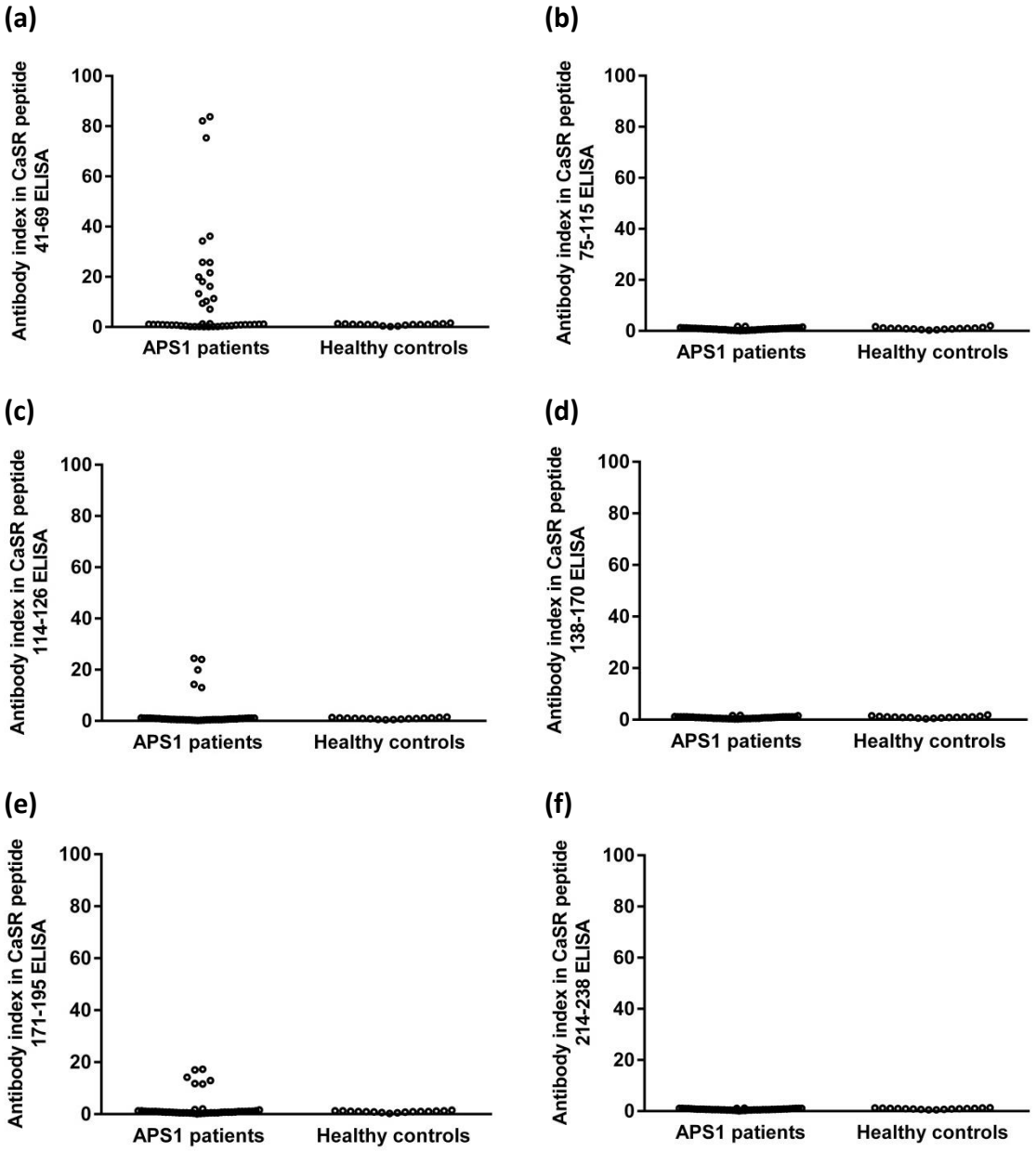
(a)
Antibody index in CaSR peptide 41-69 ELISA
100
80
60
40
20
0
APS1 patients
Healthy controls
(b)
Antibody index in CaSR peptide 75-115 ELISA
100
80
60
40
20
0
APS1 patients
Healthy controls
(c)
Antibody index in CaSR peptide 114-126 ELISA
100
80
60
40
20
0
APS1 patients
Healthy controls
(d)
Antibody index in CaSR peptide 138-170 ELISA
100
80
60
40
20
0
APS1 patients
Healthy controls
(e)
Antibody index in CaSR peptide 171-195 ELISA
100
80
60
40
20
0
APS1 patients
Healthy controls
(f)
Antibody index in CaSR peptide 214-238 ELISA
100
80
60
40
20
0
APS1 patients
Healthy controls

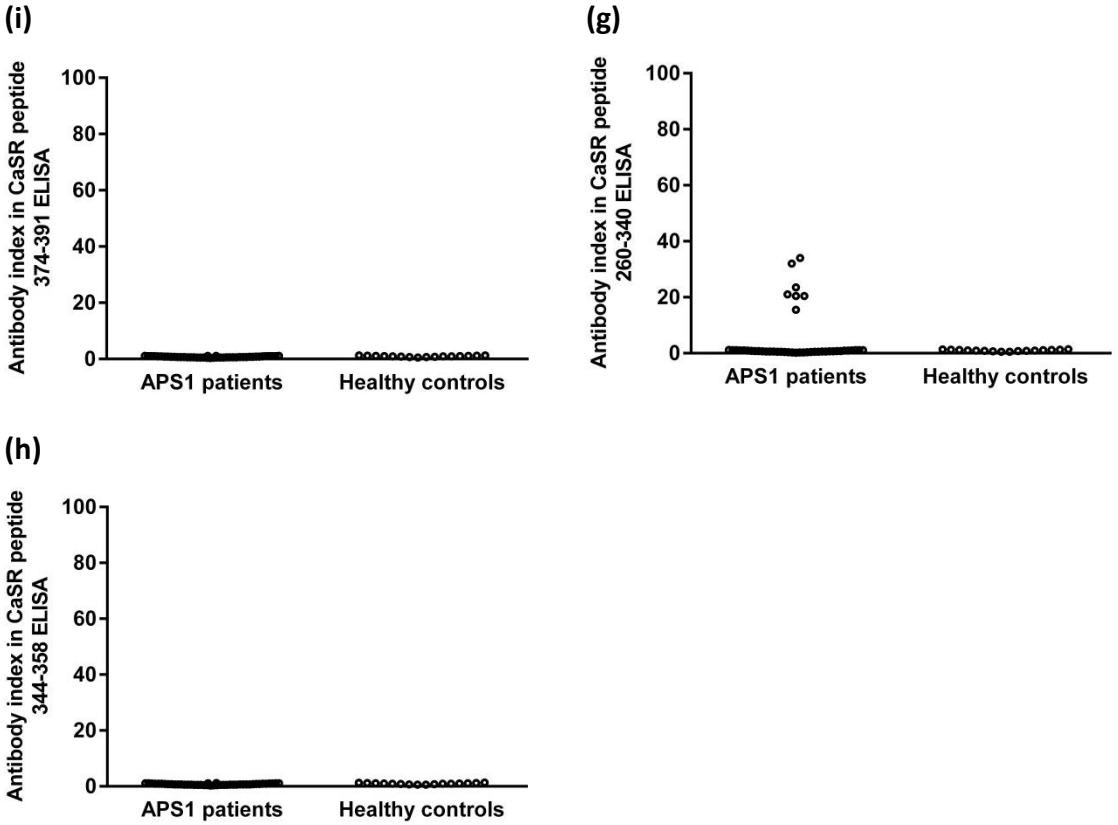

Figure 4.6: Antibody indices of APS1 patient and control sera in CaSR peptide ELISAs

Sera from 44 APS1 patients and 16 healthy controls were evaluated for antibodies against CaSR peptides using ELISAs with **(a)** CaSR 41-69 peptide, **(b)** CaSR 75-115 peptide, **(c)** CaSR 114-126 peptide, **(d)** CaSR 138-170 peptide, **(e)** CaSR 171-195 peptide, **(f)** CaSR 214-238 peptide, **(g)** CaSR 260-340 peptide, **(h)** CaSR 344-358 peptide, and **(i)** CaSR 374-391 peptide. The antibody index is shown for each APS1 patient and control serum and is the mean antibody index of at least two experiments.

Table 4.8: Summary of data from CaSR peptide ELISAs

CaSR peptide ELISA	Mean antibody index (± SD) of APS1 patient group (*n* = 44)	Antibody index range of APS1 patient group	Mean antibody index (± SD) of control group (*n* = 16)	Antibody index range of control group	Upper limit of normal antibody index	Intra-assay coefficient of variation	Inter-assay coefficient of variation	Antibody-positive APS1 patients (%)	Antibody-positive controls (%)
41-69[1]	11.6 ± 21.2	0.11-83.8	1.01 ± 0.39	0.47-1.64	2.17	4.3%	8.7%	16/44 (36)	0/16 (0)
75-115	0.79 ± 0.41	0.14-1.75	0.99 ± 0.44	0.25-2.00	2.32	3.1%	10.4%	0/44 (0)	0/16 (0)
114-126	2.82 ± 6.14	0.31-24.5	0.99 ± 0.30	0.46-1.50	1.91	2.9%	7.2%	5/44 (11)	0/16 (0)
138-170	0.82 ± 0.36	0.29-1.71	1.01 ± 0.39	0.36-1.86	2.18	3.6%	8.0%	0/44 (0)	0/16 (0)
171-195	2.68 ± 4.71	0.27-17.3	1.00 ± 0.32	0.32-1.52	1.96	4.3%	6.9%	6/44 (14)	0/16 (0)
214-238[2]	0.72 ± 0.27	0.31-1.19	0.98 ± 0.26	0.54-1.39	1.77	4.5%	7.6%	0/44 (0)	0/16 (0)
260-340	4.41 ± 8.93	0.23-34.1	1.01 ± 0.29	0.53-1.41	1.87	5.1%	8.3%	7/44 (16)	0/16 (0)
344-358	0.77 ± 0.24	0.30-1.20	1.00 ± 0.23	0.60-1.35	1.70	3.0%	11.2%	0/44 (0)	0/16 (0)
374-391	0.79 ± 0.21	0.45-1.15	0.99 ± 0.22	0.58-1.33	1.66	3.3%	10.1%	0/44 (0)	0/16 (0)

[1]The CaSR antibody index of the anti-CaSR antibody ab79829 in the 41-69 CaSR peptide ELISA was 61.95.
[2]The CaSR antibody index of the anti-CaSR antibody ab19347 in the 214-238 CaSR peptide ELISA was 222.3.

Table 4.9: Antibody indices of APS1 patient sera in CaSR peptide ELISAs

Patient number	Antibody index in each CaSR peptide ELISA[1,2]								
	41-69	75-115	114-126	138-170	171-195	214-238	260-340	344-358	374-391
APS1-1	**82.11**	1.17	0.81	1.14	0.80	0.83	0.83	0.88	0.83
APS1-2	**75.39**	0.75	0.19	0.79	0.11	0.39	0.30	0.48	0.39
APS1-3	**11.39**	0.67	0.61	0.57	**14.23**	0.69	**23.58**	0.70	0.72
APS1-4	**13.31**	1.07	1.08	1.13	**17.08**	1.10	**32.00**	1.07	1.06
APS1-5	**19.97**	1.04	**14.31**	1.05	1.78	0.88	0.93	0.93	0.95
APS1-6	**9.43**	0.75	**19.94**	0.85	1.25	0.27	0.53	0.40	0.55
APS1-7	**7.16**	0.14	**13.03**	0.43	0.56	0.42	0.63	0.53	0.65
APS1-8	**25.76**	0.79	0.81	0.88	0.82	0.77	0.85	0.83	0.88
APS1-9	**21.59**	0.36	0.44	0.58	**11.79**	0.31	**21.05**	0.43	0.58
APS1-10	**18.10**	0.36	**24.00**	0.58	1.60	0.46	0.65	0.57	0.68
APS1-11	**16.22**	0.50	0.56	0.68	0.67	0.46	0.65	0.57	0.68
APS1-12	**34.32**	0.36	0.44	0.58	**17.25**	0.31	**15.55**	0.43	0.58
APS1-13	**10.27**	1.11	1.09	1.10	1.06	1.12	1.08	1.13	1.10
APS1-14	**25.73**	0.21	0.31	0.48	**11.60**	0.15	**20.45**	0.30	0.48
APS1-15	**36.20**	0.54	0.59	0.70	**12.95**	0.50	**20.48**	0.60	0.70
APS1-16	**83.83**	1.83	**24.46**	1.71	2.01	0.75	**34.07**	0.80	0.75
APS1-17	0.57	0.68	0.72	0.80	0.83	0.65	0.78	0.73	0.80
APS1-18	0.18	1.11	1.09	1.10	1.06	1.12	1.08	1.13	1.10
APS1-19	0.22	1.18	1.16	1.15	1.14	1.19	1.13	1.20	1.15
APS1-20	1.11	1.17	0.92	1.14	1.09	0.92	0.93	0.95	0.92
APS1-21	0.11	0.17	0.31	0.29	0.27	0.47	0.40	0.55	0.47
APS1-22	0.44	1.17	0.46	1.14	0.55	0.58	0.53	0.65	0.58
APS1-23	0.36	0.33	0.35	0.43	0.48	0.50	0.43	0.58	0.50
APS1-24	0.53	0.17	0.50	0.29	0.61	0.61	0.57	0.68	0.61
APS1-25	1.33	1.75	1.15	1.64	1.27	1.08	1.13	1.10	1.08
APS1-26	0.19	0.25	0.50	0.36	0.34	0.61	0.57	0.68	0.61
APS1-27	0.19	0.25	0.35	0.36	0.34	0.50	0.43	0.58	0.50
APS1-28	1.00	1.25	1.15	1.21	1.00	1.08	1.13	1.10	1.08
APS1-29	1.39	1.58	1.23	1.50	1.32	1.14	1.20	1.15	1.14
APS1-30	0.44	0.75	0.54	0.79	0.55	0.64	0.60	0.70	0.64
APS1-31	0.96	0.79	0.75	0.73	0.76	0.81	0.69	0.80	0.82
APS1-32	0.85	0.93	0.92	0.93	0.85	0.95	0.81	0.93	0.94
APS1-33	0.96	0.55	0.47	0.40	0.53	0.57	0.31	0.59	0.62
APS1-34	0.24	0.64	0.58	0.53	0.58	0.67	0.23	0.67	0.70
APS1-35	0.11	0.86	0.83	0.83	0.86	0.88	0.73	0.87	0.88
APS1-36	0.84	0.57	0.50	0.43	0.48	0.60	0.35	0.61	0.64
APS1-37	1.24	1.07	1.08	1.13	1.03	1.10	1.00	1.07	1.06
APS1-38	0.93	0.67	0.61	0.57	0.73	0.69	0.60	0.70	0.72
APS1-39	0.79	0.57	0.50	0.43	0.55	0.60	0.33	0.61	0.64
APS1-40	0.78	1.02	1.11	0.79	1.00	1.04	1.14	1.05	1.01
APS1-41	1.06	0.93	0.94	1.15	1.12	1.12	0.92	0.96	0.84
APS1-42	0.75	0.84	0.81	1.03	0.99	0.67	0.74	0.95	0.88
APS1-43	1.02	0.92	0.67	1.02	1.04	0.81	0.78	0.64	1.05
APS1-44	1.16	1.09	0.98	0.86	0.77	0.89	1.09	0.88	1.02

[1]Bold type-face indicates antibody-positive APS1 patient serum.
[2]The antibody index is the mean of two experiments.

4.4.5 Summary of CaSR epitope identification

The identified CaSR epitope domains mapped by phage display and CaSR peptide ELISAs are given in **Table 4.10**. There was concordance between the majority of epitopes identified by phage display and those subsequently verified by CaSR peptide ELISAs. The exceptions were **(a)** antibody reactivity against CaSR peptide 260-340 in the ELISA, which was not identified as a target by phage display in patients APS1-3, APS1-9, APS1-12, APS1-14, APS1-15, and APS1-16, **(b)** antibody reactivity against CaSR peptide 171-195 in the ELISA, which was not identified as a target by phage display in patient APS1-4, and **(c)** no reactivity against CaSR peptides 114-126 and 138-170 in the ELISAs, although the consensus peptide of CaSR residues 117-144 was identified as a target by phage display in patient APS1-4.

All patients in the APS1 group had CaSR antibodies that recognised epitope/s within the domain 41-69 (**Table 4.11**). None of the patients had antibodies that bound to amino acid residues 75-115, 138-170, 214-238, 344-358 or 374-391 of the CaSR (**Table 4.11**). In addition, 31% (5/16), 38% (6/16) and 44% (7/16) of the APS1 patients showed immunoreactivity against CaSR peptides 114-126, 171-195 and 260-340, respectively (**Table 4.11**). Furthermore, the CaSR antibodies in 5/16 (31%), 4/16 (25%), and 7/16 (44%) of the APS1 patients recognised one, two and three different epitopes, respectively (**Table 4.12**). **Table 4.12** also gives the clinical details of the 16 CaSR antibody-positive patients and their respective CaSR epitope recognition patterns.

Table 4.10: CaSR epitope domains identified by phage display and/or CaSR peptide ELISA

APS1 patient	Epitope domain identified by phage-display	Epitope domain identified or confirmed by CaSR peptide ELISAs
APS1-1	26-71	41-69
APS1-2	41-71	41-69
APS1-3	19-44; 138-190	41-69; 171-195; 260-340
APS1-4	23-45; 117-144; 260-340	41-69; 171-195; 260-340
APS1-5	27-71; 106-131	41-69; 114-126
APS1-6	41-71; 106-130	41-69; 114-126
APS1-7	41-71; 114-126	41-69; 114-126
APS1-8	41-71	41-69
APS1-9	26-69; 171-195	41-69; 171-195; 260-340
APS1-10	30-70; 103-133	41-69; 114-126
APS1-11	26-71	41-69
APS1-12	26-71; 171-195	41-69; 171-195; 260-340
APS1-13	26-71	41-69
APS1-14	41-69; 171-195	41-69; 171-195; 260-340
APS1-15	41-69; 171-195	41-69; 171-195; 260-340
APS1-16	26-71; 103-133	41-69; 114-126; 260-340

Table 4.11: Summary of epitopes recognised by CaSR antibodies in APS1 patients

Epitope domain	Number of CaSR antibody-positive APS1 patients (*n* = 16) with antibodies against epitope (%)	APS1 patients with CaSR antibodies
41-69	16 (100)	APS1-1, -2, -3, -4, -5, -6, -7, -8, -9, -10, -11, -12, -13, -14, -15, -16
75-115	0 (0)	None detected
114-126	5 (31)	APS1-5, -6, -7, -10, -16
138-170	0 (0)	None detected
171-195	6 (38)	APS1-3, -4, -9, -12, -14, -15
214-238	0 (0)	None detected
260-340	7 (44)	APS1-3, -4, -9, -12, -14, -15, -16
344-358	0 (0)	None detected
374-391	0 (0)	None detected

Table 4.12: Summary of APS1 patient details and CaSR epitopes

Patient	Sex	Age at sample (years)	Age at onset (years)	Disease duration (years)	Clinical details[1]	Number of CaSR epitopes	Epitopes
APS1-1	F	46	2	44	CMC; HP; AD; HT; POF; AA; AS; TIN	1	41-69
APS1-2	M	46	7	39	CMC; HP; AD; HT; HG; AA; V; T1D; AS; K	1	41-69
APS1-3	F	51	3	48	CMC; HP; AD; POF; T1D; AS; OBS	3	41-69; 171-195; 260-340
APS1-4	M	37	2	35	CMC; HP; AD; T1D;	3	41-69; 171-195; 260-340
APS1-5	F	10	5	5	CMC; HP; AD	2	41-69; 114-126
APS1-6	F	12	3	9	CMC; HP; AD; POF; GHD	2	41-69; 114-126
APS1-7	M	9	4	5	CMC; HP; AD; K	2	41-69; 114-126
APS1-8	M	13	5	8	CMC; HP; AD; K; V; CD; AS	1	41-69
APS1-9	M	30	7	21	CMC; HP; AD; T1D	3	41-69; 171-195; 260-340
APS1-10	M	47	15	32	CMC; AD; PA; AA	2	41-69; 114-126
APS1-11	F	16	4	12	CMC; HP; AD; H; POF; OBS	1	41-69
APS1-12	F	27	2	25	CMC; HP; AD; K; AA; POF; OBS	3	41-69; 171-195; 260-340
APS1-13	M	25	4	21	CMC; HP; AD; K; AA; V; OBS; AS; HG	1	41-69
APS1-14	F	43	5	38	CMC; HP; AD; POF; AA; V; CD	3	41-69; 171-195; 260-340
APS1-15	M	9	5	4	CMC; HP; AD	3	41-69; 171-195; 260-340
APS1-16	F	11	5	6	CMC; HP; AD	3	41-69; 114-126; 260-340

[1]AA, alopecia areata; AD, Addison's disease; AS, asplenia; CD, chronic diarrhoea; CMC, chronic mucocutaneous candidiasis; GHD, growth hormone deficiency; H, hepatitis; HG, hypogonadism (male); HP, hypoparathyroidism; HT, autoimmune hypothyroidism; K, keratoconjunctivitis; OBS, chronic obstipation; PA, pernicious anaemia; POF, premature ovarian failure; T1D, type 1 diabetes mellitus; TIN, tubulonephritis; V, vitiligo.

4.4.6 Features of the identified CaSR epitopes

All the identified epitopes domains were in the extracellular domain of the CaSR (**Figure 4.7**). The epitope at amino acids 41-69 overlaps the CaSR loop 1 domain (Hu and Spiegel, 2007), and the epitope constituting amino acids 114-126 overlaps the CaSR loop 2 domain (Hu and Spiegel, 2007). The epitope encompassing amino acids 171-195 includes residues that have been predicted to participate in calcium binding (S147, S170, and D190) (Silve et al., 2005). The 260-340 epitope domain contains a critical amino acid residue E297 that forms part a Ca^{2+} binding pocket in the CaSR (Silve et al., 2005).

The mapped epitopes were visualised on a 3D representation of the CaSR extracellular domain using PyMOL molecular graphics system software. The results indicated that in all four epitopes, there were several amino acid residues exposed on the surface of the receptor (**Figure 4.8**). This would indicate accessibility as antibody targets.

Antigenicity predictions on the CaSR extracellular domain were made using the Immune Epitope Database and Analysis Resource. The analysis revealed several antigenic peptides within the CaSR extracellular domain (**Figure 4.9 and Table 4.13**). Comparison of the predicted CaSR antigenic peptides with the CaSR epitopes determined experimentally by phage-display and CaSR peptide ELISAs indicated there was overlap between them, particularly in the case of the antibody binding site identified between amino acid residues 260-340 (**Table 4.13**).

In searches of relevant protein databases, amino acid homologies between the identified epitopes and either microbial or viral polypeptides were not demonstrated.

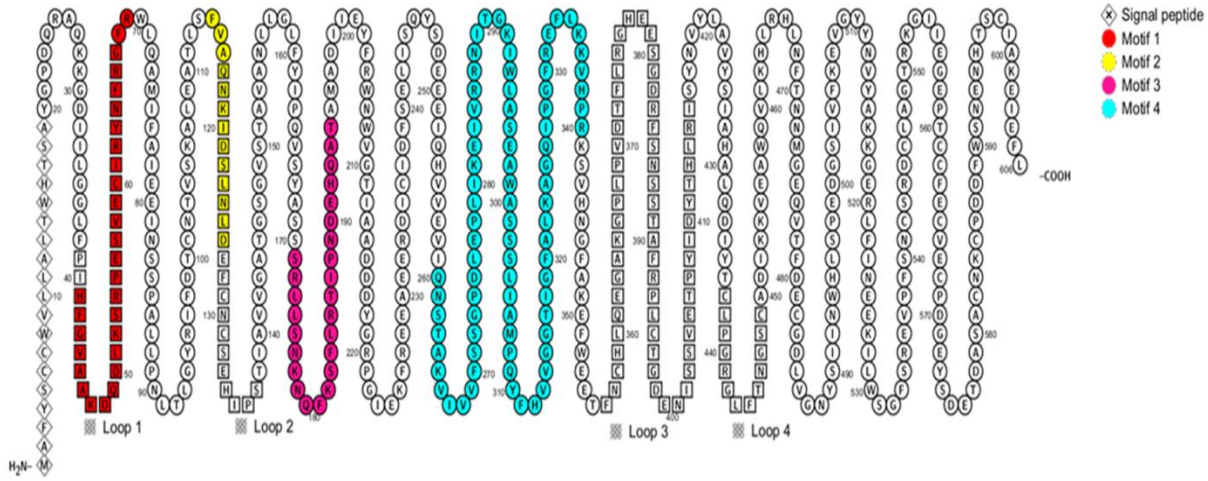

Figure 4.7: Position of identified epitopes on the linear sequence of the CaSR extracellular domain.

The figure of the CaSR extracellular domain was created using the web-based service Protter (wlab.ethz.ch/protter) (Omasits et al., 2014). Amino acids forming the CaSR loop domains (Hu and Spiegel, 2007) are shown in squares. The epitope at amino acids 41-69 overlaps the CaSR loop 1 domain (Hu and Spiegel, 2007), and the epitope constituting amino acids 114-126 overlaps the CaSR loop 2 domain (Hu and Spiegel, 2007). The epitope encompassing amino acids 171-195 includes residues that have been predicted to participate in calcium binding (S147, S170, and D190) (Silve et al., 2005). The 260-340 epitope domain contains a critical amino acid residue E297 that forms part a Ca^{2+} binding pocket in the CaSR (Silve et al., 2005).

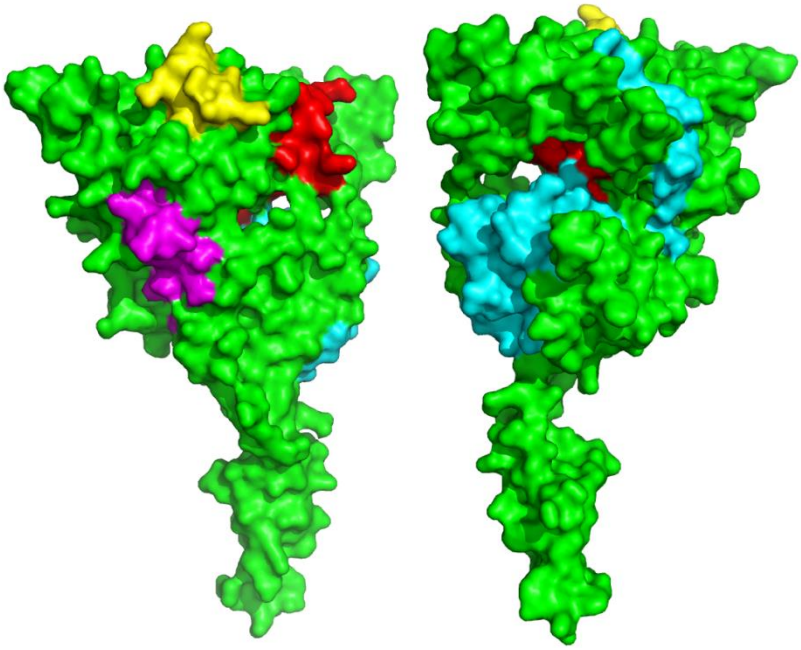

Figure 4.8: 3D representation of the CaSR extracellular domain showing antibody binding sites.

Identified CaSR epitopes were visualised on a 3D representation of the CaSR extracellular domain using PyMOL molecular graphics system software. The epitopes highlighted are at amino acids 41-69 (red), 114-126 (yellow), 171-195 (pink), and 260-340 (blue).

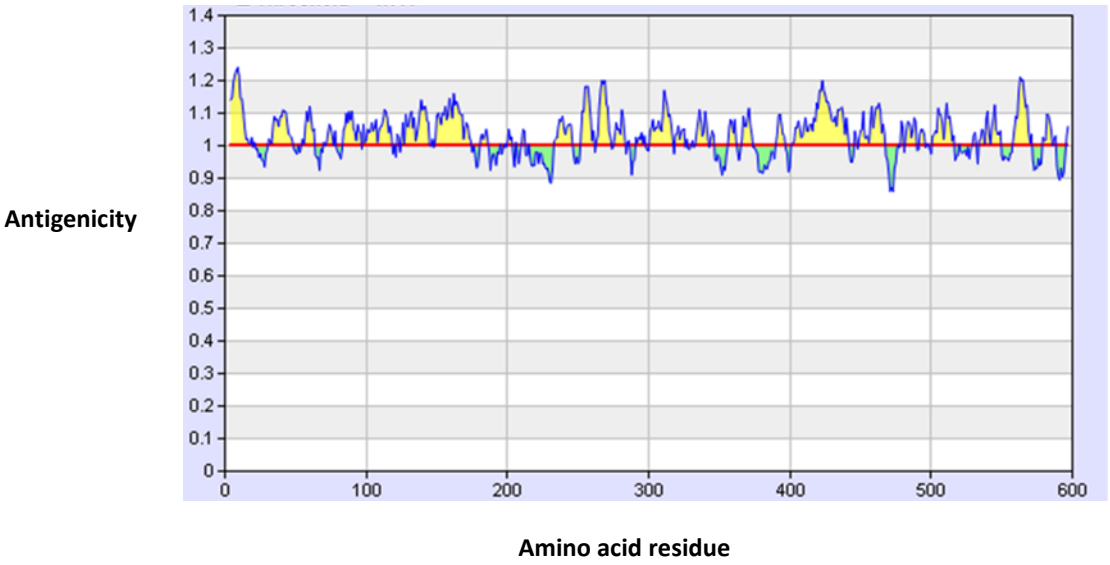

Figure 4.9: Antigenicity predictions within the CaSR extracellular domain.

Antigenicity predictions within the CaSR extracellular domain were carried out using the Immune Epitope Database and Analysis Resource. Local antigenicity values, calculated as previously detailed (Kolaskar and Tongaonkar, 1990), are plotted against the amino acid residues of the CaSR extracellular domain. The *y*-axis from 0-1.4 reflects increasing antigenicity.

Table 4.13: Comparison of predicted antigenic peptides on the CaSR extracellular domain to the CaSR epitopes determined experimentally

Predicted antigenic peptide[1]	Epitope domain[2]
4-19 (YSCCWVLLALTWHTSA)	-
31-48 (DIILGGLFPIHFGVAAKD)	41-69 (HFGVAAKDQDLKSRPESVECIRYNFRGFR)
55-63 (PESVECIRY)	41-69 (HFGVAAKDQDLKSRPESVECIRYNFRGFR)
70-76 (WLQAMIF)	-
84-96 (SPALLPNLTLGYR)	
98-118 (FDTCNTVSKALEATLSFVAQN)	114-126 (FVAQNKIDSLNLD)
125-144 (LDEFCNCSEHIPSTIAVVGA)	114-126 (FVAQNKIDSLNLD)
149-174 (VSTAVANLLGLFYIPQVSYASSSRLL)	171-195 (SRLLSNKNQFKSFLRTIPNDEHQAT)
181-186 (KSFLRT)	171-195 (SRLLSNKNQFKSFLRTIPNDEHQAT)
233-246 (RDICIDFSELISQY)	
252-261 (IQHVVEVIQN)	
263-273 (TAKVIVVFSSG)	260-340 (QNSTAKVIVVFSSGPDLEPLIKEIVRRNITGKIWLASEAWAS SSLIAMPQYFHVVGGTIGFALKAGQIPGFREFLKKVHPR)
276-283 (LEPLIKEI)	260-340 (QNSTAKVIVVFSSGPDLEPLIKEIVRRNITGKIWLASEAWAS SSLIAMPQYFHVVGGTIGFALKAGQIPGFREFLKKVHPR)
291-297 (KIWLASE)	260-340 (QNSTAKVIVVFSSGPDLEPLIKEIVRRNITGKIWLASEAWAS SSLIAMPQYFHVVGGTIGFALKAGQIPGFREFLKKVHPR)
301-317 (SSSLIAMPQYFHVVGGT)	260-340 (QNSTAKVIVVFSSGPDLEPLIKEIVRRNITGKIWLASEAWAS SSLIAMPQYFHVVGGTIGFALKAGQIPGFREFLKKVHPR)
319-325 (GFALKAG)	260-340 (QNSTAKVIVVFSSGPDLEPLIKEIVRRNITGKIWLASEAWAS SSLIAMPQYFHVVGGTIGFALKAGQIPGFREFLKKVHPR)
333-342 (FLKKVHPRKS)	260-340 (QNSTAKVIVVFSSGPDLEPLIKEIVRRNITGKIWLASEAWAS SSLIAMPQYFHVVGGTIGFALKAGQIPGFREFLKKVHPR)
357-362 (NCHLQE)	-
366-373 (GPLPVDTF)	-
390-396 (AFRPLCT)	-
401-441 (ISSVETPYIDYTHLRISYNVYLAVYSIAHALQDIYTCLP GR)	-
449-467 (CADIKKVEAWQVLKHLRHL)	-
482-489 (CGDLVGNY)	-
501-516 (GSIVFKEVGYYNVYAK)	-
543-549 (SREVPFSNCSRDCLAG)	-
558-571 (EPTCCFECVECPDG)	-
579-588 (ASACNKCPDD)	-

[1]Antigenic peptides predicted using the Immune Epitope Database and Analysis Resource.
[2]Epitopes on the CaSR identified by phage-display and CaSR peptide ELISAs.

4.5 Discussion

Identification of CaSR epitopes The aim of this part of the study was to use phage-display technology to identify the epitopes of APS1 patient CaSR antibodies. This method has been employed in identifying the binding sites of autoantibodies found in several autoimmune diseases (Myers et al., 2000, Dromey et al., 2004). Here, a phage-display library of CaSR peptides was used in panning experiments with anti-CaSR antibody ab79829, as a positive control, and with APS1 patient sera. Following five rounds of panning of the phage display library with anti-CaSR antibody ab79829, sequence analysis revealed that 80% of the phagemid contained an amino acid consensus sequence of residues 26-70, encompassing the target sequence (amino acids 41-69) of the antibody. This initial control experiment demonstrated that the phage display library could be screened successfully, at least with a specific antibody.

Subsequent panning of the phage-display library with sera from CaSR antibody-positive APS1 patients resulted in the identification of at least one CaSR peptide consensus sequence, presumably representing a CaSR epitope, for each patient. In addition, two patients (APS1-2 and APS1-4) had each enriched one in-frame CaSR peptide (amino acids 850-909 and 260-340, respectively) that was only represented once within the set of analysed sequences. Nevertheless, these sequences could represent CaSR epitopes as they would have been expressed on the phage surface and therefore accessible to antibody interaction during the panning process. The APS1 CaSR antibody-negative patient did not enrich any consensus peptide.

To confirm the presence or not of antibodies against the potential epitope domains identified by phage display, serum samples from all 44 APS1 patients were analysed in an ELISA format with specific CaSR peptides. There was concordance between the majority of epitopes identified by phage display and those subsequently verified by CaSR peptide ELISAs. However, a lack of immunoreactivity against CaSR peptides 114-126 and 138-170 in ELISAs in patient APS1-4, even though a consensus peptide of CaSR residues 117-144 was identified as a target by phage-display, may indicate that the CaSR antibody binding site lies between amino acids 127 and 137, residues which were not present in the

peptides tested in the ELISAs. In addition, there were two examples of epitopes (171-195 and 260-340) that were not identified as antibody targets by phage display by certain APS1 patient sera (171-195 by APS1-4; and 260-340 by APS1-3, APS1-9, APS1-12, APS1-14, APS1-15, and APS1-16), but were subsequently characterised as binding sites in peptide ELISAs. Such discordance could be explained by a failure to screen sufficient numbers of clones in order to identify the particular peptide sequence following panning experiments. Indeed, the CaSR peptide 260-340 was only represented once amongst the set of clones isolated after panning of serum from patient APS1-4.

Overall, CaSR antibody epitopes were identified between amino acid residues 41-69 (all patients), 114-126 (31% of patients), 171-195 (38% of patients) and 260-340 (44% of patients) at the N-terminal of the receptor's extracellular domain. The first three epitope domains have been reported previously for CaSR antibodies in 12 APS1 patients (Kemp et al., 2010) and were found again here. Amino acid sequence 260-340 constituted a novel CaSR epitope. As before (Kemp et al., 2010), epitopes at amino acids 214-236, 374-391 and 344-358 were not identified in this study, although all three binding sites have been reported as targets for CaSR autoantibodies in patients with hypocalciuric hypercalcaemia or autoimmune hypoparathyroidism (Kifor et al., 2003, Kifor et al., 2004, Pallais et al., 2004). Furthermore, epitopes were not apparent in the CaSR extracellular domain between amino acids 75-115 and 138-170.

Except for the potential epitope between amino acids 850-909, which was isolated in panning experiments with serum from patient APS1-2, but was not analysed in CaSR peptide ELISAs, antibody binding sites in either the membrane spanning region or the intracellular part of the CaSR were not characterised. As B cell epitopes are generally up to 20 amino acids (von Mikecz et al., 1995), the larger two represented by amino acids 260-340 (81 residues) and 41-69 (38 residues) require finer mapping experiments to determine the exact antibody binding sites. Of interest, is that since all patients reacted with amino acid residues 41-69, this might well be the (or part of the) immunodominant CaSR epitope and as such the peptide could form a simple assay if in future a larger panel of sera were to confirm the 100% reactivity.

Identified epitopes and CaSR function Notably, in all the identified epitopes there were several amino acid residues exposed on the surface of the CaSR such that they would be available for antibody binding. With regard to the possible effects that CaSR antibodies might have upon receptor function, the major epitope domain at amino acids 41-69 overlaps with the loop 1 domain of the receptor which, if removed, reduces activation of the receptor (Reyes-Cruz et al., 2001, Hu and Spiegel, 2007). Binding of CaSR antibodies to this site might therefore modulate the receptor's normal function.

The epitope constituting amino acids 114-126 overlaps with the loop 2 domain of the CaSR (Hu and Spiegel, 2007). Point mutations in or deletions of this part of the receptor increase the sensitivity of the CaSR to Ca^{2+}, and result in autosomal dominant hypoparathyroidism (Reyes-Cruz et al., 2001, Hu and Spiegel, 2007). From these observations, it has been suggested that loop 2 may have an important role in maintaining the inactive state of the CaSR involving disulphide links through cysteine residues C129 and C131. Indeed, mutations involving either of these amino acid residues results in autosomal dominant hypoparathyroidism (www.casrdb.mcgill.ca). Antibody binding to epitopes that are found within loop 2 could either inhibit or activate the CaSR, depending on whether antibody binding favoured the active or inactive state of the receptor, respectively.

Of particular interest is the antibody binding site at amino acids 171-195 since site-directed mutagenesis and molecular models have indicated that some of these residues (S147, S170, and D190) form part of a binding site for Ca^{2+} that is found in the crevice between the two lobes of each receptor monomer (Hauache et al., 2000, Silve et al., 2005, Hu and Spiegel, 2007). Therefore, binding of an antibody to this area of the CaSR could disrupt the interaction of Ca^{2+} with this Ca^{2+}-binding site. Furthermore, the 260-340 epitope domain also contains a critical amino acid residue E297 that forms part a Ca^{2+} binding pocket (Silve et al., 2005).

Further investigations are required to ascertain the possible functional effects of CaSR antibodies that recognise the different epitopes. Previously, antibodies that activate the receptor have been identified in two APS1 patients (Kemp et al., 2009). However, their

exact binding sites on the receptor remain to be determined. The epitopes characterised here are likely to be linear in nature as their recognition by patient CaSR antibodies was confirmed using synthetic peptide ELISAs. Nevertheless, it is possible that the identified linear binding sites contribute to discontinuous epitopes on the CaSR. It is generally assumed that autoantibodies affecting the function of a protein, and which lead to disease, bind to conformational epitopes. In Graves' disease, for example, autoantibodies against the thyrotropin receptor, which are responsible for disease activity, recognise a number of different conformational epitopes (Morgenthaler et al., 1999). Identifying CaSR antibody binding sites that depend upon the native structure of the receptor is therefore an important future goal.

Epitope spreading Immunoreactivity to more than one epitope was detected in many of the patients (11/16 = 69%), indicating a heterogeneous humoral immune response against the CaSR. Similarly, antibodies in autoimmune thyroiditis and type 1 diabetes mellitus have been reported to react against multiple epitopes on thyroid peroxidase and tyrosine phosphatase-like IA-2 autoantigens, respectively (Lampasona et al., 1996, Zanelli et al., 1992). This has been explained by 'intramolecular spreading' of an autoimmune response from one or a small number of epitopes to multiple epitopes during disease progression. For example, in type 1 diabetes mellitus, a temporal spreading of the antibody responses has been described from immunodominant epitopes in an early pre-clinical phase to lesser immunogenic domains at the manifestation of disease (Naserke et al., 1998). Unfortunately, in the absence of longitudinal serum samples, no evidence of CaSR epitope spreading can be provided in the cases described in this study.

Molecular mimicry Of note, homology between the identified epitopes and microbial proteins was not in evidence, suggesting that molecular mimicry (Wucherpfennig, 2001b) does not initiate the production of CaSR antibodies in APS1 patients. However, there may be as yet unidentified antibody binding sites on the receptor that do display cross-reactivity with bacterial or viral antigens.

Limitations of methodology A notable limitation of the study is in the use of human sera in the mapping of B cell epitopes which can be problematic because sera contain multiple

antibody species against a particular autoantigen and the immune response tends to diversify with duration. It is difficult therefore to examine the reactivity of a specific autoantibody in isolation. In order to characterise the array of autoantibodies present in a specifc serum and the epitope specificity of a particular autoantibody, the isolation of monoclonal antibodies from the patient would be needed. This has been done to identify an array of epitopes on glutamic acid decarboxylase in patients with type 1 diabetes mellitus (Syren et al., 1996). However, although the monoclonal antibody approach can allow the precise characterisation of epitopes recognised by a specific antibody, it is difficult to know the relative frequencies of the different monoclonal antibodies in the patient under investigation, and how typical these are for the general population. Despite this, the isolation of monoclonal CaSR antibodies from APS1 patients would allow a more detailed characterisation of the epitopes recognised by CaSR autoantibodies.

Conclusions To conclude, several binding sites of CaSR autoantibodies have been identified. They confirm earlier reported epitopes, although a novel binding site (amino acids 260-340) was also discovered. It will be of interest to determine if any the antibodies recognising the specific epitopes are able to affect the function of the receptor.

Chapter 5

Characterisation of the properties of CaSR autoantibodies in APS1 patients

5 Characterisation of the properties of CaSR autoantibodies in APS1 patients

5.1 Introduction

Immunoglobulin G (IgG) makes up in the region of 75% of the total immunoglobulins in the human circulation. It is a major effector of the antibody response. The remaining 25% of immunoglobulins comprises the four classes, IgM, IgA, IgD and IgE. Each class has its own distinctive functions and characteristics (Spiegelberg, 1974). Predominantly, the activity of IgG class antibodies is expressed during a secondary antibody response corresponding with repeated contact with an antigen. Antibodies of the IgG class persist in the blood for long periods, and have relatively high affinity compared with other immunoglobulin classes. The following sections will summarise some important properties of IgG antibodies that will be examined in the context of APS1 patient autoantibodies against the CaSR.

5.1.1 Antibody functional affinity (avidity)

Antibody affinity is a measure of the binding strength between one interacting antibody site and one antigenic determinant (Roitt and Delves, 1997). However, in practice, functional affinity (or avidity) is used to measure the overall strength of interaction between antibodies and multivalent antigens. Indeed, this is most applicable in describing the binding of a patient's serum to its antigenic target (Roitt and Delves, 1997). It has been suggested that high functional affinity could be an important property of antibodies in autoimmune disease (Gharavi and Reiber, 1996). However, only in a few cases have antibodies with greater functional affinity been shown to have increased pathogenicity (Takeda et al., 2001, Cucnik et al., 2004, Cucnik et al., 2011). Examples include double-stranded DNA and ribosomal P antibodies in systemic lupus erythematosus patients (Takeda et al., 2001), and antibodies against anti-β2-glycoprotein I in antiphospholipid syndrome patients (Cucnik et al., 2004, Cucnik et al., 2011). However, there are no reports on the functional affinity of CaSR autoantibodies.

5.1.2 IgG subclasses

Four subgroups of IgG have been identified in humans and these are referred to as IgG1, IgG2, IgG3 and IgG4 (Gergely et al., 1967). There are differences in some of the biological properties of the different subclasses, and these are given in **Table 5.1**. Particularly, interactions with Fc receptors (FcγR), which are expressed primarily on immune effector cells, differ between the subclasses (**Table 5.1**). Consequently, IgG1, IgG2, IgG3 and IgG4 can have different effects upon the induction of effector cell functions which may include phagocytosis, antibody-mediated cellular cytotoxicity, and antigen presentation (van de Winkel and Capel, 1993, van de Winkel and Capel, 1996). Furthermore, IgG4 cannot activate the complement system (**Table 5.1**) (Flanagan and Rabbitts, 1982, van Loghem, 1986).

In autoimmune diseases, subclass restriction of specific antibodies has been observed. For example, chiefly, autoantibodies against 21-hydroxylase, 17α-hydroxylase and side-chain cleavage enzyme, in patients with autoimmune Addison's disease and autoimmune ovarian insufficiency, are of the IgG1 subclass (Boe et al., 2004, Brozzetti et al., 2010). Similarly, in patients with type 1 diabetes mellitus, IgG1 autoantibody responses predominate against protein tyrosine phosphatase IA-2 and glutamic acid decarboxylase 65 (Bonifacio et al., 1999, Hawa et al., 2000). A predominance of IgG and IgG4 subclasses with respect to thyroid peroxidase autoantibodies has also been shown in patients with autoimmune hypothyroidism (Kohno et al., 1993, Silva et al., 2003, Xie et al., 2008). In patients with Graves' hyperthyroidism or Hashimoto's thyroiditis, IgG2 and IgG4 were the dominant subclasses, respectively, in relation to thyroglobulin autoantibodies (Caturegli et al., 1994). So far, the only report of IgG subclass in relation to CaSR autoantibodies has come from studying a patient with autoimmune hypocalciuric hypercalcemia; the anti-CaSR autoantibodies were exclusively of the IgG4 subtype (Pallais et al., 2004). No studies have reported IgG subclasses for CaSR autoantibodies found in patients with hypoparathyroidism.

5.1.3 Antibody functional effects

Several extracellular receptors are the targets of pathogenic autoantibodies in autoimmune disease. Examples are the thyroid-stimulating hormone receptor in Graves' hyperthyroidism (Morgenthaler et al., 2007), and the acetylcholine receptor in myasthenia gravis (Jacob et al., 2012). To date, only a small number of patients with hypoparathyroidism have been identified with CaSR-activating autoantibodies that could theoretically diminish PTH-secretion: IgG from two patients with APS1 (both with hypoparathyroidism) activated the CaSR expressed in HEK293 cells (Kemp et al., 2009), and sera from two patients with idiopathic hypoparathyroidism inhibited PTH-release from human parathyroid cells (Kifor et al., 2004).

Table 5.1: Properties of IgG subclasses

Property	IgG1	IgG2	IgG3	IgG4
Mean serum concentration in g/l (range)	6.98 (4.9-11.4)	3.8 (1.5-6.4)	0.51 (0.20-1.10)	0.56 (0.08-1.40)
Percentage of total IgG	43-75	16-48	1.7-7.5	0.8-11.7
Anti-protein activity[1]	++	+/-	++	+/-
Anti-polysaccharide activity[1]	+	++	-	-
Anti-allergen activity[1]	+	-	-	++
Complement C1q binding[1]	++	+	+++	-
Fc receptor for IgG binding				
FcγRI (CD64:monocytes, macrophages, neutrophils, dendritic cells)	++	-	+++	+
FcγRII (CD32):monocytes, macrophages, neutrophils, eosinophils, platelets, B cells, dendritic cells, endothelial cells)	++	-	+++	-
FcγRIIa-H131	++	+++	+++	-
FcγRIIa-R131	++	-	++	-
Fcγ RIII (CD16:neutrophils, eosinophils, macrophages, NK cells, subsets of T cells)	++	-	++	-
FcγRIIIb-NA1	+++	-	+++	-
FcγRIIIb-NA2	++	-	++	-

[1]+++, very strongly positive; ++, strongly positive; +, positive; -/+, weakly positive; -, negative.

5.2 Aims

In light of the discussed properties of IgG molecules, the aims of this part of the study were to evaluate:

- The titres of antibodies against the CaSR epitopes 41-69, 114-126, 171-195, and 260-340.
- The specificity of antibodies against the CaSR epitopes 41-69, 114-126, 171-195, and 260-340.
- The functional affinity of antibodies against the CaSR epitopes 41-69, 114-126, 171-195, and 260-340.
- The IgG subclass of antibodies against the CaSR epitopes 41-69, 114-126, 171-195, and 260-340.
- The functional effects of CaSR antibodies upon the CaSR.

5.3 Materials and Methods

5.3.1 Patient and control sera

The clinical and demographic details of the 16 CaSR antibody-positive APS1 patients used in this part of the study are given in **Table 5.2**.

5.3.2 Antibody titrations

To determine CaSR antibody titres, APS1 patient sera (*n* = up to 16, depending on the CaSR epitopes recognised by the patient's antibodies) were analysed in CaSR peptide ELISAs at a range of dilutions from 1:100 to 1:5,000. Sera from healthy individuals (*n* = 10) were used in CaSR peptide ELISAs as controls at a 1:100 dilution. All CaSR peptides (**Table 5.3**) were received dried and were solubilised and stored according to the manufacturer's instructions (Cambridge Peptides Ltd., Birmingham, UK). For ELISAs, the required peptide was diluted in phosphate-buffered saline (pH 7.4) to 0.2 µg/ml and 100-µl samples used to coat the wells of a 96-well microtitre plate. An equivalent number of wells were coated with 100 µl of 0.1% (w/v) bovine serum albumin for the measurement of non-specific binding of the sera. The plates were then incubated overnight at 4°C.

Excess peptide was removed by decanting and the wells were blocked with blocking buffer (phosphate-buffered saline, pH 7.4; 0.1% (w/v) Tween-20; 3% (w/v) bovine serum albumin) for 30 min at 37°C. Plates were washed four times with washing buffer (phosphate-buffered saline, pH 7.4; 0.1% (v/v) Tween-20). Duplicate 100-µl samples of sera at dilutions of 1:100, 1:200, 1:500, 1:1,000, 1:2,000, and 1:5,000 in blocking buffer were added to the wells. PBS was applied as a control to measure any non-specific binding of the secondary antibody. The plates were incubated at room temperature for 1 h and then washed four times with washing buffer. A 100-µl of goat anti-human IgG polyclonal antibody conjugated to alkaline phosphatase (Sigma-Aldrich, Poole, UK) diluted to 1:2000 in blocking buffer was added to each well for 1 h at room temperature. After washing five times with washing buffer, 100 µl of alkaline phosphatase substrate Sigma Fast *p*-nitrophenyl phosphate (Sigma-Aldrich) were applied to each well and plates incubated at room temperature to allow colour development. A LabSystems Integrated EIA

Management System spectrophotometer (Life Sciences International, Basingstoke, UK) was used to read absorption of the wells at 405 nm. All sera were tested in duplicate and the average OD_{405} value taken. Each mean OD_{405} value was corrected for background binding of the sera to the well without peptide.

The CaSR peptide-binding reactivity of each APS1 patient serum at each dilution and of each control serum was expressed as an antibody index calculated as: mean OD_{405} of tested serum at specified dilution/mean OD_{405} of 10 healthy control sera. Each serum was tested in three experiments and the mean antibody index ± SD calculated. The upper limit of normal for each CaSR peptide ELISA was calculated using the mean antibody index + 3SD of 10 healthy control sera.

Table 5.2: Summary of APS1 patients analysed

Patient	Sex	Age at sample (years)	Age at onset (years)	Disease duration (years)	Clinical details[1]	Number of CaSR epitopes	Epitopes
APS1-1	F	46	2	44	CMC; HP; AD; HT; POF; AA; AS; TIN	1	41-69
APS1-2	M	46	7	39	CMC; HP; AD; HT; HG; AA; V; T1D; AS; K	1	41-69
APS1-3	F	51	3	48	CMC; HP; AD; POF; T1D; AS; OBS	3	41-69; 171-195; 260-340
APS1-4	M	37	2	35	CMC; HP; AD; T1D;	3	41-69; 171-195; 260-340
APS1-5	F	10	5	5	CMC; HP; AD	2	41-69; 114-126
APS1-6	F	12	3	9	CMC; HP; AD; POF; GHD	2	41-69; 114-126
APS1-7	M	9	4	5	CMC; HP; AD; K	2	41-69; 114-126
APS1-8	M	13	5	8	CMC; HP; AD; K; V; CD; AS	1	41-69
APS1-9	M	30	7	21	CMC; HP; AD; T1D	3	41-69; 171-195; 260-340
APS1-10	M	47	15	32	CMC; AD; PA; AA	2	41-69; 114-126
APS1-11	F	16	4	12	CMC; HP; AD; H; POF; OBS	1	41-69
APS1-12	F	27	2	25	CMC; HP; AD; K; AA; POF; OBS	3	41-69; 171-195; 260-340
APS1-13	M	25	4	21	CMC; HP; AD; K; AA; V; OBS; AS; HG	1	41-69
APS1-14	F	43	5	38	CMC; HP; AD; POF; AA; V; CD	3	41-69; 171-195; 260-340
APS1-15	M	9	5	4	CMC; HP; AD	3	41-69; 171-195; 260-340
APS1-16	F	11	5	6	CMC; HP; AD	3	41-69; 114-126; 260-340

[1]AA, alopecia areata; AD, Addison's disease; AS, asplenia; CD, chronic diarrhoea; CMC, chronic mucocutaneous candidiasis; GHD, growth hormone deficiency; H, hepatitis; HG, hypogonadism (male); HP, hypoparathyroidism; HT, autoimmune hypothyroidism; K, keratoconjunctivitis; OBS, chronic obstipation; PA, pernicious anaemia; POF, premature ovarian failure; T1D, type 1 diabetes mellitus; TIN, tubulonephritis; V, vitiligo.

Table 5.3: CaSR peptides used in ELISAs

CaSR peptide[1]	Number of amino acids	Amino acid sequence of peptide
41-69	38	HFGVAAKDQDLKSRPESVECIRYNFRGFR
114-126	13	FVAQNKIDSLNLD
171-195	25	SRLLSNKNQFKSFLRTIPNDEHQAT
214-238	25	ADDDYGRPGIEKFREEAEERDICID
260-340	81	QNSTAKVIVVFSSGPDLEPLIKEIVRRNITGKIWLASEAWASSSLIA MPQYFHVVGGTIGFALKAGQIPGFREFLKKVHPR

[1]Amino acid residues are numbered according to CaSR peptide sequence with the ATG initiation codon as residue number 1.

5.3.3 Absorption experiments

To determine CaSR antibody specificity, APS1 patient sera (*n* = up to 16, depending on the CaSR epitopes recognised by the patient's antibodies) were pre-absorbed at non-saturating dilutions (**Table 5.4**), which were pre-determined by antibody titration, with a 200X molar excess of the required synthetic CaSR peptide (**Table 5.5**) in 1 ml of PBS, and then analysed in CaSR peptide ELISAs. A CaSR-unrelated peptide against the melanin-concentrating receptor 1 (Alpha Diagnostic International Inc., San Antonio, Texas, USA) was also included as a control peptide. APS1 patient sera at non-saturating dilutions and healthy control sera (*n* = 6) at 1:100 dilutions were also incubated without any peptide.

To estimate how much peptide to use in each absorption experiment, the following serves as an example. It was assumed that IgG concentration in serum was 10 mg/ml (or 0.01 g/ml). Using the molecular weight for IgG of 150,000 Da (or 150,000 g/mol), this calculated as 6.67×10^{-8} mol/ml in undiluted serum, where mol/ml = (g/ml)/(g/mol). If a 750X dilution of serum was required in the absorption experiment (**Table 5.4**), then the concentration of IgG was estimated at 8.89×10^{-11} mol/ml. The antibody concentration was then multiplied by 200 to arrive at the peptide concentration that would give a 200X molar excess of peptide in the absorption experiment. In the given example, the required concentration of peptide was therefore 1.78×10^{-8} mol/ml. If using the 41-69 CaSR peptide with a stock concentration of 1 mg/ml (or 0.001 g/ml) and a molecular weight of 3427 Da (or 3427 g/mol) (**Table 5.5**), and therefore at 2.92×10^{-7} mol/ml, where mol/ml = (g/ml)/(g/mol), the required dilution of the stock peptide in the absorption experiment was 16.4X.

After incubation at 4°C for 2 h, the pre-absorbed and unabsorbed serum samples were centrifuged in a MiniSpin microcentrifuge (Eppendorf UK Ltd., Stevenage, UK) at 13,000 rpm for 15 min and the supernatant collected. Duplicate 100-µl samples of the pre-absorbed APS1 patient sera and unabsorbed APS1 patient and unabsorbed healthy control sera were then analysed in CaSR peptide ELISAs, as detailed in **Section 5.3.2**. The CaSR peptide-binding reactivity of each serum was expressed as an antibody index calculated as: mean OD_{405} of tested serum/mean OD_{405} of six healthy unabsorbed control sera. Each

serum was tested in three experiments and the mean antibody index ± SD calculated. Antibody indices of unabsorbed and pre-absorbed APS1 patient sera were compared in Student's paired *t* tests. *P* values (two-tailed) < 0.05 were considered significant.

5.3.4 Functional affinity experiments

To analyse CaSR antibody functional affinity, APS1 patient sera (*n* = up to 16, depending on the CaSR epitopes recognised by the patient's antibodies) at non-saturating dilutions (**Table 5.4**) were pre-incubated with 0-1000 nM of the required CaSR peptide (**Table 5.5**) in 0.5 ml of PBS for 30 min. Healthy control sera (*n* = 6) at 1:100 dilutions were also pre-incubated without any peptide. Duplicate 100-µl samples of sera were then analysed in the appropriate CaSR peptide ELISA, as detailed in **Section 5.3.2**. The CaSR peptide-binding reactivity of each APS1 patient and each control serum was expressed as an antibody index calculated as: mean OD_{405} of tested serum/mean OD_{405} of six healthy control sera. Each serum was tested in three experiments and the mean antibody index ± SD calculated.

Table 5.4: Non-saturating dilutions of APS1 patient sera used in absorption and functional affinity experiments

APS1 patient	Non-saturating serum dilution used in 41-69 CaSR peptide absorption and functional affinity experiments	Non-saturating serum dilution used in 114-126 CaSR peptide absorption and functional affinity experiments	Non-saturating serum dilution used in 171-195 CaSR peptide absorption and functional affinity experiments	Non-saturating serum dilution used in 260-340 CaSR peptide absorption and functioanl affinity experiments
APS1-1	300	-	-	-
APS1-2	300	-	-	-
APS1-3	300	-	750	500
APS1-4	300	-	300	500
APS1-5	750	300	-	-
APS1-6	150	750	-	-
APS1-7	150	300	-	-
APS1-8	500	-	-	-
APS1-9	150	-	300	300
APS1-10	500	500	-	-
APS1-11	150	-	-	-
APS1-12	200	-	300	300
APS1-13	150	-	-	-
APS1-14	200	-	500	300
APS1-15	200	-	500	750
APS1-16	200	500	-	750

Table 5.5: Details of peptides used in absorption and functional affinity experiments

Peptide	Molecular weight (Da = g/mol)	Stock concentration (g/ml)	Stock concentration (mol/ml)
CaSR 41-69	3427	0.001	2.92×10^{-7}
CaSR 114-126	1468	0.001	6.81×10^{-7}
CaSR 171-195	2945	0.001	3.40×10^{-7}
CaSR 260-340	8906	0.001	1.12×10^{-7}
MCHR1	1636	0.001	6.11×10^{-7}

5.3.5 IgG subclass ELISAs

To determine CaSR antibody IgG subclass, duplicate 100-µl samples of APS1 patient (*n* = 16) and control (*n* = 10) sera were analysed in CaSR peptide ELISAs at a 1:100 dilution, as detailed in **Section 5.3.2,** with the exception that anti-human IgG1, IgG2, IgG3 and IgG4 alkaline phosphate-conjugates (SouthernBiotech, Birmingham, AL, USA) were applied as the secondary antibody at 1:2000 dilutions. The CaSR peptide-binding reactivity of each APS1 patient and control serum was expressed as an antibody index calculated as: mean OD_{405} of tested serum/mean OD_{405} of 10 healthy control sera. Each serum was tested in three experiments and the mean antibody index ± SD calculated.

The upper limit of normal for each CaSR peptide ELISA using different secondary antibodies was calculated using the mean antibody index + 3SD of 10 healthy control sera. Patient sera with an antibody index greater than the upper limit of normal were regarded as positive for binding to the CaSR peptide used in the ELISA. ELISA precision was evaluated by calculating the intra-assay coefficient of variation (expressed as a percentage) for a series of different serum samples that were measured in duplicate within the same assay run. ELISA reproducibility was evaluated by calculating the inter-assay coefficient of variation (expressed as a percentage) for a series of different serum samples that were measured in several consecutive assay runs.

5.3.6 IgG preparation

IgG was isolated from sera by affinity column chromatography using protein G-Sepharose 4 Fast Flow (Amersham Biosciences AB, Uppsala, Sweden) according to the manufacturer's instructions. Eluted IgG fractions were extensively dialysed against PBS (pH 7.4; Sigma, Poole, UK), and concentrated using an Amicon Concentrator (Amicon Inc., Beverly, MA, USA). IgG samples were sterilised with a Millex Filter Unit (Millipore Corp., Bedford, MA, USA), and the final concentrations were measured by photometry at 280 nm. All IgG samples were stored at 10 mg/ml at -20^{o}C.

5.3.7 Ca^{2+}-stimulation of the CaSR expressed in human embryonic kidney cells

The response to Ca^{2+} of the CaSR expressed in human embryonic kidney cells (HEK293-CaSR) was assessed by measuring intracellular inositol-1-phosphate (IP1) accumulation, as previously detailed (Kemp et al., 2009). The assay involves stimulating the CaSR expressed in HEK293 cells with Ca^{2+} in order to activate phospholipase C (**Figure 5.1**). The activation triggers the intracellular formation of inositol 1,4,5-triphosphate (IP3). This metabolite is transformed extremely rapidly into IP1, which in turn degrades to *myo*-inositol (**Figure 5.1**). The degradation of IP1 can be inhibited by the addition of lithium chloride to the culture medium (**Figure 5.1**). The intracellular accumulation of IP1, which reflects CaSR activation, can then be analysed by ELISA (**Section 5.3.8**).

For the assay, HEK293-CaSR cells, which were a gift from Dr Edward Brown (Division of Endocrinology, Diabetes and Hypertension, Department of Medicine, Brigham and Women's Hospital, and Harvard Medical School, Boston, MA, USA), were cultured in T75 tissue culture flasks (Nalge Nunc International, Rochester, NY, USA) in Dulbecco's DMEM medium (Invitrogen, Paisley, UK) containing 4.5 g/l glucose, 110 mg/ml sodium pyruvate, 10% (v/v) fetal calf serum, 100 units/ml penicillin G, 100 μg/ml streptomycin sulphate, 2 mM L-glutamine (all from Invitrogen) at 37°C in a 95% humidified atmosphere of 5% CO_2. To act as a control in Ca^{2+}-stimulation experiments, HEK293 cells (European Collection of Animal Cell Cultures, Salisbury, UK) were cultured in the same manner.

After reaching 80-100% confluence, the culture medium was removed from the cells which were then washed twice with PBS followed by incubation in Gibco® Cell Dissociation Buffer (Thermo Fisher Scientific, Waltham, MA, USA) at room temperature for 1 to 2 min. After discarding the buffer, cells were resuspended in culture medium and then counted in a haemocytometer.

Cells were plated in 24-well plates (Nalge Nunc International) at 4 x 10^5 cells per well in 500 μl of culture medium and incubated overnight at 37°C. Cell monolayers were washed first with serum-free medium and then with stimulation buffer containing 146 mM sodium chloride, 2.5 mM potassium chloride, 50 mM lithium chloride, 0.2 mM magnesium chloride, 2.8 mM glucose and 10 mM HEPES buffer (pH 7.4). Cells were subsequently

incubated for 1 h at 37°C in 200 µl of stimulation buffer or 200 µl of stimulation buffer containing 0.5, 1.0, 1.5, 2.0, 3.0, 5.0 or 10.0 mM calcium chloride. Following treatment, cells were lysed for 30 min at 37°C with 50 µl of 2.5% IP-One ELISA Kit Lysis Reagent (CIS Bio International, Gif-sur-Yvette, France). To assess IP1 accumulation, each cell supernatant was then analysed in an IP-One ELISA (CIS Bio International) (**Section 5.3.8**).

5.3.8 Inositol-1-phosphate ELISAs

The IP-One ELISA is based on competition between free IP1 and IP1 conjugated to horse-radish peroxidase (HRP) for binding to an anti-IP1 monoclonal antibody, as shown in **Figure 5.2**. Three 50-µl samples of each cell supernatant were tested in an IP-One ELISA. Each sample was applied to a separate well of the goat anti-mouse IgG-pre-coated ELISA plate (CIS Bio International) along with 25 µl of anti-IP1 monoclonal antibody (CIS Bio International) and 25 µl IP1-HRP conjugate (CIS Bio International). Duplicate 25 µl samples of IP1-HRP conjugate without anti-IP1 monoclonal antibody were included in each ELISA to measure any non-specific binding to the pre-coated ELISA plate. The plate was then incubated for 3 h with shaking at room temperature. The wells were washed six times with 250 µl of 0.05% (v/v) Tween 20, before the addition of 100 µl of 3,3',5,5'-tetramethylbenzidine (TMB) liquid substrate (CIS Bio International) for HRP. The plate was incubated in the dark for 30 min at room temperature, 100 µl of stop solution (CIS Bio International) added to each well, and then OD readings taken at 450 and 620 nm using a LabSystems Integrated EIA Management System spectrophotometer.

For each well, the OD at 620 nm was subtracted from OD at 450 nm, and the average of the corrected OD_{450} readings calculated for replicates. The OD_{450} readings were then corrected by subtracting the OD_{450} obtained for non-specific binding of IP1-HRP conjugate. The results for IP1 accumulation were expressed as: percentage inhibition of IP1-HRP conjugate binding = [1 – corrected OD_{450} for Ca^{2+}-stimulated cells/corrected OD_{450} in non-stimulated cells] x 100. Increasing percentage inhibition of the binding of the IP1-HRP conjugate reflects increasing amounts of IP1 in the HEK293-CaSR cell supernatants, due to CaSR activation.

5.3.9 Effect of IgG on Ca^{2+}-stimulation of the CaSR

For measuring the effects of 16 APS1 patient and 10 control IgG (**Section 5.3.6**) on Ca^{2+}-stimulation of the CaSR, HEK293-CaSR cell monolayers were washed first with serum-free medium and then with stimulation buffer. Subsequently, cells were pre-incubated either with IgG at a 1:100 dilution in 100 µl of stimulation buffer or with 100 µl of stimulation buffer without any IgG. After 10 min at 37°C, a further 100 µl of stimulation buffer or 100 µl of stimulation buffer containing 1.0, 3.0, 6.0, 12.0 or 18.0 mM calcium chloride was applied to the cells and incubation continued for 1 h at 37°C. Cells were lysed for 30 min at 37°C with 50 µl of 2.5% IP-One ELISA Kit Lysis Reagent, and IP1 accumulation analysed in an IP-One ELISA (**Section 5.3.8**). The percentage inhibition of the binding of the IP1-HRP conjugate, which reflects increasing amounts of IP1 in the HEK293-CaSR cell supernatants, were compared between Ca^{2+}-stimulated and unstimulated cells using Student's paired *t* tests. *P* values (two-tailed) < 0.05 were considered significant.

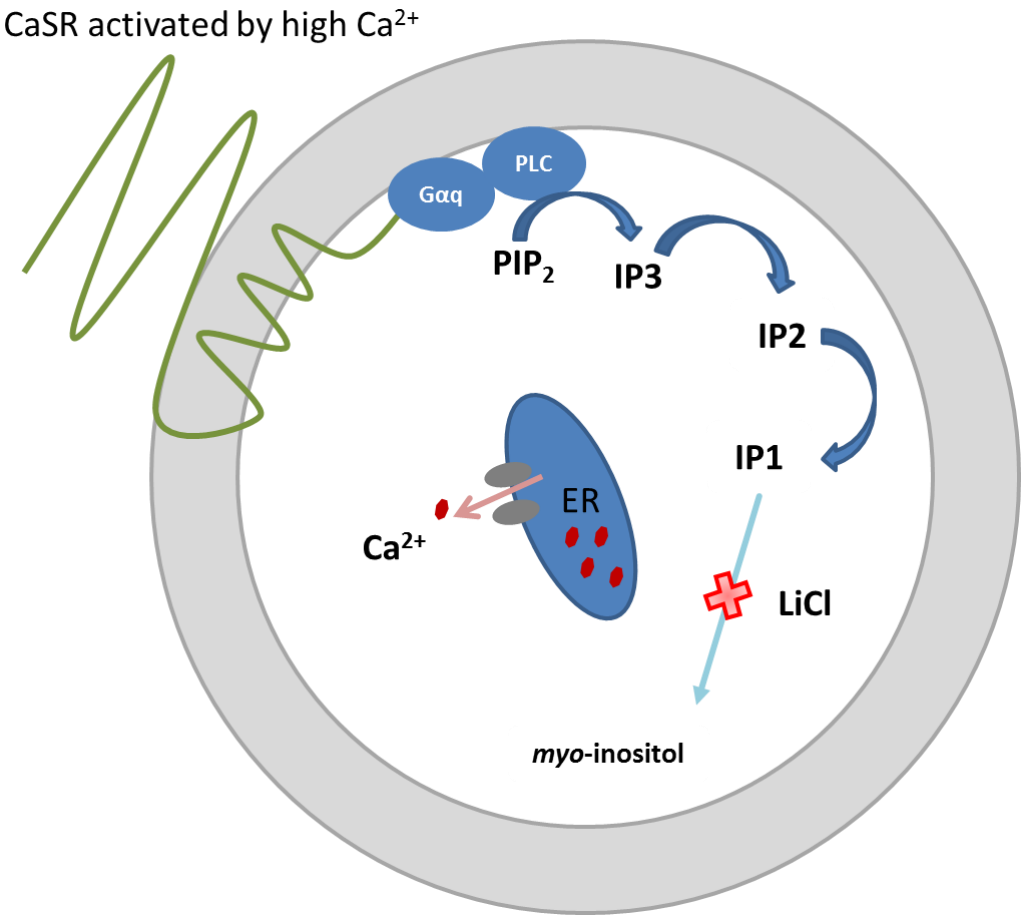

Figure 5.1: Schematic representation of the activation of the CaSR and accumulation of inositol-1-phosphate.

In HEK293-CaSR cells via the CaSR, high Ca^{2+} concentrations stimulate Gαq protein-mediated activation of phospholipase C (PLC). Phospholipase C cleaves phospholipid phosphatidylinositol 4,5-bisphosphate (PIP_2) into diacyl glycerol and inositol 1,4,5-trisphosphate (IP3). IP3 is released into the cytosol and evokes the release of Ca^{2+} from the endoplasmic reticulum (ER) by binding to IP3 receptors. IP3 is transformed extremely rapidly into inositol-1-phosphate (IP1), which in turn degrades to *myo*-inositol. The degradation of IP1 can be inhibited by the addition of lithium chloride to the culture medium. The intracellular accumulation of IP1, which indicates CaSR activation, can then be quantified by ELISA.

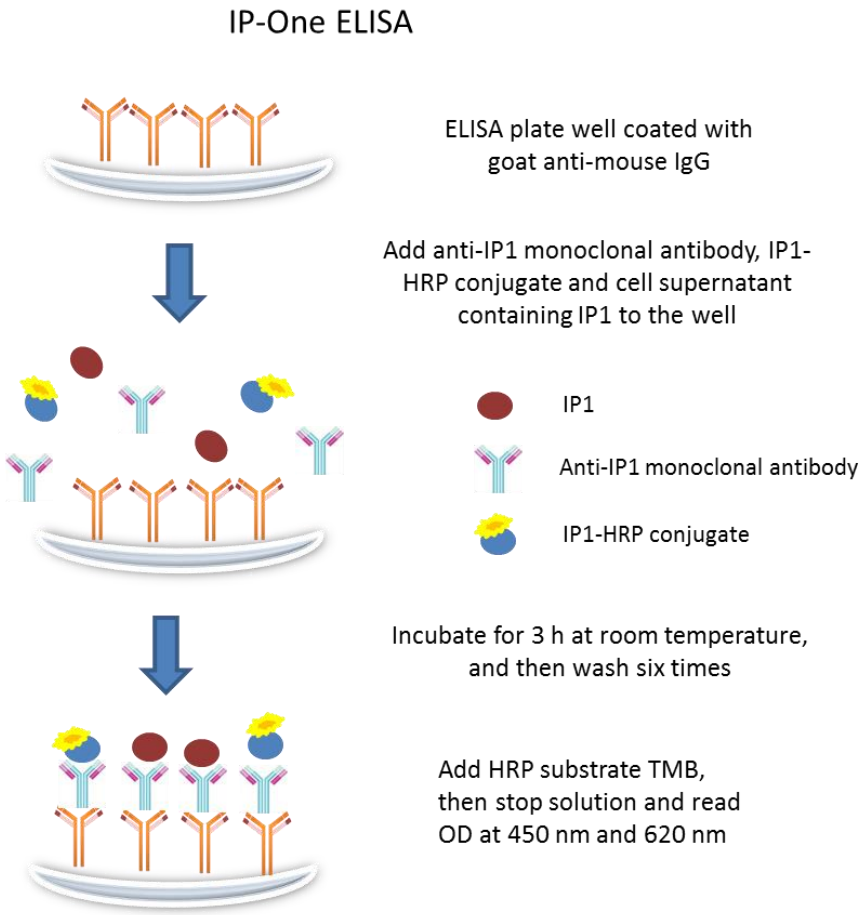

Figure 5.2: Schematic representation of the IP-One ELISA.

The IP-One ELISA is a competitive ELISA for the quantitative determination of inositol-1-phosphate (IP1) based on the competition between free IP1 and IP1 conjugated to horse-radish peroxidase (HRP) for binding to an anti-IP1 monoclonal antibody. After washing to remove unbound IP1 and IP1-HRP, HRP substrate TMB is added, followed by stop solution and the OD of the wells read at 450 nm and 620 nm. As the concentration of IP1 in the cell supernatant increases, then the $OD_{450,}$ which reflects the amount of IP1-HRP conjugate bound, decreases.

5.4 Results

5.4.1 Determination of APS1 patient CaSR antibody titres

APS1 patient antibody titres against identified CaSR epitopes (**Table 5.2**) were determined by testing a series of dilutions from 1:100 to 1:5,000 of patient sera in CaSR peptide ELISAs, as detailed in **Section 5.3.2.** Serum samples from 16, five, six, and seven APS1 patients were analysed in CaSR peptide 41-69, 114-126, 171-195, and 260-340 ELISAs, respectively, this being dependent on the CaSR epitopes recognised by the patient' serum. Sera from 10 healthy individuals were used as controls in each ELISA.

The results of the antibody titration experiments are shown in **Figures 5.3, 5.4, 5.5 and 5.6**, where the antibody index of each APS1 patient serum at each dilution is plotted against the serum dilution. In **Table 5.6,** the titration results are summarised, and show the serum dilution at which antibody reactivity could still be detected at levels above the upper limit of normal in each CaSR peptide ELISA.

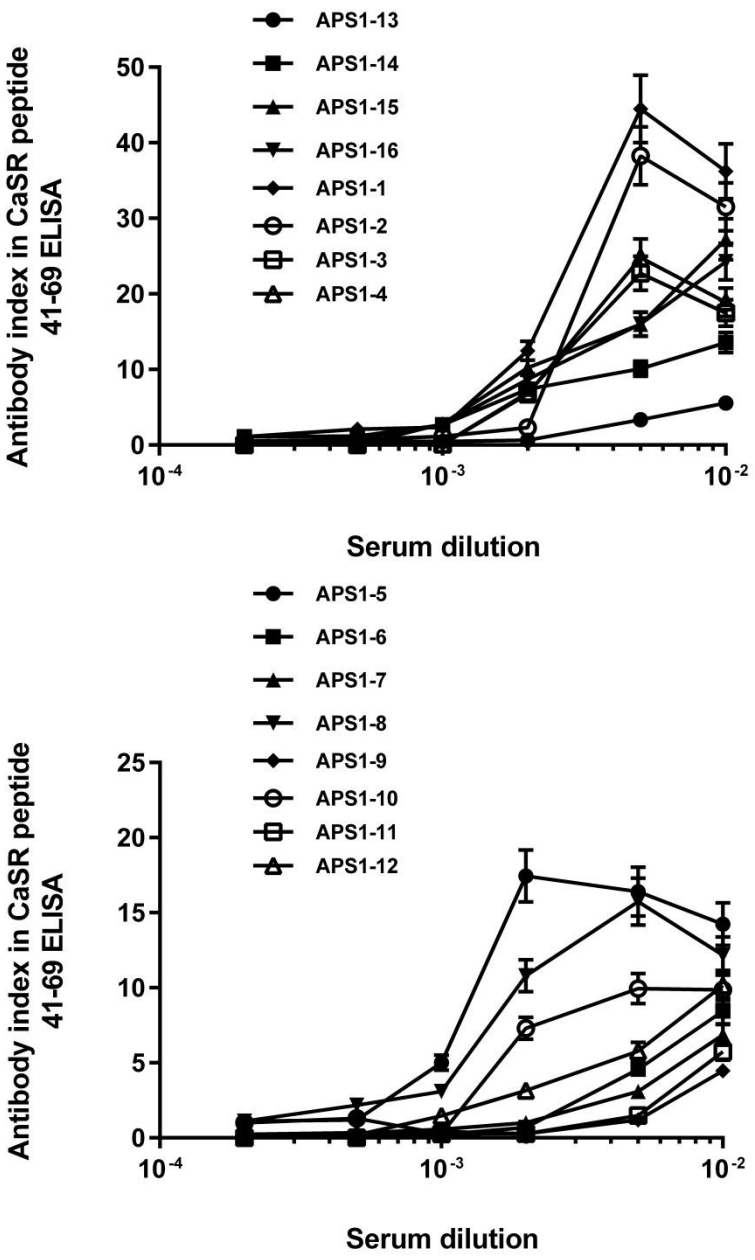

Figure 5.3: Titration of APS1 patient CaSR antibodies against CaSR 41-69 peptide.

Sixteen CaSR antibody-positive APS1 patient sera were analysed at dilutions of 1:100, 1:200, 1:500, 1:1,000, 1:2,000, and 1:5,000 in CaSR peptide 41-69 ELISAs. The antibody index (± SD) of each APS1 patient serum at each dilution is shown and is the mean of three experiments. The upper limit of normal for the CaSR peptide 41-69 ELISA was an antibody index of 2.17.

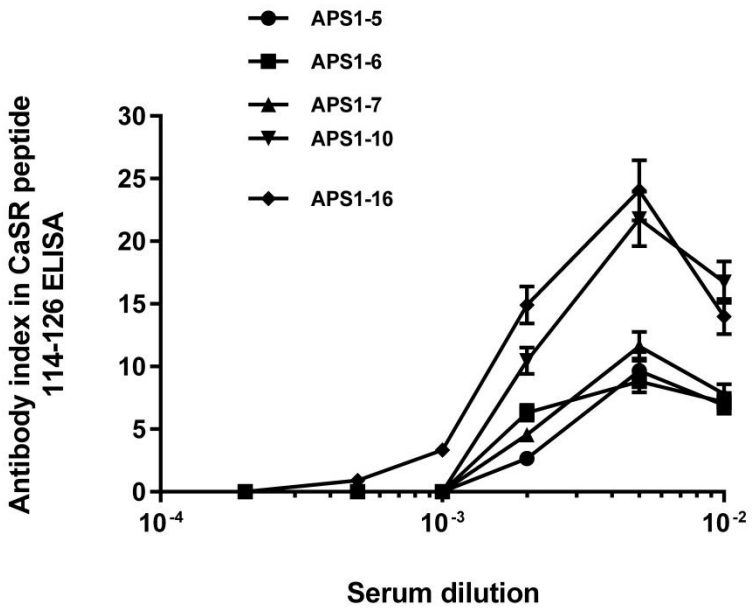

Figure 5.4: Titration of APS1 patient CaSR antibodies against the CaSR 114-126 peptide.

Five CaSR antibody-positive APS1 patient sera were analysed at dilutions of 1:100, 1:200, 1:500, 1:1,000, 1:2,000, and 1:5,000 in CaSR peptide 114-126 ELISAs. The antibody index (± SD) of each APS1 patient serum at each dilution is shown and is the mean of three experiments. The upper limit of normal for the CaSR peptide 114-126 ELISA was an antibody index of 1.91.

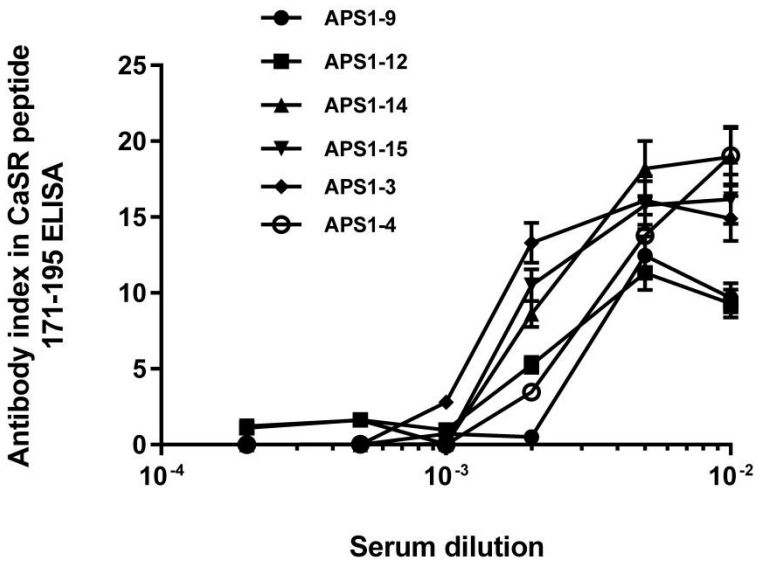

Figure 5.5: Titration of APS1 patient CaSR antibodies against the CaSR 171-195 peptide.

Six CaSR antibody-positive APS1 patient sera were analysed at dilutions of 1:100, 1:200, 1:500, 1:1,000, 1:2,000, and 1:5,000 in CaSR peptide 171-195 ELISAs. The antibody index (± SD) of each APS1 patient serum at each dilution is shown and is the mean of three experiments. The upper limit of normal for the CaSR peptide 171-195 ELISA was an antibody index of 1.96.

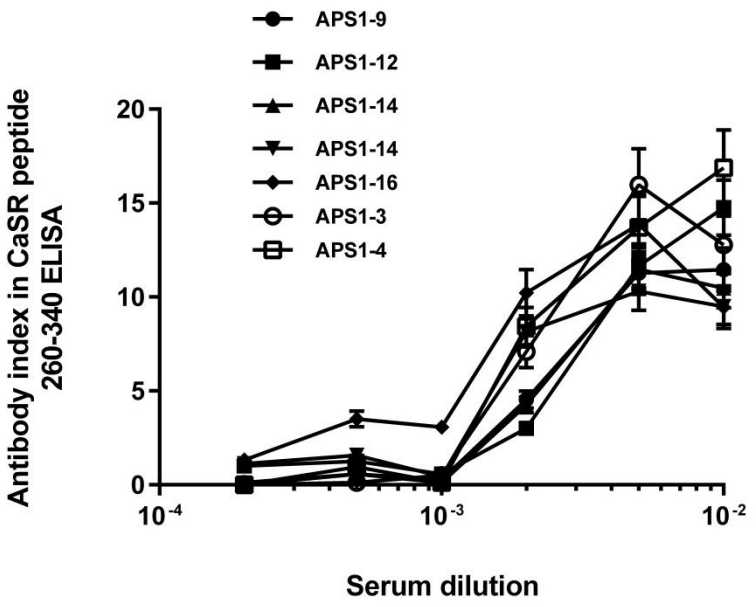

Figure 5.6: Titration of APS1 patient CaSR antibodies against the CaSR 260-340 peptide.

Seven CaSR antibody-positive APS1 patient sera were analysed at dilutions of 1:100, 1:200, 1:500, 1:1,000, 1:2,000, and 1:5,000 in CaSR peptide 260-340 ELISAs. The antibody index (± SD) of each APS1 patient serum at each dilution is shown and is the mean of three experiments. The upper limit of normal for the CaSR peptide 260-340 ELISA was an antibody index of 1.87.

Table 5.6: Summary of titration of APS1 patient autoantibodies against CaSR epitopes

APS1 patient	CaSR 41-69 antibody titre[1]	CaSR 114-126 antibody titre[1]	CaSR 171-195 antibody titre[1]	CaSR 260-340 antibody titre[1]
APS1-1	1:1000	-	-	-
APS1-2	1:500	-	-	-
APS1-3	1:500	-	1:1000	1:500
APS1-4	1:500	-	1:500	1:500
APS1-5	1:1000	1:500	-	-
APS1-6	1:200	1:500	-	-
APS1-7	1:200	1:500	-	-
APS1-8	1:1000	-	-	-
APS1-9	1:100	-	1:200	1:500
APS1-10	1:500	1:500	-	-
APS1-11	1:100	-	-	-
APS1-12	1:500	-	1:500	1:500
APS1-13	1:200	-	-	-
APS1-14	1:1000	-	1:500	1:500
APS1-15	1:1000	-	1:500	1:500
APS1-16	1:1000	1:1000	-	1:2000

[1]Each antibody titre is given as the dilution at which immunoreactivity in the serum sample could still be detected at levels above the upper limit of normal in the CaSR peptide ELISA. The upper limits of normal were CaSR autoantibody indices of 2.17, 1.91, 1.96, and 1.87 for CaSR peptides 41-69, 114-126, 171-195, and 260-340, respectively.
[2]-, denotes negative for CaSR autoantibodies.

5.4.2 Determination of APS1 patient CaSR antibody specificity

The specificity of APS1 patient CaSR antibodies was evaluated using absorption experiments, as detailed in **Section 5.3.3**. Sera from 16, five, six, and seven APS1 patients were pre-absorbed with CaSR peptides 41-69, 114-126, 171-195, and 260-340, respectively, this being dependent on the CaSR epitopes recognised by the patient' serum. As a control, a melanin-concentrating hormone receptor 1 (MCHR1) peptide was also used to pre-absorbed sera. Following pre-absorption, the CaSR antibody-binding of each of the sera was assessed in the relevant CaSR peptide ELISA, along with unabsorbed APS1 patient sera and unabsorbed sera from six healthy controls.

The results of the absorption experiments are given in **Figures 5.7, 5.8, 5.9 and 5.10**, where the antibody index of each patient serum is shown in relation to the peptide used in pre-absorption. When comparing the antibody index of unabsorbed *versus* pre-absorbed patient sera in CaSR peptide ELISAs, CaSR antibody-binding was significantly reduced by pre-absorption of APS1 patient sera with the corresponding CaSR peptide: all *P* values (two-tailed) were < 0.05 (Student's paired *t* test). In contrast, there was no significant decrease in CaSR antibody-binding following pre-absorption with either non-corresponding CaSR peptides or the MCHR1 peptide: all *P* values (two tailed) were > 0.05 (Student's paired *t* test) when comparing the antibody index of unabsorbed *versus* pre-absorbed APS1 patient sera. Overall, the results indicated that patient CaSR antibodies recognised specific CaSR epitopes and were not cross-reactive with other antibody binding sites on the receptor.

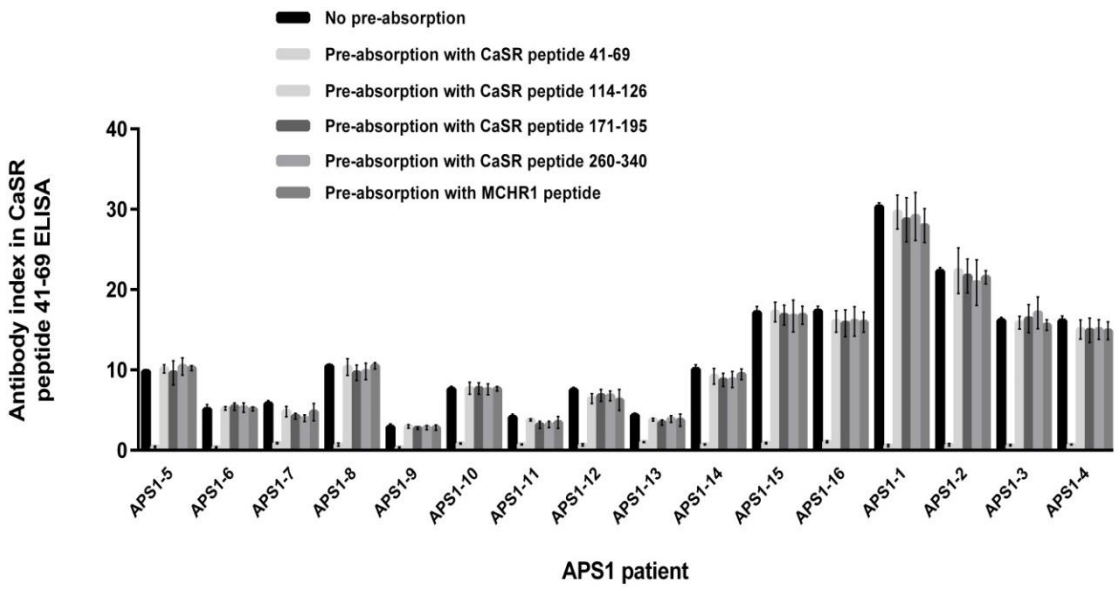

Figure 5.7: Absorption of APS1 patient CaSR antibodies with CaSR peptides prior to analysis in CaSR peptide 41-69 ELISA.

Sixteen CaSR antibody-positive APS1 patient sera were pre-absorbed with an excess of CaSR peptide before analysis in the CaSR peptide 41-69 ELISA. A melanin-concentrating hormone receptor 1 (MCHR1) peptide was used as a pre-absorption control peptide. The antibody index (± SD) of each APS1 patient serum is shown, and is the mean of three experiments. The antibody index of each patient sera pre-absorbed with CaSR peptide 41-69 was significantly reduced compared with unabsorbed sera. All *P* values (two-tailed) were < 0.05 (Student's paired *t* test): APS1-1, APS1,-2, APS1-3, < 0.0001; APS1-4, 0.0050; APS1-5, 0.0002; APS1-6, 0.0038; APS1-7, 0.0016; APS1-8, 0.0004; APS1-9, 0.0085; APS1-10, 0.0007; APS1-11, 0.0036; APS1-12, 0.0005; APS1-13, 0.0025; APS1-14, 0.0010; APS1-15, 0.0006; and APS1-16, 0.0003.There was no significant decrease in CaSR antibody-binding following pre-absorption with either non-corresponding CaSR peptides or the MCHR1 peptide: all *P* values (two tailed) were > 0.05 (Student's paired *t* test) when comparing the antibody index of unabsorbed *versus* pre-absorbed APS1 patient sera.

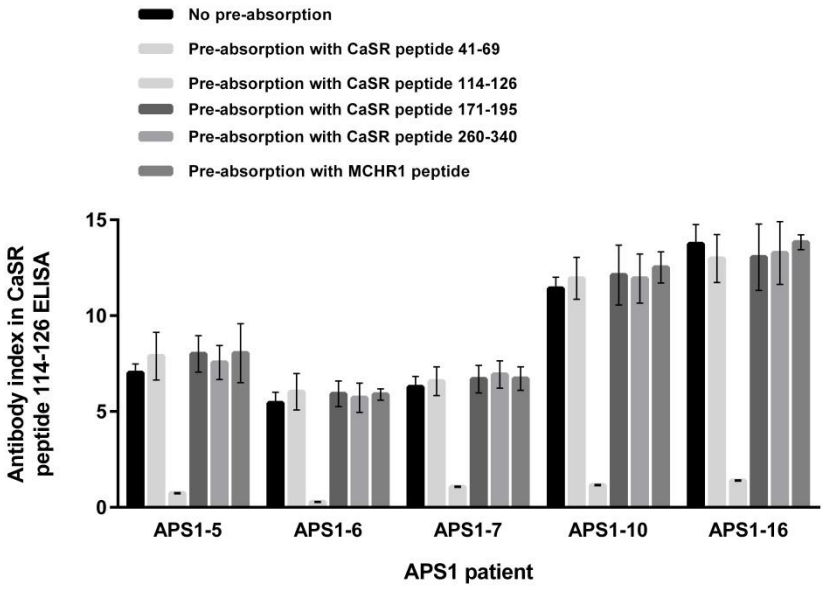

Figure 5.8: Absorption of APS1 patient CaSR antibodies with CaSR peptides prior to analysis in CaSR peptide 114-126 ELISA.

Five CaSR antibody-positive APS1 patient sera were pre-absorbed with an excess of CaSR peptide before analysis in the CaSR peptide 114-126 ELISA. A melanin-concentrating hormone receptor 1 (MCHR1) peptide was used as a pre-absorption control peptide. The antibody index (± SD) of each APS1 patient serum is shown, and is the mean of three experiments. The antibody index of each patient sera pre-absorbed with CaSR peptide 114-126 was significantly reduced compared with unabsorbed sera. All *P* values (two-tailed) were < 0.05 (Student's paired *t* test): APS1-5, 0.0028; APS1-6, 0.0040; APS1-7, 0.0036; APS1-10, 0.0011; and APS1-16, 0.0023. There was no significant decrease in CaSR antibody-binding following pre-absorption with either non-corresponding CaSR peptides or the MCHR1 peptide: all *P* values (two tailed) were > 0.05 (Student's paired *t* test) when comparing the antibody index of unabsorbed *versus* pre-absorbed APS1 patient sera.

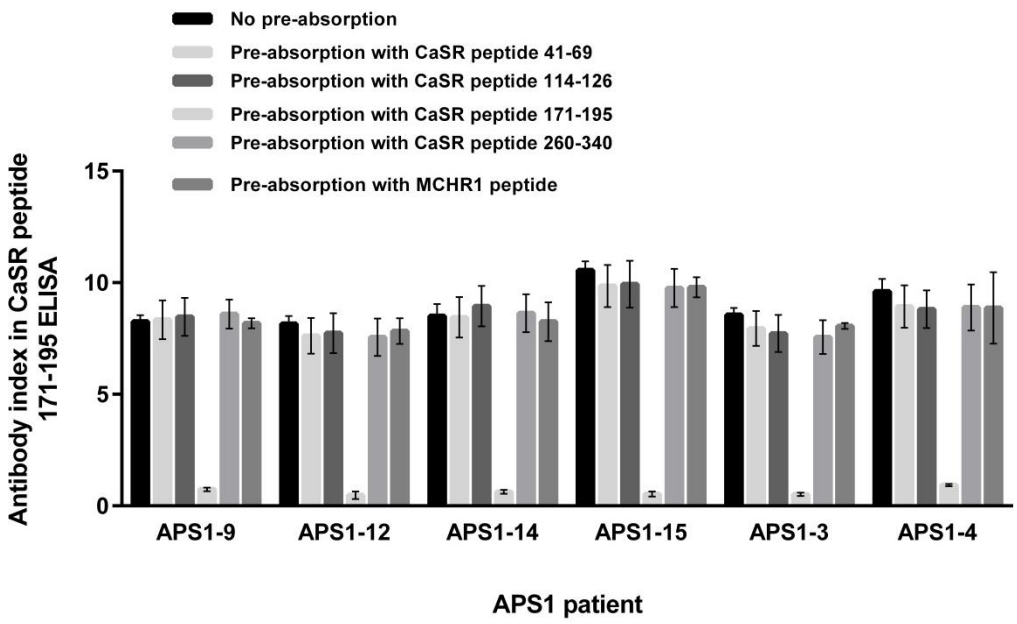

Figure 5.9: Absorption of APS1 patient CaSR antibodies with CaSR peptides prior to analysis in CaSR peptide 171-195 ELISA.

Six CaSR antibody-positive APS1 patient sera were pre-absorbed with an excess of CaSR peptide before analysis in the CaSR peptide 171-195 ELISA. A melanin-concentrating hormone receptor 1 (MCHR1) peptide was used as a pre-absorption control peptide. The antibody index (± SD) of each APS1 patient serum is shown, and is the mean of three experiments. The antibody index of each patient sera pre-absorbed with CaSR peptide 171-195 was significantly reduced compared with unabsorbed sera. All *P* values (two-tailed) were < 0.05 (Student's paired *t* test): APS1-3, 0.0004; APS1-4, 0.0017; APS1-9, 0.0007; APS1-10, 0.0010; APS1-14, 0.0019; and APS1-15, 0.0008. There was no significant decrease in CaSR antibody-binding following pre-absorption with either non-corresponding CaSR peptides or the MCHR1 peptide: all *P* values (two tailed) were > 0.05 (Student's paired *t* test) when comparing the antibody index of unabsorbed *versus* pre-absorbed APS1 patient sera.

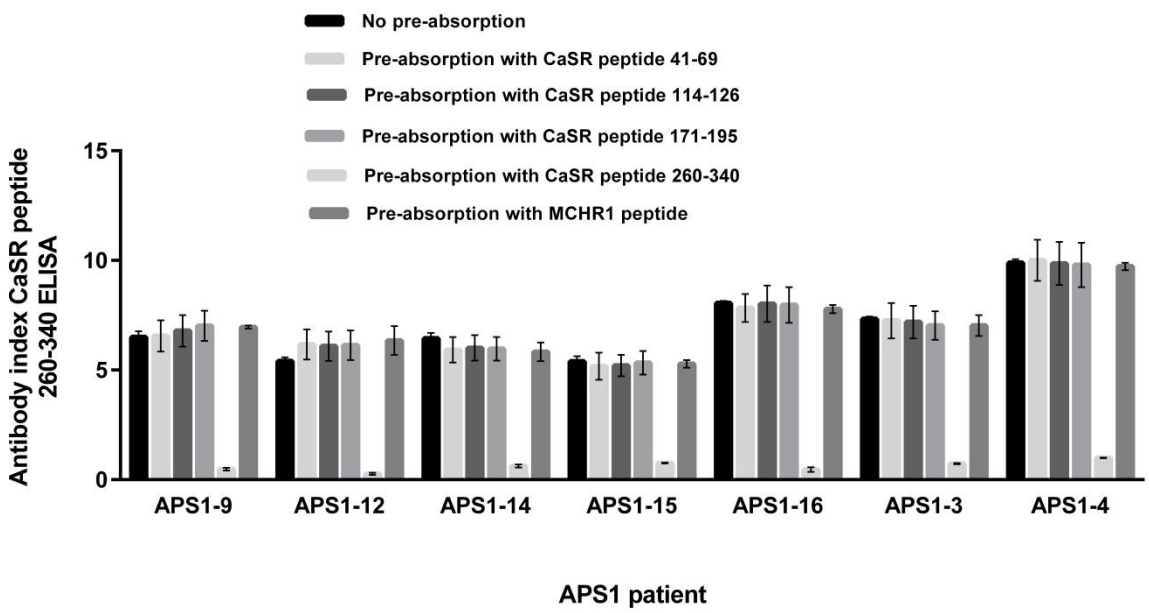

Figure 5.10: Absorption of APS1 patient CaSR antibodies with CaSR peptides prior to analysis in CaSR peptide 260-340 ELISA.

Seven CaSR antibody-positive APS1 patient sera were pre-absorbed with an excess of CaSR peptide before analysis in the CaSR peptide 260-340 ELISA. A melanin-concentrating hormone receptor 1 (MCHR1 peptide) was used as a pre-absorption control peptide. The antibody index (± SD) of each APS1 patient serum is shown, and is the mean of three experiments. The antibody index of each patient sera pre-absorbed with CaSR peptide 171-195 was significantly reduced compared with unabsorbed sera. All *P* values (two-tailed) were < 0.05 (Student's paired *t* test): APS1-3, 0.0001; APS1-4, < 0.0001; APS1-9, 0.0008; APS1-12, 0.0005; APS1-14, 0.0003; APS1-15, 0.0010; and APS1-16, 0.0002. There was no significant decrease in CaSR antibody-binding following pre-absorption with either non-corresponding CaSR peptides or the MCHR1 peptide: all *P* values (two tailed) were > 0.05 (Student's paired *t* test) when comparing the antibody index of unabsorbed *versus* pre-absorbed APS1 patient sera.

5.4.3 Determination of APS1 patient CaSR antibody functional affinity

APS1 patient CaSR antibody functional affinity was evaluated as detailed in **Section 5.3.4**. Sera from 16, five, six, and seven APS1 patients were pre-incubated with a range of concentrations (0-1000 nM) of CaSR peptides 41-69, 114-126, 171-195, and 260-340, respectively, this being dependent on the CaSR epitopes recognised by the patient' serum. Following pre-incubation, the CaSR antibody-binding of each of the APS1 patient sera was assessed in the relevant CaSR peptide ELISA, along with sera from six healthy controls which had not been pre-incubated with any peptide.

The results of the functional affinity experiments are shown in **Figures 5.11, 5.12, 5.13 and 5.14**, where the antibody index of each patient serum in the CaSR peptide ELISAs is plotted against the CaSR peptide concentration used in the pre-incubation step. From the graphs, the antibody index representing a 50% decrease in binding of sera in the CaSR peptide ELISAs was used to estimate the molar concentration of peptide that resulted in this 50% reduction. In **Table 5.7**, the functional affinity for each APS1 patient sera with each relevant CaSR peptide are summarised.

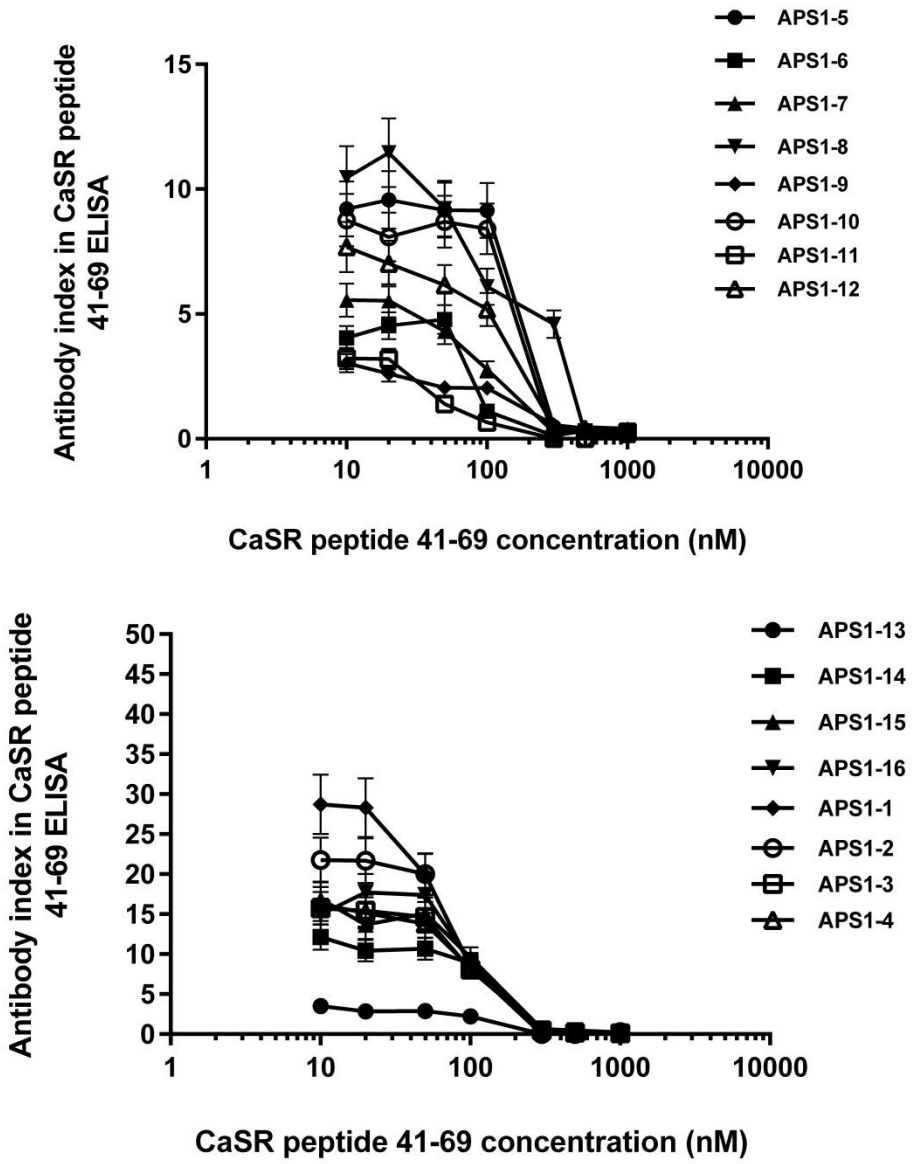

Figure 5.11: Functional affinity of APS1 patient CaSR antibodies against CaSR peptide 41-69.

Sixteen CaSR antibody-positive APS1 patient sera were pre-incubated with 0-1000 nM of CaSR peptide 41-69 before analysis in CaSR peptide 41-69 ELISAs. The antibody index (± SD) of each APS1 patient serum is shown, and is the mean of three experiments.

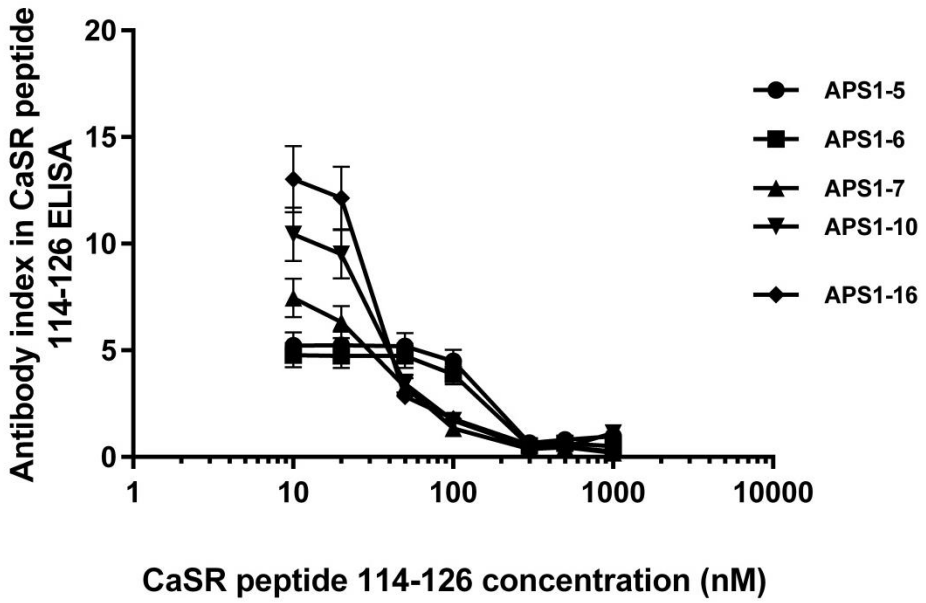

Figure 5.12: Functional affinity of APS1 patient CaSR antibodies against CaSR peptide114-126.

Five CaSR antibody-positive APS1 patient sera were pre-incubated with 0-1000 nM of CaSR peptide 114-126 before analysis in CaSR peptide 114-126 ELISAs. The antibody index (± SD) of each APS1 patient serum is shown, and is the mean of three experiments.

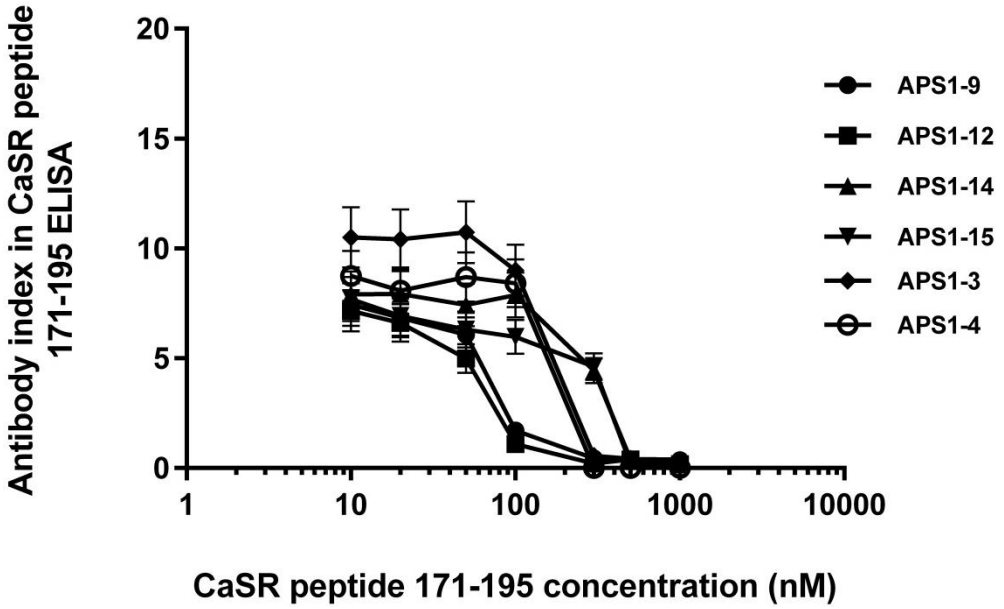

Figure 5.13: Functional affinity of APS1 patient CaSR antibodies against CaSR peptide 171-195.

Six CaSR antibody-positive APS1 patient sera were pre-incubated with 0-1000 nM of CaSR peptide 171-195 before analysis in CaSR peptide 171-195 ELISAs. The antibody index (± SD) of each APS1 patient serum is shown, and is the mean of three experiments.

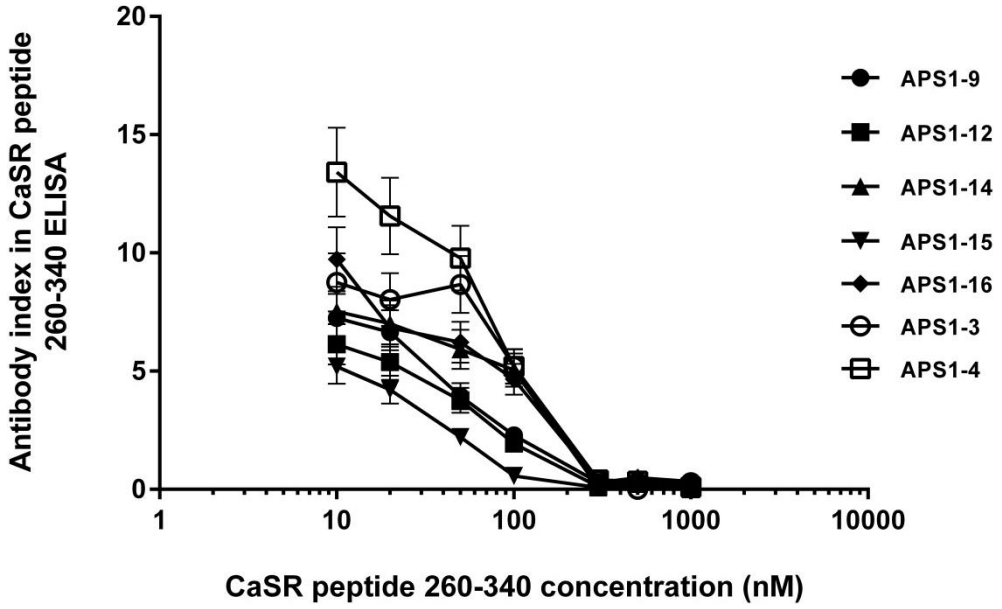

Figure 5.14: Functional affinity of APS1 patient CaSR antibodies against CaSR peptide 260-340.

Seven CaSR antibody-positive APS1 patient sera were pre-incubated with 0-1000 nM of CaSR peptide 260-340 before analysis in CaSR peptide 260-340 ELISAs. The antibody index (± SD) of each APS1 patient serum is shown, and is the mean of three experiments.

Table 5.7: Functional affinity of APS1 patient CaSR antibodies

APS1 patient	Functional affinity (M)[1]			
	CaSR 41-69 antibody	CaSR 114-126 antibody	CaSR 171-195 antibody	CaSR 260-340 antibody
APS1-1	7.50×10^{-08}	-	-	-
APS1-2	1.00×10^{-07}	-	-	-
APS1-3	1.00×10^{-07}	-	2.50×10^{-07}	1.50×10^{-07}
APS1-4	1.00×10^{-07}	-	2.50×10^{-07}	1.50×10^{-07}
APS1-5	2.50×10^{-07}	2.00×10^{-07}	-	-
APS1-6	9.00×10^{-08}	2.00×10^{-07}	-	-
APS1-7	1.50×10^{-07}	5.00×10^{-08}	-	-
APS1-8	3.00×10^{-07}	-	-	-
APS1-9	2.00×10^{-07}	-	8.00×10^{-08}	7.50×10^{-08}
APS1-10	2.50×10^{-07}	4.00×10^{-08}	-	-
APS1-11	4.00×10^{-08}	-	-	-
APS1-12	1.50×10^{-07}	-	7.50×10^{-08}	7.20×10^{-08}
APS1-13	1.50×10^{-07}	-	-	-
APS1-14	2.00×10^{-07}	-	3.50×10^{-07}	7.50×10^{-08}
APS1-15	2.00×10^{-07}	-	3.50×10^{-07}	5.00×10^{-08}
APS1-16	2.00×10^{-07}	4.00×10^{-08}	-	1.50×10^{-07}

[1]Antibody functional affinity is given as the molar concentration of peptide that resulted in a 50% reduction of antibody binding as represented by the antibody index of the sera.

5.4.4 Determination of APS1 patient CaSR antibody IgG subclass

APS1 patient CaSR antibody subclass was evaluated as detailed in **Section 5.3.5**. Sera from 16 APS1 patients and from 10 healthy controls were analysed in CaSR peptide ELISAs with IgG subclass-specific secondary antibodies being used to detect the binding of patient CaSR antibodies**.** The results of the CaSR peptide ELISAs are given in **Figure 5.15**, where the antibody index of each patient and control serum is shown. For each ELISA, the mean antibody index of the APS1 patient and control groups, the antibody index range of the APS1 patient and control groups, the intra- and inter-assay coefficients of variation, and the upper limit of normal are summarised in **Table 5.8**.

All control sera were negative for antibody binding, as their antibody indices were below the upper limits of normal for each ELISA (**Table 5.8**). In the APS1 patient group, some sera had an antibody index above the upper limit of normal in certain IgG subclass ELISAs and so were considered positive for antibody binding (**Table 5.8**). From the results of the IgG subclass ELISAs, the IgG subclasses of APS1 patient CaSR antibodies were determined and these are summarised in **Table 5.9**. In all APS1 patients, antibodies against the CaSR epitopes 41-69, 171-195, and 260-340 were of the IgG1 subclass. Antibody responses against CaSR epitope 114-126 were of the IgG1 and IgG3 subclasses.

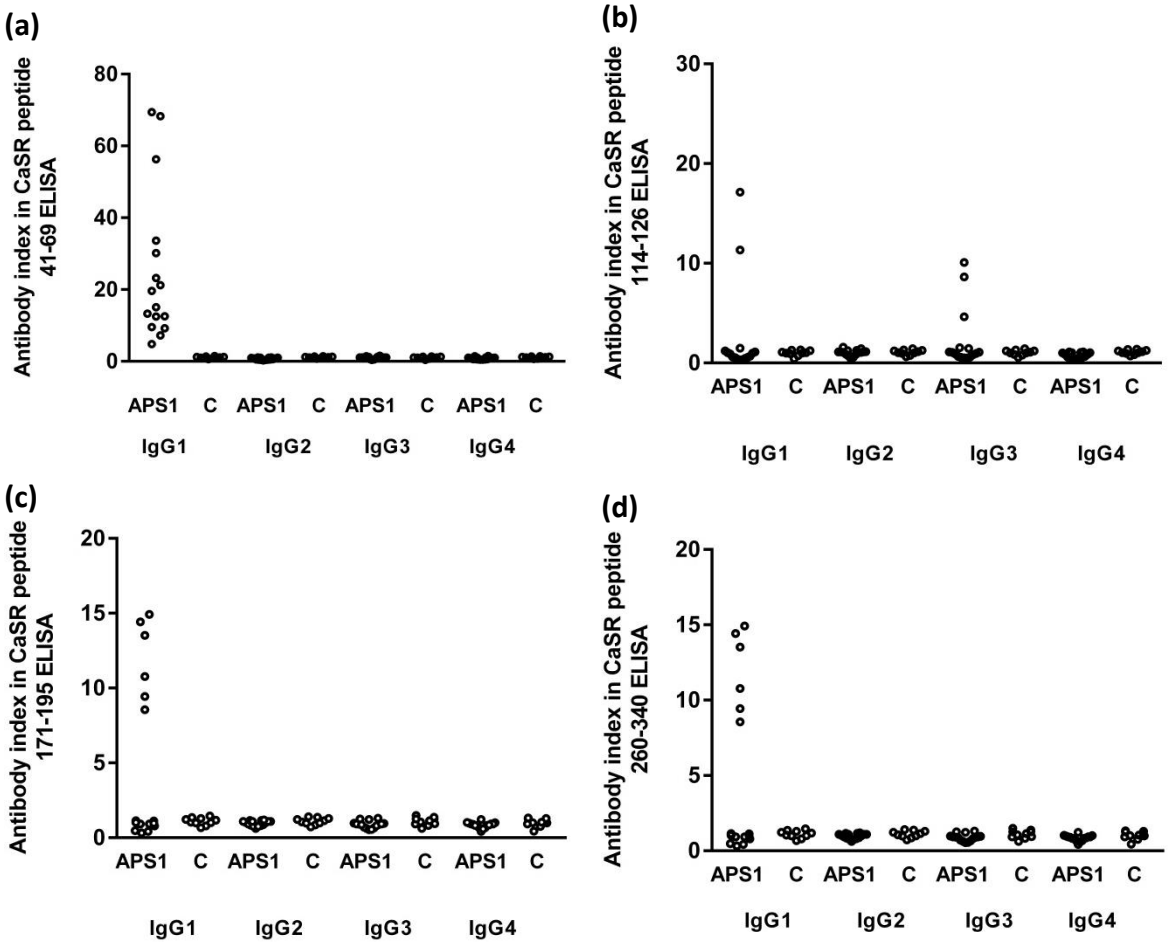

Figure 5.15: IgG subclass of APS1 patient CaSR antibodies against CaSR peptides

Sixteen CaSR antibody-positive APS1 patient sera and 10 healthy control (C) sera at a dilution of 1:100 were analysed in CaSR peptide ELISAs and IgG subclass-specific secondary antibodies. The antibody index is shown for each serum, and is the mean of three experiments. The results are shown for **(a)** CaSR peptide ELISAs with peptide 41-69; **(b)** CaSR peptide ELISAs with peptide114-126; **(c)** CaSR peptide ELISAs with peptide 171-195; and **(d)** CaSR peptide ELISAs with peptide 260-340.

Table 5.8: Summary of data from CaSR peptide IgG subclass ELISAs

CaSR peptide IgG subclass ELISA	Mean antibody index (± SD) of APS1 patient group (*n* = 16)	Antibody index range of APS1 patient group	Mean antibody index (± SD) of control group (*n* = 10)	Antibody index range of healthy control group	Upper limit of normal antibody index	Intra-assay coefficient of variation	Inter-assay coefficient of variation	Antibody positive APS1 patients (%)	Antibody positive controls (%)
41-69 IgG1	25.4 ± 21.1	4.81-69.4	1.08 ± 0.26	0.60-1.47	1.86	5.1%	9.3%	16/16 (100)	0/10 (0)
41-69 IgG2	0.74 ± 0.28	0.29-1.10	1.12 ± 0.22	0.74-1.42	1.78	3.8%	8.4%	0/16 (0)	0/10 (0)
41-69 IgG3	1.02 ± 0.29	0.41-1.56	1.03 ± 0.27	0.46-1.35	1.84	5.5%	7.3%	0/16 (0)	0/10 (0)
41-69 IgG4	0.87 ± 0.32	0.50-1.52	1.11 ± 0.25	0.67-1.46	1.85	3.2%	8.9%	0/16 (0)	0/10 (0)
114-126 IgG1	2.45 ± 4.74	0.32-17.1	1.00 ± 0.27	0.74-1.32	1.81	4.7%	10.1%	2/16 (12.5)	0/10 (0)
114-126 IgG2	1.04 ± 0.29	0.43-1.58	1.08 ± 0.25	0.76-1.43	1.82	5.3%	9.4%	0/16 (0)	0/10 (0)
114-126 IgG3	2.20 ± 2.97	0.51-10.1	1.05 ± 0.26	0.57-1.44	1.83	3.6%	8.2%	3/16 (18.8)	0/10 (0)
114-126 IgG4	0.76 ± 0.28	0.31-1.11	1.09 ± 0.22	0.71-1.39	1.75	4.7%	6.7%	0/16 (0)	0/10 (0)
171-195 IgG1	4.99 ± 5.78	0.43-14.9	1.10 ± 0.25	0.67-1.46	1.85	4.2%	9.3%	6/16 (38)	0/10 (0)
171-195 IgG2	0.97 ± 0.17	0.62-1.16	1.11 ± 0.22	0.73-1.41	1.78	4.8%	10.4%	0/16 (0)	0/10 (0)
171-195 IgG3	0.88 ± 0.23	0.54-1.31	1.09 ± 0.27	0.62-1.49	1.89	5.3%	9.2%	0/16 (0)	0/10 (0)
171-195 IgG4	0.85 ± 0.19	0.42-1.23	1.01 ± 0.27	0.44-1.33	1.82	5.7%	9.9%	0/16 (0)	0/10 (0)
260-340 IgG1	9.19 ± 9.92	0.41-25.0	1.02 ± 0.22	0.64-1.32	1.69	2.6%	6.4%	7/16 (44)	0/10 (0)
260-340 IgG2	0.92 ± 0.19	0.60-1.28	1.00 ± 0.27	0.53-1.40	1.80	3.4%	6.5%	0/16 (0)	0/10 (0)
260-340 IgG3	0.83 ± 0.14	0.63-1.14	0.92 ± 0.27	0.35-1.24	1.73	4.1%	5.1%	0/16 (0)	0/10 (0)
260-340 IgG4	0.86 ± 0.15	0.51-1.03	1.01 ± 0.25	0.58-1.37	1.76	3.3%	7.7%	0/16 (0)	0/10 (0)

Table 5.9: IgG subclasses of APS1 patient CaSR antibodies

APS1 patient	Antibody reactivity in CaSR peptide 41-69 ELISA[1]	IgG subclass	Antibody reactivity in CaSR peptide 114-126 ELISA[1]	IgG subclass	Antibody reactivity in CaSR peptide 171-195 ELISA[1]	IgG subclass	Antibody reactivity in CaSR peptide 260-340 ELISA[1]	IgG Subclass
APS1-1	+	IgG1	-	-	-	-	-	-
APS1-2	+	IgG1	-	-	-	-	-	-
APS1-3	+	IgG1	-	-	+	IgG1	+	IgG1
APS1-4	+	IgG1	-	-	+	IgG1	+	IgG1
APS1-5	+	IgG1	+	IgG1	-	-	-	-
APS1-6	+	IgG1	+	IgG1	-	-	-	-
APS1-7	+	IgG1	+	IgG3	-	-	-	-
APS1-8	+	IgG1	-	-	-	-	-	-
APS1-9	+	IgG1	-	-	+	IgG1	+	IgG1
APS1-10	+	IgG1	+	IgG3	-	-	-	-
APS1-11	+	IgG1	-	-	-	-	-	-
APS1-12	+	IgG1	-	-	+	IgG1	+	IgG1
APS1-13	+	IgG1	-	-	-	-	-	-
APS1-14	+	IgG1	-	-	+	IgG1	+	IgG1
APS1-15	+	IgG1	-	-	+	IgG1	+	IgG1
APS1-16	+	IgG1	+	IgG3	-	-	+	IgG1

[1]+, denotes positive for CaSR antibody reactivity; -, denotes negative for CaSR antibody reactivity.

5.4.5 Effect of APS1 patient IgG on the response of the CaSR to Ca^{2+}-stimulation

The results of Ca^{2+}-stimulation on HEK293-CaSR and HEK293 cells are shown in **Figure 5.16**. A response to Ca^{2+}-stimulation was only detected in HEK293-CaSR cells where IP1 accumulated with increasing Ca^{2+} concentrations up to an estimated concentration of 5.0 mM.

To determine the effects of IgG from APS1 patients (*n* = 16) and healthy controls (*n* = 10) on CaSR function, HEK293-CaSR cells were pre-incubated with IgG at a 1:100 dilution prior to stimulation with Ca^{2+} concentrations of 0.0, 0.5, 1.5, 3.0, 6.0 and 9.0 mM. Each experiment also included HEK293-CaSR cells without pre-incubation with IgG. Subsequently, IP1 accumulation was measured using an IP-One ELISA Kit and the percentage inhibition of IP1-HRP conjugate binding calculated, as detailed in **Section 5.3.8**. The results of pre-incubation of HEK293-CaSR cells with APS1 patient and control IgG samples are shown in **Figures 5.17, 5.18, 5.19 and 5.20**, where IP1 accumulation is plotted against Ca^{2+} concentration.

The percentage inhibition of the binding of the IP1-HRP conjugate, which reflects increasing amounts of IP1 in the HEK293-CaSR cell supernatants, were compared between Ca^{2+}-stimulated and unstimulated cells using Student's paired t tests. *P* values < 0.05 were considered significant. Of the 10 control IgG samples analysed, none had any statistically significant effect upon IP1 accumulation in HEK293-CaSR cells when compared with stimulation by Ca^{2+} alone: *P* values (two-tailed) were > 0.05. The same results were obtained for the effects of 12/16 of the APS1 patient IgG samples tested: there was no statistically significant increase in IP1 accumulation with all *P* values (two-tailed) were > 0.05. In contrast, IgG samples from four APS1 patients (APS1-5, APS1-9, APS1-11, and APS1-16) statistically significantly increased IP1 accumulation at Ca^{2+} concentrations of 0.5, 1.5 and 3.0 mM when compared with Ca^{2+}-stimulation alone: *P* values (two-tailed) were < 0.0001. The results indicated the presence of CaSR-stimulating activity in these four APS1 patient IgG samples. However, when Ca^{2+} was not present, the IgG samples from these four patients had no effect upon IP1 accumulation, indicating that some degree of receptor activation was needed to see the functional effect of the antibodies.

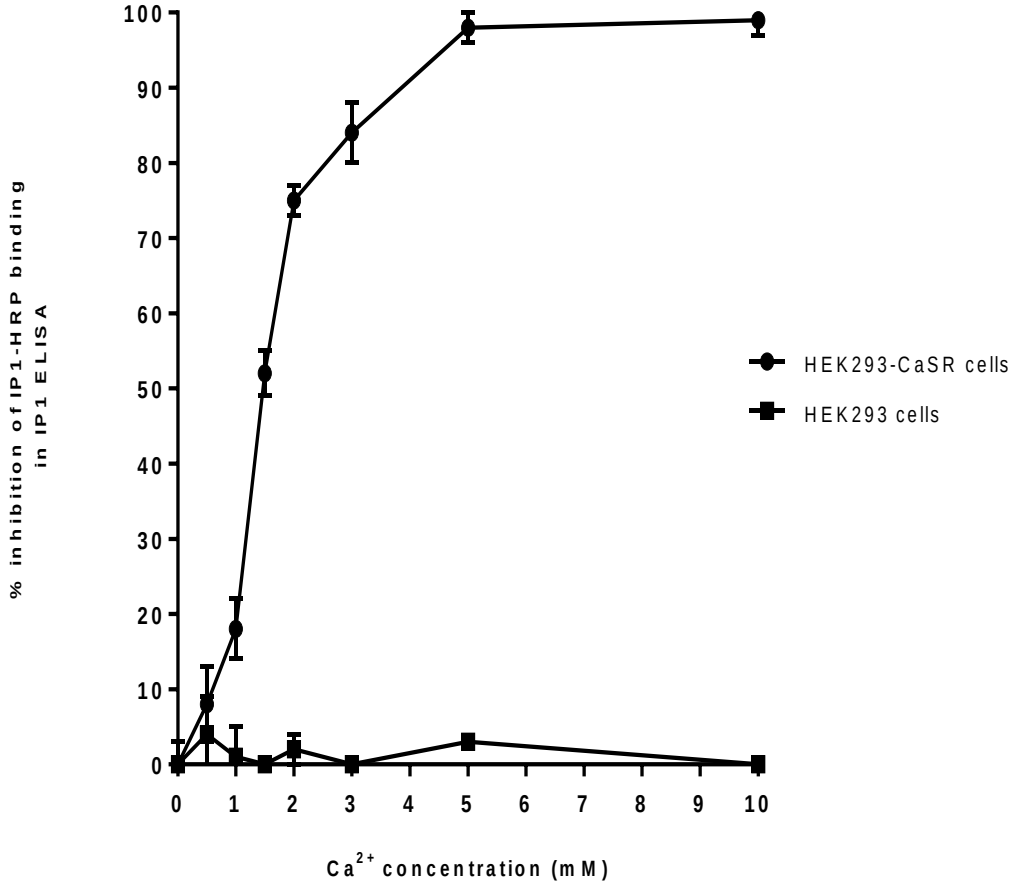

Figure 5.16: Measuring the effect of Ca^{2+}-stimulation on the CaSR.

HEK293-CaSR and HEK293 cells were treated with Ca^{2+} at 0.0, 0.5, 1.0, 1.5, 2.0, 3.0, 5.0 and 10.0 mM. Intracellular IP1 accumulation was then measured in an IP-One ELISA. The results show the mean percentage (±SD) inhibition of IP1-HRP conjugate binding from three experiments.

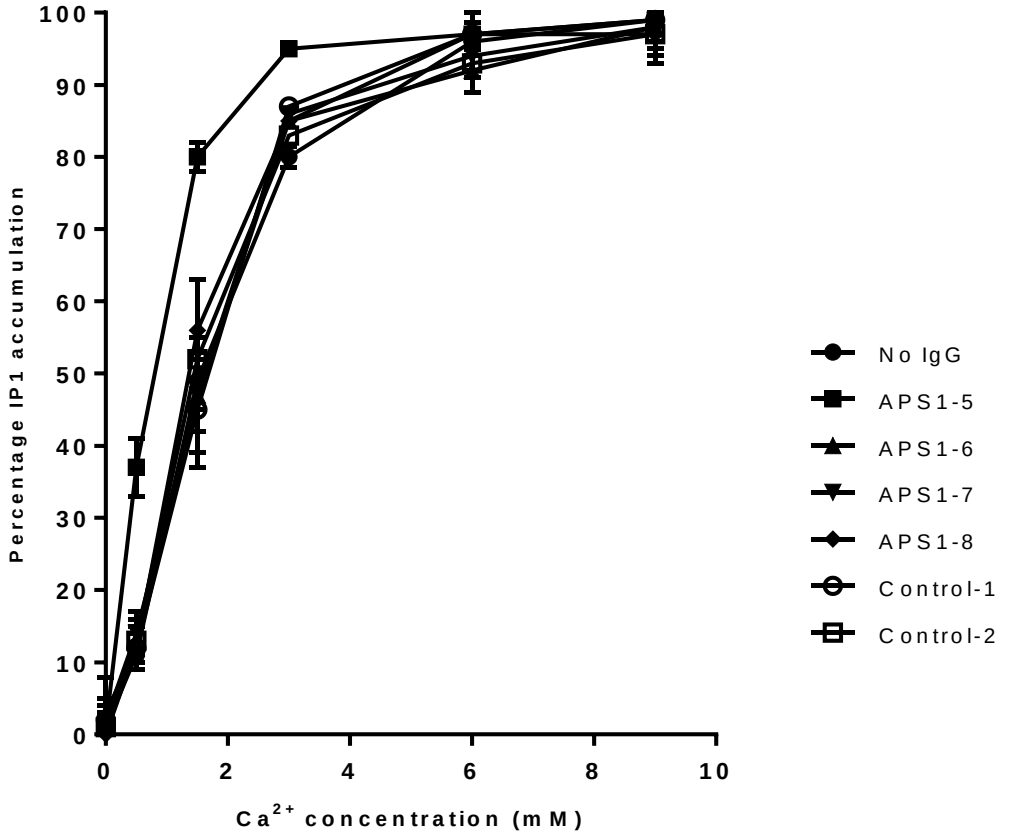

Figure 5.17: Effect of APS1 patient and control IgG on the response of the CaSR to Ca^{2+}-stimulation-1.

HEK293-CaSR cells were pre-incubated with IgG samples at a 1:100 dilution from APS1 patient (n = 16) and healthy controls (n = 10) prior to treatment with Ca^{2+} at 0.0, 0.5, 1.5, 3.0, 6.0 and 9.0 mM. Intracellular IP1 accumulation was then measured in an IP-One ELISA. The results show the mean percentage (±SD) inhibition of IP1-HRP conjugate binding from three experiments for two control and four APS1 patient IgG samples. Both controls and three of the APS1 patient IgG samples had no statistically significant effect upon IP1 accumulation in HEK293-CaSR cells when compared with cells stimulated by Ca^{2+} alone: all P values were > 0.05 (Student's paired t test). IgG samples from one APS1 patients (APS1-5) statistically significantly increased IP1 accumulation at Ca^{2+} concentrations of 0.5 mM (P = 0.0034), 1.5 mM (P = 0.0092) and 3.0 mM (P = 0.0021) when compared with Ca^{2+}-stimulation alone.

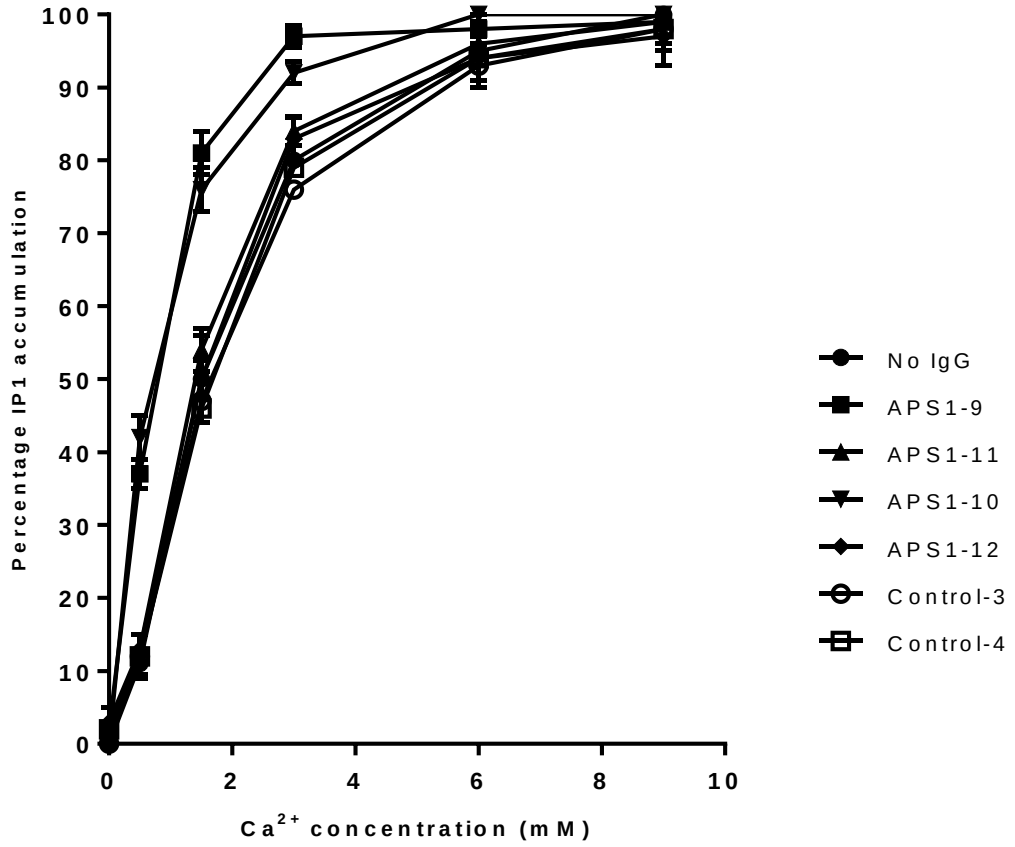

Figure 5.18: Effect of APS1 patient and control IgG on the response of the CaSR to Ca^{2+}-stimulation-2.

HEK293-CaSR cells were pre-incubated with IgG samples at a 1:100 dilution from APS1 patient (n = 16) and healthy controls (n = 10) prior to treatment with Ca^{2+} at 0.0, 0.5, 1.5, 3.0, 6.0 and 9.0 mM. Intracellular IP1 accumulation was then measured in an IP-One ELISA. The results show the mean percentage (±SD) inhibition of IP1-HRP conjugate binding from three experiments for two control and four APS1 patient IgG samples. Both controls and two of the APS1 patient IgG samples had no statistically significant effect upon IP1 accumulation in HEK293-CaSR cells when compared with cells stimulated by Ca^{2+} alone: all P values were > 0.05 (Student's paired t test). IgG samples from two APS1 patients (APS1-11 and APS1-9) statistically significantly increased IP1 accumulation at Ca^{2+} concentrations of 0.5 mM (P = 0.0015 and 0.0059, respectively), 1.5 mM (P = 0.0061 and 0.015, respectively) and 3.0 mM (P = 0.0067 and 0.0057, respectively) when compared with Ca^{2+}-stimulation alone.

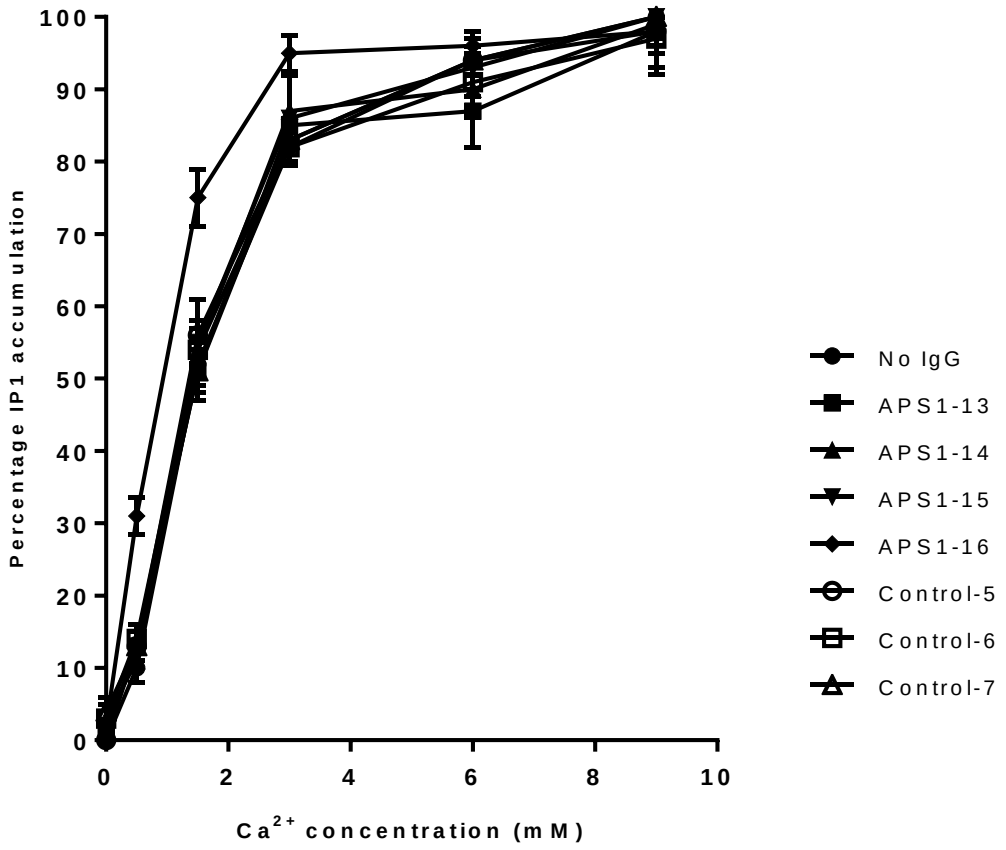

Figure 5.19: Effect of APS1 patient and control IgG on the response of the CaSR to Ca^{2+}-stimulation-3.

HEK293-CaSR cells were pre-incubated with IgG samples at a 1:100 dilution from APS1 patient (*n* = 16) and healthy controls (*n* = 10) prior to treatment with Ca^{2+} at 0.0, 0.5, 1.5, 3.0, 6.0 and 9.0 mM. Intracellular IP1 accumulation was then measured in an IP-One ELISA. The results show the mean percentage (±SD) inhibition of IP1-HRP conjugate binding from three experiments for two control and four APS1 patient IgG samples. Both controls and two of the APS1 patient IgG samples had no statistically significant effect upon IP1 accumulation in HEK293-CaSR cells when compared with cells stimulated by Ca^{2+} alone: all *P* values were > 0.05 (Student's paired t test). IgG samples from one APS1 patients (APS1-16) statistically significantly increased IP1 accumulation at Ca^{2+} concentrations of 0.5 mM (*P* = 0.015), 1.5 mM (*P* = 0.026) and 3.0 mM (*P* = 0.0006) when compared with Ca^{2+}-stimulation alone.

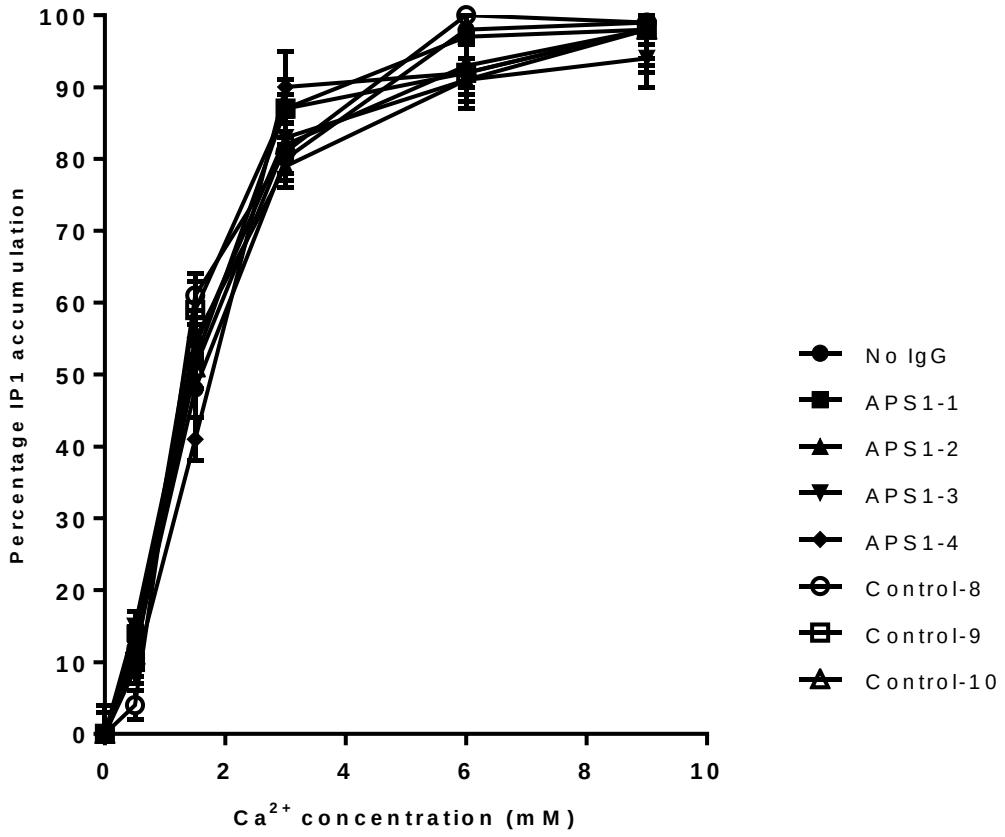

Figure 5.20: Effect of APS1 patient and control IgG on the response of the CaSR to Ca^{2+}-stimulation-4.

HEK293-CaSR cells were pre-incubated with IgG samples at a 1:100 dilution from APS1 patient (*n* = 16) and healthy controls (*n* = 10) prior to treatment with Ca^{2+} at 0.0, 0.5, 1.5, 3.0, 6.0 and 9.0 mM. Intracellular IP1 accumulation was then measured in an IP-One ELISA. The results show the mean percentage (±SD) inhibition of IP1-HRP conjugate binding from three experiments for three control and four APS1 patient IgG samples. All controls and APS1 patient IgG samples had no statistically significant effect upon IP1 accumulation in HEK293-CaSR cells when compared with cells stimulated by Ca^{2+} alone: all *P* values were > 0.05 (Student's paired t test).

5.5 Results Summary

The results from this chapter are summarised in **Tables 5.10, 5.11**, and indicated that:

CaSR autoantibody titres ranged from 1:200 to 1:2000.

- CaSR autoantibodies were specific for recognition of their CaSR binding site.
- CaSR autoantibody functional affinity ranged from 1.00×10^{-07} M to 9.00×10^{-08} M.
- Autoantibodies against the different CaSR epitopes were predominantly of the IgG1 subclass.
- Only a minority (4/16 = 25%) of APS1 patients had autoantibodies that activated the CaSR.

Table 5.10: Summary of APS1 patient CaSR antibody titres, specificity, functional affinity, and IgG subclass-1

APS1 patient	CaSR epitope 41-69 antibodies					CaSR epitope 114-126 antibodies			
	Antibody reactivity[1]	Antibody titre[2]	Functional affinity (M)[3]	IgG subclass		Antibody reactivity[1]	Antibody titre[2]	Functional affinity (M)[3]	IgG subclass
APS1-1	+	1:1000	7.50×10^{-08}	IgG1		-	-	-	-
APS1-2	+	1:500	1.00×10^{-07}	IgG1		-	-	-	-
APS1-3	+	1:500	1.00×10^{-07}	IgG1		-	-	-	-
APS1-4	+	1:500	1.00×10^{-07}	IgG1		-	-	-	-
APS1-5	+	1:1000	2.50×10^{-07}	IgG1		+	1:500	2.00×10^{-07}	IgG1
APS1-6	+	1:200	9.00×10^{-08}	IgG1		+	1:500	2.00×10^{-07}	IgG1
APS1-7	+	1:200	1.50×10^{-07}	IgG1		+	1:500	5.00×10^{-08}	IgG3
APS1-8	+	1:1000	3.00×10^{-07}	IgG1		-	-	-	-
APS1-9	+	1:100	2.00×10^{-07}	IgG1		-	-	-	-
APS1-10	+	1:500	2.50×10^{-07}	IgG1		+	1:500	4.00×10^{-08}	IgG3
APS1-11	+	1:100	4.00×10^{-08}	IgG1		-	-	-	-
APS1-12	+	1:500	1.50×10^{-07}	IgG1		-	-	-	-
APS1-13	+	1:200	1.50×10^{-07}	IgG1		-	-	-	-
APS1-14	+	1:1000	2.00×10^{-07}	IgG1		-	-	-	-
APS1-15	+	1:1000	2.00×10^{-07}	IgG1		-	-	-	-
APS1-16	+	1:1000	2.00×10^{-07}	IgG1		+	1:1000	4.00×10^{-08}	IgG3

[1]+, denotes positive for CaSR antibody reactivity; -, denotes negative for CaSR antibody reactivity.
[2]The CaSR antibody titre is given as the dilution at which immunoreactivity of the serum sample could still be detected at levels above the upper limit of normal in the specific CaSR peptide ELISA.
[3]Antibody functional affinity is given as the molar concentration of peptide that resulted in a 50% reduction of antibody binding as represented by the antibody index of the sera.

Table 5.11: Summary of APS1 patient CaSR antibody titres, specificity, functional affinity, and IgG subclass-2

APS1 patient	CaSR epitope 171-195 antibodies					CaSR epitope 260-340 antibodies			
	Antibody reactivity[1]	Antibody titre[2]	Functional affinity (M)[3]	IgG subclass		Antibody reactivity[1]	Antibody titre[2]	Functional affinity (M)[3]	IgG subclass
APS1-1	-	-	-	-		-	-	-	-
APS1-2	-	-	-	-		-	-	-	-
APS1-3	+	1:1000	2.50×10^{-07}	IgG1		+	1:500	1.50×10^{-07}	IgG1
APS1-4	+	1:500	2.50×10^{-07}	IgG1		+	1:500	1.50×10^{-07}	IgG1
APS1-5	-	-	-	-		-	-	-	-
APS1-6	-	-	-	-		-	-	-	-
APS1-7	-	-	-	-		-	-	-	-
APS1-8	-	-	-	-		-	-	-	-
APS1-9	+	1:200	8.00×10^{-08}	IgG1		+	1:500	7.50×10^{-08}	IgG1
APS1-10	-	-	-	-		-	-	-	-
APS1-11	-	-	-	-		-	-	-	-
APS1-12	+	1:500	7.50×10^{-08}	IgG1		+	1:500	7.20×10^{-08}	IgG1
APS1-13	-	-	-	-		-	-	-	-
APS1-14	+	1:500	3.50×10^{-07}	IgG1		+	1:500	7.50×10^{-08}	IgG1
APS1-15	+	1:500	3.50×10^{-07}	IgG1		+	1:500	5.00×10^{-08}	IgG1
APS1-16	-	-	-	-		+	1:2000	1.50×10^{-07}	IgG1

[1]+, denotes positive for CaSR antibody reactivity; -, denotes negative for CaSR antibody reactivity.
[2]The CaSR antibody titre is given as the dilution at which immunoreactivity of the serum sample could still be detected at levels above the upper limit of normal in the specific CaSR peptide ELISA.
[3]Antibody functional affinity is given as the molar concentration of peptide that resulted in a 50% reduction of antibody binding as represented by the antibody index of the sera.

5.6 Discussion

Titre and specificity Antibody titres can present a simple and effective method for determining the progression of an autoimmune disorder. Such examples include anti-alpha-galactosyl autoantibody levels in Graves' disease (Etienne-Decerf et al., 1987). In the case of autoantibodies against the CaSR, assessment of one patient with autoimmune hypocalciuric hypercalcemia showed that their CaSR autoantibody titres were strongly correlated with high serum calcium and elevated PTH levels (Pallais et al., 2004). Furthermore, there was a dramatic decrease in CaSR autoantibody levels in response to steroid therapy (Pallais et al., 2004). However, in the case of CaSR autoantibody titres in the APS1 patients included in this study, longitudinal serum samples were not analysed in relation to disease progression so conclusions are unable to be drawn at this stage.

Interestingly, the CaSR autoantibodies showed specificity for their particular epitope on the receptor and did not appear to be cross-reactive, suggesting that patients may have an array of different CaSR autoantibodies in their sera. Indeed, patients with type 1 diabetes mellitus have an array of autoantibodies against glutamic acid decarboxylase 65 that recognise specific antibody-binding sites (Syren et al., 1996).

Functional affinity The functional affinity of the CaSR autoantibodies varied between the individual APS1 patients. Previously, it has been suggested that the avidity of autoantibodies could be an important feature in autoimmune disease (Gharavi and Reiber, 1996). For example, in the case of β2-glycoprotein I autoantibodies in patients with antiphospholipid syndrome, autoantibodies with high avidity have been shown to be associated with increased pathogenicity (Cucnik et al., 2004, Cucnik et al., 2011). However, further studies will be needed, with respect to CaSR autoantibodies in APS1, to investigate potential pathogenic properties such as complement-fixation, antibody-dependent cellular cytotoxicity, and CaSR-activation before these can be related or not to antibody avidity.

IgG subclasses Similar to previous studies on IgG subclass determination in autoimmune disease (Boe et al., 2004, Brozzetti et al., 2010), CaSR autoantibodies against all identified epitopes were mainly of the IgG1 subclass. In a minority of APS1 patients, antibodies

against epitope 114-126 were of the IgG3 subclass. CaSR antibodies of the IgG2 and IgG4 subclasses were not identified. This is the first report regarding IgG subclass for antibodies against the CaSR in patients with hypoparathyroidism in the context of APS1, although CaSR autoantibodies exclusively of the IgG4 subtype have been found in a patient with autoimmune hypocalciuric hypercalcemia (Pallais et al, 2004). Interestingly, both IgG1 and IgG3 subclass antibodies can induce cell-mediated effector mechanisms as well as having the capacity to activate complement (Flanagan and Rabbitts, 1982, van Loghem, 1986). However, these pathomechanisms require investigation in relation to autoantibodies against the CaSR. It is possible that affinity purification of IgG subclasses might show less restriction than was found here in relation to CaSR autoantibodies. Indeed, fractionation into IgG subclasses has revealed the presence of all IgG subclass antibodies, including IgG4, with respect to thyroglobulin and thyroid peroxidase autoantibodies in Hashimoto's thyroiditis (Weetman et al., 1989).

The T helper cell Th1/Th2 balance of the immune response influences the profile of IgG subtypes (Finkelman et al., 1990, Snapper and Paul, 1987). The Th1 cell subset induces the activation of macrophage and cytotoxic T lymphocytes as well as immunoglobulin IgG subclass switching in favour of complement-fixation and opsonisation (Romagnani, 1995, Mosmann and Sad, 1996). Indeed, the levels of IgG1 and IgG3 have been related to a Th1 immune response (Finkelman et al., 1990, Snapper and Paul, 1987), which is characterised also by the production of IFN-γ, IL-2, and TNF-β. In contrast, a predominant Th2 cell immune response, defined by the secretion of IL-4, IL-5, and IL-10, induces the selection of IgG4 subclass antibodies (Finkelman et al., 1990, Snapper and Paul, 1987). However, in APS1, there are no available studies on the potential immunopolarisation to a Th1-type immune profile which could be related to the finding that CaSR autoantibodies are mainly of the IgG1 subclass.

Effects of CaSR autoantibodies on CaSR function Only a minority of patients (4/16 = 25%) had CaSR autoantibodies that stimulated the receptor. Indeed, to date, only a small number of patients with hypoparathyroidism have been identified with CaSR-activating antibodies that could potentially reduce PTH-secretion. Firstly, sera from two patients with idiopathic hypoparathyroidism inhibited PTH-release from human parathyroid cells

(Kifor et al., 2004). Secondly, IgG from two patients with APS1 both of whom had hypoparathyroidism, activated the CaSR expressed in HEK293 cells (Kemp et al., 2009). However, it was not determined if these IgG samples would consequently affect PTH secretion from parathyroid chief cells. In patients with CaSR-stimulating autoantibodies, it could be that their hypoparathyroidism is caused by autoantibody activity against the CaSR instead of parathyroid gland destruction. This would be analogous to the action of pathogenic autoantibodies against the thyroid-stimulating hormone receptor in Graves' disease (Morgenthaler et al., 2007). However, there were no data on whether or not the parathyroid of the APS1 patients with CaSR autoantibodies did or did not have lymphocyte infiltration.

Chapter 6

Development of an ELISA for the Detection of CaSR Autoantibodies

6 Development of an ELISA for the Detection of CaSR Autoantibodies

6.1 Introduction

One of the main aims of this project was investigate the prevalence of CaSR autoantibodies in APS1 patients. However, there is no gold standard method to detect CaSR autoantibodies. The few methods established already are either labour-intensive, time-consuming or are not quantitative. The detection methods used have included radioligand binding assays (RLBAs), immunoprecipitation, immunoblotting, and ELISA (**Table 6.1**).

Radioligand binding assays using *in vitro* translated CaSR were initially used to detect CaSR autoantibodies (Li et al., 1996, Gylling et al., 2003). Such assays are often the gold standard for measuring autoantibodies in patients with APS1 (Soderbergh et al., 2004). One of the advantages of this methodology is that there is less background compared to the assays that use autoantigens expressed in a cell system which may therefore be contaminated with other proteins. Although Tomar and colleagues (Tomar et al., 2013) showed that this assay was very specific in recognising CaSR autoantibodies, earlier work by our group did not manage to detect the reactivity of such receptor autoantibodies using this assay (Gavalas et al., 2007). Similar results were reported also by Soderbergh and co-workers (Soderbergh et al., 2004).

Immunoblotting of the CaSR expressed in HEK293 cells (Li et al., 1996, Kifor et al., 2003, Tomar et al., 2013) or recombinant CaSR extracellular domain expressed in *E. coli* (Mayer et al., 2004) are other strategies which have been used to detect autoantibodies against the receptor. However, it is more difficult to use immunoblotting as an accurate quantitative measurement of autoantibodies present in patient serum samples. Immunoprecipitation using extracts of HEK293 cells expressing the receptor has also been employed to detect immunoreactivity against the CaSR (Gavalas et al., 2007). This assay method probably allows the detection of autoantibodies that recognise the native receptor as the antibody-antigen binding is done in solution under non-denaturing conditions. However, the technique is labour-intensive, involving several stages, so it is

difficult to test many samples at one time. Flow cytometry has also been successfully used in the detection of autoantibodies against the CaSR expressed in HEK293 cells (Gavalas et al., 2007). However, the technique appeared less sensitive than immunoprecipitation, detecting CaSR autoantibodies at a lesser frequency. The method is also less amenable to automation than an ELISA, for example.

Compared to other immunoassay methods, there are many advantages of ELISAs. They are considered highly sensitive, specific, possess the added advantage of not needing radioisotopes and large numbers of samples can be analysed at one time. This method was, therefore, chosen as the basis for an assay for CaSR autoantibodies. Previously, synthetic peptides which correspond to specific parts of the CaSR have been used was used as targets to detect autoantibodies against the receptor in an ELISA format (Kifor et al., 2003, Kemp et al., 2010, Tomar et al., 2013). Although specific peptides have shown a high specificity in the detection of CaSR autoantibodies, this approach is less useful as it cannot detect all at once the array of autoantibodies against the receptor that might be present in a patient (Kemp et al., 2010). It was necessary, therefore, to consider using at least the extracellular domain of the CaSR as the antigen in an ELISA.

Since glycosylation of the CaSR is not seemingly required for antigen-antibody interaction (Li et al., 1996), and several non-conformational CaSR epitopes in the extracellular domain are recognised by APS1 patient autoantibodies (Mayer et al., 2004, Kemp et al., 2010), it was decided to express the extracellular domain of the receptor in *E. coli*. This would provide a large quantity of the antigen when compared to expression in mammalian cells. Indeed, one commercially available kit (Alpco Immunoassays, Salem, NH, USA), which has been made available during the course of this study, uses the CaSR extracellular domain as the antigen in an ELISA system.

Table 6.1: Summary of CaSR antibody detection methods

Source of antigen	Method of antibody detection	Reference
In vitro translation of the CaSR	Radioligand binding assay	(Li et al., 1996, Gylling et al., 2003)
Full-length CaSR expressed in HEK293 cells	Immunoblotting	(Tomar et al., 2013)
Extracellular domain of the CaSR expressed in *E. coli*	Immunoblotting	(Mayer et al., 2004, Tomar et al., 2013)
Full-length CaSR expressed in HEK293 cells	Immunoprecipitation	(Kifor et al., 2003, Gavalas et al., 2007)
Full-length CaSR expressed in HEK293 cells	Flow cytometry	(Gavalas et al., 2007)
Synthetic peptides representing parts of the CaSR extracellular domain	ELISA	(Kifor et al., 2003, Tomar et al., 2013)

6.2 Aims

The broad aims of this part of the study were:

- To express His-tagged CaSR-ECD in bacterial cells and purify the fusion protein using nickel-chelation chromatography.
- To investigate the usefulness of the purified CaSR-ECD for detecting CaSR antibodies in an ELISA format.

6.3 Strategy for expressing the CaSR extracellular domain

As explained in the previous section, *E. coli* was chosen to express the extracellular domain of the CaSR. Plasmid pET14b vector (**Figure 6.1**) was chosen for this purpose. In this vector, the DNA of interest is cloned such that a 6XHis-tag is located at the N-terminal of the expressed fusion protein. The His-tag can subsequently be used to purify the expressed protein using metal affinity chromatography. The His-tag was chosen because it is small in size and has been shown to result in high yields of protein without affecting the structure and function of the protein (Bornhorst and Falke, 2000). Although the elution buffers used in the purification of His-tag proteins are mild, the His-tag can be used under conditions where there is detergent or a strong ionic environment (Bornhorst and Falke, 2000).

In the pET14b vector, expression of the cloned DNA is under the control of the T7 promotor and T7 RNA polymerase (**Figure 6.2**). So that expression of the required protein can take place, *E. coli* strains are used in which the T7 RNA polymerase gene is integrated into the bacterial genome under the control of the *lac* operon promoter (**Figure 6.2**) (Rosano and Ceccarelli, 2014). Expression of T7 RNA polymerase is therefore inducible by isopropyl β-D-1-thiogalactopyranoside (IPTG) (**Figure 6.2**) (Bell and Lewis, 2000, Daber et al., 2007). Several strains are available for using with the pET14b expression system. Strain *E. coli* BL21 (DE3) expresses high levels of protein, but can show protein expression before IPTG-induction (Rosano and Ceccarelli, 2014). This can be overcome in *E. coli* BL21 (DE3)pLysS which is better in terms of controlling leaky expression (Rosano and Ceccarelli, 2014). The strain encodes T7 lysozyme which degrades any T7 RNA polymerase produced due to leaky expression. The *E. coli* BL21 GOLD (DE3) and BL21 GOLD (DE3)pLysS strains are engineered to be deficient for proteases such that expressed proteins are not degraded (Greener et al., 1997). Finally, the *E. coli* BL21 CODONPLUS (DE3)-RIPL strain is engineered to contain extra copies of genes that encode the tRNAs that most frequently limit the translation of proteins in *E. coli* (Carstens et al., 2002). The availability of such tRNAs allows high-level expression of recombinant genes in this strain.

The signal peptide of the CaSR is highly hydrophobic (Hu and Spiegel, 2007), and removing this part of the protein has been shown to increase the solubility of the extracellular domain of the CaSR when expressed in bacterial cells (Tomar et al., 2013). Plasmid pPROEX-HTb-CaSREx containing the CaSR extracellular domain cDNA but without a signal peptide (**Figure 6.3**) (Tomar et al., 2013) was therefore used as a second option to express the extracellular domain of the receptor. In this plasmid, the CaSR extracellular domain is also linked to a His-tag at the N-terminal. Protein expression is driven from the synthetic IPTG-inducible *trc* promoter (Brosius et al., 1985), derived from the *E. coli trp* and *lac*UV5 promoters.

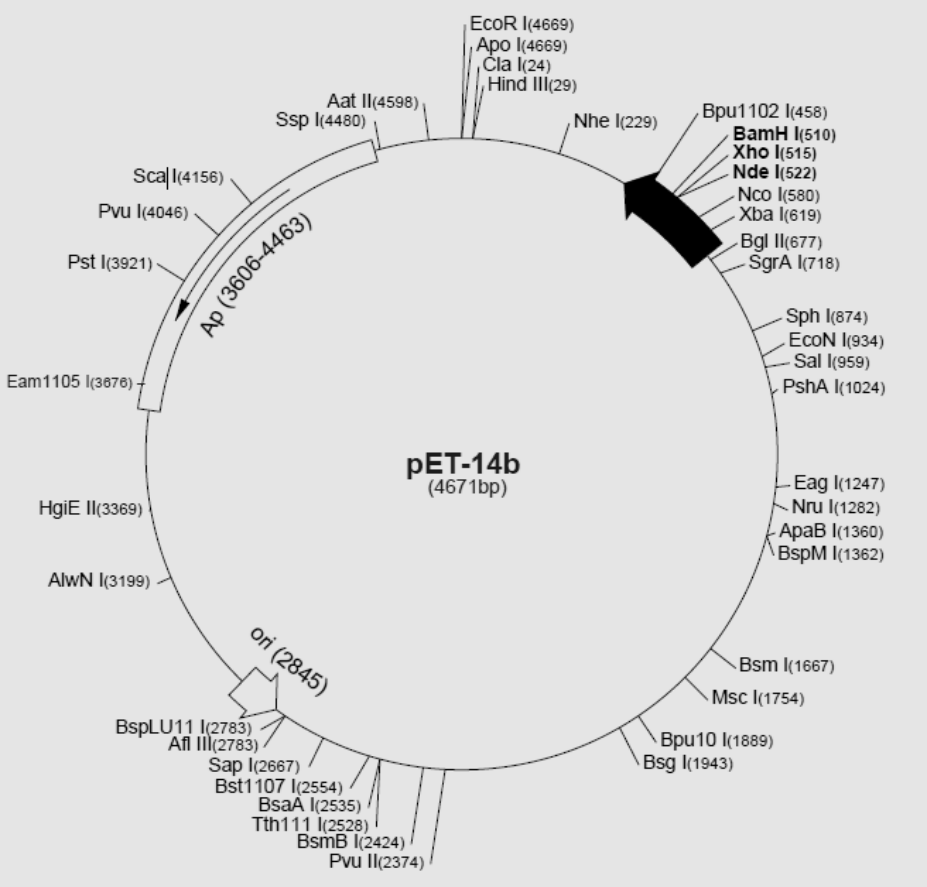

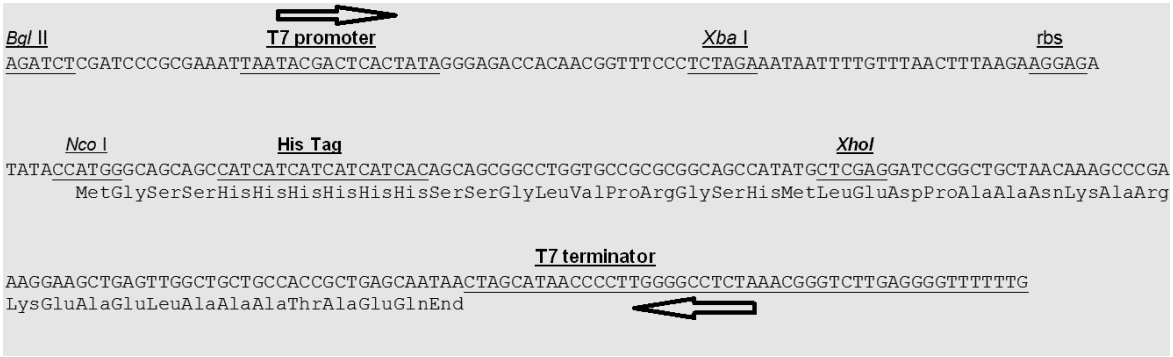

Figure 6.1: Plasmid vector pET14b.

The cloning sites and sequencing primer binding sites are illustrated.

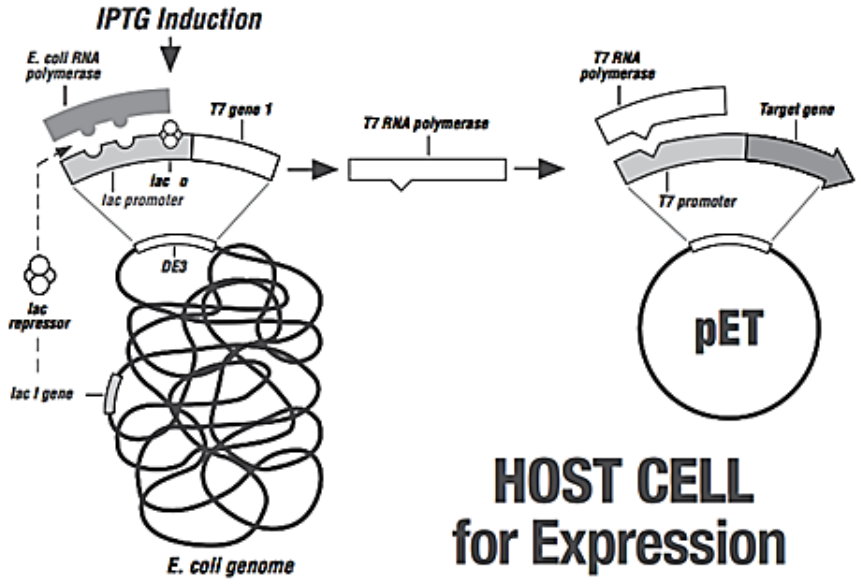

Figure 6.2: Expression of target genes in the pET14b expression system.

In the pET14b vector, expression of the cloned DNA is under the control of the T7 promotor and T7 RNA polymerase. So that expression of the required protein can take place, *E. coli* strains are used in which the T7 RNA polymerase gene is integrated into the bacterial genome under the control of the *lac* operon promoter. Expression of T7 RNA polymerase is therefore inducible by isopropyl β-D-1-thiogalactopyranoside (IPTG). As a result, T7 RNA polymerase is produced, which then promotes the transcription of the cloned DNA of interest.

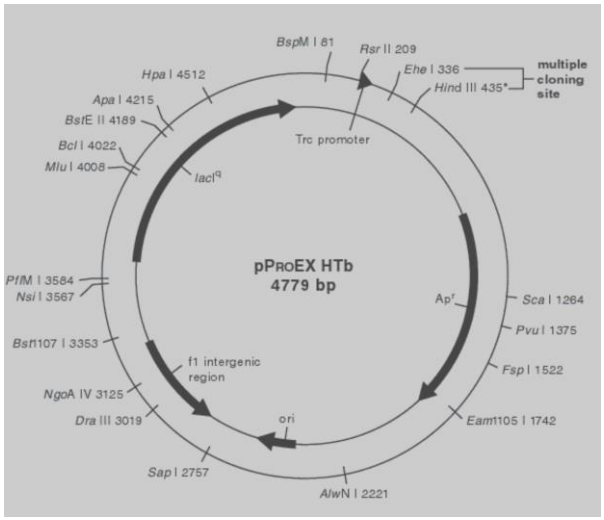

Amino acid sequence of cDNA-encoded CaSR-ECD

YGPDQRAQKKGDIILGGLFPIHFGVAAKDQDLKSRPE
SVECIRYNFRGFRWLQAMIFAIEEINSSPALLPNLTL
GYRIFDTCNTVSKALEATLSFVAQNKIDSLNLDEFCN
CSEHIPSTIAVVGATGSGVSTAVANLLGLFYIPQVSY
ASSSRLLSNKNQFKSFLRTIPNDEHQATAMADIIEYF
RWNWVGTIAADDDYGRPGIEKFREEAEERDICIDFSE
LISQYSDEEEIQHVVEVIQNSTAKVIVVFSSGPDLEP
LIKEIVRRNITGKIWLASEAWASSSLIAMPQYFHVVG
GTIGFALKAGQIPGFREFLKKVHPRKSVHNGFAKEFW
EETFNCHLQEGAKGPLPVDTFLRGHEESGDRFSNSST
AFRPLCTGDENISSVETPYIDYTHLRISYNVYLAVYS
IAHALQDIYTCLPGRGLFTNGSCADIKKVEAWQVLKH
LRHLNFTNNMGEQVTFDECGDLVGNYSIINWHLSPED
GSIVFKEVGYYNVYAKKGERLFINEEKILWSGFSREV
PFSNCSRDCLAGTRKGIIEGEPTCCFECVECPDGEYS
DETDASACNKCPDDFWSNENHTSCIA

Nucleotide sequence of CaSR-ECD cDNA in plasmid pPROEX-HTb-CaSREx

TACGGCCCCGACCAGAGGGCCCAGAAGAAGGGCGACATCATCCTGGGCGGCCTGTTCCCCATCCACTTCGGCGTGGCCGCCAAGGACCAGGA
CCTGAAGAGCAGGCCCGAGAGCGTGGAGTGCATCAGGTACAACTTCAGGGGCTTCAGGTGGCTGCAGGCCATGATCTTCGCCATCGAGGAGA
TCAACAGCAGCCCCGCCCTGCTGCCCAACCTGACCCTGGGCTACAGGATCTTCGACACCTGCAACACCGTGAGCAAGGCCCTGGAGGCCACC
CTGAGCTTCGTGGCCCAGAACAAGATCGACAGCCTGAACCTGGACGAGTTCTGCAACTGCAGCGAGCACATCCCCAGCACCATCGCCGTGGT
GGGCGCCACCGGCAGCGGCGTGAGCACCGCCGTGGCCAACCTGCTGGGCCTGTTCTACATCCCCCAGGTGAGCTACGCCAGCAGCAGCAGGC
TGCTGAGCAACAAGAACCAGTTCAAGAGCTTCCTGAGGACCATCCCCAACGACGAGCACCAGGCCACCGCCATGGCCGACATCATCGAGTAC
TTCAGGTGGAACTGGGTGGGCACCATCGCCGCCGACGACGACTACGGCAGGCCCGGCATCGAGAAGTTCAGGGAGGAGGCCGAGGAGAGGGA
CATCTGCATCGACTTCAGCGAGCTGATCAGCCAGTACAGCGACGAGGAGGAGATCCAGCACGTGGTGGAGGTGATCCAGAACAGCACCGCCA
AGGTGATCGTGGTGTTCAGCAGCGGCCCCGACCTGGAGCCCCTGATCAAGGAGATCGTGAGGAGGAACATCACCGGCAAGATCTGGCTGGCC
AGCGAGGCCTGGGCCAGCAGCAGCCTGATCGCCATGCCCCAGTACTTCCACGTGGTGGGCGGCACCATCGGCTTCGCCCTGAAGGCCGGCCA
GATCCCCGGCTTCAGGGAGTTCCTGAAGAAGGTGCACCCCAGGAAGAGCGTGCACAACGGCTTCGCCAAGGAGTTCTGGGAGGAGACCTTCA
ACTGCCACCTGCAGGAGGGCGCCAAGGGCCCCCTGCCCGTGGACACCTTCCTGAGGGGCCACGAGGAGAGCGGCGACAGGTTCAGCAACAGC
AGCACCGCCTTCAGGCCCCTGTGCACCGGCGACGAGAACATCAGCAGCGTGGAGACCCCCTACATCGACTACACCCACCTGAGGATCAGCTA
CAACGTGTACCTGGCCGTGTACAGCATCGCCCACGCCCTGCAGGACATCTACACCTGCCTGCCCGGCAGGGGCCTGTTCACCAACGGCAGCT
GCGCCGACATCAAGAAGGTGGAGGCCTGGCAGGTGCTGAAGCACCTGAGGCACCTGAACTTCACCAACAACATGGGCGAGCAGGTGACCTTC
GACGAGTGCGGCGACCTGGTGGGCAACTACAGCATCATCAACTGGCACCTGAGCCCCGAGGACGGCAGCATCGTGTTCAAGGAGGTGGGCTA
CTACAACGTGTACGCCAAGAAGGGCGAGAGGCTGTTCATCAACGAGGAGAAGATCCTGTGGAGCGGCTTCAGCAGGGAGGTGCCCTTCAGCA
ACTGCAGCAGGGACTGCCTGGCCGGCACCAGGAAGGGCATCATCGAGGGCGAGCCCACCTGCTGCTTCGAGTGCGTGGAGTGCCCCGACGGC
GAGTACAGCGACGAGACCGACGCCAGCGCCTGCAACAAGTGCCCCGACGACTTCTGGAGCAACGAGAACCACACCAGCTGCATCGCC

Nucleotide sequence from the start of the 6XHis-CaSR-ECD fusion protein:

ATGTCGTACTACCATCACCATCACCATCACGATTACGATATCCCAAGGACCGAAAACCTGTATTTTGAGGGCG
CCATGG*GATTC*TAC

Amino acid sequence from the start of the 6XHis-CaSR-ECD fusion protein:

MSYYHHHHHHDYDIPTTENLYFQGAMGSYGPD

Figure 6.3: Details of plasmid pPROEX-HTb-CaSREx.

Plasmid pPROEX-HTb-CaSREx is vector pPROEX-HTb containing the cDNA of the extracellular domain (ECD) of the CaSR (1743 base pairs) without the receptor signal sequence. The CaSR extracellular domain cDNA was cloned between the *Bam*HI and *Hin*dIII restriction sites and was in the correct orientation for expression in *E. coli* from the *trc* promoter present in pPROEX-HTb. The selectable marker for propagation in bacteria was ampicillin resistance. In the nucleotide sequence, the 6XHis codons are underlined and the ATG start codon is given in bold type. The 5' *Bam*HI restriction site is in italics. In the amino acid sequence, the 6XHis-tag is underlined and the start methionine residue is given in bold.

6.4 Experiments and Results

6.4.1 Preparation of pPROEX-HTb-CaSREx

Plasmid pPROEX-HTb-CaSREx (**Figure 6.3**) containing the CaSR extracellular domain (CaSR-ECD) cDNA, but without the CaSR signal sequence was a kind gift from Professor Ravinder Goswami (Department of Endocrinology and Metabolism, All India Institute of Medical Sciences, New Delhi, India). Initially, the plasmid was used to transform *E. coli* JM109, as detailed earlier (**Section 2.13**). One transformant was purified by streaking onto a fresh LB agar plate (**Section 2.3**) containing ampicillin at 100 µg/ml (**Section 2.3**) followed by incubation overnight at 37°C. The purified bacterial clone was then inoculated into 10 ml of LB medium (**Section 2.3**) containing ampicillin at 100 µg/ml and incubated at 37°C overnight. Subsequently, plasmid DNA was purified from the bacterial culture using a Wizard Miniprep DNA Purification System (**Section 2.6**). Successful preparation of the plasmid was confirmed by electrophoresis in a 1% (w/v) agarose gel (**Section 2.8**). A large-scale plasmid preparation of pPROEX-HTb-CaSREx was carried out, as detailed in **Section 2.7.** Finally, the CaSR-ECD cDNA sequence in the plasmid was verified using primers M13 forward, M13 Reverse, CaSR-451, CaSR-951, and CaSR-1151 (**Section 2.15; Table 2.5**).

6.4.2 Cloning of the CaSR extracellular domain for expression in *E. coli*

The experiment to clone the CaSR-ECD cDNA into pET14b (**Figure 6.1**), for ultimate use in the expression of a 6XHis-CaSR-ECD fusion protein, is detailed in the following sections.

6.4.2.1 PCR amplification of the CaSR extracellular domain

A cDNA fragment of the CaSR-ECD, encompassing base pairs 1-1800 of the CaSR cDNA sequence (**Figure 3.2**), was generated from the full-length CaSR cDNA present in pDEST14-CaSR (**Figure 6.4**) by PCR amplification (**Section 2.10**). The oligonucleotide primers CaSR-ECD-F and CaSR-ECD-R, which were used to generate the CaSR-ECD cDNA, are listed in **Table 2.4**. A restriction site for *Xho*I was incorporated into each of the primers in order to allow eventual cloning of the PCR amplification product into the *Xho*I restriction site of the expression vector pET14b. The composition of the PCR amplification reaction and the PCR

amplification conditions used with the template pDEST14-CaSR DNA were as previously described (**Section 2.10**). To check the PCR amplification product, a 5-µl aliquot of the PCR amplification reaction was electrophoresed in a 1% (w/v) agarose gel (**Section 2.8**). The result is shown in **Figure 6.5**, and this indicated a PCR amplification product with an estimated size of 1.8 kb.

6.4.2.2 TOPO® cloning of the CaSR-ECD cDNA PCR product

According to a TOPO® TA Cloning Kit (**Section 2.14**), a TOPO® cloning reaction was used to clone the CaSR-ECD cDNA PCR amplification product directly into plasmid vector pCR®2.1-TOPO® (**Figure 6.6**). Following transformation of *E. coli* TOP10F' cells the TOPO® cloning reaction, individual colonies were purified by streaking onto fresh LB agar plates (**Section 2.3**) with kanamycin at 50 µg/ml (**Section 2.3**) and growing them overnight at 37°C.

For screening of *E. coli* TOP10F' transformants for recombinant plasmids that contained the correct CaSR cDNA fragment, 10 individual bacterial clones were inoculated separately into 10 ml of LB medium (**Section 2.3**) containing kanamycin at 50 µg/ml (**Section 2.3**), and then incubated at 37°C overnight. Subsequently, plasmid DNA was purified from individual transformants using a Wizard Miniprep DNA Purification System (**Section 2.6**). Plasmids were then checked for the presence of a DNA insert of the correct size by restriction enzyme digestion of a 0.5-µg sample with *Xho*I in a 25-µl reaction (**Section 2.9**), followed by analysis by electrophoresis in a 1% (w/v) agarose gel (**Section 2.8**).

The results indicated that the frequency of recombinant plasmids was 90%, with 9/10 plasmids having a DNA insert of the expected size at 1.8 kb (**Figure 6.7**). One recombinant plasmid was designated as pCR®2.1-TOPO®-CaSR-ECD (**Figure 6.8**), and this was further analysed.

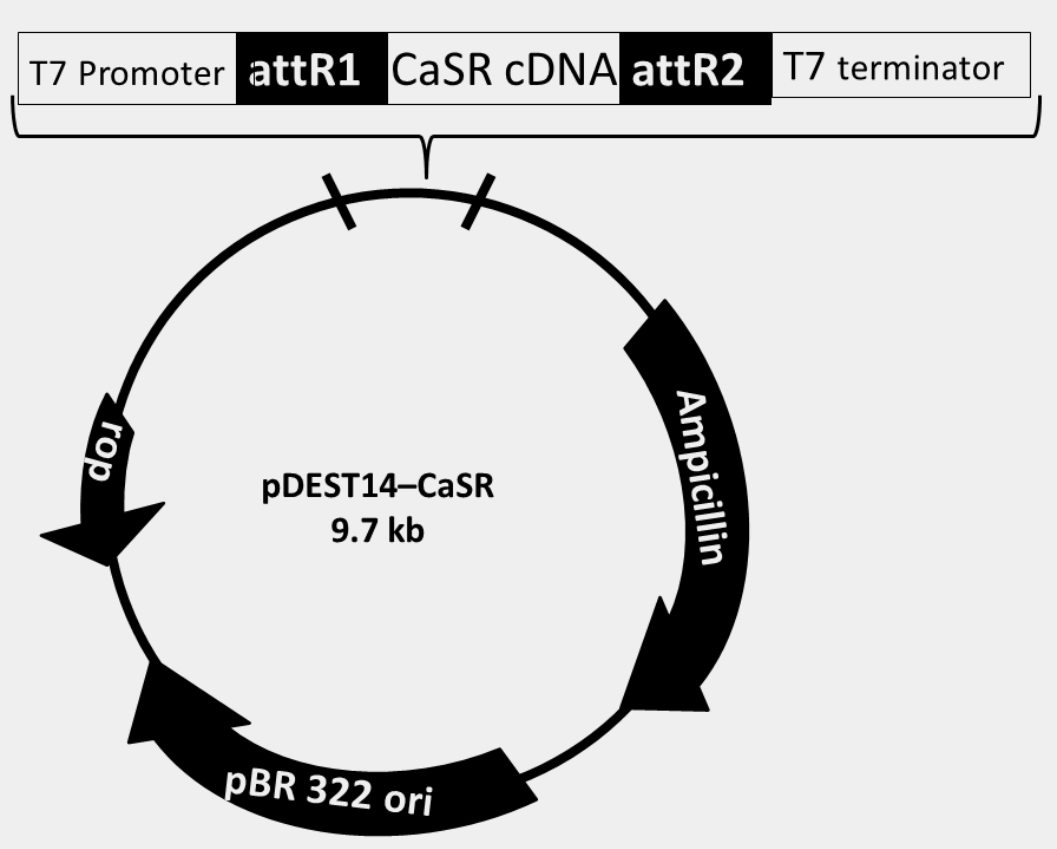

Figure 6.4: A map of the pDEST14-CaSR plasmid.

Restriction enzyme sites and sequencing primer binding sites (T7 promoter and T7 terminator) are shown. The CaSR cDNA is cloned as a 3234-base pair fragment into the 6.4-kilobase pDEST14 vector.

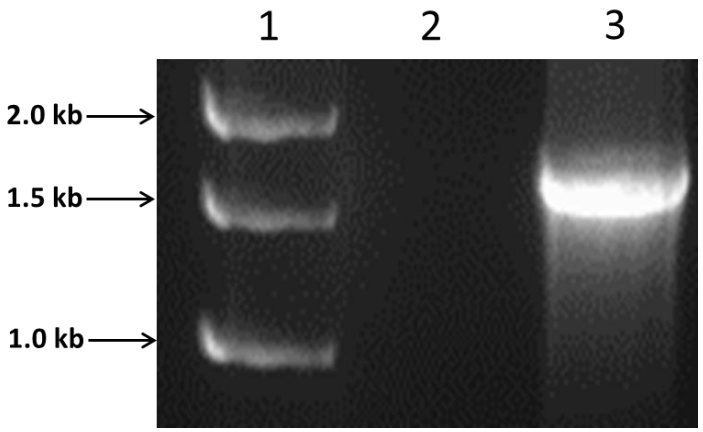

Figure 6.5: Agarose gel of PCR amplification product amplified from pDEST14-CaSR.

Plasmid pDEST-CaSR was subjected to PCR amplification using primers CASR-ECD-F and CASR-ECD-R. The PCR amplification products were analysed by electrophoresis in a 1% (w/v) agarose gel. The gel shows: 1-kb DNA Ladder with DNA fragments from 500 to 10,000 bp (lane 1); no DNA control with primers CASR-ECD-F and CASR-ECD-R (lane 2); plasmid pDEST-CaSR amplified with primers CASR-ECD-F and CASR-ECD-R (lane 3).

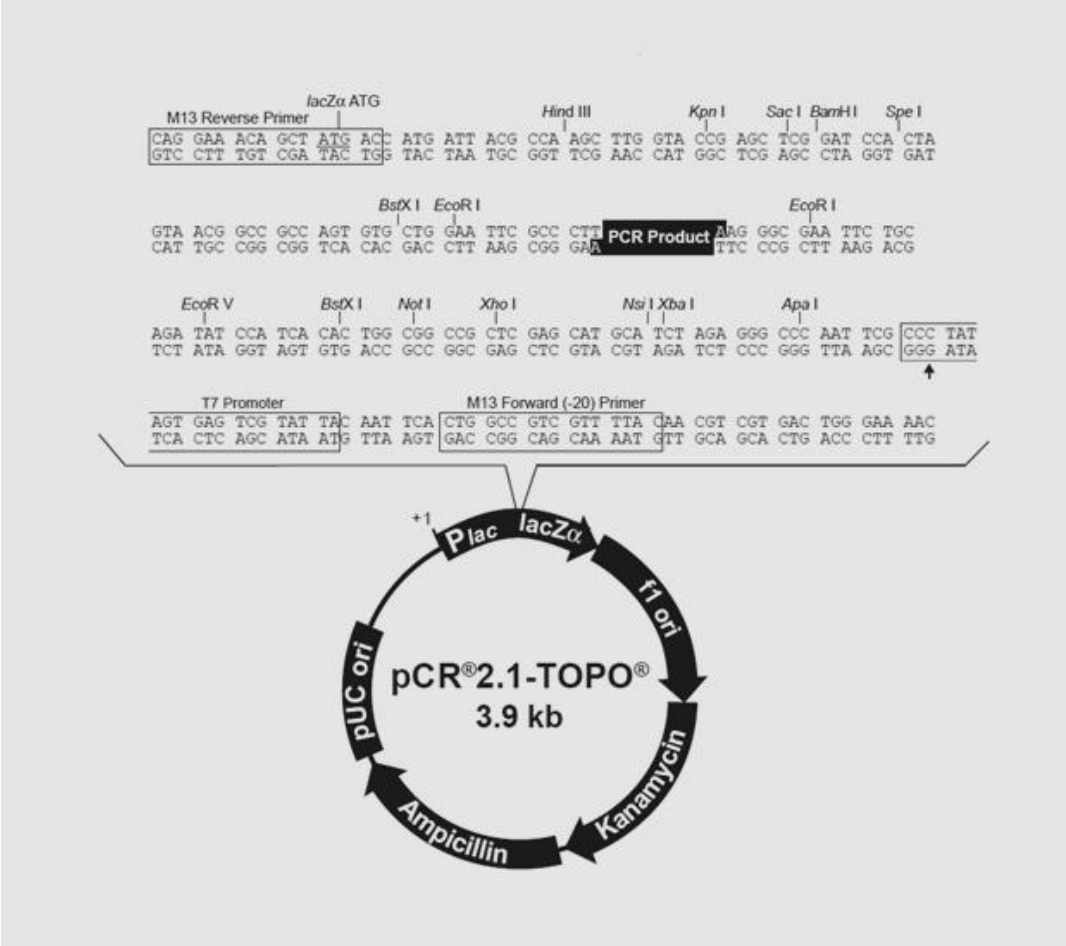

Figure 6.6: Plasmid vector pCR®2.1-TOPO®.

The PCR product insertion site and sequencing primer binding sites are illustrated.

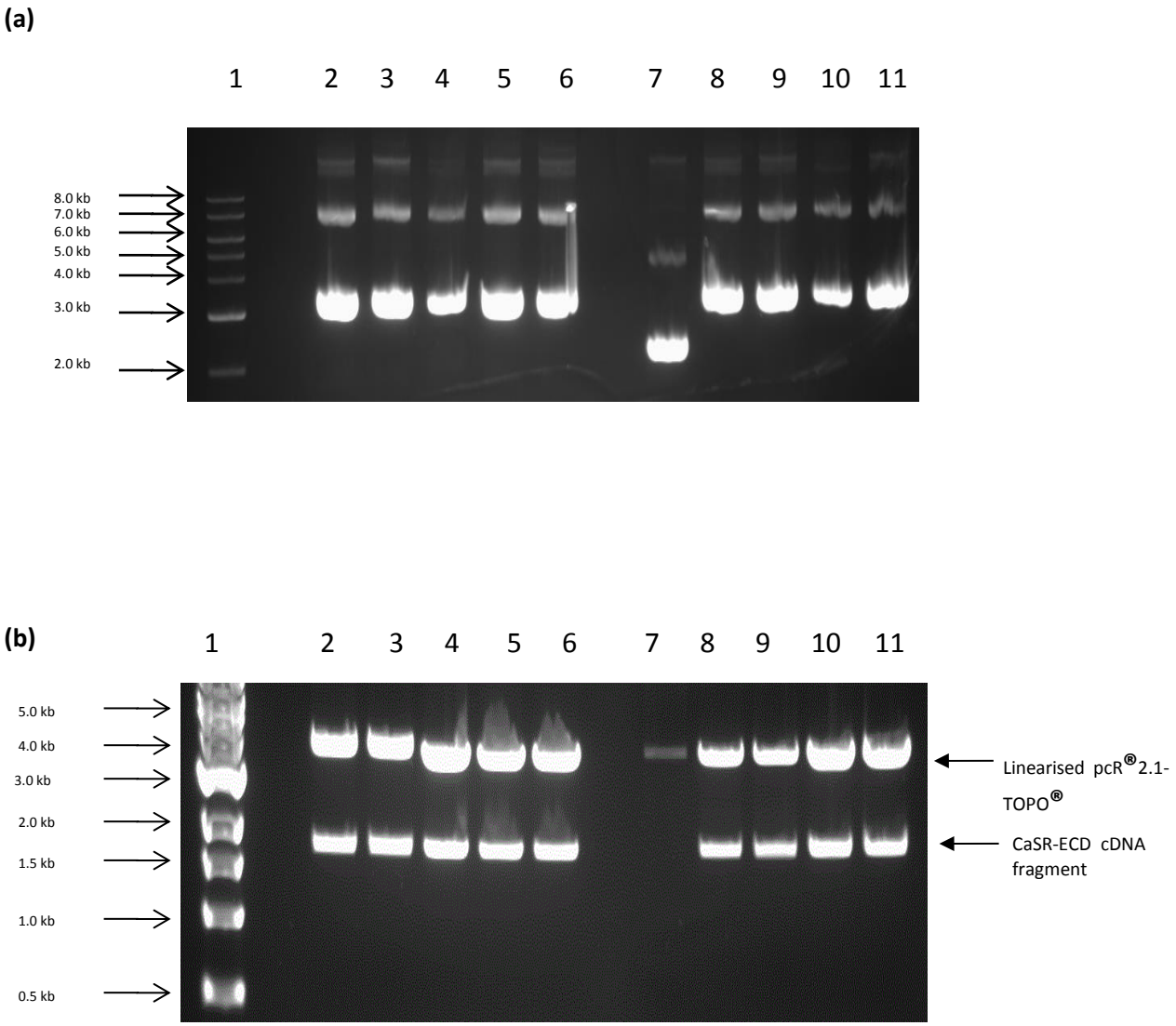

Figure 6.7: Agarose gel of plasmids prepared from *E. coli* TOP10F' clones.

The plasmids prepared from ten *E. coli* TOP10F' clones were restricted with *Xho*I to determine the presence of a CaSR-ECD cDNA insert. **(a)** The 1% (w/v) agarose gel shows: 1-kb DNA Markers with DNA fragments from 500-10,000 bp (lane 1); unrestricted plasmids (lanes 2-11). **(b)** The gel 1% (w/v) agarose shows: 1-kb DNA Markers with DNA fragments from 500-10,000 bp (lane 1); *Xho*I-restricted plasmids (lanes 2-11).

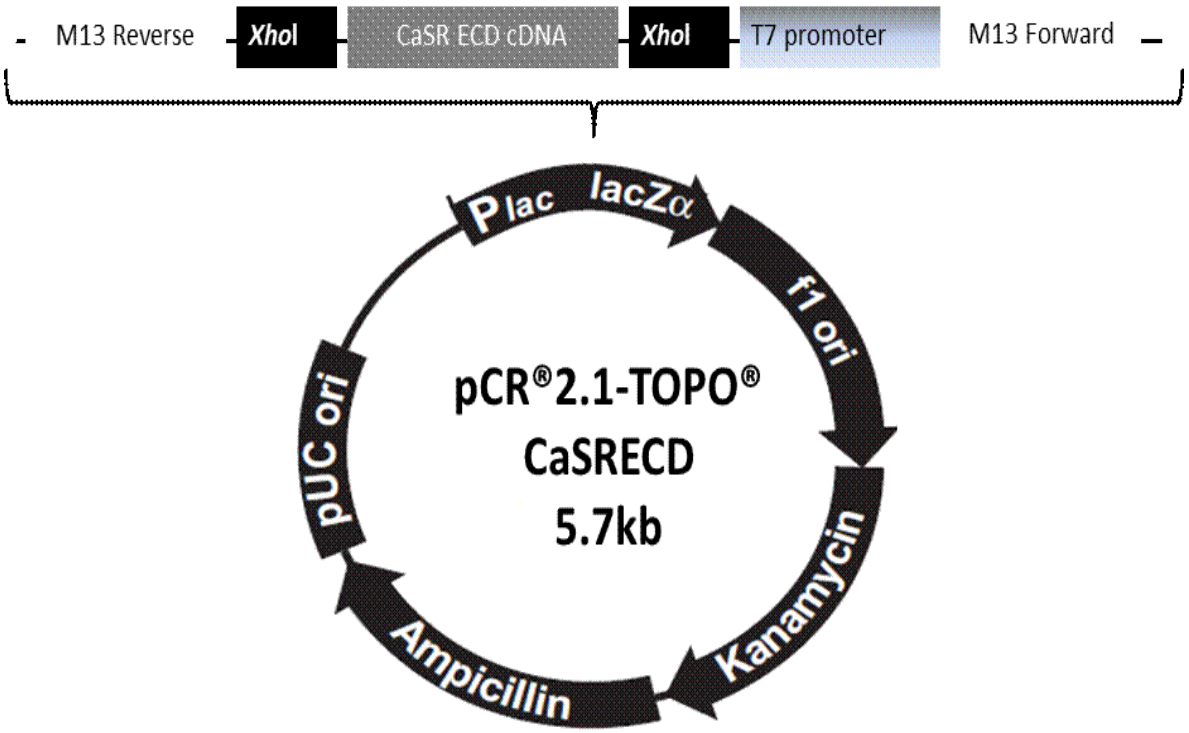

Figure 6.8: Schematic diagram of plasmid pCR®2.1-TOPO®-CaSR-ECD.

The CaSR-ECD cDNA is cloned into the PCR cloning site of pCR2.1-TOPO as a fragment with *Xho*I restriction sites incorporated at the 5' and 3' ends. The positions of the T7 promoter, M13 reverse and M13 forward primers are indicated.

6.4.2.3 Sequencing of cloned CaSR-ECD cDNA fragment

To verify that no sequence errors had been introduced into the CaSR-ECD cDNA fragment during PCR amplification, plasmid pCR®2.1-TOPO®-CaSR-ECD was subjected to DNA sequencing (**Section 2.15**) using primers T7 Promoter, M13 Reverse and CASR646-F (**Table 2.5**). The results verified that the recombinant plasmid contained the correct CaSR-ECD cDNA fragment when compared with the sequence of the CaSR cDNA template (**Figure 3.2**) using the Pairwise Alignment tool at the network facilities of the EBI-EMBL (**Section 2.16**). This plasmid was used in subsequent cloning experiments as the source of the cloned CaSR-ECD.

6.4.2.4 Preparation of the CaSR-ECD cDNA fragment for cloning into pET14b

To prepare the CaSR-ECD cDNA fragment, 1 µg of pCR®2.1-TOPO®-CaSR-ECD was digested with *Xho*I in a 25-µl reaction and then electrophoresed in a 1% (w/v) agarose gel. Subsequently, the 1.8-kb DNA fragment was purified from the gel using a Wizard PCR Preps DNA Purification System (**Section 2.11**). Finally, a 3-µl aliquot of the restricted and purified product was analysed by agarose gel electrophoresis in a 1% (w/v) gel, and the concentration determined by spectrophotometry (**Section 2.6**).

6.4.2.5 Preparation of vector pET14b

Plasmid vector pET14 (Novagen/Merck KgaA, Darmstadt, Germany) was already available in the laboratory (Dr Helen Kemp, University of Sheffield). For cloning of the CaSR-ECD fragment into pET14b, 1 µg of the plasmid vector was digested with *Xho*I in a 25-µl reaction. The linearised vector was purified from a 1% (w/v) agarose gel using a Wizard PCR Preps DNA Purification System. A 3-µl aliquot of the restricted and purified vector was checked on a 1% (w/v) agarose gel, and the concentration determined by spectrophotometry.

6.4.2.6 Cloning of CaSR-ECD cDNA fragment into pET14b

The *Xho*I-restricted CaSR-ECD cDNA fragment was cloned into *Xho*I-digested pET14b by setting up 20-µl ligation reaction (**Section 2.12**). A 5-µl aliquot of the ligation reaction was then used to transform 100 µl of chemically competent *E. coli* JM109 cells (**Section 2.13**) with transformants being selected on LB agar containing ampicillin at 100 µg/ml. Following overnight incubation at 37°C, 60 individual bacterial colonies from the transformation were purified by streaking on to fresh LB agar containing ampicillin at 100 µg/ml and subsequently incubating at 37°C overnight.

For screening of *E. coli* JM109 transformants for recombinant plasmid that contained the CaSR-ECD cDNA fragment, 60 individual bacterial clones were subjected to PCR amplification. For this, a small amount of each bacterial clone was taken from the selective LB agar plate and suspended in 100 µl of nuclease-free water in a 0.5-ml tube. After heating at 95°C for 5 min, the lysed cells were centrifuged for 5 min at 12,000 *g* to remove cellular debris. The supernatant containing DNA was removed to a clean 0.5-ml tube. Using primers CaSR-ECD-F and CaSR-ECD-R, a 2-µl aliquot of each DNA sample was subjected to PCR amplification. To check the PCR amplification products, a 5-µl aliquot of each of the PCR amplification reactions was electrophoresed in a 1% (w/v) agarose gel. The results are illustrated in **Figure 6.9**, and these indicated that a product with an estimated size of 1.8 kb was produced in 2/60 (3%) clones.

The two bacterial clones carrying recombinant plasmids were inoculated separately into 10 ml of LB medium with ampicillin at 100 µg/ml, and then incubated at 37°C overnight. Plasmid DNA was purified from the bacterial cultures using a Wizard Miniprep DNA Purification System. Plasmids were then checked for the presence of the correctly sized DNA insert by restriction enzyme digestion of a 0.5-µg sample with *Xho*I in a 25-µl reaction, followed by analysis by electrophoresis in 1% (w/v) agarose gels. The results are given in **Figure 6.10**, and these indicated that both recombinant plasmids contained a DNA insert of the expected size at 1.8 kb.

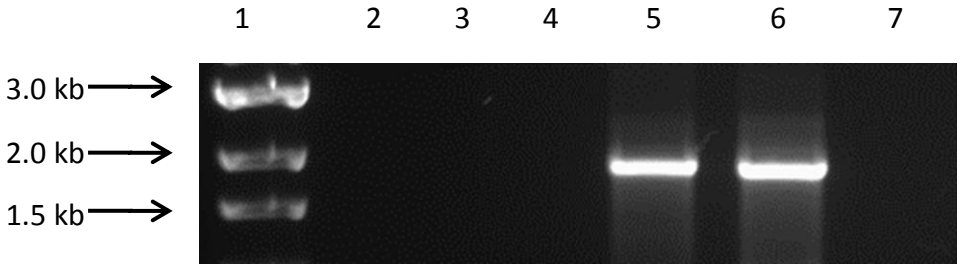

Figure 6.9: Agarose gel of PCR amplification products arising from the screening of *E. coli* JM109 clones isolated from the pET14b/CaSR-ECD cDNA cloning experiment.

DNA prepared from *E. coli* JM109 clones (*n* = 60) was subjected to PCR amplification using primers CASR-ECD-F and CASR-ECD-R. The PCR amplification products were analysed by electrophoresis in 1% (w/v) agarose gels. The gel shows: 1-kb DNA Ladder with DNA fragments from 500 to 10,000 bp (lane 1); clone 1 DNA amplified with primers CASR-ECD-F and CASR-ECD-R (lane 2); clone 2 DNA amplified with primers CASR-ECD-F and CASR-ECD-R (lane 3); clone 3 DNA amplified with primers CASR-ECD-F and CASR-ECD-R (lane 4); clone 4 DNA amplified with primers CASR-ECD-F and CASR-ECD-R (lane 5); clone 5 DNA amplified with primers CASR-ECD-F and CASR-ECD-R (lane 6); and no DNA control with primers CASR-ECD-F and CASR-ECD-R (lane 7).

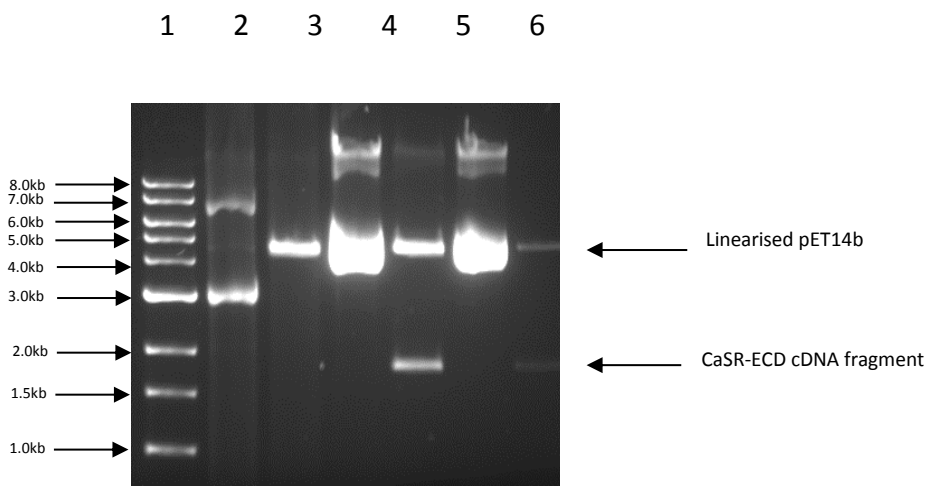

Figure 6.10: Agarose gel of recombinant plasmids from the pET14b/CaSR-ECD cDNA cloning experiment.

The recombinant plasmids prepared from two *E. coli* JM109 clones were restricted with *Xho*I to determine the presence of a CaSR-ECD cDNA insert. The 1% (w/v) agarose gel shows: 1-kb DNA Markers with DNA fragments from 500-10,000 base pairs (lane 1); unrestricted pET14b (lane 2); *Xho*I-restricted pET14b (lane 3); unrestricted recombinant plasmid 1 (lane 4); *Xho*I-restricted recombinant plasmid 1 (lane 5); unrestricted recombinant plasmid 2 (lane 6); *Xho*I-restricted recombinant plasmid 2 (lane 7).

6.4.2.7 Sequencing of the CaSR-ECD cDNA fragment cloned in pET14b

To determine the orientation of the DNA insert and to verify that the CaSR-ECD cDNA was in-frame with the 6XHis-tag in pET14b, both recombinant plasmids were subjected to DNA sequencing using the T7 Promoter primer. The results verified that the recombinant plasmids contained the CaSR-ECD cDNA fragment in the correct reading frame for expression as a 6XHis-CaSR-ECD fusion protein (**Figure 6.11**). One recombinant plasmid was designated as pET14b-CaSR-ECD (**Figure 6.11**), and this was used in further experiments. A large-scale plasmid preparation of pET14b-CaSR-ECD was carried out as detailed in **Section 2.7.**

6.4.3 Expression of the CaSR-ECD in *E. coli* BL21 strains

6.4.3.1 Transformation of *E. coli* BL21 strains with pET14b-CaSR-ECD, pET14b, and pPROEX-HTb-CaSREX

Initially, *E. coli* strains BL21 (DE3), BL21 (DE3)pLysS, BL21 GOLD (DE3)pLysS, BL21 GOLD (DE3), and BL21 CODONPLUS (DE3)-RIPL (Agilent Technologies Inc., Santa Clara, CA, USA) were transformed with plasmids pET14b-CaSR-ECD, pET14b, and pPROEX-HTb-CaSREx, as detailed earlier (**Section 2.13**). Transformants were selected on LB agar containing ampicillin at 100 µg/ml. Following overnight incubation at 37°C, 10 individual bacterial colonies from the transformation were purified by streaking on to fresh LB agar containing ampicillin at 100 µg/ml and subsequently incubating at 37°C overnight.

For screening of *E. coli* BL21 transformants for recombinant plasmids, 10 individual bacterial clones were inoculated separately into 10 ml of LB medium with ampicillin at 100 µg/ml, and then incubated at 37°C overnight. Subsequently, plasmid DNA was purified from individual transformants using a Wizard Miniprep DNA Purification System, and plasmids analysed by electrophoresis in a 1% (w/v) agarose gel. One transformant of each *E. coli* BL21 strain containing pET14b-CaSR-ECD, pET14b or pPROEX-HTb-CaSREx was kept as a frozen stock at -80°C, as detailed in **Section 2.4.**

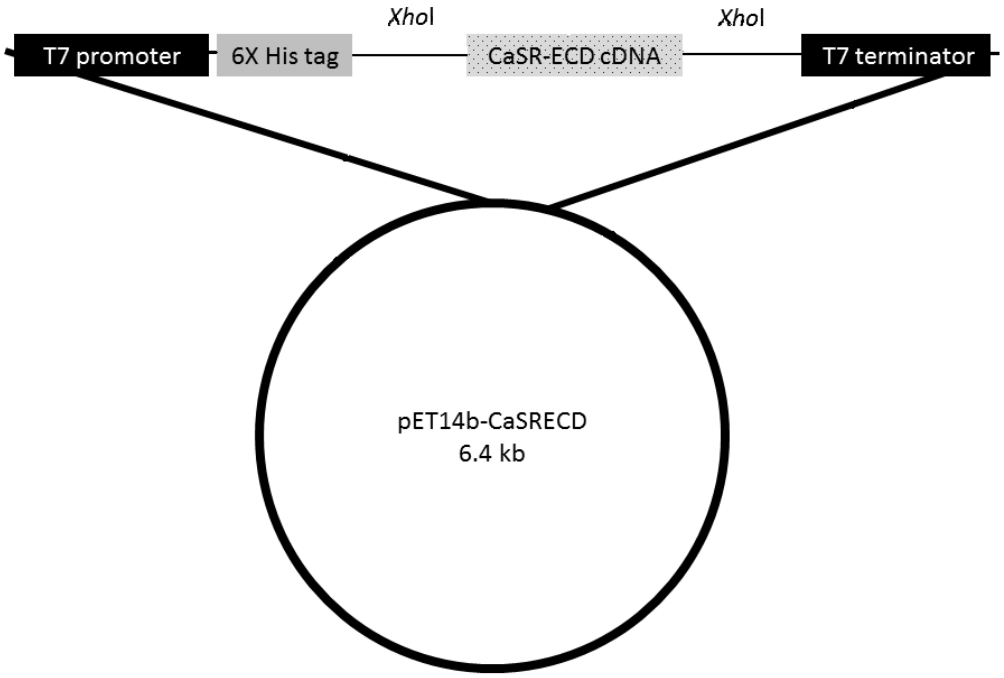

Nucleotide sequence from the start of the 6XHis-CaSR-ECD fusion protein:

ATGGGCAGCAGCCATCATCATCATCATCACAGCAGCGGCCTGGTGCCGCGCGGCAGCCATATG*CTCGAG*ATG

Amino acid sequence from the start of the 6XHis-CaSR-ECD fusion protein:

MGSSHHHHHHSSGLVPRGSH**M**LEMAFYSCCWVLLALTWHTSAYGPDQRAQKKGDIILGGLFPIHFGVAA
KDQDLKSRPESVECIRYNFRGFRWLQAMIFAIEEINSSPALLPNLTLGYRIFDTCNTVSKALEATLSFV
AQNKIDSLNLDEFCNCSEHIPSTIAVVGATGSGVSTAVANLLGLFYIPQVSYASSSRLLSNKNQFKSFL
RTIPNDEHQATAMADIIEYFRWNWVGTIAADDDYGRPGIEKFREEAEERDICIDFSELISQYSDEEEIQ
HVVEVIQNSTAKVIVVFSSGPDLEPLIKEIVRRNITGKIWLASEAWASSSLIAMPQYFHVVGGTIGFAL
KAGQIPGFREFLKKVHPRKSVHNGFAKEFWEETFNCHLQEGAKGPLPVDTFLRGHEESGDRFSNSSTAF
RPLCTGDENISSVETPYIDYTHLRISYNVYLAVYSIAHALQDIYTCLPGRGLFTNGSCADIKKVEAWQV
LKHLRHLNFTNNMGEQVTFDECGDLVGNYSIINWHLSPEDGSIVFKEVGYYNVYAKKGERLFINEEKIL
WSGFSREVPFSNCSRDCLAGTRKGIIEGEPTCCFECVECPDGEYSDETDASACNKCPDDFWSNENHTSC
IA

Figure 6.11: Schematic diagram of plasmid pET14b-CaSR-ECD.

The nucleotide and amino acid sequences of the N-terminal of the 6XHis-CaSR-ECD fusion protein are shown. In the nucleotide sequence, the 6XHis codons are underlined and the ATG codon is given in bold. The 5' *Xho*I restriction site is in *italics* and underlined. In the amino acid sequence, the 6XHis-tag is underlined and the methionine start is given in bold. The positions of the T7 promoter and T7 terminator primers are indicated.

6.4.3.2 Small-scale expression of the CaSR-ECD in *E. coli* BL21 strains

For small-scale expression of the CaSR-ECD, a fresh overnight colony of the required *E. coli* BL21 strain was inoculated into 10 ml of LB medium containing ampicillin at 100 µg/ml. The culture was incubated with shaking at 37°C until an OD_{600} of 0.5 was reached after approximately 2-3 h. Subsequently, 3 ml of the culture was transferred to 50 ml of LB without antibiotics and incubated with shaking at 37°C until an OD_{600} of 0.5 was reached. At this point, a 1-ml aliquot of the culture was removed into a 1.5-ml microfuge tube on ice and designated as the uninduced sample (T=0). To the remaining culture, isopropyl β-D-1-thiogalactopyranoside (IPTG) (Sigma-Aldrich) was added to a final concentration of 1 mM and incubation of the culture continued in order to induce the expression of the CaSR-ECD. At time points of 1 h (T=1), 2 h (T=2), 3 h (T=3) and 4 h (T=4), the OD_{600} of the culture was taken, and a 1-ml sample was removed to a 1.5-ml microfuge tube on ice. The collected samples were centrifuged at 13,000 *g* and the cell pellet stored at -80°C. Identical experiments were undertaken with *E. coli* BL21 strains containing pET14b.

Before analysis by SDS-PAGE, the resuspended cell pellets were diluted with PBS to equivalent OD_{600} values so that the same amount of cell extract was loaded on to SDS-polyacrylamide gels. Samples of cell extract (10 µl) from uninduced and IPTG-induced BL21/pET14b-CaSR-ECD, BL21/pET14b and BL21/pPROEX-HTb-CaSREx strains were mixed with 10 µl of SDS-sample buffer (**Section 2.17**), heated at 95°C, and applied to 10% (w/v) SDS-polyacrylamide gels. Following SDS-PAGE (**Section 2.17**), gels were stained with Coomassie® Blue stain and then destained to reveal the separated proteins (**Section 2.17**).

For the BL21/pET14b strains, no difference was evident between the proteins in the cell extracts made from uninduced and IPTG-induced cultures. This is illustrated as a hourly time-course for BL21 (DE3)/pET14b in **Figure 6.12a**. For the BL21/pET14b-CaSR-ECD strains, a band of increased intensity at 70 kDa was clearly visible in cell extracts that were made from cultures 1 h after IPTG had been added. This is illustrated as a hourly time-course for strain BL21 (DE3)/pET14b-CaSR-ECD in **Figure 6.12b**. The expected size of the CaSR-ECD protein was 66 kDa. **Figures 6.13a and b** show expression of the CaSR-ECD in all of the BL21/pET14b-CaSR-ECD strains analysed at times T=0 and T=4. **Figure 6.13c** shows

the expression of the CaSR-ECD in strain BL21 CODONPLUS (DE3)-RIPL/pPROEX-HTb-CaSREx at T=0 and T=4.

6.4.3.3 Western blotting of uninduced and induced *E. coli* BL21/pET14b-CaSR-ECD cell extracts

Before analysis by western blotting, samples of cell extract (10 µl) from uninduced and IPTG-induced BL21/pET14b-CaSR-ECD strains were mixed with 10 µl of SDS-sample buffer (**Section 2.17**), heated at 95°C, and applied to 10% (w/v) SDS-polyacrylamide gels. Following SDS-PAGE (**Section 2.17**), gels were subjected to western blotting as detailed in **Section 2.19**. After the transfer of proteins to PVDF membrane, the blots were probed with either primary anti-His-tag antibody (**Table 2.6**) (Life Technologies Ltd., Paisley, UK) or anti-CaSR antibody ab79829 against the CaSR (**Table 2.6**) (Abcam, Inc., Cambridge, MA, USA). Both were used at a 1:500 dilution. Appropriate secondary antibodies were anti-mouse IgG-HRP (**Table 2.6**) and anti-rabbit IgG-HRP (**Table 2.6**), respectively, and these were used at a 1:2000 dilution.

The results indicated that following IPTG-induction, a protein band of approximately 70 kDa, which reacted with both primary anti-His-tag and anti-CaSR antibodies, was present in cell extracts made from all the different BL21/pET14b-CaSR-ECD strains used for expression. However, the protein band was not seen in cell extracts prepared from uninduced cultures. This is illustrated in **Figures 6.14a and b** for strain BL21 CODONPLUS (DE3)-RIPL/pET14b-CaSR-ECD.

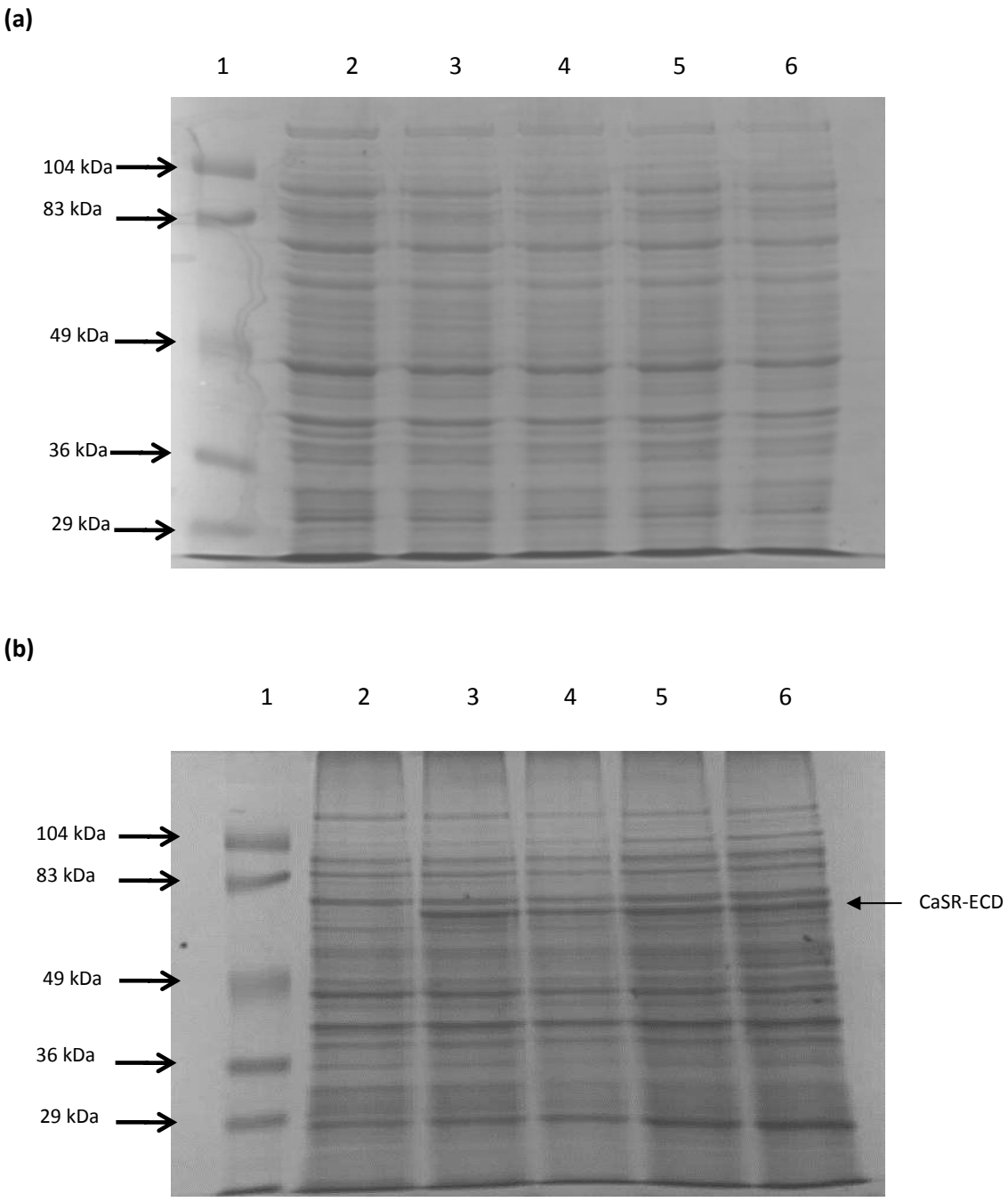

Figure 6.12: SDS-PAGE and Coomassie blue staining of gels containing cell extracts of *E. coli* BL21 (DE3)/pET14b-CaSR-ECD and *E. coli* BL21 (DE3)/pET14b strains

Cell extracts were prepared from *E. coli* BL21 (DE3)/pET14b-CaSR-ECD and BL21 (DE3)/pET14b strains prior to and following the addition of IPTG. The 10% (w/v) SDS-polyacrylamide gels show: **(a)** Prestained SDS-PAGE Standards, Low Range (20-104 kDa) (lane 1); uninduced (T=0) BL21 (DE3)/pET14b (lane 2); post induction (T=1) BL21 (DE3)/pET14b (lane 3); post induction (T=2) BL21 (DE3)/pET14b (lane 4); post induction (T=3) BL21 (DE3)/pET14b (lane 5); and post induction (T=4) BL21 (DE3)/pET14b (lane 6). **(b)** Prestained SDS-PAGE Standards, Low Range (lane 1); uninduced (T=0) BL21 (DE3)/pET14b-CaSR-ECD (lane 2); post induction (T=1) BL21 (DE3)/pET14b-CaSR-ECD (lane 3); post induction (T=2) BL21 (DE3)/pET14b-CaSR-ECD (lane 4); post induction (T=3) BL21 (DE3)/pET14b-CaSR-ECD (lane 5); and post induction (T=4) BL21 (DE3)/pET14b-CaSR-ECD (lane 6).

(a)

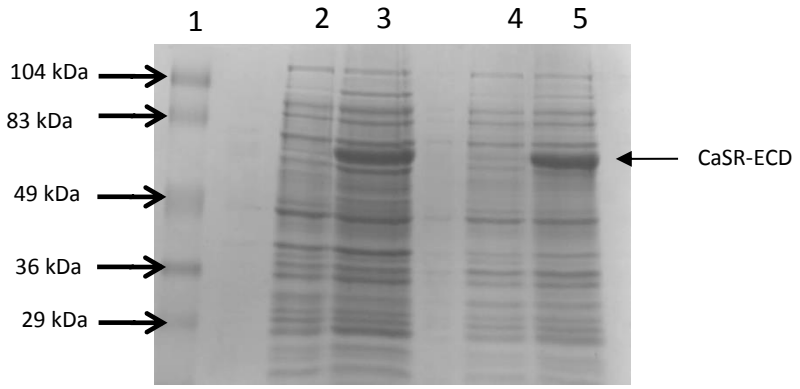

(b)

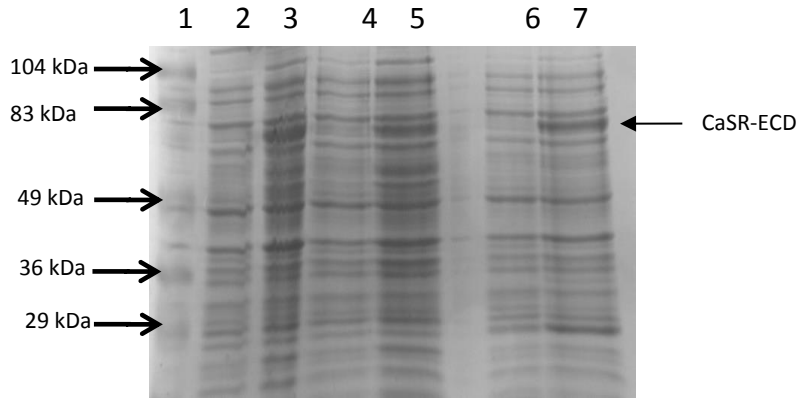

Figure 6.13: SDS-PAGE and Coomassie blue staining of gels containing cell extracts of *E. coli* BL21/pET14b-CaSR-ECD strains.

Cell extracts were prepared from *E. coli* BL21/pET14b-CaSR-ECD strains prior to and following the addition of IPTG to induce the expression of CaSR-ECD. The 10% (w/v) SDS-polyacrylamide gels show: **(a)** Prestained SDS-PAGE Standards, Low Range (20-104 kDa) (lane 1); uninduced (T=0) BL21 (DE3)pLysS/pET14b-CaSR-ECD (lane 2); post induction (T=4) BL21 (DE3)pLysS/pET14b-CaSR-ECD (lane 3); uninduced (T=0) BL21 GOLD (DE3)pLysS/pET14b-CaSR-ECD (lane 4); and post induction (T=4) BL21 GOLD (DE3)pLysS/pET14b-CaSR-ECD (lane 5). **(b)** Prestained SDS-PAGE Standards, Low Range (lane 1); uninduced (T=0) BL21 (DE3)/pET14b-CaSR-ECD (lane 2); post induction (T=4) BL21 (DE3)/pET14b-CaSR-ECD (lane 3); uninduced (T=0) BL21 GOLD (DE3)/pET14b-CaSR-ECD (lane 4); post induction (T=4) BL21 GOLD (DE3)/pET14b-CaSR-ECD (lane 5); uninduced (T=0) BL21 CODONPLUS (DE3)-RIPL/pET14b-CaSR-ECD (lane 6); and post induction (T=4) BL21 CODONPLUS (DE3)-RIPL/pET14b-CaSR-ECD (lane 7). **(c)** Prestained SDS-PAGE Precision Plus Protein™ Standards (20-250 kDa) (lane 1); uninduced (T=0) BL21 CODONPLUS (DE3)-RIPL/pPROEX-HTb-CaSREx (lane 2); and post induction (T=4) BL21 CODONPLUS (DE3)-RIPL/pPROEX-HTb-CaSR-Ex (lane 3).

(c)

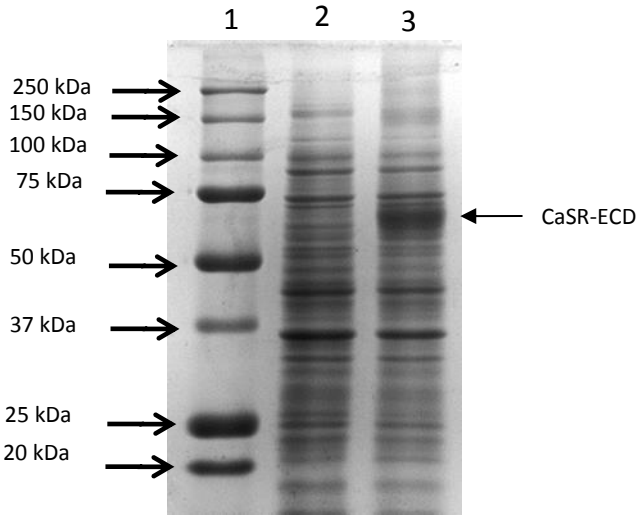

Figure 6.13: SDS-PAGE and Coomassie blue staining of gels containing cell extracts of *E. coli* BL21/pET14b-CaSR-ECD strains.

Cell extracts were prepared from *E. coli* BL21/pET14b-CaSR-ECD strains prior to and following the addition of IPTG to induce the expression of CaSR-ECD. The 10% (w/v) SDS-polyacrylamide gels show: **(a)** Prestained SDS-PAGE Standards, Low Range (20-104 kDa) (lane 1); uninduced (T=0) BL21 (DE3)pLysS/pET14b-CaSR-ECD (lane 2); post induction (T=4) BL21 (DE3)pLysS/pET14b-CaSR-ECD (lane 3); uninduced (T=0) BL21 GOLD (DE3)pLysS/pET14b-CaSR-ECD (lane 4); and post induction (T=4) BL21 GOLD (DE3)pLysS/pET14b-CaSR-ECD (lane 5). **(b)** Prestained SDS-PAGE Standards, Low Range (lane 1); uninduced (T=0) BL21 (DE3)/pET14b-CaSR-ECD (lane 2); post induction (T=4) BL21 (DE3)/pET14b-CaSR-ECD (lane 3); uninduced (T=0) BL21 GOLD (DE3)/pET14b-CaSR-ECD (lane 4); post induction (T=4) BL21 GOLD (DE3)/pET14b-CaSR-ECD (lane 5); uninduced (T=0) BL21 CODONPLUS (DE3)-RIPL/pET14b-CaSR-ECD (lane 6); and post induction (T=4) BL21 CODONPLUS (DE3)-RIPL/pET14b-CaSR-ECD (lane 7). **(c)** Prestained SDS-PAGE Precision Plus Protein™ Standards (20-250 kDa) (lane 1); uninduced (T=0) BL21 CODONPLUS (DE3)-RIPL/pPROEX-HTb-CaSREx (lane 2); and post induction (T=4) BL21 CODONPLUS (DE3)-RIPL/pPROEX-HTb-CaSR-Ex (lane 3).

(a)

(b)

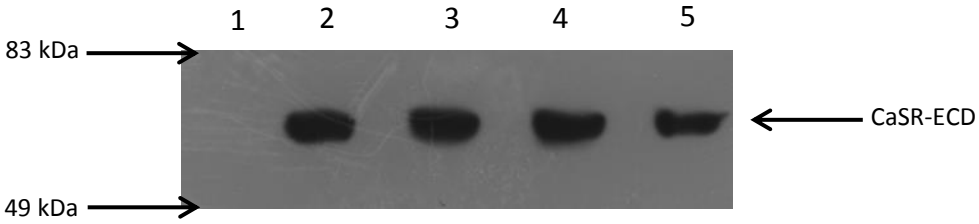

Figure 6.14: Western blotting of cell extracts of *E. coli* BL21 CODONPLUS (DE3)-RIPL/pET14b-CaSR-ECD.

Cell extracts were prepared from *E. coli* BL21 CODONPLUS (DE3)-RIPL/pET14b-CaSR-ECD prior to and following the addition of IPTG to induce the expression of CaSR-ECD. The extracts were applied to 10% (w/v) SDS-polyacrylamide gels, and then the separated proteins subjected to western blotting with primary anti-His-tag and anti-CaSR antibodies. **(a)** Western blot of cell extracts probed with anti-CaSR antibody. Uninduced (T=0) BL21 CODONPLUS (DE3)-RIPL/pET14b-CaSR-ECD (lane 1); post induction (T=2) BL21 CODONPLUS (DE3)-RIPL/pET14b-CaSR-ECD (lane 2); and post induction (T=4) BL21 CODONPLUS (DE3)-RIPL/pET14b-CaSR-ECD (lane 3). **(b)** Western blot of cell extracts probed with anti-His-tag antibody. Uninduced (T=0) BL21 CODONPLUS (DE3)-RIPL/pET14b-CaSR-ECD (lane 1); post induction (T=1) BL21 CODONPLUS (DE3)-RIPL/pET14b-CaSR-ECD (lane 2); post induction (T=2) BL21 CODONPLUS (DE3)-RIPL/pET14b-CaSR-ECD (lane 3); post induction (T=3) BL21 CODONPLUS (DE3)-RIPL/pET14b-CaSR-ECD (lane 2); and post induction (T=4) BL21 CODONPLUS (DE3)-RIPL/pET14b-CaSR-ECD (lane 3). Prestained SDS-PAGE Standards, Low Range (20-104 kDa) were included in the gels.

6.4.4 Purification of the His-tagged CaSR-ECD

6.4.4.1 Large-scale expression of the His-tagged CaSR-ECD

E. coli BL21 CODONPLUS (DE3)-RIPL/pET14b-CaSR-ECD and BL21 CODONPLUS (DE3)-RIPL/pPROEX-HTb-CaSREx were chosen for large-scale expression of His-tagged CaSR-ECD, as they showed the best results for the expression of the His-tagged CaSR-ECD, based on the results of the Coomassie blue staining of gels and western blotting. A small-scale culture was prepared by inoculating a single colony of the bacterial strain into 10 ml of LB medium with ampicillin at 100 µg/ml. This was grown with shaking at 37°C until an OD_{600} of 0.5 was reached after approximately 2-3 h. Subsequently, 5 ml of the culture was transferred to 100 ml of LB medium with ampicillin at 100 µg/ml and incubated with shaking at 37°C until an OD_{600} of 0.5 was reached. Then, 50 ml of the culture were transferred to 500 ml of LB medium and the culture incubated with shaking at 37°C until an OD_{600} of 1.0 was reached. Samples (1-ml) of the culture were collected and labelled as uninduced (T=0). Following this, IPTG was added to a final concentration of 1 mM and incubation of the culture continued for 3 h to induce the expression of the His-tagged CaSR-ECD. After measuring the OD_{600}, samples of 1 ml were collected and labelled as induced (T=3). All culture samples were spun at 13,000 *g* and the pellets kept for analysis at -80°C. The remainder of the culture was harvested at 6,000 *g* for 15 min at 4°C. The cell pellet was weighed and then stored at -80°C until analysis. The 1-ml culture samples were used to confirm His-tagged CaSR-ECD expression using SDS-PAGE, as described in **Section 6.4.3.2**, before proceeding with purification of the His-tagged CaSR-ECD from the cell pellet of the large-scale culture.

6.4.4.2 Solubility of the His-tagged CaSR-ECD

Solubility analysis was undertaken to determine whether the His-tagged CaSR-ECD was in soluble form or was present as an insoluble form as inclusion bodies. The cell pellet from the 500-ml culture containing expressed His-tagged CaSR-ECD was resuspended in 10 ml of phosphate-buffered saline containing Protease Inhibitor Cocktail (Roche, Mannheim, Germany). To lyse the cells, lysozyme (Sigma-Aldrich) was added to concentration of 200

µg/ml followed by incubation on ice for 20 min. Subsequently, sodium deoxycholate (Sigma-Aldrich) was added to a final concentration of 200 µg/ml, and the lysed cells left for 20 min on ice with gentle mixing. The lysed cells were sonicated for four times for 10 sec and then centrifuged at 20,000 *g* for 20 min at 4°C. The supernatant was removed and the pellet of inclusion bodies was resuspended in 20 ml of inclusion body wash buffer (30 mM Tris-hydrochloride, pH 8.0; 5 mM dithiothreitol; 2 M urea; 2% (v/v) Triton X-100) using a SHM1 handheld homogeniser (Bibby Scientific Limited, Stone, UK) for three 20-sec bursts at 10,000 rpm at 4°C with a 20-sec break between bursts.

Samples of 10 µl of the supernatant and the resuspended inclusion bodies were added to 10 µl of SDS-sample buffer (**Section 2.17**), heated at 95°C**,** and analysed by SDS-PAGE (**Section 2.17**). The results of Coomassie blue staining of the gel are illustrated in **Figure 6.15**, with the His-tagged CaSR-ECD clearly present in the insoluble inclusion body fraction.

(a)

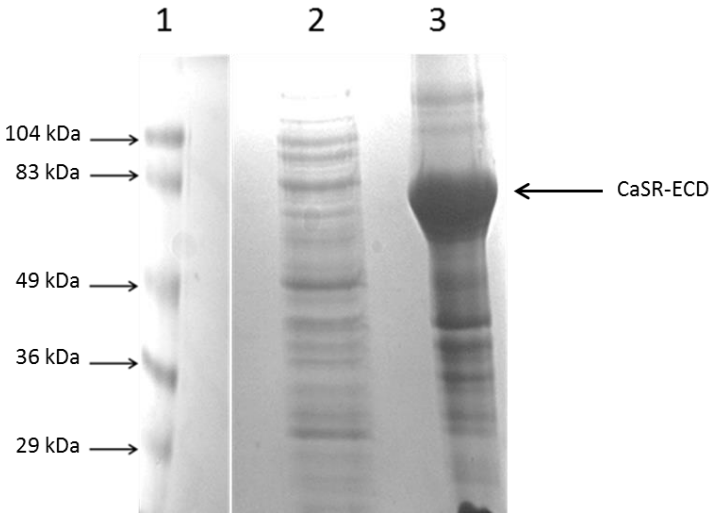

(b)

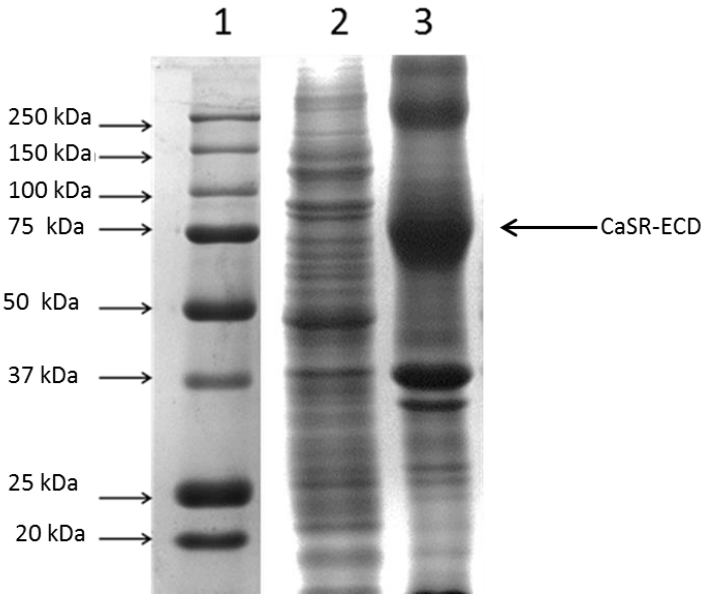

Figure 6.15: Solubility of the His-tagged CaSR-ECD.

Samples (10 µl) of the soluble and insoluble fractions from the large-scale cell extracts were applied to a 10% (w/v) SDS-polyacrylamide gel. The results show: **(a)** Prestained SDS-PAGE Standards, Low Range (20-104 kDa) (lane 1); soluble fraction of extract of BL21 CODONPLUS (DE3)-RIPL/pET14b-CaSR-ECD (lane 2); and insoluble fraction (inclusion bodies) of extract of BL21 CODONPLUS (DE3)-RIPL/pET14b-CaSR-ECD (lane 3). **(b)** Prestained SDS-PAGE Precision Plus Protein™ Standards (20-250 kDa) (lane 1); soluble fraction of extract of BL21 CODONPLUS (DE3)-RIPL/pPROEX-HTb-CaSREx (lane 2); and insoluble fraction (inclusion bodies) of extract of BL21 CODONPLUS (DE3)-RIPL/pPROEX-HTb-CaSREx (lane 3).

6.4.4.3 Purification and solubilisation of inclusion bodies containing the His-tagged CaSR-ECD

Resuspended inclusion bodies (**Section 6.4.4.2**) were collected by centrifugation at 30,000 *g* for 30 min at 4°C. A 20-µl sample of the supernatant was saved and remainder was discarded. The pelleted inclusion bodies were washed three times (washes 1-3) using inclusion body wash buffer (**Section 6.4.4.2**). Samples (20-µl) of the supernatant were retained after each wash. The final wash (wash 4) was done with inclusion body wash buffer without Triton X-100, and with centrifugation at 40,000 *g* for 40 min at 4°C. Again, a 20-µl sample of the supernatant was saved.

The pellet of inclusion bodies was resuspended in buffer (20 mM Tris-hydrochloride, pH 8.0; 1 M sodium chloride), and centrifuged at 40,000 *g* for 20 min at 4°C. A 20-µl sample of supernatant was retained (wash 5). Next, the inclusion body pellet was resuspended in 20 mM Tris-hydrochloride (pH 8.0) and centrifuged as before (wash 6), and a 20-µl sample of the supernatant was saved. The inclusion body pellet was solubilised in buffer containing 30 mM Tris-hydrochloride (pH 8.0), 6 M guanidine hydrochloride and 100 mM sodium chloride, overnight at 4°C. The solubilised inclusion bodies were then centrifuged at 40,000 *g* for 45 min at 4°C, and the supernatant containing the solubilised His-tagged CaSR-ECD protein was collected and stored at 4°C.

The supernatants from the washing procedures and the final solubilised protein were analysed by SDS-PAGE. Samples of 10 µl were added to 10 µl of SDS-sample buffer (**Section 2.17**), heated at 95°C**,** and analysed by SDS-PAGE (**Section 2.17**). The results of Coomassie blue staining of the gel are illustrated in **Figure 6.16**, and show the His-tagged CaSR-ECD protein remaining in the pellet at each stage of washing.

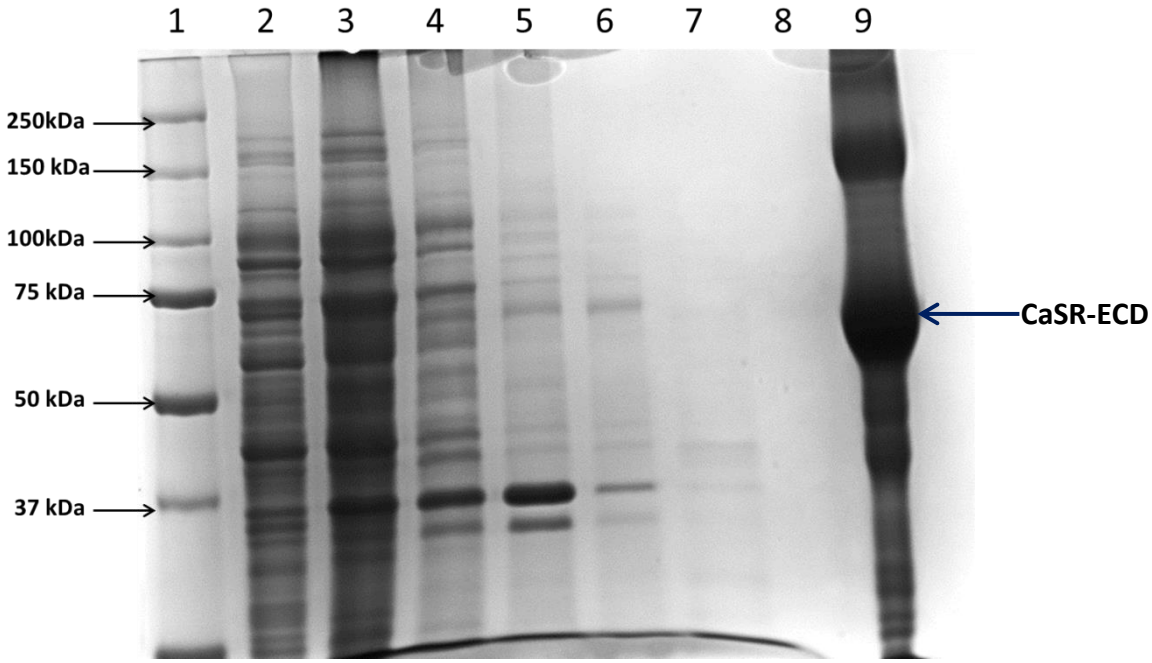

Figure 6.16: SDS-PAGE analysis of the preparation of inclusion bodies of the His-tagged CaSR-ECD.

Samples (10 µl) of the soluble and insoluble fractions and washes from the inclusion body preparation were analysed by SDS-PAGE in a 10% (w/v) SDS-polyacrylamide gel. The result shows: Prestained SDS-PAGE Standards Precision Plus Protein™ (range 20-250 kDa) (lane 1); soluble fraction of extract of BL21 CODONPLUS (DE3)-RIPL/pPROEX-HTb-CaSREx cells (lane 2); supernatant from wash 1 of inclusion bodies (lane 3); supernatant from wash 2 of inclusion bodies (lane 4); supernatant from wash 3 of inclusion bodies (lane 5); supernatant from wash 4 of inclusion bodies (lane 6); supernatant from wash 5 of inclusion bodies (lane 7); supernatant from wash 6 of inclusion bodies (lane 8); and solubilised inclusion bodies of the His-tagged CaSR-ECD (lane 9).

6.4.4.4 Purification of His-tagged CaSR-ECD by Ni^{2+}-chelation chromatography

6.4.4.4.1 Use of HisTrap FF Crude columns

Initial attempts to purify the solubilised His-tagged CaSR-ECD (obtained from both *E. coli* BL21 CODONPLUS (DE3)-RIPL/pET14b-CaSR-ECD and BL21 CODONPLUS (DE3)-RIPL/pPROEX-HTb-CaSREx) (**Section 6.4.4.2**) used HisTrap FF Crude 1-ml columns (GE Healthcare, Little Chalfont, UK). The columns were prepacked with pre-charged Ni Sepharose 6 Fast Flow. The column was rinsed with 10 column volumes of filtered water at 2 ml per min and then equilibrated with 10 column volumes of equilibration buffer (30 mM Tris-hydrochloride, pH 8.0; 6 M guanidine hydrochloride; 100 mM sodium chloride; 20 mM imidazole) at 2 ml per min. Before the solubilised his-tagged CaSR-ECD protein was loaded onto the column, 20 mM imidazole was to the protein added to reduce the chance of non-specific binding of the protein to the column. His-tagged CaSR-ECD protein was loaded on to the column at 2 ml per min and the flow-through collected. Attempts were then made to wash the with 10 column volumes of wash buffer (30 mM Tris-hydrochloride, pH 8.0; 100 mM sodium chloride; 50 mM imidazole) at 2 ml per min. However, there was no flow through the column at this point. In order to alleviate the problem with flow through the column, 6 M guanidine hydrochloride was included in the wash buffer, in order to keep the His-tagged CaSR-ECD protein solubilised. However, there was no improvement in flow through the column when washing buffer was applied.

6.4.4.4.2 Use of cOmplete™ His-Tag purification resin

A second protocol for purifying the His-tagged CaSR-ECD protein used cOmplete™ His-Tag purification resin (Roche Mannheim, Germany). The resin was used to pack a disposable 5-ml Polypropylene Column (Qiagen, Manchester, UK). The column was rinsed with 10 column volumes of filtered water at 2 ml per min and then equilibrated with 10 column volumes of equilibration buffer (30 mM Tris-hydrochloride, pH 8.0; 6 M guanidine hydrochloride; 100 mM sodium chloride; 20 mM imidazole) at 2 ml per min. Before the solubilised his-tagged CaSR-ECD protein was loaded onto the column, 20 mM imidazole was to the protein added to reduce the chance of non-specific binding of the protein to the column. His-tagged CaSR-ECD protein was loaded on to the column at 2 ml per min

and the flow-through collected. The column was washed with 10 column volumes of wash buffer (30 mM Tris-hydrochloride, pH 8.0; 6 M guanidine hydrochloride; 100 mM sodium chloride; 50 mM imidazole) at 2 ml per min. The elution of the protein was performed in two stages. Firstly, elution buffer 1 (30 mM Tris-hydrochloride, pH 8.0; 6 M guanidine hydrochloride; 100 mM sodium chloride; 150 mM imidazole) was applied to the column followed by elution buffer 2 (30 mM Tris-hydrochloride, pH 8.0; 6 M guanidine hydrochloride; 100 mM sodium chloride; 500 mM imidazole). Seven 1-ml fractions were collected during each of the two elution steps. A sample of each fraction was analysed qualitatively in a Bradford protein assay according to the manufacturer's protocol (Bio-Rad Laboratories Ltd. Hemel Hempstead, UK), in order to determine which fractions contained protein.

Of the 14 fractions analysed, fractions 8-11 obtained after elution with buffer containing 500 mM imidazole were the ones that contained the protein. The four fractions containing the protein were pooled. Then, to remove guanidine hydrochloride and imidazole, the pooled protein fractions were dialysed in SnakeSkin™ Dialysis Tubing, 10K MWCO (Life Technologies Ltd., Paisley, UK) against dialysis buffer containing 30 mM Tris-hydrochloride (pH 8.0) and 100 mM sodium chloride. This was carried out at 4°C overnight. However, during dialysis, the His-tagged CaSR-ECD precipitated from solution.

6.4.4.5 Purification of His-tagged CaSR-ECD using gel-filtration chromatography

6.4.4.5.1 Gel-filtration

As there was no success with using Ni^{2+}-chelation chromatography, gel-filtration chromatography was used as an alternative method to purify the His-tagged CaSR-ECD. This method separates molecules according to their size as they pass through a matrix filled column.

For gel-filtration chromatography, a XK 16/100 column (GE Healthcare) was packed with 150 ml of Superdex™ 200 beads (GE Healthcare) to a height of 70 cm. The column was washed with 200 ml of filtered water to remove the preservation buffer containing 20% (v/v) ethanol. The column was then by equilibrated with equilibration buffer (30 mM Tris-

hydrochloride, pH 8.0; 4 M guanidine hydrochloride; 100 mM sodium chloride) at 1 ml per min. Solubilised inclusion bodies (obtained from *E. coli* BL21 CODONPLUS (DE3)-RIPL/pPROEX-HTb-CaSREx) (**Section 6.4.4.3**) in buffer containing 30 mM Tris-hydrochloride (pH 8.0), 4 M guanidine hydrochloride, and 100 mM sodium chloride were then loaded on to the column. Elution buffer (30 mM Tris-hydrochloride, pH 8.0; 4 M guanidine hydrochloride; 100 mM sodium chloride) was applied to the column at 1 ml per min. The elution of the protein was monitored against time by a BioLogic LP UV detector (Bio-Rad Laboratories Ltd. Hemel Hempstead, UK) at an absorbance of 280 nm. During the elution, approximately 40 fractions of 1.5 ml were collected and these were stored at 4°C. The results of the elution process are given in **Figure 6.17** and show that the protein was eluted between fractions 38 and 42 min from the start of the elution process. From the absorbance, the protein was indicated to be in three fractions (25, 26 and 27) of the eluate.

6.4.4.5.2 Western blot of eluted protein samples

For western blotting analysis of the eluted proteins, samples (10 µl) from the eluted fractions containing the His-tagged CaSR-ECD were mixed with 10 µl of SDS-sample buffer (**Section 2.17**), heated at 95°C, and separated on 10% (w/v) SDS-polyacrylamide gels. Following SDS-PAGE (**Section 2.17**), gels were subjected to western blotting as detailed above in **Section 6.4.3.3**. After the transfer of proteins to PVDF membrane, the blots were probed with anti-CaSR antibody ab79829 (**Table 2.6**) as the primary antibody which was used at a 1:500 dilution. The secondary antibody anti-rabbit IgG-HRP (**Table 2.6**) was used at a 1:2000 dilution.

The results indicated the presence of the His-tagged CaSR-ECD protein in the eluted fractions as a band running at the predicted molecular weight of 70 kDa was detected by the anti-CaSR antibody ab79829 (**Figure 6.18**). A smaller molecular weight band was seen at 50 kDa. This was assumed to be a degradation product of the His-tagged CaSR-ECD protein since it was detected by the anti-CaSR antibody (**Figure 6.18**). No other proteins were visible in the His-tagged CaSR-ECD protein samples when analysed by Coomassie blue staining following SDS-PAGE.

6.4.4.5.3 Concentration of the eluted protein

Fractions containing the His-tagged CaSR-ECD protein were pooled. The concentration of the eluted protein was measured using a Bradford assay according to the manufacturer's protocol (Bio-Rad Laboratories Ltd.). The concentration of the protein was 200 µg/ml. The protein was stored in 20% (v/v) glycerol at -20°C.

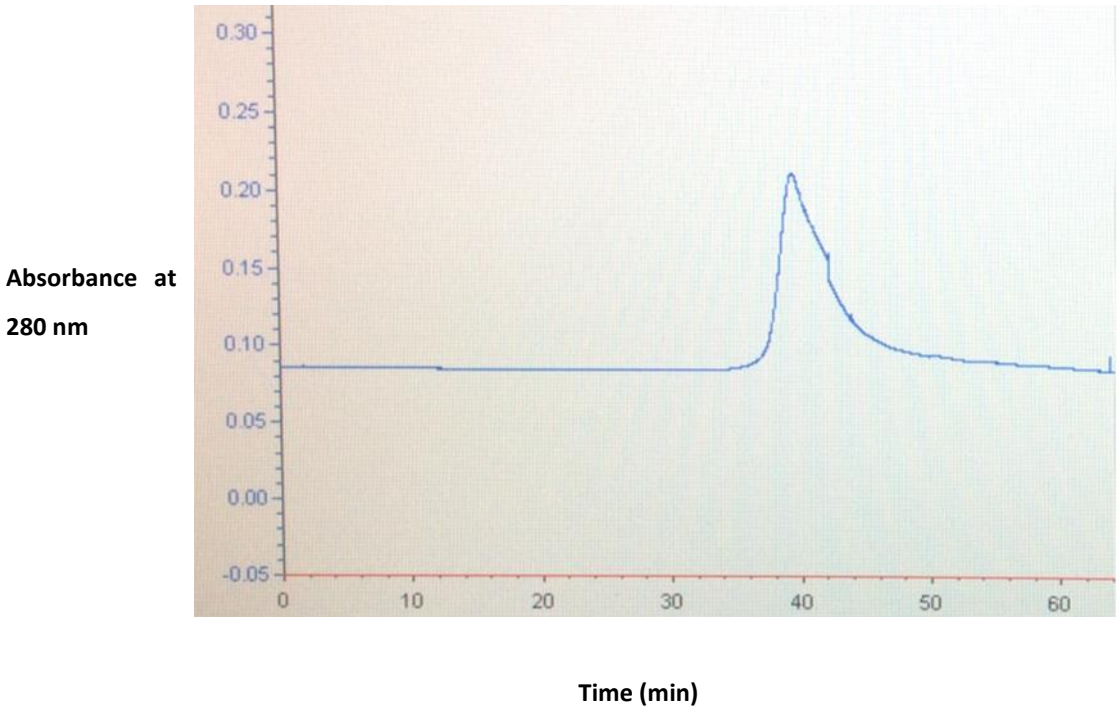

Figure 6.17: The elution of protein by gel-filtration chromatography.

Solubilised inclusion bodies in buffer containing 30 mM Tris-hydrochloride (pH8.0), 4 M guanidine hydrochloride, and 100 mM sodium chloride were loaded on to the gel-filtration column. Elution buffer (30 mM Tris-hydrochloride, pH 8.0; 4 M guanidine hydrochloride; 100 mM sodium chloride) was then applied to the column at 1 ml per min. The elution of the protein was monitored against time at an absorbance of 280 nm, which is shown by the blue line. During elution, fractions of 1.5 ml were collected. The peak shows the time at which the protein was eluted from the column.

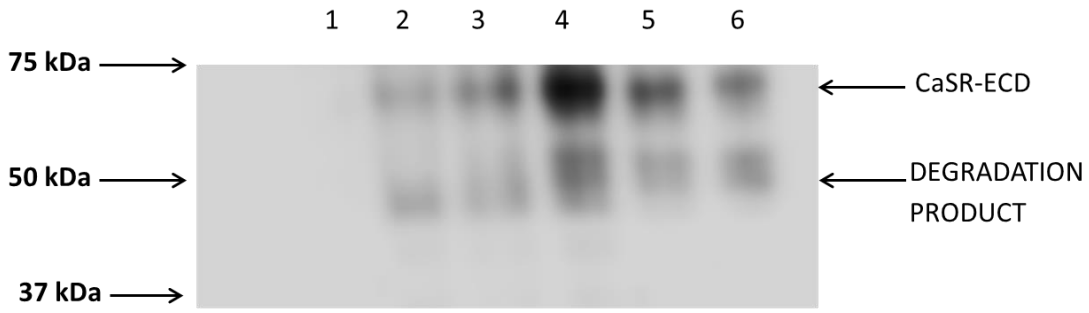

Figure 6.18: Western blotting of fractions eluted from the gel-filtration column during the purification of His-tagged CaSR-ECD expressed in *E. coli* BL21 CODONPLUS (DE3)-RIPL/pPROEX-HTb-CaSREx.

Samples of 10 µl of the fractions from the gel-filtration column, which were presumed to contain the His-tagged CaSR-ECD protein, were applied to a 10% (w/v) SDS-polyacrylamide gel. The separated samples were transferred to PVDF membrane and the blot probed with anti-CaSR antibody ab79829 and secondary antibody anti-rabbit IgG-HRP. The blot shows: Elution fraction 23 (lane 1); elution fraction 24 (lane 2); elution fraction 25 (lane 3); elution fraction 26 (lane 4); elution fraction 27 (lane 5); and elution fraction 28 (lane 6). Prestained SDS-PAGE Standards Precision Plus Protein™ (range 20-250 kDa) were included in the gel.

6.4.5 Use of the purified CaSR-ECD in an ELISA format

6.4.5.1 Assay procedure

For ELISAs, the purified CaSR-ECD was diluted in coating buffer (1.5 mM sodium carbonate; 3.5 mM sodium hydrogen carbonate; pH 9.2) to 200 ng/ml. Samples of 100 µl were used to coat the wells of a 96-well microtitre plate. Plates were then incubated overnight at 4°C. The coating buffer was removed by decanting and the wells were blocked with blocking buffer (PBS; 0.1% (w/v) Tween-20; 3% (w/v) bovine serum albumin) for 30 min at 37°C.

Plates were washed four times with washing buffer (PBS/0.1% (v/v) Tween-20). To avoid possible cross-reactivity with any remaining *E. coli* proteins, all serum samples and antibodies were pre-incubated with *E. coli* BL21 cell lysate (a gift from Dr Helen Kemp, Department of Oncology and Metabolism, University of Sheffield, Sheffield, UK) at 100 µg per 50 µl of diluted serum sample for 30 min. Aliquots of 100 µl of serum at a 1:100 dilution in blocking buffer were added to the wells. Phosphate-buffered saline (pH 7.4) was applied as a control to measure any non-specific binding of the secondary antibody. Anti-CaSR antibodies ab79829 (**Table 2.6**) and CaSR11-S (**Table 2.6**) were used as positive controls at a 1:100 dilution. The plates were incubated at room temperature for 1 h and then washed four times with washing buffer. To detect primary antibody binding, a 100-µl sample of horse-radish peroxidase conjugated to either goat anti-human IgG or goat anti-rabbit IgG (Sigma-Aldrich) diluted to 1:2000 in blocking buffer was added to each well for 1 h at room temperature. After washing five times with washing buffer, 100 µl of 3,3',5,5'-tetramethylbenzidine (TMB) (Sigma-Aldrich) were applied to each well and plates incubated at room temperature away from light for 30-45 min to allow colour development. Stop the colour-forming reaction by the addition of 100 µl of 0.5 M hydrochloric acid. A LabSystems Integrated EIA Management System spectrophotometer was used to read absorption of the wells at 450 nm. All sera were tested in duplicate and the average OD_{450} value taken. Each mean OD_{450} value was corrected for background binding of the sera to the well without antigen.

In each ELISA, the binding reactivity of each patient and control sera to the peptide was expressed as an antibody index calculated as: mean OD_{450} of tested serum/mean OD_{450} of a population of healthy control sera. The antibody index was the mean of three experiments. The upper limit of normal for the ELISA was calculated using the mean antibody index + 3SD of a population of healthy control sera. Sera with an antibody index greater than the upper limit of normal were regarded as antibody-positive.

6.4.5.2 Assay of APS1 patient sera in the CaSR-ECD ELISA

To confirm the presence or not of antibodies against the CaSR-ECD, serum samples from 44 APS1 patients and 10 healthy controls were analysed in an ELISA format, as detailed in **Section 6.4.5.1.** Positive control anti-CaSR antibodies ab79829 and CASR11-S were included in the ELISA.

The results of three experiments testing the 44 APS1 patient and 10 control sera in the CaSR-ECD ELISA are shown in **Figure 6.19.** All control sera were negative for antibodies against the CaSR-ECD, as their antibody indices were below the upper limit of normal (mean antibody index + 3SD of 10 healthy individuals) in the ELISA (**Figure 6.19**). This was calculated as an antibody index of 1.23. In the APS1 patient group, the antibody indices of 15 (34%) patients were above this upper limit of normal (**Figure 6.19**). The mean CaSR antibody index ± SD for the APS1 patient group and for the control group was, respectively, 6.28 ± 9.29 (range: 0.58-28.3) and 1.00 ± 0.08 (range: 0.88-1.10). Anti-CaSR antibodies ab79829 and CASR11-S had an antibody index of 20.1 and 1.04, respectively. The negativity of binding of the CASR11-S to the CaSR-ECD was expected in that the antibody recognises a C-terminal peptide in the full-length receptor which is not present in the purified CaSR-ECD.

6.4.5.3 Analysis of the results of the CaSR-ECD ELISA

Antibody assay precision was evaluated by calculating the intra-assay coefficient of variation (expressed as a percentage) for a series of ten serum samples that were measured in duplicate within the same assay run. The intra-assay coefficient of variation for the CaSR-ECD ELISA was in the range of 7.2-8.4%. Antibody assay reproducibility was

evaluated by calculating the inter-assay coefficient of variation (expressed as a percentage) for a series of six serum samples that were measured in three consecutive assay runs. The inter-assay coefficient of variation for the CaSR-ECD ELISA was 12.2%.

Cohen's kappa was used to measure the agreement between the CaSR immunoprecipitation assay (**Chapter 3**) and the CaSR-ECD ELISA for detecting CaSR autoantibodies (www.statstodo.com/CohenKappa_Pgm.php). Conventionally, a Cohen's kappa is considered of poor agreement at a value of < 0.2, fair at 0.21-0.4, moderate at 0.41-0.6, strong at 0.61-0.8, and near complete agreement at > 0.8. Of the 16 CaSR autoantibody-positive APS1 patient sera, as measured in the CaSR immunoprecipitation assay (**Chapter 3**), 15 were also sero-positive in the CaSR-ECD ELISA. The remaining 29 APS1 patient sera were CaSR autoantibody-negative in the ELISA. The two methods of measuring CaSR autoantibodies concurred in 98% of APS1 cases with near complete agreement between the two assays (Cohen's kappa = 0.95; standard error = 0.05; 95% confidence interval = 0.85-1.05).

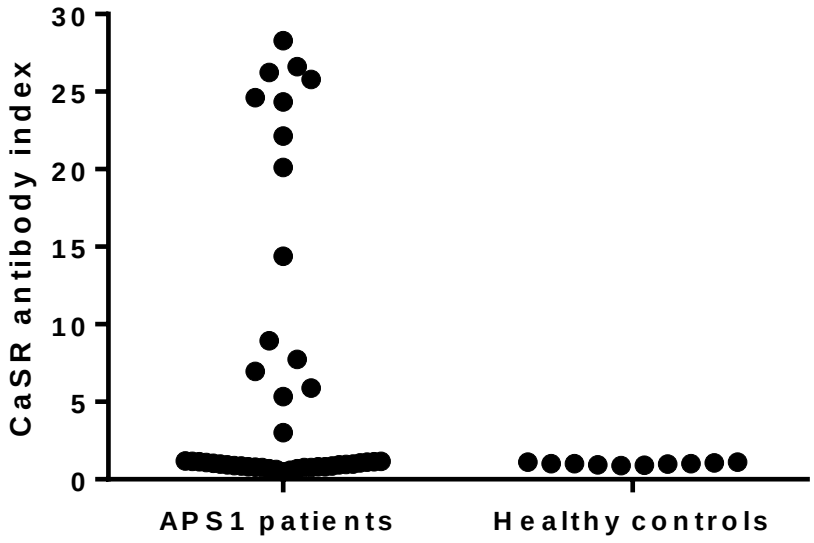

Figure 6.19: CaSR antibody indices of APS1 patient and control sera.

Sera from 44 APS1 patients and 10 healthy controls were evaluated for CaSR antibodies using the CaSR-ECD ELISA. The CaSR antibody index (mean of three experiments) is shown for each APS1 patient and control serum. The mean CaSR antibody index ± SD for the APS1 patient group and for the control group was, respectively, 6.28 ± 9.29 (range: 0.58-28.3) and 1.00 ± 0.08 (range: 0.88-1.10).

6.5 Discussion

All the current assays for CaSR autoantibodies are either labour-intensive, time-consuming or are not quantitative. The aim of this part of the project was to develop an ELISA method that would allow the measurement of CaSR autoantibodies in patient serum samples. This would be based on the CaSR-ECD as antigen for ELISA plate coating. Initially, the CaSR-ECD was expressed in *E. coli* using the pET system. Although this was successful, difficulties were accounted with protein purification using nickel-chelation chromatography to bind the His-tagged CaSR-ECD. Eventually, the CaSR-ECD was purified using gel-filtration chromatography. Future experiments will use a specific antibody column to prepare the CaSR-ECD. A polyclonal or monoclonal antibody will be bound to an activated solid support matrix using a mild and irreversible coupling method that will retain biological activity of the antibody. In the case of the antibodies against the CaSR, several polyclonal and monoclonal antibodies are available which recognise different epitopes on the receptor. As antigen-binding affinity varies between different antibodies, binding and elution conditions will need to be optimised.

The purified CaSR-ECD was then used in an ELISA format to detect autoantibodies against the receptor's ECD in APS1 patient sera. All of the 15 APS1 patient sera that were considered positive for autoantibodies against the CaSR-ECD had previously been classed as antibody-positive by the CaSR immunoprecipitation assay (**Chapter 3**). Indeed, the two methods of measuring CaSR autoantibodies concurred in 98% of APS1 cases with near complete agreement between the two assays (Cohen's kappa = 0.95). The serum sample from one APS1 patient (APS1-1), which had previously tested positive for CaSR autoantibodies in the CaSR immunoprecipitation assay, was negative for immunoreactivity against the CaSR-ECD. This anomaly requires further investigation. For intra- and inter-assay precision, the CaSR-ECD ELISA had coefficients of variation of 7.2-8.4% and 12.2%, respectively. This is line generally with the values reported for measuring autoantibodies in patients with autoimmune disease (Van Campenhout et al., 2007).

In these preliminary ELISAs, antibody binding was expressed as an antibody index and the cut-off point for antibody positivity set as the mean + 3SD of a population of controls. To

improve the ELISA, a better calibration system needs to be devised where a standard curve is generated by plotting the absorbance values against the respective antibody concentration in each of a set of CaSR antibody primary reference standards (Wright et al., 1993). The concentration of human anti-CaSR autoantibody in test samples could then be determined directly from this standard curve. In addition, a set of internal quality control CaSR antibody samples will need to be defined which will represent defined binding reactivities within the ELISA (Wright et al., 1993). These will need to be included in every assay run, and will be used to verify or not that the ELISA is operating within acceptable limits, and to monitor variability within and between ELISAs. The ELISA needs to be further developed to establish antigen reproducibility between batches as this is a critical reagent in the ELISA. This would be addressed by preparing at least four different batches of the CaSR-ECD and testing each batch in the ELISA protocol.

Overall, the preliminary results for the CaSR antibody ELISA are encouraging, but the assay requires further refinement and validation for use in testing patient sera.

Chapter 7

General Discussion

7 General Discussion

The CaSR is involved the control of serum calcium levels via its effects upon the secretion of PTH (Brown et al., 1993). Previously, the receptor was identified as autoantigen in APS1 in a small cohort of patients (Gavalas et al., 2007). In some patients, CaSR autoantibodies increased the activity of the receptor in response to Ca^{2+}-stimulation (Kemp et al., 2009). The binding sites (epitopes) of CaSR autoantibodies were determined for, and appeared to be restricted to, the extracellular domain of the receptor (Kemp et al., 2010). Following on from these initial studies, the aims of my study were **(i)** to investigate the prevalence of CaSR autoantibodies in a larger group of 44 APS1 patients, **(ii)** to determine if there were any associations between the presence of CaSR autoantibodies and hypoparathyroidism in APS1 patients, **(iii)** to determine the CaSR autoantibody binding sites (epitopes) on the receptor, **(iv)** to investigate the characteristics of CaSR autoantibodies in terms of their subclasses, functional affinities and affects upon the function of the CaSR, and **(v)** to design an ELISA for CaSR measurement in APS1 patient sera.

Initially, the prevalence of immunoreactivity against the CaSR in APS1 patients was investigated (Kemp et al., 2014). Autoantibodies against the receptor were detected in 36% of patients. This prevalence was lower than that found in a previous study carried out in our laboratory (Gavalas et al., 2007). Most likely, this is due to the difference in cohort size (44 APS1 patients *versus* 14 APS1 patients), as the same CaSR immunoprecipitation assay was used with APS1 patients of the same ethnic origin. Although CaSR autoantibodies were detected at an increased of patients with hypoparathyroidism compared to those without (39% *versus* 17%, respectively), the difference in their frequency did not reach statistical significance ($P = 0.392$), suggesting that autoantibodies against the receptor were not clinically useful markers for parathyroid dysfunction. In this way, they may resemble thyroid autoantibodies which are found in patients with overt thyroid diseases and in those who are at risk of developing it. However, it must be stressed that only six patients without hypoparathyroidism were available for study, and that there may have been CaSR autoantibodies in some patients that might not have been detected by the assay methods used.

As part of characterising CaSR autoantibodies, phage-display technology was applied to identify the targets of autoantibodies against the receptor, which were confirmed subsequently using ELISAs with the relevant CaSR peptide (Kemp et al., 2010). Autoantibody targets resided in the extracellular domain of the receptor confirming previous results (Kemp et al., 2010). As before (Kemp et al., 2010), a major epitope was identified between amino acid residues 41 and 69, with minor epitopes at residues 114-126, and 171-195. A novel epitope was found in the current study, different from those reported before (Kemp et al., 2010). The binding site was between residues 260 and 340. Immunoreactivity against more than one CaSR epitope was found in nine out of 16 (56%) APS1 patients, indicating there was a heterogeneous antibody response against the receptor. Similarly, in autoimmune thyroid disease and in type 1 diabetes mellitus, multiple epitopes have been detected on thyroid peroxidase and tyrosine phosphatase-like IA-2 autoantigen, respectively (Lampasona et al., 1996). In the case of in type 1 diabetes mellitus this has been explained by the 'spreading' of autoimmune responses against a single or a few epitopes from early childhood to multiple and different epitopes with the advancing years (Naserke et al., 1998). However, in the context of this study, serum samples taken at different disease durations from the same individual APS1 patient were not analysed, so the possibility of epitope spreading was not evaluated.

All the epitopes identified overlapped with domains on the CaSR that are thought to be involved in receptor function (Hauache et al., 2000, Silve et al., 2005, Hu and Spiegel, 2007). However, how exactly the CaSR autoantibodies with different epitope specificities might affect CaSR function needs more investigation. Further studies are also required to determine the exact epitope/s recognised by the CaSR-stimulating autoantibodies which were detected in four of the APS1 patients. The characterised CaSR epitopes were linear by nature, so further studies need to be undertaken to identify autoantibodies that may recognise conformational epitopes which would depend on the native structure of the receptor. Such antibodies are usually important in disease (Pettersson, 1992, Morgenthaler et al., 1999). For example, in Graves' disease, pathogenic autoantibodies against the thyrotropin receptor target several different conformational epitopes

(Morgenthaler et al., 1999). This is also the case for pathogenic autoantibodies against thyroid peroxidase in autoimmune hypothyroidism (Gora et al., 2004).

The IgG isotypes of APS1 patient CaSR autoantibodies were determined also in this study. Autoantibodies against the receptor were mainly of the IgG1 subclass. In a minority of APS1 patients, antibodies against epitope 114-126 were of the IgG3 subclass. CaSR antibodies of the IgG2 and IgG4 subclasses were not identified. This is the first report regarding IgG subclass for antibodies against the CaSR in patients with hypoparathyroidism in the context of APS1, although CaSR autoantibodies exclusively of the IgG4 subtype were found in one patient with autoimmune hypocalciuric hypercalcemia (Pallais et al., 2004). Interestingly, both IgG1 and IgG3 subclass antibodies can induce antibody-dependent cellular cytotoxicity, as well as having the capacity to activate complement (Flanagan and Rabbitts, 1982, van Loghem, 1986). However, these pathogenic mechanisms require investigation in relation to autoantibodies against the CaSR. It is possible that affinity purification of IgG subclasses might show less restriction than was found here in relation to CaSR autoantibodies: fractionation into IgG subclasses has revealed the presence of all IgG subclass antibodies, including IgG4, with respect to thyroglobulin and thyroid peroxidase autoantibodies in Hashimoto's thyroiditis (Weetman et al., 1989).

Autoantibodies that affect CaSR function are more likely to have a role in disease pathogenesis than autoantibodies that simply bind to the receptor. For example, thyroid-stimulating autoantibodies activate the thyrotropin receptor leading to hyperthyroidism in Graves' disease by mimicking the binding of thyroid-stimulating hormone (Weetman and McGregor, 1994). Autoantibodies against the acetylcholine receptor block the acetylcholine-binding site and provoke accelerated receptor degradation causing myasthenia gravis (Hoedemaekers et al., 1997). Indeed, a small number of patients with either APS1 or isolated autoimmune hypoparathyroidism have been identified with CaSR-stimulating autoantibodies that could potentially reduce PTH secretion (Posillico et al., 1986, Kifor et al., 2004, Kemp et al., 2009). In this study, four patients with APS1 had CaSR autoantibodies that activated the receptor in the presence of calcium. However, further studies are needed to investigate if these autoantibodies also consequently inhibit the

release of PTH from the parathyroid glands. This could be done *in vitro* initially using a parathyroid cell line (Fabbri et al., 2014). It could be that in the aforementioned cases of hypoparathyroidism, the CaSR autoantibodies cause dysfunction of the parathyroid without causing irreversible damage to the glands (Kifor et al., 2004). This would need to be clarified in the APS1 patients used in this study.

Further to affecting the function of the CaSR, autoantibodies against the receptor could also destroy parathyroid cells through complement-fixation or antibody-dependent cellular cytotoxicity. Such activities of anti-parathyroid autoantibodies from patients with autoimmune hypoparathyroidism have been reported previously, although their molecular target was not defined (Brandi et al., 1986). This potential activity needs further analysis in relation to CaSR autoantibodies. Of course, it is also possible that CaSR autoantibodies are an epiphenomenon and play no part in APS1 pathogenesis, but rather they indicate the presence of autoreactive anti-CaSR T lymphocytes.

The targets of autoreactive T cells have been little studied in APS1 compared with that of the humoral immune response, although the autoimmune diseases found in the syndrome are thought to result from T cell-mediated damage of the specific organs. This has been supported by the examination of available tissue samples from various endocrine glands which show lymphocytic infiltration (Betterle and Zanchetta, 2003). In a study of an ASP1 patient with alopecia, in addition to other diseases, a biopsy of the affected scalp showed a significant infiltration of T cells in the hair follicles (Faiyaz-Ul-Haque et al., 2009). To date, however, the targets of T cells in APS1 patients have not been studied extensively, but there are some examples such as aromatic L-amino acid decarboxylase (Kluger et al., 2015). This autoantigen was recognised by cytotoxic T cells in 43% of APS1 patients with gastrointestinal dysfunction (Kluger et al., 2015). However, autoreactive T cells against the CaSR in patients with APS1 have not been investigated so far.

There are many questions to be answered regarding the development of self-tolerance towards the CaSR. Many well-known targets of immune responses in autoimmune endocrine disease are controlled by *AIRE*. For example, the thyrotropin receptor, thyroglobulin, thyroid peroxidase and the sodium-iodide symporter, which are

autoantigens in autoimmune thyroid disease, are reliant upon *AIRE* for their expression and the consequent induction of tolerance to them (Misharin et al., 2009); so too are the pemphigus vulgaris-related autoantigen desmoglein 3 (Wada et al., 2011), and the vitiligo-associated autoantigen gp100 (Trager et al., 2012, van den Boorn et al., 2009). However, certain vitiligo-associated autoantigens such as tyrosinase-related protein-2 are not under *AIRE* control (Trager et al., 2012). Future questions include: Is the CaSR under *AIRE* control? Is this centrally or peripherally controlled? Are Tregs responsible for tolerance to the CaSR? Understanding the CaSR tolerance mechanism may improve our understanding of the presence of immune responses against the receptor in APS1.

This study aimed to develop a fast and quantitative ELISA for detecting CaSR autoantibodies in APS1 patient sera using the CaSR extracellular domain expressed in *E. coli* as the antibody-capture antigen. Although the ELISA developed was able to detect the presence of CaSR autoantibodies in APS1 patient sera, further work is required to optimise and validate the method.

This thesis has concentrated on characterising autoantibodies against the CaSR in APS1 patients. However, their relevance to the pathogenesis of hypoparathyroidism in APS1 has yet to be fully established. The possibility that CaSR autoantibodies play no part in APS1 pathogenesis, but rather indicate the presence of autoreactive anti-CaSR T lymphocytes, needs to be investigated. Future investigations should aim also to identify whether any other novel parathyroid antigens exist besides CaSR and NALP5. By analogy with other autoimmune endocrinopathies, T cells are likely to play the major role in parathyroid destruction in hypoparathyroidism in APS1, and so it will also be essential to characterise any parathyroid autoantigens and the epitopes that are targeted by T cells.

References

ABRAMSON, J., GIRAUD, M., BENOIST, C. & MATHIS, D. 2010. Aire's partners in the molecular control of immunological tolerance. *Cell,* 140**,** 123-35.

ADAMSON, K. A., PEARCE, S. H., LAMB, J. R., SECKL, J. R. & HOWIE, S. E. 2004. A comparative study of mRNA and protein expression of the autoimmune regulator gene (Aire) in embryonic and adult murine tissues. *J Pathol,* 202**,** 180-7.

AHONEN, P., MYLLARNIEMI, S., SIPILA, I. & PERHEENTUPA, J. 1990. Clinical variation of autoimmune polyendocrinopathy-candidiasis-ectodermal dystrophy (APECED) in a series of 68 patients. *N Engl J Med,* 322**,** 1829-36.

AL-BUKHARI, T. A., TIGHE, P. & TODD, I. 2002. An immuno-precipitation assay for determining specific interactions between antibodies and phage selected from random peptide expression libraries. *J Immunol Methods,* 264**,** 163-71.

AL-OWAIN, M., KAYA, N., AL-ZAIDAN, H., BIN HUSSAIN, I., AL-MANEA, H., AL-HINDI, H., KENNEDY, S., IQBAL, M. A., AL-MOJALLI, H., AL-BAKHEET, A., PUEL, A., CASANOVA, J. L. & AL-MUHSEN, S. 2010. Renal failure associated with APECED and terminal 4q deletion: evidence of autoimmune nephropathy. *Clin Dev Immunol,* 2010**,** 586342.

ALIMOHAMMADI, M., BJORKLUND, P., HALLGREN, A., PONTYNEN, N., SZINNAI, G., SHIKAMA, N., KELLER, M. P., EKWALL, O., KINKEL, S. A., HUSEBYE, E. S., GUSTAFSSON, J., RORSMAN, F., PELTONEN, L., BETTERLE, C., PERHEENTUPA, J., AKERSTROM, G., WESTIN, G., SCOTT, H. S., HOLLANDER, G. A. & KAMPE, O. 2008. Autoimmune polyendocrine syndrome type 1 and NALP5, a parathyroid autoantigen. *N Engl J Med,* 358**,** 1018-28.

ALIMOHAMMADI, M., DUBOIS, N., SKOLDBERG, F., HALLGREN, A., TARDIVEL, I., HEDSTRAND, H., HAAVIK, J., HUSEBYE, E. S., GUSTAFSSON, J., RORSMAN, F., MELONI, A., JANSON, C., VIALETTES, B., KAJOSAARI, M., EGNER, W., SARGUR, R., PONTEN, F., AMOURA, Z., GRIMFELD, A., DE LUCA, F., BETTERLE, C., PERHEENTUPA, J., KAMPE, O. & CAREL, J. C. 2009. Pulmonary autoimmunity as a feature of autoimmune polyendocrine syndrome type 1 and identification of KCNRG as a bronchial autoantigen. *Proc Natl Acad Sci U S A,* 106**,** 4396-401.

ALTENAHR, E. & JENKE, W. 1974. Experimental parathyroiditis in the rat by passive immunisation. *Virchows Arch A Pathol Anat Histol,* 363**,** 333-42.

AMIT, A. G., MARIUZZA, R. A., PHILLIPS, S. E. & POLJAK, R. J. 1986. Three-dimensional structure of an antigen-antibody complex at 2.8 A resolution. *Science,* 233**,** 747-53.

ANDERSON, M. S., VENANZI, E. S., KLEIN, L., CHEN, Z., BERZINS, S. P., TURLEY, S. J., VON BOEHMER, H., BRONSON, R., DIERICH, A., BENOIST, C. & MATHIS, D. 2002. Projection of an immunological self shadow within the thymus by the aire protein. *Science,* 298**,** 1395-401.

BAI, M. 2004. Structure-function relationship of the extracellular calcium-sensing receptor. *Cell Calcium,* 35**,** 197-207.

BAI, M., JANICIC, N., TRIVEDI, S., QUINN, S. J., COLE, D. E., BROWN, E. M. & HENDY, G. N. 1997. Markedly reduced activity of mutant calcium-sensing receptor with an inserted Alu element from a kindred with familial hypocalciuric hypercalcemia and neonatal severe hyperparathyroidism. *J Clin Invest,* 99**,** 1917-25.

BARBAS, C. F., 3RD 1993. Recent advances in phage display. *Curr Opin Biotechnol,* 4**,** 526-30.

BASS, S., GREENE, R. & WELLS, J. A. 1990. Hormone phage: an enrichment method for variant proteins with altered binding properties. *Proteins,* 8**,** 309-14.

BAZAN, J., CAŁKOSIŃSKI, I. & GAMIAN, A. 2012. Phage display—A powerful technique for immunotherapy: 1. Introduction and potential of therapeutic applications. *Human vaccines & immunotherapeutics,* 8**,** 1817-1828.

BELL, C. E. & LEWIS, M. 2000. A closer view of the conformation of the Lac repressor bound to operator. *Nat Struct Biol,* 7**,** 209-14.

BENSING, S., FETISSOV, S. O., MULDER, J., PERHEENTUPA, J., GUSTAFSSON, J., HUSEBYE, E. S., OSCARSON, M., EKWALL, O., CROCK, P. A., HOKFELT, T., HULTING, A. L. & KAMPE, O. 2007. Pituitary autoantibodies in autoimmune polyendocrine syndrome type 1. *Proc Natl Acad Sci U S A,* 104**,** 949-54.

BETTERLE, C., CARETTO, A., ZEVIANI, M., PEDINI, B. & SALVIATI, C. 1985. Demonstration and Characterization of Anti-Human Mitochondria Autoantibodies in Idiopathic Hypoparathyroidism and in Other Conditions. *Clinical and Experimental Immunology,* 62**,** 353-360.

BETTERLE, C., DAL PRA, C., MANTERO, F. & ZANCHETTA, R. 2002. Autoimmune adrenal insufficiency and autoimmune polyendocrine syndromes: Autoantibodies, autoantigens, and their applicability in diagnosis and disease prediction. *Endocrine Reviews,* 23**,** 327-364.

BETTERLE, C., GREGGIO, N. A. & VOLPATO, M. 1998. Clinical review 93: Autoimmune polyglandular syndrome type 1. *J Clin Endocrinol Metab,* 83**,** 1049-55.

BETTERLE, C. & ZANCHETTA, R. 2003. Update on autoimmune polyendocrine syndromes (APS). *Acta Biomed,* 74**,** 9-33.

BJORSES, P., HALONEN, M., PALVIMO, J. J., KOLMER, M., AALTONEN, J., ELLONEN, P., PERHEENTUPA, J., ULMANEN, I. & PELTONEN, L. 2000. Mutations in the AIRE gene: effects on subcellular location and transactivation function of the autoimmune polyendocrinopathy-candidiasis-ectodermal dystrophy protein. *Am J Hum Genet,* 66**,** 378-92.

BLIZZARD, R. M., CHEE, D. & DAVIS, W. 1966. The incidence of parathyroid and other antibodies in the sera of patients with idiopathic hypoparathyroidism. *Clinical and Experimental Immunology,* 1**,** 119-28.

BOE, A. S., BREDHOLT, G., KNAPPSKOG, P. M., HJELMERVIK, T. O., MELLGREN, G., WINQVIST, O., KAMPE, O. & HUSEBYE, E. S. 2004. Autoantibodies against 21-hydroxylase and side-chain cleavage enzyme in autoimmune Addison's disease are mainly immunoglobulin G1. *Eur J Endocrinol,* 150**,** 49-56.

BOITARD, C. 2012. Pancreatic islet autoimmunity. *Presse Med,* 41**,** e636-50.

BONIFACIO, E., SCIRPOLI, M., KREDEL, K., FUCHTENBUSCH, M. & ZIEGLER, A. G. 1999. Early autoantibody responses in prediabetes are IgG1 dominated and suggest antigen-specific regulation. *Journal of Immunology,* 163**,** 525-32.

BORNHORST, J. A. & FALKE, J. J. 2000. [16] Purification of Proteins Using Polyhistidine Affinity Tags. *Methods in enzymology,* 326**,** 245-254.

BRANDI, M. L., AURBACH, G. D., FATTOROSSI, A., QUARTO, R., MARX, S. J. & FITZPATRICK, L. A. 1986. Antibodies cytotoxic to bovine parathyroid cells in autoimmune hypoparathyroidism. *Proc Natl Acad Sci U S A,* 83**,** 8366-9.

BRATLAND, E., MAGITTA, N. F., WOLFF, A. S. B., EKERN, T., KNAPPSKOG, P. M., KAMPE, O., HAAVIK, J. & HUSEBYE, E. S. 2013. Autoantibodies against aromatic amino acid hydroxylases in patients with autoimmune polyendocrine syndrome type 1 target multiple antigenic determinants and reveal regulatory regions crucial for enzymatic activity. *Immunobiology,* 218**,** 899-909.

BRATLAND, E., SKINNINGSRUD, B., UNDLIEN, D. E., MOZES, E. & HUSEBYE, E. S. 2009. T cell responses to steroid cytochrome P450 21-hydroxylase in patients with autoimmune primary adrenal insufficiency. *J Clin Endocrinol Metab,* 94**,** 5117-24.

BRAUNER-OSBORNE, H., JENSEN, A. A., SHEPPARD, P. O., O'HARA, P. & KROGSGAARD-LARSEN, P. 1999. The agonist-binding domain of the calcium-sensing receptor is located at the amino-terminal domain. *Journal of Biological Chemistry,* 274**,** 18382-18386.

BROSIUS, J., ERFLE, M. & STORELLA, J. 1985. Spacing of the -10 and -35 regions in the tac promoter. Effect on its in vivo activity. *J Biol Chem,* 260**,** 3539-41.

BROWN, E. M. 1999. Physiology and pathophysiology of the extracellular calcium-sensing receptor. *American Journal of Medicine,* 106**,** 238-253.

BROWN, E. M. 2007. Clinical lessons from the calcium-sensing receptor. *Nat Clin Pract End Met,* 3**,** 122-133.

BROWN, E. M., GAMBA, G., RICCARDI, D., LOMBARDI, M., BUTTERS, R., KIFOR, O., SUN, A., HEDIGER, M. A., LYTTON, J. & HEBERT, S. C. 1993. Cloning and characterization of an extracellular Ca(2+)-sensing receptor from bovine parathyroid. *Nature,* 366**,** 575-80.

BROWN, E. M. & MACLEOD, R. J. 2001. Extracellular calcium sensing and extracellular calcium signaling. *Physiological Reviews,* 81**,** 239-297.

BROWN, E. M., POLLAK, M. & HEBERT, S. C. 1995. Sensing of Extracellular Ca2+ by Parathyroid and Kidney-Cells - Cloning and Characterization of an Extracellular Ca2+-Sensing Receptor. *American Journal of Kidney Diseases,* 25**,** 506-513.

BROWN, E. M., POLLAK, M. & HEBERT, S. C. 1998. The extracellular calcium-sensing receptor: its role in health and disease. *Annu Rev Med,* 49**,** 15-29.

BROZZETTI, A., MARZOTTI, S., LA TORRE, D., BACOSI, M. L., MORELLI, S., BINI, V., AMBROSI, B., GIORDANO, R., PERNIOLA, R., DE BELLIS, A., BETTERLE, C. & FALORNI, A. 2010. Autoantibody responses in autoimmune ovarian insufficiency and in Addison's disease are IgG1 dominated and suggest a predominant, but not exclusive, Th1 type of response. *Eur J Endocrinol,* 163**,** 309-17.

BUTTERONI, C., DE FELICI, M., SCHÖLER, H. R. & PESCE, M. 2000. Phage Display Screening Reveals an Association Between Germline-specific Transcription Factor Oct-4 and Multiple Cellular Proteins. *Journal of Molecular Biology,* 304**,** 529-540.

CARSTENS, C.-P., BONNARDEL, J., ALLEN, O. & WAESCHE, A. 2002. BL21-CodonPlus™ Cells Correct Expression Problems Caused by Codon Bias. *Stratagene,* 14**,** 50-52.

CATUREGLI, P., KUPPERS, R. C., MARIOTTI, S., BUREK, C. L., PINCHERA, A., LADENSON, P. W. & ROSE, N. R. 1994. IgG subclass distribution of thyroglobulin antibodies in patients with thyroid disease. *Clin Exp Immunol,* 98**,** 464-469.

CERVATO, S., MARINIELLO, B., LAZZAROTTO, F., MORLIN, L., ZANCHETTA, R., RADETTI, G., DE LUCA, F., VALENZISE, M., GIORDANO, R., RIZZO, D., GIORDANO, C. & BETTERLE, C. 2009. Evaluation of the autoimmune regulator (AIRE) gene mutations in a cohort of Italian patients with autoimmune-polyendocrinopathy-candidiasis-ectodermal-dystrophy (APECED) and in their relatives. *Clin Endocrinol (Oxf),* 70**,** 421-8.

CERVATO, S., MORLIN, L., ALBERGONI, M. P., MASIERO, S., GREGGIO, N., MEOSSI, C., CHEN, S., LAROSA, M. D., FURMANIAK, J., SMITH, B. R., ALIMOHAMMADI, M., KAMPE, O., VALENZISE, M. & BETTERLE, C. 2010. AIRE gene mutations and autoantibodies to interferon omega in patients with chronic hypoparathyroidism without APECED. *Clinical Endocrinology,* 73**,** 630-636.

CETANI, F., BARBESINO, G., BORSARI, S., PARDI, E., CIANFEROTTI, L., PINCHERA, A. & MARCOCCI, C. 2001. A novel mutation of the autoimmune regulator gene in an Italian kindred with autoimmune polyendocrinopathy-candidiasis-ectodermal dystrophy, acting in a dominant fashion and strongly cosegregating with hypothyroid autoimmune thyroiditis. *J Clin Endocrinol Metab,* 86**,** 4747-52.

CHANG, W., CHEN, T. H., PRATT, S. & SHOBACK, D. 2000. Amino acids in the second and third intracellular loops of the parathyroid Ca2+-sensing receptor mediate efficient coupling to phospholipase C. *J Biol Chem,* 275**,** 19955-63.

CHATTOPADHYAY, N., MITHAL, A. & BROWN, E. M. 1996. The calcium-sensing receptor: A window into the physiology and pathophysiology of mineral ion metabolism. *Endocrine Reviews,* 17**,** 289-307.

CHENG, M. H., FAN, U., GREWAL, N., BARNES, M., MEHTA, A., TAYLOR, S., HUSEBYE, E. S., MURPHY, E. J. & ANDERSON, M. S. 2010. Acquired autoimmune polyglandular syndrome, thymoma, and an AIRE defect. *N Engl J Med,* 362**,** 764-6.

CHIGNOLA, F., GAETANI, M., REBANE, A., ORG, T., MOLLICA, L., ZUCCHELLI, C., SPITALERI, A., MANNELLA, V., PETERSON, P. & MUSCO, G. 2009. The solution structure of the first PHD finger of autoimmune regulator in complex with non-modified histone H3 tail reveals the antagonistic role of H3R2 methylation. *Nucleic Acids Res,* 37**,** 2951-61.

CIHAKOVA, D., TREBUSAK, K., HEINO, M., FADEYEV, V., TIULPAKOV, A., BATTELINO, T., TAR, A., HALASZ, Z., BLUMEL, P., TAWFIK, S., KROHN, K., LEBL, J. & PETERSON, P. 2001. Novel AIRE mutations and P450 cytochrome autoantibodies in Central and Eastern European patients with APECED. *Hum Mutat,* 18**,** 225-32.

CLEMENTE, M. G., MELONI, A., OBERMAYER-STRAUB, P., FRAU, F., MANNS, M. P. & DE VIRGILIIS, S. 1998. Two cytochromes P450 are major hepatocellular autoantigens in autoimmune polyglandular syndrome type 1. *Gastroenterology,* 114**,** 324-8.

CLEMENTE, M. G., OBERMAYERSTRAUB, P., MELONI, A., STRASSBURG, C. P., ARANGINO, V., TUKEY, R. H., DEVIRGILIIS, S. & MANNS, M. P. 1997. Cytochrome P450 1A2 is a hepatic autoantigen in autoimmune polyglandular syndrome type 1. *Journal of Clinical Endocrinology & Metabolism,* 82**,** 1353-1361.

COLLINS, S. M., DOMINGUEZ, M., ILMARINEN, T., COSTIGAN, C. & IRVINE, A. D. 2006. Dermatological manifestations of autoimmune polyendocrinopathy-candidiasis-ectodermal dystrophy syndrome. *Br J Dermatol,* 154**,** 1088-93.

CRAMERI, R., JAUSSI, R., MENZ, G. & BLASER, K. 1994. Display of expression products of cDNA libraries on phage surfaces. A versatile screening system for selective isolation of genes by specific gene-product/ligand interaction. *Eur J Biochem,* 226**,** 53-8.

CUCNIK, S., KVEDER, T., KRIZAJ, I., ROZMAN, B. & BOZIC, B. 2004. High avidity anti-beta 2-glycoprotein I antibodies in patients with antiphospholipid syndrome. *Ann Rheum Dis,* 63**,** 1478-82.

CUCNIK, S., KVEDER, T., ULCOVA-GALLOVA, Z., SWADZBA, J., MUSIAL, J., VALESINI, G., AVCIN, T., ROZMAN, B. & BOZIC, B. 2011. The avidity of anti-beta2-glycoprotein I antibodies in patients with or without antiphospholipid syndrome: a collaborative study in the frame of the European forum on antiphospholipid antibodies. *Lupus,* 20**,** 1166-71.

CUTOLO, M. 2014. Autoimmune polyendocrine syndromes. *Autoimmun Rev,* 13**,** 85-9.

DABER, R., STAYROOK, S., ROSENBERG, A. & LEWIS, M. 2007. Structural analysis of lac repressor bound to allosteric effectors. *J Mol Biol,* 370**,** 609-19.

DAL PRA, C., CHEN, S., BETTERLE, C., ZANCHETTA, R., MCGRATH, V., FURMANIAK, J. & REES SMITH, B. 2004. Autoantibodies to human tryptophan hydroxylase and aromatic L-amino acid decarboxylase. *Eur J Endocrinol,* 150**,** 313-21.

DAWOODJI, A., CHEN, J. L., SHEPHERD, D., DALIN, F., TARLTON, A., ALIMOHAMMADI, M., PENNA-MARTINEZ, M., MEYER, G., MITCHELL, A. L., GAN, E. H., BRATLAND, E., BENSING, S., HUSEBYE, E. S., PEARCE, S. H., BADENHOOP, K., KAMPE, O. & CERUNDOLO, V. 2014. High frequency of cytolytic 21-hydroxylase-specific CD8+ T cells in autoimmune Addison's disease patients. *J Immunol,* 193**,** 2118-26.

DEL RINCON, I., ZEIDEL, M., REY, E., HARLEY, J. B., JAMES, J. A., FISCHBACH, M. & SANZ, I. 2000. Delineation of the Human Systemic Lupus Erythematosus Anti-Smith Antibody Response Using Phage-Display Combinatorial Libraries. *The Journal of Immunology,* 165**,** 7011-7016.

DELANO, W. L., ULTSCH, M. H., DE VOS, A. M. & WELLS, J. A. 2000. Convergent solutions to binding at a protein-protein interface. *Science,* 287**,** 1279-1283.

DEVOSS, J. J., SHUM, A. K., JOHANNES, K. P., LU, W., KRAWISZ, A. K., WANG, P., YANG, T., LECLAIR, N. P., AUSTIN, C., STRAUSS, E. C. & ANDERSON, M. S. 2008. Effector mechanisms of the

autoimmune syndrome in the murine model of autoimmune polyglandular syndrome type 1. *Journal of Immunology,* 181**,** 4072-9.

DOBES, J., NEUWIRTH, A., DOBESOVA, M., VOBORIL, M., BALOUNOVA, J., BALLEK, O., LEBL, J., MELONI, A., KROHN, K., KLUGER, N., RANKI, A. & FILIPP, D. 2015. Gastrointestinal Autoimmunity Associated With Loss of Central Tolerance to Enteric alpha-Defensins. *Gastroenterology,* 149**,** 139-50.

DOMINGUEZ, M., CRUSHELL, E., ILMARINEN, T., MCGOVERN, E., COLLINS, S., CHANG, B., FLEMING, P., IRVINE, A. D., BROSNAHAN, D., ULMANEN, I., MURPHY, N. & COSTIGAN, C. 2006. Autoimmune polyendocrinopathy-candidiasis-ectodermal dystrophy (APECED) in the Irish population. *J Pediatr Endocrinol Metab,* 19**,** 1343-52.

DRAGOJEVIĆ-DIKIĆ, S., MARISAVLJEVIĆ, D., MITROVIĆ, A., DIKIĆ, S., JOVANOVIĆ, T. & JANKOVIĆ-RAŽNATOVIĆ, S. 2010. An immunological insight into premature ovarian failure (POF). *Autoimmunity Reviews,* 9**,** 771-774.

DROMEY, J. A., WEENINK, S. M., PETERS, G. H., ENDL, J., TIGHE, P. J., TODD, I. & CHRISTIE, M. R. 2004. Mapping of epitopes for autoantibodies to the type 1 diabetes autoantigen IA-2 by peptide phage display and molecular modeling: overlap of antibody and T cell determinants. *J Immunol,* 172**,** 4084-90.

EKWALL, O., HEDSTRAND, H., GRIMELIUS, L., HAAVIK, J., PERHEENTUPA, J., GUSTAFSSON, J., HUSEBYE, E., KAMPE, O. & RORSMAN, F. 1998. Identification of tryptophan hydroxylase as an intestinal autoantigen. *Lancet,* 352**,** 279-283.

ELDERSHAW, S. A., SANSOM, D. M. & NARENDRAN, P. 2011. Expression and function of the autoimmune regulator (Aire) gene in non-thymic tissue. *Clin Exp Immunol,* 163**,** 296-308.

ETIENNE-DECERF, J., MALAISE, M., MAHIEU, P. & WINAND, R. 1987. Elevated anti-α-galactosyl antibody titres. A marker of progression in autoimmune thyroid disorders and in endocrine ophthalmopathy? *Acta Endocrinol (Copenh),* 115**,** 67-74.

FABBRI, S., CIUFFI, S., NARDONE, V., GOMES, A. R., MAVILIA, C., ZONEFRATI, R., GALLI, G., LUZI, E., TANINI, A. & BRANDI, M. L. 2014. PTH-C1: a rat continuous cell line expressing the parathyroid phenotype. *Endocrine,* 47**,** 90-9.

FAIYAZ-UL-HAQUE, M., BIN-ABBAS, B., AL-ABDULLATIF, A., ABDULLAH ABALKHAIL, H., TOULIMAT, M., AL-GAZLAN, S., ALMUTAWA, A. M., AL-SAGHEIR, A., PELTEKOVA, I., AL-DAYEL, F. & ZAIDI, S. H. 2009. Novel and recurrent mutations in the AIRE gene of autoimmune polyendocrinopathy syndrome type 1 (APS1) patients. *Clin Genet,* 76**,** 431-40.

FAN, G. F., RAY, K., ZHAO, X. M., GOLDSMITH, P. K. & SPIEGEL, A. M. 1998. Mutational analysis of the cysteines in the extracellular domain of the human Ca2+ receptor: effects on cell surface expression, dimerization and signal transduction. *FEBS Lett,* 436**,** 353-6.

FARILLA, L., TIBERTI, C., LUZZAGO, A., YU, L., EISENBARTH, G. S., CORTESE, R., DOTTA, F. & DI MARIO, U. 2002. Application of phage display peptide library to autoimmune diabetes: identification of IA-2/ICA512bdc dominant autoantigenic epitopes. *Eur J Immunol,* 32**,** 1420-7.

FATTOROSSI, A., AURBACH, G. D., SAKAGUCHI, K., CAMA, A., MARX, S. J., STREETEN, E. A., FITZPATRICK, L. A. & BRANDI, M. L. 1988. Anti-endothelial cell antibodies: detection and characterization in sera from patients with autoimmune hypoparathyroidism. *Proc Natl Acad Sci U S A,* 85**,** 4015-9.

FERGUSON, B. J., ALEXANDER, C., ROSSI, S. W., LIIV, I., REBANE, A., WORTH, C. L., WONG, J., LAAN, M., PETERSON, P., JENKINSON, E. J., ANDERSON, G., SCOTT, H. S., COOKE, A. & RICH, T. 2008. AIRE's CARD revealed, a new structure for central tolerance provokes transcriptional plasticity. *J Biol Chem,* 283**,** 1723-31.

FINKELMAN, F. D., HOLMES, J., KATONA, I. M., URBAN, J. F., JR., BECKMANN, M. P., PARK, L. S., SCHOOLEY, K. A., COFFMAN, R. L., MOSMANN, T. R. & PAUL, W. E. 1990. Lymphokine control of in vivo immunoglobulin isotype selection. *Annu Rev Immunol,* 8**,** 303-33.

FINNISH-GERMAN, A. C. 1997. An autoimmune disease, APECED, caused by mutations in a novel gene featuring two PHD-type zinc-finger domains. *Nat Genet,* 17**,** 399-403.

FLANAGAN, J. G. & RABBITTS, T. H. 1982. Arrangement of human immunoglobulin heavy chain constant region genes implies evolutionary duplication of a segment containing gamma, epsilon and alpha genes. *Nature,* 300**,** 709-13.

FRIEDMAN, T. C., THOMAS, P. M., FLEISHER, T. A., FEUILLAN, P., PARKER, R. I., CASSORLA, F. & CHROUSOS, G. P. 1991. Frequent occurrence of asplenism and cholelithiasis in patients with autoimmune polyglandular disease type I. *Am J Med,* 91**,** 625-30.

GAETANI, M., MATAFORA, V., SAARE, M., SPILIOTOPOULOS, D., MOLLICA, L., QUILICI, G., CHIGNOLA, F., MANNELLA, V., ZUCCHELLI, C., PETERSON, P., BACHI, A. & MUSCO, G. 2012. AIRE-PHD fingers are structural hubs to maintain the integrity of chromatin-associated interactome. *Nucleic Acids Res,* 40**,** 11756-68.

GAMA, L., WILT, S. G. & BREITWIESER, G. E. 2001. Heterodimerization of calcium sensing receptors with metabotropic glutamate receptors in neurons. *J Biol Chem,* 276**,** 39053-9.

GARDNER, J. M., DEVOSS, J. J., FRIEDMAN, R. S., WONG, D. J., TAN, Y. X., ZHOU, X., JOHANNES, K. P., SU, M. A., CHANG, H. Y., KRUMMEL, M. F. & ANDERSON, M. S. 2008. Deletional tolerance mediated by extrathymic Aire-expressing cells. *Science,* 321**,** 843-7.

GARRETT, J. E., CAPUANO, I. V., HAMMERLAND, L. G., HUNG, B. C., BROWN, E. M., HEBERT, S. C., NEMETH, E. F. & FULLER, F. 1995. Molecular cloning and functional expression of human parathyroid calcium receptor cDNAs. *J Biol Chem,* 270**,** 12919-25.

GAVALAS, N. G., GOTTUMUKKALA, R. V., GAWKRODGER, D. J., WATSON, P. F., WEETMAN, A. P. & KEMP, E. H. 2009. Mapping of melanin-concentrating hormone receptor 1 B cell epitopes predicts two major binding sites for vitiligo patient autoantibodies. *Exp Dermatol,* 18**,** 454-63.

GAVALAS, N. G., KEMP, E. H., KROHN, K. J. E., BROWN, E. M., WATSON, P. F. & WEETMAN, A. P. 2007. The calcium-sensing receptor is a target of autoantibodies in patients with autoimmune polyendocrine syndrome type 1. *Journal of Clinical Endocrinology & Metabolism,* 92**,** 2107-2114.

GEBRE-MEDHIN, G., HUSEBYE, E. S., GUSTAFSSON, J., WINQVIST, O., GOKSOYR, A., RORSMAN, F. & KAMPE, O. 1997. Cytochrome P450IA2 and aromatic L-amino acid decarboxylase are hepatic autoantigens in autoimmune polyendocrine syndrome type I. *FEBS Lett,* 412**,** 439-45.

GERGELY, J., STANWORTH, D. R., JEFFERIS, R., NORMANSELL, D. E., HENNEY, C. S. & PARDOE, G. I. 1967. Structural studies of immunoglobulins—I. The role of cysteine in papain hydrolysis. *Immunochemistry,* 4**,** 101-111.

GEVORKIAN, G., MANOUTCHARIAN, K., ALMAGRO, J. C., GOVEZENSKY, T. & DOMINGUEZ, V. 1998. Identification of autoimmune thrombocytopenic purpura-related epitopes using phage-display peptide library. *Clin Immunol Immunopathol,* 86**,** 305-9.

GHARAVI, A. & REIBER, H. 1996. Affinity and avidity of autoantibodies. *In:* PETER JB & Y, S. (eds.) *Autoantibodies.* Amsterdam: Elsevier Science.

GIANANI, R. & EISENBARTH, G. S. 2003. Autoimmunity to gastrointestinal endocrine cells in autoimmune polyendocrine syndrome type I. *J Clin Endocrinol Metab,* 88**,** 1442-4.

GORA, M., GARDAS, A., WATSON, P. F., HOBBY, P., WEETMAN, A. P., SUTTON, B. J. & BANGA, J. P. 2004. Key residues contributing to dominant conformational autoantigenic epitopes on thyroid peroxidase identified by mutagenesis. *Biochem Biophys Res Commun,* 320**,** 795-801.

GREENER, A., CALLAHAN, M. & JERPSETH, B. 1997. An efficient random mutagenesis technique using an E. coli mutator strain. *Mol Biotechnol,* 7**,** 189-95.

GYLLING, M., KAARIAINEN, E., VAISANEN, R., KEROSUO, L., SOLIN, M. L., HALME, L., SAARI, S., HALONEN, M., KAMPE, O., PERHEENTUPA, J. & MIETTINEN, A. 2003. The

hypoparathyroidism of autoimmune polyendocrinopathy-candidiasis-ectodermal dystrophy protective effect of male sex. *Journal of Clinical Endocrinology & Metabolism,* 88**,** 4602-4608.

GYLLING, M., TUOMI, T., BJORSES, P., KONTIAINEN, S., PARTANEN, J., CHRISTIE, M. R., KNIP, M., PERHEENTUPA, J. & MIETTINEN, A. 2000. beta-cell autoantibodies, human leukocyte antigen II alleles, and type 1 diabetes in autoimmune polyendrocrionopathy-candidiasis-ectodermal dystrophy. *Journal of Clinical Endocrinology & Metabolism,* 85**,** 4434-4440.

HAGER-BRAUN, C. & TOMER, K. B. 2005. Determination of protein-derived epitopes by mass spectrometry. *Expert Rev Proteomics,* 2**,** 745-56.

HALONEN, M., ESKELIN, P., MYHRE, A. G., PERHEENTUPA, J., HUSEBYE, E. S., KAMPE, O., RORSMAN, F., PELTONEN, L., ULMANEN, I. & PARTANEN, J. 2002. AIRE mutations and human leukocyte antigen genotypes as determinants of the autoimmune polyendocrinopathy-candidiasis-ectodermal dystrophy phenotype. *J Clin Endocrinol Metab,* 87**,** 2568-74.

HAUACHE, O. M., HU, J., RAY, K., XIE, R., JACOBSON, K. A. & SPIEGEL, A. M. 2000. Effects of a calcimimetic compound and naturally activating mutations on the human Ca2+ receptor and on Ca2+ receptor/metabotropic glutamate chimeric receptors. *Endocrinology,* 141**,** 4156-63.

HAWA, M. I., FAVA, D., MEDICI, F., DENG, Y. J., NOTKINS, A. L., DE MATTIA, G. & LESLIE, R. D. 2000. Antibodies to IA-2 and GAD65 in type 1 and type 2 diabetes: isotype restriction and polyclonality. *Diabetes Care,* 23**,** 228-33.

HEDSTRAND, H., EKWALL, O., HAAVIK, J., LANDGREN, E., BETTERLE, C., PERHEENTUPA, J., GUSTAFSSON, J., HUSEBYE, E., RORSMAN, F. & KAMPE, O. 2000. Identification of tyrosine hydroxylase as an autoantigen in autoimmune polyendocrine syndrome type I. *Biochemical and Biophysical Research Communications,* 267**,** 456-461.

HEDSTRAND, H., EKWALL, O., OLSSON, M. J., LANDGREN, E., KEMP, E. H., WEETMAN, A. P., PERHEENTUPA, J., HUSEBYE, E., GUSTAFSSON, J., BETTERLE, C., KAMPE, O. & RORSMAN, F. 2001. The transcription factors SOX9 and SOX10 are vitiligo autoantigens in autoimmune polyendocrine syndrome type I. *Journal of Biological Chemistry,* 276**,** 35390-35395.

HEINO, M., PETERSON, P., KUDOH, J., NAGAMINE, K., LAGERSTEDT, A., OVOD, V., RANKI, A., RANTALA, I., NIEMINEN, M., TUUKKANEN, J., SCOTT, H. S., ANTONARAKIS, S. E., SHIMIZU, N. & KROHN, K. 1999. Autoimmune regulator is expressed in the cells regulating immune tolerance in thymus medulla. *Biochemical and Biophysical Research Communications,* 257**,** 821-825.

HEINO, M., PETERSON, P., KUDOH, J., SHIMIZU, N., ANTONARAKIS, S. E., SCOTT, H. S. & KROHN, K. 2001. APECED mutations in the autoimmune regulator (AIRE) gene. *Hum Mutat,* 18**,** 205-11.

HERMANS, E. & CHALLISS, R. A. 2001. Structural, signalling and regulatory properties of the group I metabotropic glutamate receptors: prototypic family C G-protein-coupled receptors. *Biochem J,* 359**,** 465-84.

HERMITTE, L., ATLAN-GEPNER, C., MATTEI, C., DUFAYET, D., JANNOT, M. F., CHRISTOFILIS, M. A., NERVI, S. & VIALETTES, B. 1998. Diverging evolution of anti-GAD and anti-IA-2 antibodies in long-standing diabetes mellitus as a function of age at onset: No association with complications. *Diabetic Medicine,* 15**,** 586-591.

HOEDEMAEKERS, A. C., VAN BREDA VRIESMAN, P. J. & DE BAETS, M. H. 1997. Myasthenia gravis as a prototype autoimmune receptor disease. *Immunol Res,* 16**,** 341-354.

HOFER, A. M. & BROWN, E. M. 2003. Extracellular calcium sensing and signalling. *Nature Reviews Molecular Cell Biology,* 4**,** 530-538.

HORE, P. 2015. *Nuclear magnetic resonance*, Oxford University Press.

HU, J., HAUACHE, O. & SPIEGEL, A. M. 2000. Human Ca2+ receptor cysteine-rich domain. Analysis of function of mutant and chimeric receptors. *J Biol Chem,* 275**,** 16382-9.

HU, J., REYES-CRUZ, G., GOLDSMITH, P. K., GANTT, N. M., MILLER, J. L. & SPIEGEL, A. M. 2007. Functional effects of monoclonal antibodies to the purified amino-terminal extracellular domain of the human Ca(2+) receptor. *J Bone Miner Res,* 22**,** 601-608.

HU, J. & SPIEGEL, A. M. 2007. Structure and function of the human calcium-sensing receptor: insights from natural and engineered mutations and allosteric modulators. *J Cell Mol Med,* 11**,** 908-22.

HUANG, Y., ZHOU, Y., YANG, W., BUTTERS, R., LEE, H. W., LI, S., CASTIBLANCO, A., BROWN, E. M. & YANG, J. J. 2007. Identification and dissection of Ca(2+)-binding sites in the extracellular domain of Ca(2+)-sensing receptor. *J Biol Chem,* 282**,** 19000-10.

HUSEBYE, E. S., GEBRE-MEDHIN, G., TUOMI, T., PERHEENTUPA, J., LANDIN-OLSSON, M., GUSTAFSSON, J., RORSMAN, F. & KAMPE, O. 1997. Autoantibodies against aromatic L-amino acid decarboxylase in autoimmune polyendocrine syndrome type I. *J Clin Endocrinol Metab,* 82**,** 147-50.

HUSEBYE, E. S., PERHEENTUPA, J., RAUTEMAA, R. & KAMPE, O. 2009. Clinical manifestations and management of patients with autoimmune polyendocrine syndrome type I. *J Intern Med,* 265**,** 514-29.

ILMARINEN, T., ESKELIN, P., HALONEN, M., RUPPELL, T., KILPIKARI, R., TORRES, G. D., KANGAS, H. & ULMANEN, I. 2005. Functional analysis of SAND mutations in AIRE supports dominant inheritance of the G228W mutation. *Hum Mutat,* 26**,** 322-31.

IRVINE, W. J. & SCARTH, L. 1969. Antibody to the oxyphil cells of the human parathyroid in idiopathic hypoparathyroidism. *Clinical and Experimental Immunology,* 4**,** 505-10.

JACOB, S., VIEGAS, S., LEITE, M. I., WEBSTER, R., COSSINS, J., KENNETT, R., HILTON-JONES, D., MORGAN, B. P. & VINCENT, A. 2012. Presence and Pathogenic Relevance of Antibodies to Clustered Acetylcholine Receptor in Ocular and Generalized Myasthenia Gravis. *Archives of Neurology,* 69**,** 994-1001.

JIANG, W., ANDERSON, M. S., BRONSON, R., MATHIS, D. & BENOIST, C. 2005. Modifier loci condition autoimmunity provoked by Aire deficiency. *J Exp Med,* 202**,** 805-15.

JIANG, Y. F., ZHANG, Z., KIFOR, O., LANE, C. R., QUINN, S. J. & BAI, M. 2002. Protein kinase C (PKC) phosphorylation of the Ca2+ o-sensing receptor (CaR) modulates functional interaction of G proteins with the CaR cytoplasmic tail. *J Biol Chem,* 277**,** 50543-9.

KAHALY, G. J. 2009. Polyglandular autoimmune syndromes. *Eur J Endocrinol,* 161**,** 11-20.

KAHALY, G. J. 2012. Polyglandular autoimmune syndrome type II. *Presse Med,* 41**,** e663-70.

KEKALAINEN, E., TUOVINEN, H., JOENSUU, J., GYLLING, M., FRANSSILA, R., PONTYNEN, N., TALVENSAARI, K., PERHEENTUPA, J., MIETTINEN, A. & ARSTILA, T. P. 2007. A defect of regulatory T cells in patients with autoimmune polyendocrinopathy-candidiasis-ectodermal dystrophy. *J Immunol,* 178**,** 1208-15.

KELLEY, L. A., MEZULIS, S., YATES, C. M., WASS, M. N. & STERNBERG, M. J. 2015. The Phyre2 web portal for protein modeling, prediction and analysis. *Nat Protoc,* 10**,** 845-58.

KELLEY, L. A. & STERNBERG, M. J. E. 2009. Protein structure prediction on the Web: a case study using the Phyre server. *Nature Protocols,* 4**,** 363-371.

KEMP, E. H., GAVALAS, N. G., AKHTAR, S., KROHN, K. J., PALLAIS, J. C., BROWN, E. M., WATSON, P. F. & WEETMAN, A. P. 2010. Mapping of human autoantibody binding sites on the calcium-sensing receptor. *J Bone Miner Res,* 25**,** 132-40.

KEMP, E. H., GAVALAS, N. G., GAWKRODGER, D. J. & WEETMAN, A. P. 2007. Autoantibody responses to melanocytes in the depigmenting skin disease vitiligo. *Autoimmun Rev,* 6**,** 138-42.

KEMP, E. H., GAVALAS, N. G., KROHN, K. J., BROWN, E. M., WATSON, P. F. & WEETMAN, A. P. 2009. Activating autoantibodies against the calcium-sensing receptor detected in two patients with autoimmune polyendocrine syndrome type 1. *J Clin Endocrinol Metab,* 94**,** 4749-56.

KEMP, E. H., HABIBULLAH, M., KLUGER, N., RANKI, A., SANDHU, H. K., KROHN, K. J. & WEETMAN, A. P. 2014. Prevalence and clinical associations of calcium-sensing receptor and NALP5 autoantibodies in Finnish APECED patients. *J Clin Endocrinol Metab,* 99**,** 1064-71.

KEMP, E. H., HERD, L. M., WATERMAN, E. A., WILSON, A. G., WEETMAN, A. P. & WATSON, P. P. 2002. Immunoscreening of phage-displayed cDNA-encoded polypeptides identifies B cell targets in autoimmune disease. *Biochem Biophys Res Commun,* 298**,** 169-77.

KIFOR, O., MCELDUFF, A., LEBOFF, M. S., MOORE, F. D., JR., BUTTERS, R., GAO, P., CANTOR, T. L., KIFOR, I. & BROWN, E. M. 2004. Activating antibodies to the calcium-sensing receptor in two patients with autoimmune hypoparathyroidism. *J Clin Endocrinol Metab,* 89**,** 548-56.

KIFOR, O., MOORE, F. D., DELANEY, M., GARBER, J., HENDY, G. N., BUTTERS, R., GAO, P., CANTOR, T. L., KIFOR, I., BROWN, E. M. & WYSOLMERSKI, J. 2003. A syndrome of hypocalciuric hypercalcemia caused by autoantibodies directed at the calcium-sensing receptor. *Journal of Clinical Endocrinology & Metabolism,* 88**,** 60-72.

KISAND, K., LILIC, D., CASANOVA, J. L., PETERSON, P., MEAGER, A. & WILLCOX, N. 2011. Mucocutaneous candidiasis and autoimmunity against cytokines in APECED and thymoma patients: Clinical and pathogenetic implications. *European Journal of Immunology,* 41**,** 1517-1527.

KISAND, K., LINK, M., WOLFF, A. S. B., MEAGER, A., TSEREL, L., ORG, T., MURUMAGI, A., UIBO, R., WILLCOX, N., PODKRAJSEK, K. T., BATTELINO, T., LOBELL, A., KAMPE, O., LIMA, K., MELONI, A., ERGUN-LONGMIRE, B., MACLAREN, N. K., PERHEENTUPA, J., KROHN, K. J. E., SCOTT, H. S., HUSEBYE, E. S. & PETERSON, P. 2008. Interferon autoantibodies associated with AIRE deficiency decrease the expression of IFN-stimulated genes. *Blood,* 112**,** 2657-2666.

KISAND, K. & PETERSON, P. 2011. Autoimmune polyendocrinopathy candidiasis ectodermal dystrophy: known and novel aspects of the syndrome. *Ann N Y Acad Sci,* 1246**,** 77-91.

KISAND, K. & PETERSON, P. 2015. Autoimmune polyendocrinopathy candidiasis ectodermal dystrophy. *J Clin Immunol,* 35**,** 463-78.

KISAND, K., WOLFF, A. S. B., PODKRAJSEK, K. T., TSEREL, L., LINK, M., KISAND, K. V., ERSVAER, E., PERHEENTUPA, J., ERICHSEN, M. M., BRATANIC, N., MELONI, A., CETANI, F., PERNIOLA, R., ERGUN-LONGMIRE, B., MACLAREN, N., KROHN, K. J. E., PURA, M., SCHALKE, B., STROBEL, P., LEITE, M. I., BATTELINO, T., HUSEBYE, E. S., PETERSON, P., WILLCOX, N. & MEAGER, A. 2010. Chronic mucocutaneous candidiasis in APECED or thymoma patients correlates with autoimmunity to Th17-associated cytokines. *Journal of Experimental Medicine,* 207**,** 299-308.

KLUGER, N., JOKINEN, M., KROHN, K. & RANKI, A. 2013. Gastrointestinal manifestations in APECED syndrome. *J Clin Gastroenterol,* 47**,** 112-20.

KLUGER, N., JOKINEN, M., LINTULAHTI, A., KROHN, K. & RANKI, A. 2015. Gastrointestinal immunity against tryptophan hydroxylase-1, aromatic L-amino-acid decarboxylase, AIE-75, villin and Paneth cells in APECED. *Clin Immunol,* 158**,** 212-20.

KLUGER, N., RANKI, A. & KROHN, K. 2012. APECED: is this a model for failure of T cell and B cell tolerance? *Front Immunol,* 3**,** 232.

KOCH, D., LILIC, D. & CARMICHAEL, A. J. 2009. Autosomal dominant chronic mucocutaneous candidiasis and primary hypothyroidism complicated by oesophageal carcinoma. *Clin Exp Dermatol,* 34**,** e818-20.

KOHNO, Y., KIJIMA, M., YAMAGUCHI, F., SAITO, K., TSUNOO, H., HOSOYA, T. & NIIMI, H. 1993. Comparison of the IgG subclass distribution of anti-thyroid peroxidase antibodies in healthy subjects with that in patients with chronic thyroiditis. *Endocr J,* 40**,** 317-321.

KOLASKAR, A. S. & TONGAONKAR, P. C. 1990. A semi-empirical method for prediction of antigenic determinants on protein antigens. *FEBS Lett,* 276**,** 172-4.

KOPIC, S. & GEIBEL, J. P. 2013. Gastric acid, calcium absorption, and their impact on bone health. *Physiol Rev,* 93**,** 189-268.

KOSSLING, F. K. & EMMRICH, P. 1971. [Demonstration of a case of Addison's disease and hypoparathyroidism in childhood (author's transl)]. *Verh Dtsch Ges Pathol,* 55**,** 155-60.

KUNISHIMA, N., SHIMADA, Y., TSUJI, Y., SATO, T., YAMAMOTO, M., KUMASAKA, T., NAKANISHI, S., JINGAMI, H. & MORIKAWA, K. 2000. Structural basis of glutamate recognition by a dimeric metabotropic glutamate receptor. *Nature,* 407**,** 971-7.

KUROBE, H., LIU, C., UENO, T., SAITO, F., OHIGASHI, L., SEACH, N., ARAKAKI, R., HAYASHI, Y., KITAGAWA, T., LIPP, M., BOYD, R. L. & TAKAHAMA, Y. 2006. CCR7-Dependent cortex-to-medulla migration of positively selected thymocytes is essential for establishing central tolerance. *Immunity,* 24**,** 165-177.

KUROKAWA, K. 1994. The Kidney and Calcium Homeostasis. *Kidney International,* 45**,** S97-S105.

LAAKSO, S. M., KEKALAINEN, E., HEIKKILA, N., MANNERSTROM, H., KISAND, K., PETERSON, P., RANKI, A. & ARSTILA, T. P. 2014. In vivo analysis of helper T cell responses in patients with autoimmune polyendocrinopathy - candidiasis - ectodermal dystrophy provides evidence in support of an IL-22 defect. *Autoimmunity,* 47**,** 556-562.

LAAKSO, S. M., KEKALAINEN, E., ROSSI, L. H., LAURINOLLI, T. T., MANNERSTROM, H., HEIKKILA, N., LEHTOVIITA, A., PERHEENTUPA, J., JARVA, H. & ARSTILA, T. P. 2011. IL-7 dysregulation and loss of CD8+ T cell homeostasis in the monogenic human disease autoimmune polyendocrinopathy-candidiasis-ectodermal dystrophy. *J Immunol,* 187**,** 2023-30.

LAAKSO, S. M., LAURINOLLI, T. T., ROSSI, L. H., LEHTOVIITA, A., SAIRANEN, H., PERHEENTUPA, J., KEKALAINEN, E. & ARSTILA, T. P. 2010. Regulatory T cell defect in APECED patients is associated with loss of naive FOXP3(+) precursors and impaired activated population. *Journal of Autoimmunity,* 35**,** 351-357.

LAMPASONA, V., BEARZATTO, M., GENOVESE, S., BOSI, E., FERRARI, M. & BONIFACIO, E. 1996. Autoantibodies in insulin-dependent diabetes recognize distinct cytoplasmic domains of the protein tyrosine phosphatase-like IA-2 autoantigen. *J Immunol,* 157**,** 2707-2711.

LEI, Y., RIPEN, A. M., ISHIMARU, N., OHIGASHI, I., NAGASAWA, T., JEKER, L. T., BOSL, M. R., HOLLANDER, G. A., HAYASHI, Y., MALEFYT, R. D., NITTA, T. & TAKAHAMA, Y. 2011. Aire-dependent production of XCL1 mediates medullary accumulation of thymic dendritic cells and contributes to regulatory T cell development. *Journal of Experimental Medicine,* 208**,** 383-394.

LI, Y., SONG, Y. H., RAIS, N., CONNOR, E., SCHATZ, D., MUIR, A. & MACLAREN, N. 1996. Autoantibodies to the extracellular domain of the calcium sensing receptor in patients with acquired hypoparathyroidism. *J Clin Invest,* 97**,** 910-4.

LIANG, S. C., TAN, X. Y., LUXENBERG, D. P., KARIM, R., DUNUSSI-JOANNOPOULOS, K., COLLINS, M. & FOUSER, L. A. 2006. Interleukin (IL)-22 and IL-17 are coexpressed by Th17 cells and cooperatively enhance expression of antimicrobial peptides. *Journal of Experimental Medicine,* 203**,** 2271-2279.

LIBLAU, R. S., SINGER, S. M. & MCDEVITT, H. O. 1995. Th1 and Th2 CD4+ T cells in the pathogenesis of organ-specific autoimmune diseases. *Immunol Today,* 16**,** 34-8.

LIENHARDT, A., BAI, M., LAGARDE, J. P., RIGAUD, M., ZHANG, Z., JIANG, Y., KOTTLER, M. L., BROWN, E. M. & GARABEDIAN, M. 2001. Activating mutations of the calcium-sensing receptor: management of hypocalcemia. *J Clin Endocrinol Metab,* 86**,** 5313-23.

LINDH, E., BRANNSTROM, J., JONES, P., WERMELING, F., HASSLER, S., BETTERLE, C., GARTY, B., STRIDSBERG, M., HERRMANN, B., KARLSSON, M. C. I. & WINQVIST, O. 2013. Autoimmunity and cystatin SA1 deficiency behind chronic mucocutaneous candidiasis in autoimmune polyendocrine syndrome type 1. *Journal of Autoimmunity,* 42**,** 1-6.

LINDH, E., LIND, S. M., LINDMARK, E., HASSLER, S., PERHEENTUPA, J., PELTONEN, L., WINQVIST, O. & KARLSSON, M. C. I. 2008. AIRE regulates T-cell-independent B-cell responses through BAFF. *Proceedings of the National Academy of Sciences of the United States of America,* 105**,** 18466-18471.

LISTON, A., LESAGE, S., WILSON, J., PELTONEN, L. & GOODNOW, C. C. 2003. Aire regulates negative selection of organ-specific T cells. *Nature Immunology,* 4**,** 350-354.

LUPULESCU, A., PETROVICI, A., POP, A. & HEITMANEK, C. 1968a. Electron microscopic observations on the parathyroid gland in experimental hypoparathyroidism. *Experientia,* 24**,** 62-3.

LUPULESCU, A., POTORAC, E., POP, A., HEITMANEK, C., MERCULIEV, E., CHISIU, N., OPRISAN, R. & NEACSU, C. 1968b. Experimental investigations on immunology of the parathyroid gland. *Immunology,* 14**,** 475-82.

MAGITTA, N. F., PURA, M., WOLFF, A. S. B., VANUGA, P., MEAGER, A., KNAPPSKOG, P. M. & HUSEBYE, E. S. 2008. Autoimmune polyendocrine syndrome type I in Slovakia: relevance of screening patients with autoimmune Addison's disease. *European Journal of Endocrinology,* 158**,** 705-709.

MALCHOW, S., LEVENTHAL, D. S., NISHI, S., FISCHER, B. I., SHEN, L., PANER, G. P., AMIT, A. S., KANG, C., GEDDES, J. E., ALLISON, J. P., SOCCI, N. D. & SAVAGE, P. A. 2013. Aire-dependent thymic development of tumor-associated regulatory T cells. *Science,* 339**,** 1219-24.

MANOLAGAS, S. C. & JILKA, R. L. 1995. Mechanisms of Disease - Bone-Marrow, Cytokines, and Bone Remodeling - Emerging Insights into the Pathophysiology of Osteoporosis. *New England Journal of Medicine,* 332**,** 305-311.

MATSUMOTO, M. 2011. Contrasting models for the roles of Aire in the differentiation program of epithelial cells in the thymic medulla. *Eur J Immunol,* 41**,** 12-7.

MAYER, A., PLOIX, C., ORGIAZZI, J., DESBOS, A., MOREIRA, A., VIDAL, H., MONIER, J. C., BIENVENU, J. & FABIEN, N. 2004. Calcium-sensing receptor autoantibodies are relevant markers of acquired hypoparathyroidism. *J Clin Endocrinol Metab,* 89**,** 4484-8.

MAZZA, C., BUZI, F., ORTOLANI, F., VITALI, A., NOTARANGELO, L. D., WEBER, G., BACCHETTA, R., SORESINA, A., LOUGARIS, V., GREGGIO, N. A., TADDIO, A., PASIC, S., DE VROEDE, M., PAC, M., KILIC, S. S., OZDEN, S., RUSCONI, R., MARTINO, S., CAPALBO, D., SALERNO, M., PIGNATA, C., RADETTI, G., MAGGIORE, G., PLEBANI, A., NOTARANGELO, L. D. & BADOLATO, R. 2011. Clinical heterogeneity and diagnostic delay of autoimmune polyendocrinopathy-candidiasis-ectodermal dystrophy syndrome. *Clin Immunol,* 139**,** 6-11.

MCINTOSH, R. S., ASGHAR, M. S., KEMP, E. H., WATSON, P. F., GARDAS, A., BANGA, J. P. & WEETMAN, A. P. 1997. Analysis of immunoglobulin G kappa antithyroid peroxidase antibodies from different tissues in Hashimoto's thyroiditis. *J Clin Endocrinol Metab,* 82**,** 3818-3825.

MEAGER, A., VISVALINGAM, K., PETERSON, P., MOLL, K., MURUMAGI, A., KROHN, K., ESKELIN, P., PERHEENTUPA, J., HUSEBYE, E., KADOTA, Y. & WILLCOX, N. 2006. Anti-interferon autoantibodies in autoimmune polyendocrinopathy syndrome type 1. *PLoS Med,* 3**,** e289.

MELONI, A., PERNIOLA, R., FAA, V., CORVAGLIA, E., CAO, A. & ROSATELLI, M. C. 2002. Delineation of the molecular defects in the AIRE gene in autoimmune polyendocrinopathy-candidiasis-ectodermal dystrophy patients from Southern Italy. *J Clin Endocrinol Metab,* 87**,** 841-6.

MELONI, A., WILLCOX, N., MEAGER, A., ATZENI, M., WOLFF, A. S., HUSEBYE, E. S., FURCAS, M., ROSATELLI, M. C., CAO, A. & CONGIA, M. 2012. Autoimmune polyendocrine syndrome type 1: an extensive longitudinal study in Sardinian patients. *J Clin Endocrinol Metab,* 97**,** 1114-24.

MERENMIES, L. & TARKKANEN, A. 2000. Chronic bilateral keratitis in autoimmune polyendocrinopathy-candidiadis-ectodermal dystrophy (APECED). A long-term follow-up and visual prognosis. *Acta Ophthalmol Scand,* 78**,** 532-5.

METZGER, T. C. & ANDERSON, M. S. 2011. Control of central and peripheral tolerance by Aire. *Immunol Rev,* 241**,** 89-103.

MEZGUELDI, E., BERTHOLET-THOMAS, A., MILAZZO, S., MORRIS, M., BACCHETTA, J., FABIEN, N., COCHAT, P., WEETMAN, A. P., KEMP, E. H. & BELOT, A. 2015. Early-onset hypoparathyroidism and chronic keratitis revealing APECED. *Clin Case Rep,* 3**,** 809-13.

MICHELS, A. W. & EISENBARTH, G. S. 2009. Autoimmune polyendocrine syndrome type 1 (APS-1) as a model for understanding autoimmune polyendocrine syndrome type 2 (APS-2). *Journal of Internal Medicine,* 265**,** 530-540.

MISHARIN, A. V., NAGAYAMA, Y., ALIESKY, H. A., RAPOPORT, B. & MCLACHLAN, S. M. 2009. Studies in mice deficient for the autoimmune regulator (Aire) and transgenic for the thyrotropin receptor reveal a role for Aire in tolerance for thyroid autoantigens. *Endocrinology,* 150**,** 2948-56.

MIYARA, M., YOSHIOKA, Y., KITOH, A., SHIMA, T., WING, K., NIWA, A., PARIZOT, C., TAFLIN, C., HEIKE, T., VALEYRE, D., MATHIAN, A., NAKAHATA, T., YAMAGUCHI, T., NOMURA, T., ONO, M., AMOURA, Z., GOROCHOV, G. & SAKAGUCHI, S. 2009. Functional delineation and differentiation dynamics of human CD4+ T cells expressing the FoxP3 transcription factor. *Immunity,* 30**,** 899-911.

MORGENTHALER, N. G., HO, S. C. & MINICH, W. B. 2007. Stimulating and blocking thyroid-stimulating hormone (TSH) receptor autoantibodies from patients with Graves' disease and autoimmune hypothyroidism have very similar concentration, TSH receptor affinity, and binding sites. *Journal of Clinical Endocrinology & Metabolism,* 92**,** 1058-1065.

MORGENTHALER, N. G., HODAK, K., SEISSLER, J., STEINBRENNER, H., PAMPEL, I., GUPTA, M., MCGREGOR, A. M., SCHERBAUM, W. A. & BANGA, J. P. 1999. Direct binding of thyrotropin receptor autoantibody to in vitro translated thyrotropin receptor: a comparison to radioreceptor assay and thyroid stimulating bioassay. *Thyroid,* 9**,** 466-75.

MORRIS, G. E. 2001. Epitope Mapping: B-cell Epitopes. *eLS.* John Wiley & Sons, Ltd.

MOSMANN, T. R. & SAD, S. 1996. The expanding universe of T-cell subsets: Th1, Th2 and more. *Immunol Today,* 17**,** 138-146.

MYERS, M. A., DAVIES, J. M., TONG, J. C., WHISSTOCK, J., SCEALY, M., MACKAY, I. R. & ROWLEY, M. J. 2000. Conformational epitopes on the diabetes autoantigen GAD65 identified by peptide phage display and molecular modeling. *J Immunol,* 165**,** 3830-8.

MYHRE, A. G., HALONEN, M., ESKELIN, P., EKWALL, O., HEDSTRAND, H., RORSMAN, F., KAMPE, O. & HUSEBYE, E. S. 2001. Autoimmune polyendocrine syndrome type 1 (APS I) in Norway. *Clin Endocrinol (Oxf),* 54**,** 211-7.

NAGAMINE, K., PETERSON, P., SCOTT, H. S., KUDOH, J., MINOSHIMA, S., HEINO, M., KROHN, K. J. E., LALIOTI, M. D., MULLIS, P. E., ANTONARAKIS, S. E., KAWASAKI, K., ASAKAWA, S., ITO, F. & SHIMIZU, N. 1997. Positional cloning of the APECED gene. *Nature Genetics,* 17**,** 393-398.

NASERKE, H. E., ZIEGLER, A. G., LAMPASONA, V. & BONIFACIO, E. 1998. Early development and spreading of autoantibodies to epitopes of IA-2 and their association with progression to type 1 diabetes. *J Immunol,* 161**,** 6963-6969.

NEUFELD, M., MACLAREN, N. K. & BLIZZARD, R. M. 1981. Two types of autoimmune Addison's disease associated with different polyglandular autoimmune (PGA) syndromes. *Medicine (Baltimore),* 60**,** 355-62.

NIKI, S., OSHIKAWA, K., MOURI, Y., HIROTA, F., MATSUSHIMA, A., YANO, M., HAN, H., BANDO, Y., IZUMI, K., MATSUMOTO, M., NAKAYAMA, K. I., KURODA, N. & MATSUMOTO, M. 2006. Alteration of intra-pancreatic target-organ specificity by abrogation of Aire in NOD mice. *J Clin Invest,* 116**,** 1292-301.

NOKOFF, N. J., REWERS, M. & CREE GREEN, M. 2012. The interplay of autoimmunity and insulin resistance in type 1 diabetes. *Discov Med,* 13**,** 115-22.

O'DWYER, D. T., MCELDUFF, P., PETERSON, P., PERHEENTUPA, J. & CROCK, P. A. 2007. Pituitary autoantibodies in autoimmune polyendocrinopathy-candidiasis-ectodermal dystrophy (APECED). *Acta Biomed,* 78 Suppl 1**,** 248-54.

OBERMAYER-STRAUB, P., PERHEENTUPA, J., BRAUN, S., KAYSER, A., BARUT, A., LOGES, S., HARMS, A., DALEKOS, G., STRASSBURG, C. P. & MANNS, M. P. 2001. Hepatic autoantigens in patients with autoimmune polyendocrinopathy-candidiasis-ectodermal dystrophy. *Gastroenterology,* 121**,** 668-77.

OFTEDAL, B. E., HELLESEN, A., ERICHSEN, M. M., BRATLAND, E., VARDI, A., PERHEENTUPA, J., KEMP, E. H., FISKERSTRAND, T., VIKEN, M. K., WEETMAN, A. P., FLEISHMAN, S. J., BANKA, S., NEWMAN, W. G., SEWELL, W. A., SOZAEVA, L. S., ZAYATS, T., HAUGARVOLL, K., ORLOVA, E. M., HAAVIK, J., JOHANSSON, S., KNAPPSKOG, P. M., LOVAS, K., WOLFF, A. S., ABRAMSON, J. & HUSEBYE, E. S. 2015. Dominant Mutations in the Autoimmune Regulator AIRE Are Associated with Common Organ-Specific Autoimmune Diseases. *Immunity,* 42**,** 1185-96.

OLIVA-HEMKER, M., BERKENBLIT, G. V., ANHALT, G. J. & YARDLEY, J. H. 2006. Pernicious anemia and widespread absence of gastrointestinal endocrine cells in a patient with autoimmune polyglandular syndrome type I and malabsorption. *J Clin Endocrinol Metab,* 91**,** 2833-8.

OMASITS, U., AHRENS, C. H., MULLER, S. & WOLLSCHEID, B. 2014. Protter: interactive protein feature visualization and integration with experimental proteomic data. *Bioinformatics,* 30**,** 884-6.

ORLOVA, E. M., BUKINA, A. M., KUZNETSOVA, E. S., KAREVA, M. A., ZAKHAROVA, E. U., PETERKOVA, V. A. & DEDOV, II 2010. Autoimmune polyglandular syndrome type 1 in Russian patients: clinical variants and autoimmune regulator mutations. *Horm Res Paediatr,* 73**,** 449-57.

OSMAN, A. A., GÜNNEL, T., DIETL, A., UHLIG, H. H., AMIN, M., FLECKENSTEIN, B., RICHTER, T. & MOTHES, T. 2000. B cell epitopes of gliadin. *Clinical & Experimental Immunology,* 121**,** 248-254.

PALLAIS, J. C., KIFOR, O., CHEN, Y. B., SLOVIK, D. & BROWN, E. M. 2004. Brief report - Acquired hypocalciuric hypercalcemia due to autoantibodies against the calcium-sensing receptor. *New England Journal of Medicine,* 351**,** 362-369.

PARKER, R. I., O'SHEA, P. & FORMAN, E. N. 1990. Acquired splenic atrophy in a sibship with the autoimmune polyendocrinopathy-candidiasis syndrome. *J Pediatr,* 117**,** 591-3.

PAVLIC, A. & WALTIMO-SIREN, J. 2009. Clinical and microstructural aberrations of enamel of deciduous and permanent teeth in patients with autoimmune polyendocrinopathy-candidiasis-ectodermal dystrophy. *Arch Oral Biol,* 54**,** 424-31.

PEARCE, S. H., BAI, M., QUINN, S. J., KIFOR, O., BROWN, E. M. & THAKKER, R. V. 1996. Functional characterization of calcium-sensing receptor mutations expressed in human embryonic kidney cells. *J Clin Invest,* 98**,** 1860-6.

PELLETIER-MOREL, L., FABIEN, N., MOUHOUB, Y., BOITARD, C. & LARGER, E. 2008. Hyperparathyroidism in a patient with autoimmune polyglandular syndrome. *Intern Med,* 47**,** 1911-5.

PERHEENTUPA, J. 2006. Autoimmune polyendocrinopathy-candidiasis-ectodermal dystrophy. *J Clin Endocrinol Metab,* 91**,** 2843-50.

PERNIOLA, R., FALORNI, A., CLEMENTE, M. G., FORINI, F., ACCOGLI, E. & LOBREGLIO, G. 2000. Organ-specific and non-organ-specific autoantibodies in children and young adults with autoimmune polyendocrinopathy-candidiasis-ectodermal dystrophy (APECED). *Eur J Endocrinol,* 143**,** 497-503.

PERNIOLA, R., FILOGRANA, O., GRECO, G. & PELLEGRINO, V. 2008. High prevalence of thyroid autoimmunity in Apulian patients with autoimmune polyglandular syndrome type 1. *Thyroid,* 18**,** 1027-1029.

PERNIOLA, R., LOBREGLIO, G., ROSATELLI, M. C., PITOTTI, E., ACCOGLI, E. & DE RINALDIS, C. 2005. Immunophenotypic characterisation of peripheral blood lymphocytes in autoimmune polyglandular syndrome type 1: clinical study and review of the literature. *J Pediatr Endocrinol Metab,* 18**,** 155-64.

PERRET, C., WIESNER-MENZEL, L. & HAPPLE, R. 1984. Immunohistochemical analysis of T-cell subsets in the peribulbar and intrabulbar infiltrates of alopecia areata. *Acta Derm Venereol,* 64**,** 26-30.

PETERSON, P., ORG, T. & REBANE, A. 2008. Transcriptional regulation by AIRE: molecular mechanisms of central tolerance. *Nat Rev Immunol,* 8**,** 948-57.

PETERSON, P. & PELTONEN, L. 2005. Autoimmune polyendocrinopathy syndrome type 1 (APS1) and AIRE gene: New views on molecular basis of autoimmunity. *Journal of Autoimmunity,* 25**,** 49-55.

PETTERSSON, I. 1992. Methods of epitope mapping. *Molecular Biology Reports,* 16**,** 149-153.

PITKANEN, J., REBANE, A., ROWELL, J., MURUMAGI, A., STROBEL, P., MOLL, K., SAARE, M., HEIKKILA, J., DOUCAS, V., MARX, A. & PETERSON, P. 2005. Cooperative activation of transcription by autoimmune regulator AIRE and CBP. *Biochem Biophys Res Commun,* 333**,** 944-53.

PODKRAJSEK, K. T., BRATANIC, N., KRZISNIK, C. & BATTELINO, T. 2005. Autoimmune regulator-1 messenger ribonucleic acid analysis in a novel intronic mutation and two additional novel AIRE gene mutations in a cohort of autoimmune polyendocrinopathy-candidiasis-ectodermal dystrophy patients. *J Clin Endocrinol Metab,* 90**,** 4930-5.

PODKRAJSEK, K. T., MILENKOVIC, T., ODINK, R. J., CLAASEN-VAN DER GRINTEN, H. L., BRATANIC, N., HOVNIK, T. & BATTELINO, T. 2008. Detection of a complete autoimmune regulator gene deletion and two additional novel mutations in a cohort of patients with atypical phenotypic variants of autoimmune polyglandular syndrome type 1. *Eur J Endocrinol,* 159**,** 633-9.

POLIANI, P. L., KISAND, K., MARRELLA, V., RAVANINI, M., NOTARANGELO, L. D., VILLA, A., PETERSON, P. & FACCHETTI, F. 2010. Human peripheral lymphoid tissues contain autoimmune regulator-expressing dendritic cells. *Am J Pathol,* 176**,** 1104-12.

POLLAK, M. R., BROWN, E. M., ESTEP, H. L., MCLAINE, P. N., KIFOR, O., PARK, J., HEBERT, S. C., SEIDMAN, C. E. & SEIDMAN, J. G. 1994. Autosomal dominant hypocalcaemia caused by a Ca(2+)-sensing receptor gene mutation. *Nat Genet,* 8**,** 303-7.

POLLAK, U., BAR-SEVER, Z., HOFFER, V., MARCUS, N., SCHEUERMAN, O. & GARTY, B. Z. 2009. Asplenia and functional hyposplenism in autoimmune polyglandular syndrome type 1. *Eur J Pediatr,* 168**,** 233-5.

POSILLICO, J. T., WORTSMAN, J., SRIKANTA, S., EISENBARTH, G. S., MALLETTE, L. E. & BROWN, E. M. 1986. Parathyroid Cell-Surface Autoantibodies That Inhibit Parathyroid-Hormone Secretion from Dispersed Human Parathyroid Cells. *Journal of Bone and Mineral Research,* 1**,** 475-483.

PROUST-LEMOINE, E., SAUGIER-VEBER, P., LEFRANC, D., DUBUCQUOI, S., RYNDAK, A., BUOB, D., LALAU, J. D., DESAILLOUD, R., WEILL, J., PRIN, L., LEFEBVRE, H. & WEMEAU, J. L. 2010. Autoimmune Polyendocrine Syndrome Type 1 in North-Western France: AIRE Gene Mutation Specificities and Severe Forms Needing Immunosuppressive Therapies. *Hormone Research in Paediatrics,* 74**,** 275-284.

PROUST-LEMOINE, E., SAUGIER-VEBER, P. & WÉMEAU, J.-L. 2012. Polyglandular Autoimmune Syndrome Type I. *La Presse Médicale,* 41**,** e651-e662.

PUEL, A., DOFFINGER, R., NATIVIDAD, A., CHRABIEH, M., BARCENAS-MORALES, G., PICARD, C., COBAT, A., OUACHEE-CHARDIN, M., TOULON, A., BUSTAMANTE, J., AL-MUHSEN, S., AL-OWAIN, M., ARKWRIGHT, P. D., COSTIGAN, C., MCCONNELL, V., CANT, A. J., ABINUN, M., POLAK, M., BOUGNERES, P. F., KUMARARATNE, D., MARODI, L., NAHUM, A., ROIFMAN, C.,

BLANCHE, S., FISCHER, A., BODEMER, C., ABEL, L., LILIC, D. & CASANOVA, J. L. 2010. Autoantibodies against IL-17A, IL-17F, and IL-22 in patients with chronic mucocutaneous candidiasis and autoimmune polyendocrine syndrome type I. *J Exp Med,* 207**,** 291-7.

RAMSEY, C., WINQVIST, O., PUHAKKA, L., HALONEN, M., MORO, A., KAMPE, O., ESKELIN, P., PELTO-HUIKKO, M. & PELTONEN, L. 2002. Aire deficient mice develop multiple features of APECED phenotype and show altered immune response. *Hum Mol Genet,* 11**,** 397-409.

RAY, K., CLAPP, P., GOLDSMITH, P. K. & SPIEGEL, A. M. 1998. Identification of the sites of N-linked glycosylation on the human calcium receptor and assessment of their role in cell surface expression and signal transduction. *J Biol Chem,* 273**,** 34558-67.

REDL, B., MERSCHAK, P., ABT, B. & WOJNAR, P. 1999. Phage display reveals a novel interaction of human tear lipocalin and thioredoxin which is relevant for ligand binding. *FEBS Lett,* 460**,** 182-6.

REYES-CRUZ, G., HU, J. X., GOLDSMITH, P. K., STEINBACH, P. J. & SPIEGEL, A. M. 2001. Human Ca2+ receptor extracellular domain - Analysis of function of lobe I loop deletion mutants. *Journal of Biological Chemistry,* 276**,** 32145-32151.

ROITT, I. M. & DELVES, P. J. 1997. *Roitt's essential immunology,* Oxford, Blackwell Science.

ROMAGNANI, S. 1995. Biology of human TH1 and TH2 cells. *J Clin Immunol,* 15**,** 121-129.

ROSA, D. D., PASQUALOTTO, A. C. & DENNING, D. W. 2008. Chronic mucocutaneous candidiasis and oesophageal cancer. *Med Mycol,* 46**,** 85-91.

ROSANO, G. L. & CECCARELLI, E. A. 2014. Recombinant protein expression in Escherichia coli: advances and challenges. *Frontiers in Microbiology,* 5**,** 172.

ROSATELLI, M. C., MELONI, A., MELONI, A., DEVOTO, M., CAO, A., SCOTT, H. S., PETERSON, P., HEINO, M., KROHN, K. J. E., NAGAMINE, K., KUDOH, J., SHIMIZU, N. & ANTONARAKIS, S. E. 1998. A common mutation in Sardinian autoimmune polyendocrinopathy-candidiasis-ectodermal dystrophy patients. *Human Genetics,* 103**,** 428-434.

ROSE, N. R. & BONA, C. 1993. Defining criteria for autoimmune diseases (Witebsky's postulates revisited). *Immunology Today,* 14**,** 426-430.

ROTTEMBOURG, D., DEAL, C., LAMBERT, M., MALLONE, R., CAREL, J. C., LACROIX, A., CAILLAT-ZUCMAN, S. & LE DEIST, F. 2010. 21-Hydroxylase epitopes are targeted by CD8 T cells in autoimmune Addison's disease. *J Autoimmun,* 35**,** 309-15.

ROWLEY, M. J., SCEALY, M., WHISSTOCK, J. C., JOIS, J. A., WIJEYEWICKREMA, L. C. & MACKAY, I. R. 2000. Prediction of the immunodominant epitope of the pyruvate dehydrogenase complex E2 in primary biliary cirrhosis using phage display. *J Immunol,* 164**,** 3413-9.

RUSSEL, M., LOWMAN, H. B. & CLACKSON, T. 2004. Introduction to phage biology and phage display. *Phage Display: A practical approach***,** 1-26.

RYAN, K. R., LAWSON, C. A., LORENZI, A. R., ARKWRIGHT, P. D., ISAACS, J. D. & LILIC, D. 2005. CD4+CD25+ T-regulatory cells are decreased in patients with autoimmune polyendocrinopathy candidiasis ectodermal dystrophy. *J Allergy Clin Immunol,* 116**,** 1158-9.

SARKADI, A. K., TASKO, S., CSORBA, G., TOTH, B., ERDOS, M. & MARODI, L. 2014. Autoantibodies to IL-17A may be correlated with the severity of mucocutaneous candidiasis in APECED patients. *J Clin Immunol,* 34**,** 181-93.

SATO, K., NAKAJIMA, K., IMAMURA, H., DEGUCHI, T., HORINOUCHI, S., YAMAZAKI, K., YAMADA, E., KANAJI, Y. & TAKANO, K. 2002. A novel missense mutation of AIRE gene in a patient with autoimmune polyendocrinopathy, candidiasis and ectodermal dystrophy (APECED), accompanied with progressive muscular atrophy: Case report and review of the literature in Japan. *Endocrine Journal,* 49**,** 625-633.

SCHERUBL, H., SCHULTZ, G. & HESCHELER, J. 1991. Electrophysiological Properties of Rat Calcitonin-Secreting Cells. *Molecular and Cellular Endocrinology,* 82**,** 293-301.

SCOTT, H. S., HEINO, M., PETERSON, P., MITTAZ, L., LALIOTI, M. D., BETTERLE, C., COHEN, A., SERI, M., LERONE, M., ROMEO, G., COLLIN, P., SALO, M., METCALFE, R., WEETMAN, A., PAPASAVVAS, M.-P., ROSSIER, C., NAGAMINE, K., KUDOH, J., SHIMIZU, N., KROHN, K. J. E. & ANTONARAKIS, S. E. 1998. Common Mutations in Autoimmune Polyendocrinopathy-Candidiasis-Ectodermal Dystrophy Patients of Different Origins. *Molecular Endocrinology,* 12**,** 1112-1119.

SHUM, A. K., ALIMOHAMMADI, M., TAN, C. L., CHENG, M. H., METZGER, T. C., LAW, C. S., LWIN, W., PERHEENTUPA, J., BOUR-JORDAN, H., CAREL, J. C., HUSEBYE, E. S., DE LUCA, F., JANSON, C., SARGUR, R., DUBOIS, N., KAJOSAARI, M., WOLTERS, P. J., CHAPMAN, H. A., KAMPE, O. & ANDERSON, M. S. 2013. BPIFB1 is a lung-specific autoantigen associated with interstitial lung disease. *Sci Transl Med,* 5**,** 206ra139.

SILVA, A. M., ROSARIO, L. M. & SANTOS, R. M. 1994. Background Ca2+ Influx Mediated by a Dihydropyridine-Insensitive and Voltage-Insensitive Channel in Pancreatic Beta-Cells - Modulation by Ni2+, Diphenylamine-2-Carboxylate, and Glucose-Metabolism. *Journal of Biological Chemistry,* 269**,** 17095-17103.

SILVA, L. M., CHAVEZ, J., CANALLI, M. H. & ZANETTI, C. R. 2003. Determination of IgG subclasses and avidity of antithyroid peroxidase antibodies in patients with subclinical hypothyroidism - a comparison with patients with overt hypothyroidism. *Horm Res,* 59**,** 118-124.

SILVE, C., PETREL, C., LEROY, C., BRUEL, H., MALLET, E., ROGNAN, D. & RUAT, M. 2005. Delineating a Ca2+ binding pocket within the Venus flytrap module of the human calcium-sensing receptor. *Journal of Biological Chemistry,* 280**,** 37917-37923.

SKOLDBERG, F., PORTELA-GOMES, G. M., GRIMELIUS, L., NILSSON, G., PERHEENTUPA, J., BETTERLE, C., HUSEBYE, E. S., GUSTAFSSON, J., RONNBLOM, A., RORSMAN, F. & KAMPE, O. 2003. Histidine decarboxylase, a pyridoxal phosphate-dependent enzyme, is an autoantigen of gastric enterochromaffin-like cells. *Journal of Clinical Endocrinology & Metabolism,* 88**,** 1445-1452.

SMITH, G. P. 1985. Filamentous fusion phage: novel expression vectors that display cloned antigens on the virion surface. *Science,* 228**,** 1315-7.

SNAPPER, C. M. & PAUL, W. E. 1987. Interferon-gamma and B cell stimulatory factor-1 reciprocally regulate Ig isotype production. *Science,* 236**,** 944-7.

SODERBERGH, A., MYHRE, A. G., EKWALL, O., GEBRE-MEDHIN, G., HEDSTRAND, H., LANDGREN, E., MIETTINEN, A., ESKELIN, P., HALONEN, M., TUOMI, T., GUSTAFSSON, J., HUSEBYE, E. S., PERHEENTUPA, J., GYLLING, M., MANNS, M. P., RORSMAN, F., KAMPE, O. & NILSSON, T. 2004. Prevalence and clinical associations of 10 defined autoantibodies in autoimmune polyendocrine syndrome type I. *Journal of Clinical Endocrinology & Metabolism,* 89**,** 557-562.

SPIEGELBERG, H. L. 1974. Biological activities of immunoglobulins of different classes and subclasses. *Adv Immunol,* 19**,** 259-294.

SQUIRES, P. E. 2000. Non-Ca2+-homeostatic functions of the extracellular Ca2+-sensing receptor (CaR) in endocrine tissues. *J Endocrinol,* 165**,** 173-7.

STOLARSKI, B., PRONICKA, E., KORNISZEWSKI, L., POLLAK, A., KOSTRZEWA, G., ROWINSKA, E., WLODARSKI, P., SKORKA, A., GREMIDA, M., KRAJEWSKI, P. & PLOSKI, R. 2006. Molecular background of polyendocrinopathy-candidiasis-ectodermal dystrophy syndrome in a Polish population: novel AIRE mutations and an estimate of disease prevalence. *Clin Genet,* 70**,** 348-54.

SYREN, K., LINDSAY, L., STOEHRER, B., JURY, K., LUHDER, F., BAEKKESKOV, S. & RICHTER, W. 1996. Immune reactivity of diabetes-associated human monoclonal autoantibodies defines multiple epitopes and detects two domain boundaries in glutamate decarboxylase. *Journal of Immunology,* 157**,** 5208-14.

TAKEDA, I., RAYNO, K., MOVAFAGH, F. B., WOLFSON-REICHLIN, M. & REICHLIN, M. 2001. Dual binding capabilities of anti-double-stranded DNA antibodies and anti-ribosomal phosphoprotein (P) antibodies. *Lupus,* 10**,** 857-65.

TARKKANEN, A. & MERENMIES, L. 2001. Corneal pathology and outcome of keratoplasty in autoimmune polyendocrinopathy-candidiasis-ectodermal dystrophy (APECED). *Acta Ophthalmol Scand,* 79**,** 204-7.

TODES-TAYLOR, N., TURNER, R., WOOD, G. S., STRATTE, P. T. & MORHENN, V. B. 1984. T cell subpopulations in alopecia areata. *J Am Acad Dermatol,* 11**,** 216-23.

TOH, B. H., VAN DRIEL, I. R. & GLEESON, P. A. 1997. Pernicious anemia. *N Engl J Med,* 337**,** 1441-8.

TOMAR, N., GUPTA, N. & GOSWAMI, R. 2013. Calcium-sensing receptor autoantibodies and idiopathic hypoparathyroidism. *J Clin Endocrinol Metab,* 98**,** 3884-91.

TOMAR, N., KAUSHAL, E., DAS, M., GUPTA, N., BETTERLE, C. & GOSWAMI, R. 2012. Prevalence and Significance of NALP5 Autoantibodies in Patients with Idiopathic Hypoparathyroidism. *Journal of Clinical Endocrinology & Metabolism,* 97**,** 1219-1226.

TOTH, B., WOLFF, A. S., HALASZ, Z., TAR, A., SZUTS, P., ILYES, I., ERDOS, M., SZEGEDI, G., HUSEBYE, E. S., ZEHER, M. & MARODI, L. 2010. Novel sequence variation of AIRE and detection of interferon-omega antibodies in early infancy. *Clin Endocrinol (Oxf),* 72**,** 641-7.

TRAGER, U., SIERRO, S., DJORDJEVIC, G., BOUZO, B., KHANDWALA, S., MELONI, A., MORTENSEN, M. & SIMON, A. K. 2012. The immune response to melanoma is limited by thymic selection of self-antigens. *PLoS One,* 7**,** e35005.

TUOMI, T., BJORSES, P., FALORNI, A., PARTANEN, J., PERHEENTUPA, J., LERNMARK, A. & MIETTINEN, A. 1996. Antibodies to glutamic acid decarboxylase and insulin-dependent diabetes in patients with autoimmune polyendocrine syndrome type I. *J Clin Endocrinol Metab,* 81**,** 1488-94.

ULINSKI, T., PERRIN, L., MORRIS, M., HOUANG, M., CABROL, S., GRAPIN, C., CHABBERT-BUFFET, N., BENSMAN, A., DESCHENES, G. & GIURGEA, I. 2006. Autoimmune polyendocrinopathy-candidiasis-ectodermal dystrophy syndrome with renal failure: impact of posttransplant immunosuppression on disease activity. *J Clin Endocrinol Metab,* 91**,** 192-5.

VAN CAMPENHOUT, C. M., VAN COTTHEM, K. A., STEVENS, W. J. & DE CLERCK, L. S. 2007. Performance of automated measurement of antibodies to cyclic citrullinated peptide in the routine clinical laboratory. *Scand J Clin Lab Invest,* 67**,** 859-67.

VAN DE WINKEL, J. G. & CAPEL, P. J. 1993. Human IgG Fc receptor heterogeneity: molecular aspects and clinical implications. *Immunol Today,* 14**,** 215-21.

VAN DE WINKEL, J. G. & CAPEL, P. J. 1996. *Human IgG Fc receptors,* Austin Landes Company.

VAN DEN BOORN, J. G., KONIJNENBERG, D., DELLEMIJN, T. A. M., VAN DER VEEN, J. P. W., BOS, J. D., MELIEF, C. J. M., VYTH-DREESE, F. A. & LUITEN, R. M. 2009. Autoimmune Destruction of Skin Melanocytes by Perilesional T Cells from Vitiligo Patients. *Journal of Investigative Dermatology,* 129**,** 2220-2232.

VAN DEN DRIESSCHE, A., EENKHOORN, V., VAN GAAL, L. & DE BLOCK, C. 2009. Type 1 diabetes and autoimmune polyglandular syndrome: a clinical review. *Neth J Med,* 67**,** 376-87.

VAN LOGHEM, E. 1986. Allotypic markers. *Monogr Allergy,* 19**,** 40-51.

VANDECAS, M. & GEPTS, W. 1973. Primary (Autoimmune Questionable) Parathyroiditis. *Virchows Archiv Abteilung a Pathologische Anatomie,* 361**,** 257-261.

VON MIKECZ, A. H., HEMMERICH, P. H., PETER, H. H. & KRAWINKEL, U. 1995. Autoantigenic epitopes on eukaryotic L7. *Clin Exp Immunol,* 100**,** 205-213.

WADA, N., NISHIFUJI, K., YAMADA, T., KUDOH, J., SHIMIZU, N., MATSUMOTO, M., PELTONEN, L., NAGAFUCHI, S. & AMAGAI, M. 2011. Aire-dependent thymic expression of desmoglein 3, the autoantigen in pemphigus vulgaris, and its role in T-cell tolerance. *J Invest Dermatol,* 131**,** 410-7.

WALTER, W. 2000. PIcture of the month. *Archives of Pediatrics & Adolescent Medicine,* 154**,** 746-746.

WANG, C. Y., DAVOODI-SEMIROMI, A., HUANG, W., CONNOR, E., SHI, J. D. & SHE, J. X. 1998. Characterization of mutations in patients with autoimmune polyglandular syndrome type 1 (APS1). *Hum Genet,* 103**,** 681-5.

WANG, X. P., LAAN, M., BICHELE, R., KISAND, K., SCOTT, H. S. & PETERSON, P. 2012. Post-Aire maturation of thymic medullary epithelial cells involves selective expression of keratinocyte-specific autoantigens. *Frontiers in Immunology,* 3.

WATERMAN, E. A., GAWKRODGER, D. J., WATSON, P. F., WEETMAN, A. P. & HELEN KEMP, E. 2010. Autoantigens in Vitiligo Identified by the Serological Selection of a Phage-Displayed Melanocyte cDNA Expression Library. *Journal of Investigative Dermatology,* 130**,** 230-240.

WEETMAN, A. P. 2004. Cellular immune responses in autoimmune thyroid disease. *Clin Endocrinol (Oxf),* 61**,** 405-13.

WEETMAN, A. P., BLACK, C. M., COHEN, S. B., TOMLINSON, R., BANGA, J. P. & REIMER, C. B. 1989. Affinity purification of IgG subclasses and the distribution of thyroid auto-antibody reactivity in Hashimoto's thyroiditis. *Scandinavian Journal of Immunology,* 30**,** 73-82.

WEETMAN, A. P. & MCGREGOR, A. M. 1994. Autoimmune thyroid disease: further developments in our understanding. *Endocr Rev,* 15**,** 788-830.

WESTWOOD, O. M. R. & HAY, F. C. 2001. *Epitope mapping : a practical approach,* Oxford ; New York, Oxford University Press.

WILLIAMS, S., VAN DER LOGT, P. & GERMASCHEWSKI, V. 2001. Phage display libraries. *In:* WESTWOOD, O. M. R. & HAY, F. C. (eds.) *Epitope mapping: A practical approach.* Oxford: Oxford University Press.

WILSON, D. R. & FINLAY, B. B. 1998. Phage display: applications, innovations, and issues in phage and host biology. *Can J Microbiol,* 44**,** 313-29.

WINTER, W. E., SILVERSTEIN, J. H., MACLAREN, N. K., RILEY, W. J. & CHIARO, J. J. 1983. Autosomal dominant hypoparathyroidism with variable, age-dependent severity. *J Pediatr,* 103**,** 387-90.

WOLFF, A. S., ERICHSEN, M. M., MEAGER, A., MAGITTA, N. F., MYHRE, A. G., BOLLERSLEV, J., FOUGNER, K. J., LIMA, K., KNAPPSKOG, P. M. & HUSEBYE, E. S. 2007. Autoimmune polyendocrine syndrome type 1 in Norway: phenotypic variation, autoantibodies, and novel mutations in the autoimmune regulator gene. *J Clin Endocrinol Metab,* 92**,** 595-603.

WOLFF, A. S., OFTEDAL, B. E., KISAND, K., ERSVAER, E., LIMA, K. & HUSEBYE, E. S. 2010. Flow cytometry study of blood cell subtypes reflects autoimmune and inflammatory processes in autoimmune polyendocrine syndrome type I. *Scand J Immunol,* 71**,** 459-67.

WOLFF, A. S., SARKADI, A. K., MARODI, L., KARNER, J., ORLOVA, E., OFTEDAL, B. E., KISAND, K., OLAH, E., MELONI, A., MYHRE, A. G., HUSEBYE, E. S., MOTAGHEDI, R., PERHEENTUPA, J., PETERSON, P., WILLCOX, N. & MEAGER, A. 2013. Anti-cytokine autoantibodies preceding onset of autoimmune polyendocrine syndrome type I features in early childhood. *J Clin Immunol,* 33**,** 1341-8.

WORTSMAN, J., MCCONNACHIE, P., BAKER, J. R., JR. & MALLETTE, L. E. 1992. T-lymphocyte activation in adult-onset idiopathic hypoparathyroidism. *Am J Med,* 92**,** 352-6.

WRIGHT, P. F., NILSSON, E., VAN ROOIJ, E. M., LELENTA, M. & JEGGO, M. H. 1993. Standardisation and validation of enzyme-linked immunosorbent assay techniques for the detection of antibody in infectious disease diagnosis. *Rev Sci Tech,* 12**,** 435-50.

WUCHERPFENNIG, K. W. 2001a. Mechanisms for the induction of autoimmunity by infectious agents. *J Clin Invest,* 108**,** 1097-1104.

WUCHERPFENNIG, K. W. 2001b. Structural basis of molecular mimicry. *Journal of Autoimmunity,* 16**,** 293-302.

XIE, L. D., GAO, Y., LI, M. R., LU, G. Z. & GUO, X. H. 2008. Distribution of immunoglobulin G subclasses of anti-thyroid peroxidase antibody in sera from patients with Hashimoto's thyroiditis with different thyroid functional status. *Clin Exp Immunol,* 154**,** 172-176.

YANG, S., FUJIKADO, N., KOLODIN, D., BENOIST, C. & MATHIS, D. 2015. Immune tolerance. Regulatory T cells generated early in life play a distinct role in maintaining self-tolerance. *Science,* 348**,** 589-94.

YEH, S. & MATOBA, A. Y. 2007. Successful nonsurgical management of corneal perforation in a patient with autoimmune polyendocrinopathy-candidiasis-ectodermal dystrophy. *Cornea,* 26**,** 880-2.

ZAIDI, G., SAHU, R. P., ZHANG, L., GEORGE, G., BHAVANI, N., SHAH, N., BHATIA, V., BHANSALI, A., JEVALIKAR, G., JAYAKUMAR, R. V., EISENBARTH, G. S. & BHATIA, E. 2009. Two novel AIRE mutations in autoimmune polyendocrinopathy-candidiasis-ectodermal dystrophy (APECED) among Indians. *Clin Genet,* 76**,** 441-8.

ZANELLI, E., HENRY, M. & MALTHIERY, Y. 1992. Use of recombinant epitopes to study the heterogeneous nature of the autoantibodies against thyroid peroxidase in autoimmune thyroid disease. *Clin Exp Immunol,* 87**,** 80-86.

ZHANG, C., MILLER, C. L., BROWN, E. M. & YANG, J. J. 2015. The calcium sensing receptor: from calcium sensing to signaling. *Sci China Life Sci,* 58**,** 14-27.

ZLOTOGORA, J. & SHAPIRO, M. S. 1992. Polyglandular autoimmune syndrome type I among Iranian Jews. *J Med Genet,* 29**,** 824-6.

ZUKLYS, S., BALCIUNAITE, G., AGARWAL, A., FASLER-KAN, E., PALMER, E. & HOLLANDER, G. A. 2000. Normal thymic architecture and negative selection are associated with Aire expression, the gene defective in the autoimmune-polyendocrinopathy-candidiasis-ectodermal dystrophy (APECED). *Journal of Immunology,* 165**,** 1976-1983.